ANL/ES-25

TEMPERATURE AND VELOCITY MEASUREMENTS AND PREDICTIVE MODEL COMPARISONS IN THE NEAR-FIELD REGION OF SURFACE THERMAL DISCHARGES

by

R. A. Paddock, A. J. Policastro,
A. A. Frigo, D. E. Frye,
and J. V. Tokar

ARGONNE NATIONAL LABORATORY

ANL
CES

CENTER FOR ENVIRONMENTAL STUDIES

Prepared for the U.S. ATOMIC ENERGY COMMISSION
Division of Reactor Research and Development
under Contract W-31-109-Eng-38

DISCLAIMER

The facilities of Argonne National Laboratory are owned by the United States Government. Under the terms of a contract (W-31-109-Eng-38) between the U. S. Atomic Energy Commission, Argonne Universities Association and The University of Chicago, the University employs the staff and operates the Laboratory in accordance with policies and programs formulated, approved and reviewed by the Association.

MEMBERS OF ARGONNE UNIVERSITIES ASSOCIATION

The University of Arizona	Kansas State University	The Ohio State University
Carnegie-Mellon University	The University of Kansas	Ohio University
Case Western Reserve University	Loyola University	The Pennsylvania State University
The University of Chicago	Marquette University	Purdue University
University of Cincinnati	Michigan State University	Saint Louis University
Illinois Institute of Technology	The University of Michigan	Southern Illinois University
University of Illinois	University of Minnesota	The University of Texas at Austin
Indiana University	University of Missouri	Washington University
Iowa State University	Northwestern University	Wayne State University
The University of Iowa	University of Notre Dame	The University of Wisconsin

Printed in the United States of America
Available from
U.S. Atomic Energy Commission
Technical Information Center
P.O. Box 62
Oak Ridge, Tennessee 37830
Price: Printed Copy $7.60

ANL/ES-25
Heat Rejection and
Utilization (UC-12)

ARGONNE NATIONAL LABORATORY
9700 South Cass Avenue
Argonne, Illinois 60439

TEMPERATURE AND VELOCITY MEASUREMENTS AND PREDICTIVE MODEL COMPARISONS IN THE NEAR-FIELD REGION OF SURFACE THERMAL DISCHARGES

by

R. A. Paddock, A. J. Policastro,
A. A. Frigo, D. E. Frye,
and J. V. Tokar

Center for Environmental Studies

October 1973

THIS PAGE

WAS INTENTIONALLY

LEFT BLANK

TABLE OF CONTENTS

TABLE OF CONTENTS

LIST OF FIGURES

LIST OF FIGURES

LIST OF FIGURES

LIST OF FIGURES

LIST OF FIGURES

LIST OF FIGURES

LIST OF FIGURES

LIST OF TABLES

TEMPERATURE AND VELOCITY MEASUREMENTS AND PREDICTIVE MODEL COMPARISONS IN THE NEAR-FIELD REGION OF SURFACE THERMAL DISCHARGES

by

R. A. Paddock, A. J. Policastro,
A. A. Frigo, D. E. Frye,
and J. V. Tokar

ABSTRACT

Simultaneous temperature and velocity measurements were made in the near-field region of the surface thermal discharge at the Point Beach Unit 1 and Palisades Nuclear Power Plants on Lake Michigan. Data collected include measurements of temperature and velocity at the 0.5-, 1.0-, 1.5-, 2.0-, 2.5-, and 3.0-m depths, along with measurements of ambient lake and meteorological conditions. Bottom depth was also measured at various locations. Four such surveys were made at the Point Beach plant, three at the Palisades plant.

To examine the jet features from the above surveys and facilitate a comparison with analytical model predictions, a computer program was written to smooth the data, extracting such jet characteristics as trajectory, centerline temperature decay and temperature half-widths, centerline velocity decay and velocity half-widths, temperature and velocity half-depths, and isotherm areas.

Four near-field analytical models often used in environmental impact evaluations of power-plant surface discharges are compared to the jet characteristics determined from the smoothed jet data. The Pritchard model compares rather well with these limited data and is often conservative when model-data discrepancies exist. The Stolzenbach-Harleman and Prych models predict too rapid a temperature and velocity decay accompanying too great a lateral spread. The Motz-Benedict model is too sensitive to an entrainment coefficient E with little consistent data available for its determination for accurate prediction.

Recommendations for future research, encompassing the field-data acquisition, the smoothing procedure, and the presently available models are included.

I. INTRODUCTION

Under the auspices of the U.S. Atomic Energy Commission, the Argonne Center for Environmental Studies has been studying the physical effects of heated condenser discharges from steam-electric power plants on the Great Lakes since FY 1970. Appendix A lists the reports published under this program to the present. Two of the primary objectives of this program have been and continue to be the acquisition of reasonably complete prototype thermal-plume field data and the verification of analytical predictive plume models. To this end, field data in the jet regime of two nuclear power plants on Lake Michigan have been collected and compared to models, with the results reported herein.

The jet regime (the near field) is that region of the discharge in which the heated effluent enters the receiving body of water possessing a velocity and temperature disparity with respect to the receiving body. Thus, as a heated effluent enters an ambient environment from a particular plant outfall, viscous shear between the effluent and the ambient fluid creates turbulence in the contact region. This turbulence works its way both inward toward the jet centerline and outward toward the ambient fluid, with a resultant net outward flux of momentum and heat away from the jet axis. Within this regime of the discharge, it is the mechanical mixing action induced by the kinetic energy of the discharge itself that dominates the eddy transport mechanisms. At some distance from the outfall, the kinetic energy of the discharge will be sufficiently dissipated to allow the natural turbulence existing within the ambient receiving water, together with buoyant forces, to dictate plume dispersion. It is nominally assumed that the effluent is no longer jetlike in character when this situation is reached.

From a regulatory point of view, the jet regime is of particular interest. It is often within this region that outfall architects must design their discharges to meet thermal water-quality criteria that limit the temperature rise in the thermal plume beyond a prescribed distance from the point of discharge. This is commonly referred to as a mixing-zone limitation. Some states have adopted very restrictive mixing-zone criteria; others have none at all. Therefore, depending on the nature of the receiving body, the size of plant, and a multitude of different factors including the thermal criteria, each plant outfall design is more or less tailored to the particular siting situation. On the Great Lakes, the predominant outfall design happens to be a shoreline, open, rectangular discharge canal. Several more recent plant designs have used more sophisticated offshore multiorifice submerged discharges, called diffusers.

The literature contains numerous models that attempt to predict the behavior of shoreline canal discharges. Some of these models are qualitative in nature; others profess to be quantitative as well. One thing all these models have in common is that none has been generally verified with prototype field data. To compound the problem, a survey of the literature reveals surprisingly little actual jet-regime field data with which models can be tested. Since there

is such a paucity of data in the jet regime, a field program was developed by the Center for Environmental Studies specifically to acquire prototype data near canal-type discharges. This program has been partially described in Refs. 21 and 25 of Appendix A. A description of experimental methods and detailed information concerning the results of seven jet studies obtained during 1972 are presented herein.

Since it would have been difficult to compare the field data directly to results obtained from analytical models, a data-smoothing technique was developed to help in this endeavor. The smoothing method was primarily developed to glean as much information from the experimental data as possible, considering the limited number of data points collected using the present field technique. A complete description of the smoothing method appears in Sec. V. While one should recognize that the smoothing method has some obvious limitations and biases, it nevertheless has worked out quite well for the purposes for which it was designed.

Lastly, the results of the smoothing procedure are compared to four analytical models that have been used, in some cases quite extensively, for predictive purposes. These comparisons and a discussion of them appear in Sec. VII. Note that the success or apparent lack of success displayed by a particular model should not, at this point, be considered as a total test of the model. Many more data comparisons under different outfall situations must be made before any model can be realistically evaluated.

In summary, this report brings together details concerning the acquisition, smoothing, and model analysis of a relatively unique set of jet-regime plume field data. We hope this report will stimulate more interest than has been shown in the literature in attempting to validate existing predictive models. In our opinion, too many predictive models existing in the literature have not been adequately tested. Much reliable field data is just now becoming available, and it should be the immediate goal of those interested in applying predictive models to test these models with actual field data. Only in this way can we hope for a positive improvement in the existing state of the art.

II. EXPERIMENTAL TECHNIQUE

A two- or three-point mooring system was used to hold Argonne's $5\frac{1}{2}$-m (18-ft) cathedral-hull fiberglass boat, the R. V. Aha, steady while obtaining simultaneous temperature and velocity measurements in the near-field region of the thermal plume (see Fig. 1). Anchors were located on either side of the plume, and for regions very near the outfall, a third line was sometimes attached to the outfall itself. Transects across the plume centerline were then made at various distances from the outfall. The position of the boat was held relatively constant at the various measuring stations, and the position of each station was determined by using a Motorola Mini-Ranger range positioning system (Fig. 2). This positioning system consists of two shore-based transponders with a receiver-transmitter unit and range console on board the boat that displays the range information

Fig. 1. Boat with Current Meter Used in Jet-regime Studies

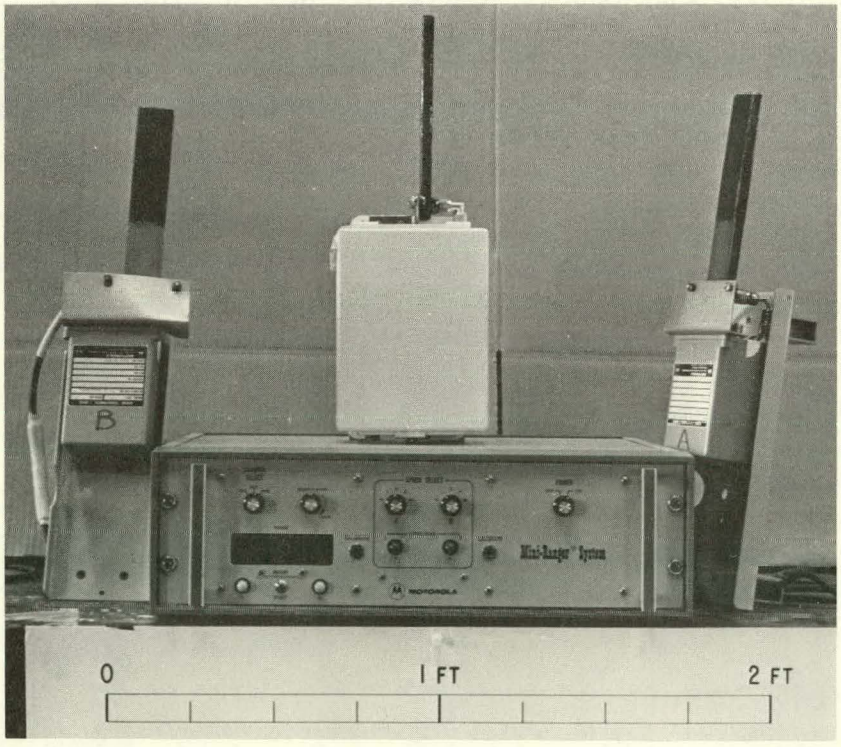

Fig. 2. Motorola Mini-Ranger Range Positioning System

from each transponder. The boat's position can then be found by trilateration. The Mini-Ranger is powered by 110 V ac (available from a 24-V dc high-efficiency Flitetronics PC 16 Aircraft Static Inverter). The usable range of the system with omnidirectional antennas is about 16 km.

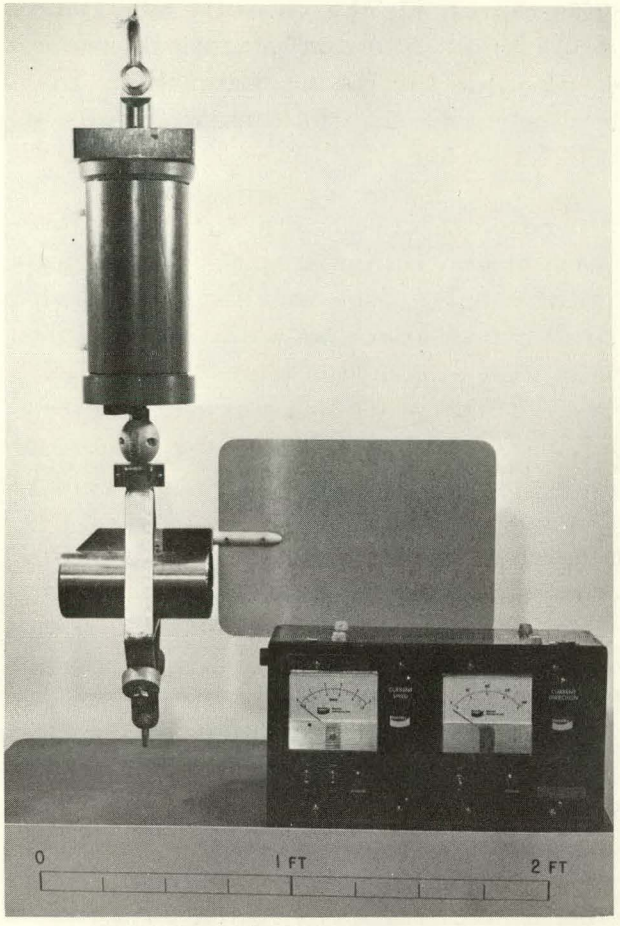

Fig. 3. Bendix Q-15 Geomagnetic Ducted Current Meter. ANL Neg. No. 190-568-11.

A Bendix Q-15 geomagnetic ducted current meter (Fig. 3), with an attached YSI thermistor, was used to measure the velocity and temperature of the discharge waters. The Q-15 has a five-bladed impeller that rotates in both directions and is enclosed in a duct. The ducted assembly is aligned with the current by a vane of adjustable length. The effects of wave and boat motion are nulled out by electronic averaging (over about 25 sec) of the number of turns of the impeller and by the presence of the duct. Current speed and direction are displayed on deck by means of a readout unit, Bendix Model No. S-232, which is connected to the current meter through a four-conductor cable. The current meter is powered by six 9-V batteries. The meter was lowered over the side of the boat and suspended at 0.5-m intervals to a depth of 3.0 m or to the bottom. The first time the experiment was being conducted, it was discovered that time variations in velocity and temperature occur. Thus, in order to obtain average values of velocity and temperature along with any variation, strip chart recorders were connected to the current-meter and thermistor outputs.

Note at this point that a variety of factors inherent in making measurements in the jet regime may cause uncertainties in the data. These problems must be understood if proper use is to be made of the data.

An important aspect of the experimental uncertainty is the short-term variations in the velocity and temperature of the discharge jet (see Ref. 30). The cause of these variations is not clear at present, but they may be due to eddies created at the interface between the jet and the ambient water, to surging which is apparent in the discharge canal, or to other factors. These fluctuations appear to have periods ranging from a few seconds to a few minutes.

Since point-by-point measurements in the jet were typically made over a period of 1-2 min, it is apparent that an unrepresentative value might be obtained at a given point. The scale of the short-term temperature fluctuations is on the order of several Centigrade degrees or less; the velocity variations are on the order of 50% of the mean value or less. These fluctuations were not present at all locations. A more typical value for the uncertainty in the temperature measurement is ±0.5C°; a typical value for the uncertainty in the current speed is ±20%.

Another source of uncertainty, in terms of data analysis, is the ambiguity attached to the values of ambient current and temperature. These numbers, necessarily assumed to be constants throughout the measurement (which lasted from 3 to 7 hr), vary not only in time but in space as well. Ambient-current measurements were typically made at a single location (at several depths) before and after the jet-regime measurements. Here again, current fluctuations in time and position may lead, for a variety of reasons, to an unrepresentative value for ambient-current speed. (Direction of the current is thought to be more definite.) Ambient-current speeds as reported may have an uncertainty of 20-50%; lower current speeds are the most uncertain. On some occasions, ambient-temperature measurements are as difficult to pin down as ambient-current speed and are somewhat more important in terms of the analysis to be described. We chose the ambient temperature to be the water temperature (at the appropriate depth), which appeared not to be influenced by the discharge water, yet was in the vicinity of the discharge. Unfortunately, on days when upwelling, downwelling, shoreline heating, or other disturbing phenomena occurred, the reported values of ambient water temperature may have an uncertainty of as much as 1-2C°.

In the face of the previously discussed uncertainties in the data, instrumentation accuracy may not be very important, but for completeness, Table I lists the instrument specifications. Of special interest in terms of velocity measurements is the fact that, while a ducted current meter is used to null out disturbing vertical motion, shielding of the impeller occurs if the duct is not aligned with the flow. The importance of this remains unclear, but because the meter continuously averages the speed over a 25-sec period, any shielding would result in lower values for current speed.

TABLE I. Instrument Accuracy

Instrument	Sensor	Accuracy	Threshold	Range	Time Constant	Resolution	Remarks
Bendix Q-15 Current Meter	Speed; impeller	±4% of full scale	3 cm/sec	0-1.0 knot; low scale 0-5.0 knots; high scale	25 sec; low scale 2.5 sec; high scale	1 cm/sec; low scale 5 cm/sec; high scale	
	Direction; compass with vane	±12°	-	0-360°	-	5°	Vane has adjustable length; 0.3-3.0 m
Temperature Recorder[a]	Thermistor	±0.5C°	-	0-30°C	~2.5 sec	0.2C°	Consisting of a Rustrak Model No. 2133 temperature recorder and YSI No. 409 thermistor probe
Temperature Recorder[b]	Thermistor	±0.2C°	-	0-50°C	~2.5 sec	0.1C°	Consisting of YSI No. 709 probe and digital readout built at Argonne
Motorola Mini-Ranger	-	±3 m	-	0.1-35 km	-	1 m	Accuracy applies to each range measurement. System accuracy varies with position of transponders relative to boat. For most of these measurements, ±3 m would apply.

[a]Used in temperature measurements up to and including July 19, 1972.
[b]Used in temperature measurements after July 19, 1972.

III. DESCRIPTIONS OF POWER PLANTS

The jet regimes of the thermal plumes were surveyed at two power plants located on Lake Michigan. The power plants studied were the Point Beach Nuclear Power Plant, operated by the Wisconsin Electric Power Company and the Wisconsin Michigan Power Company, and the Palisades Nuclear Power Plant, operated by Consumers Power Company. Brief descriptions of these plants follow.

A. Point Beach Nuclear Power Plant

The Point Beach Nuclear Power Plant is in the town of Two Creeks, Wisconsin, on the western shore of Lake Michigan. (Figure 4 is an aerial view of the plant.) The plant is a two-unit steam-generating station. The nuclear reactors for each unit are pressurized light-water-moderated and -cooled systems. Each unit has a gross capacity of 523 MWe and a net capacity of 505 MWe. The water intake for the plant consists of a circular crib 533 m from the shore. Cooling water for the operation of the power plant is drawn from Lake Michigan and passes through the cooling condensers at a maximum rate of 25.1 m^3/sec for full-power operation of each individual unit of the plant. The water is returned to the lake about 50 m offshore through two 10.7-m-wide discharge flumes (one flume per unit). Water depth in the flumes is about 4.2 m. During most of the field year, the second unit was not operational. Late in the summer, however, the second unit was operating at about 12% power and 50% of its rated discharge flow.

B. Palisades Nuclear Power Plant

The Palisades Nuclear Power Plant is near the city of South Haven, Michigan, on the eastern shore of Lake Michigan. (Figure 5 is an aerial view of the plant.) This plant uses a pressurized-water reactor to produce a maximum gross output of 714 MWe. During the 1972 field year, the plant was operating at a net generating capacity of about 420 MWe. The cooling water is taken from Lake Michigan through an intake crib located 6.1 m below the lake's surface, 1.8 m from the lake bottom, and 1000 m from the shoreline. For the Palisades plant, as presently constructed, the cooling water passes through the cooling condenser at a maximum flow rate of 25.6 m^3/sec and is returned to Lake Michigan, via a 32.9-m-long discharge canal at the shoreline. The canal is 11.3 m wide at the shoreline outlet and diverges to a width of 28.3 m at the point of discharge. At this point, the water has an average depth of about 2.1 m.

Fig. 4. Aerial View of Point Beach Nuclear Power Plant. ANL Neg. No. 190–499.

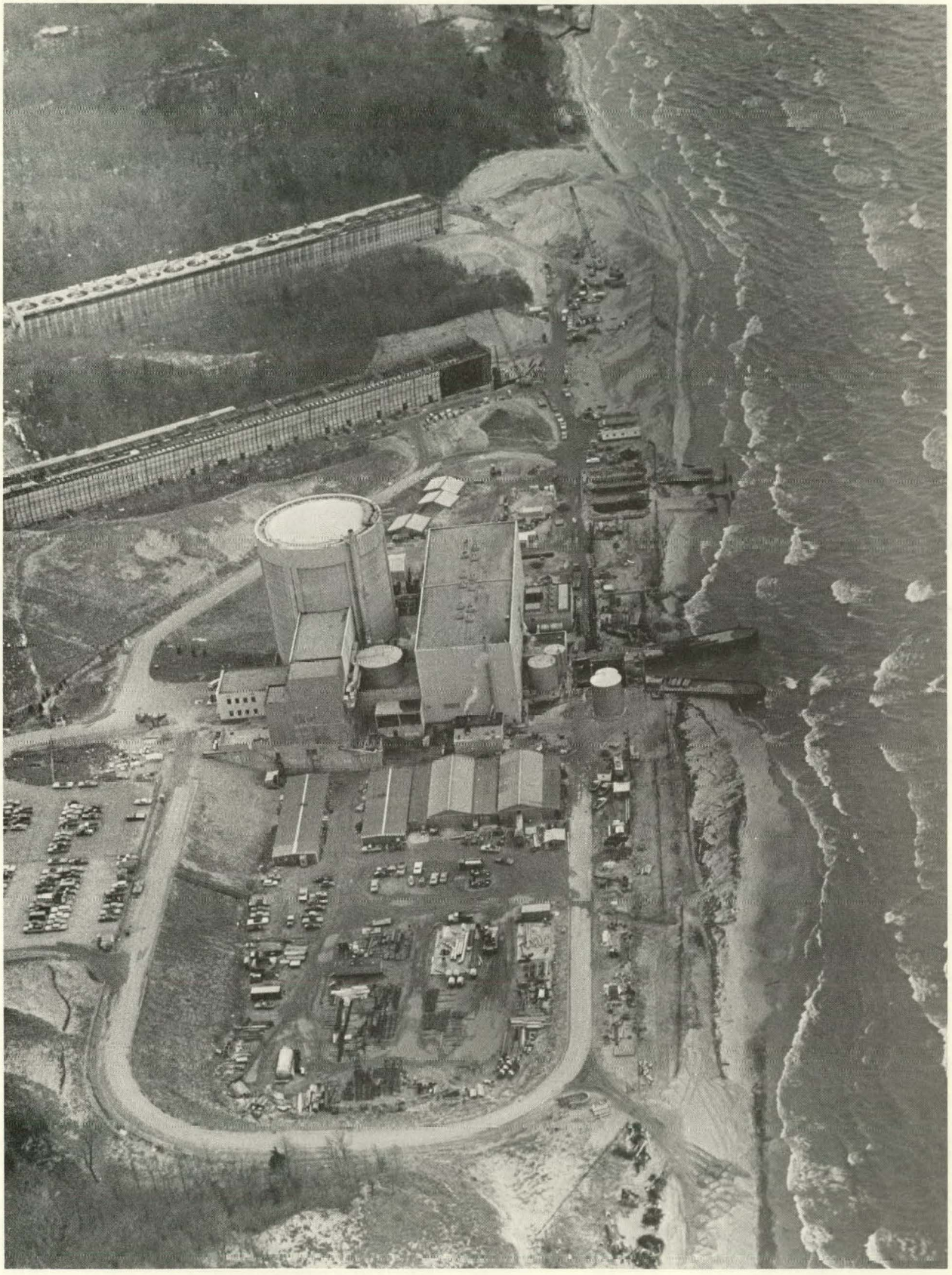

Fig. 5. Aerial View of Palisades Nuclear Power Plant

IV. RESULTS OF FIELD MEASUREMENTS

During the 1972 field year, seven jet-regime studies were conducted at the two power plants described in Sec. III. Specifically, these studies were at the Point Beach Nuclear Power Plant Unit 1 on May 18, May 23, July 13, and September 9, 1972, and at the Palisades Nuclear Power Plant on June 14, July 19, and October 10, 1972. In addition, one survey was conducted late in the 1971 field year (November 3, 1971) as a preliminary feasibility study of the technique (see Appendix B). Data collected include measurements of velocity and temperature in the near-field region of the thermal plume at the 0.5-, 1.0-, 1.5-, 2.0-, 2.5-, and 3.0-m depths, along with measurements of ambient lake and meteorological conditions. Bottom depth was also measured at various locations. From the bottom-depth data, approximate depth contours were drawn near the outfalls and are shown in Figs. 6 and 7. The points indicate positions at which data were taken.* Results of the jet-regime measurements are shown in Figs. 8-48 for the dates indicated. The figures show station locations at which jet velocities and temperatures were measured. The velocity is represented vectorially at each station location. In addition, the current speed, current direction, and temperature at each station are listed in a table on each figure. Current direction is given in degrees as measured from magnetic north. Also listed on the figures are the ambient lake and meteorological data, as well as the plant operating data. Temperature and velocity centerlines and widths are shown in most cases. The widths represent the lateral distance from the centerline at which the appropriate parameter has reached a value halfway between the centerline value and the ambient value. The mathematical fitting technique used to obtain the centerlines and widths is described in Sec. V. Centerlines and widths are not shown for any depths for the jet-regime studies conducted at the Palisades Plant on June 14 and July 19, 1972. Typically, the Palisades outfall produces a very wide jet, and the data on these dates did not lend themselves to the type of analysis necessary for determining centerlines and widths.

*Dotted lines indicate estimated contours for which no data were available.

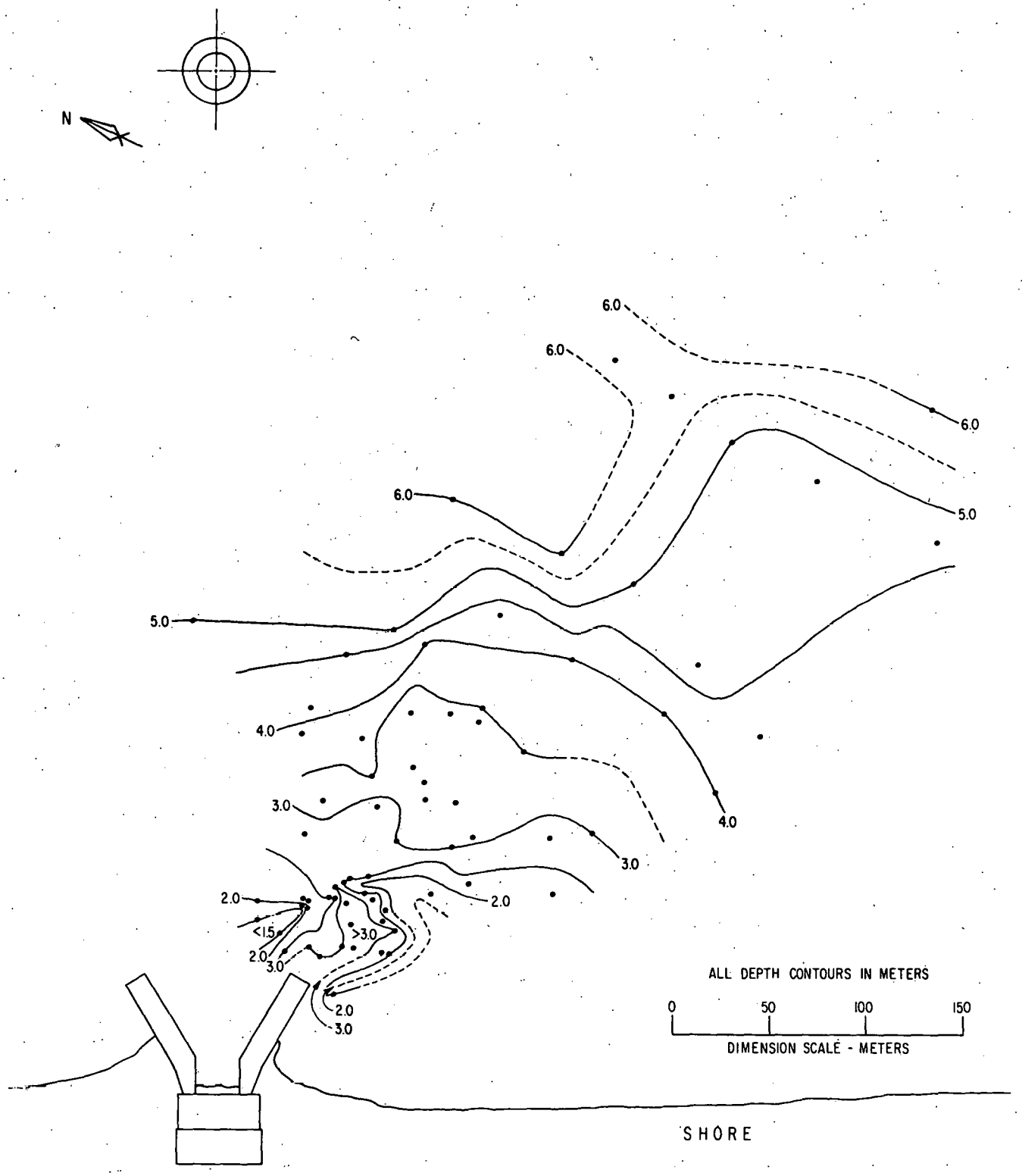

Fig. 6. Approximate Depth Contours near Point Beach Outfall. ANL Neg. No. 190-878.

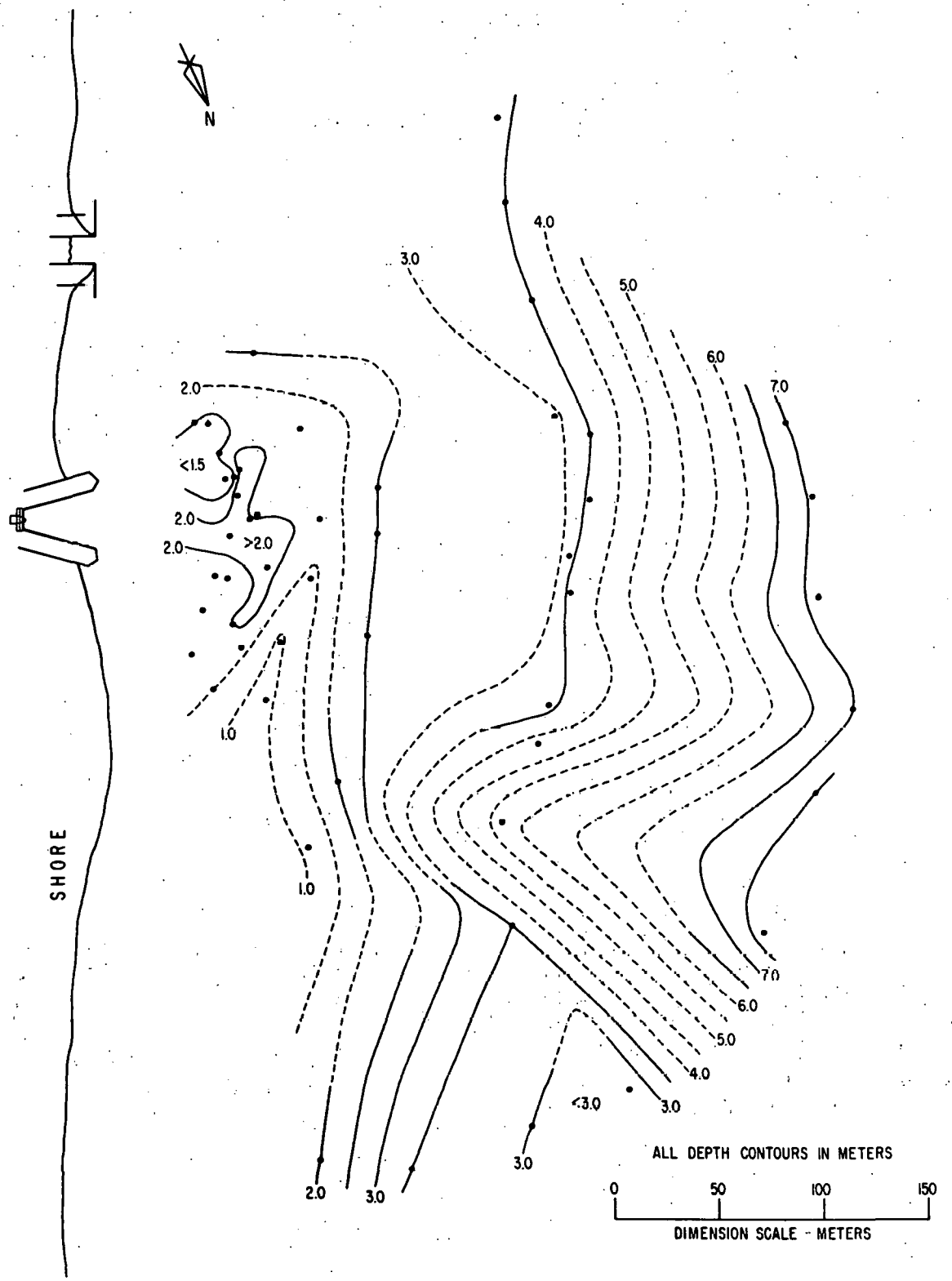

Fig. 7. Approximate Depth Contours near Palisades Outfall. ANL Neg. No. 190-880.

STATION NUMBER	CURRENT SPEED (cm/sec)	CURRENT DIRECTION (°)	TEMPERATURE (°C)
1	0	–	11.0
2	0	–	11.2
3	NOT MEASURED		
4	21.1	115	14.0
5	26.1	80	14.5
6	16.7	105	11.1
7	0	–	12.7
8	0	–	13.3
9	40.6	125	14.5
10	44.5	120	13.0
11	0	–	10.5
12	0	–	10.6
13	9.5	95	11.0
14	58.4	105	16.7
15	36.1	125	16.0
16	27.8	140	16.0
17	12.8	145	13.8
18	9.5	125	13.4
19	67.8	95	17.7

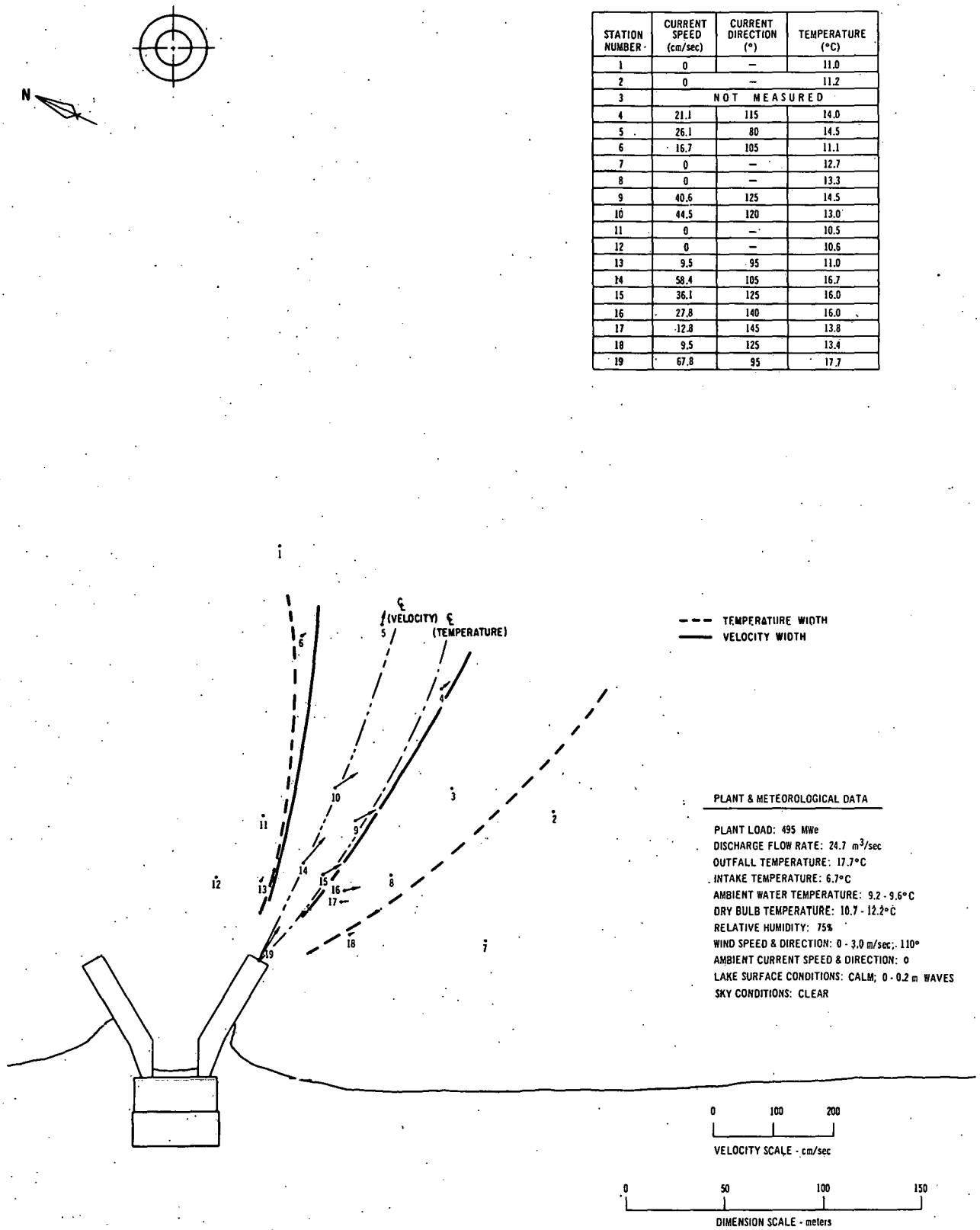

Fig. 8. Jet-regime Study for 0.5-m Depth at Point Beach Power Plant (Unit 1): May 18, 1972, 1115-1440 Hours. ANL Neg. No. 190-761 Rev. 1.

STATION NUMBER	CURRENT SPEED (cm/sec)	CURRENT DIRECTION (°)	TEMPERATURE (°C)
1	0	–	9.7
2	0	–	11.0
3	6.1	145	12.6
4	16.7	140	14.0
5	22.2	85	13.5
6	9.5	110	10.6
7	LAKE BOTTOM		
8	0	–	13.1
9	36.1	110	14.4
10	41.7	110	13.9
11	0	–	9.7
12	0	–	8.5
13	8.3	110	10.3
14	47.3	95	16.0
15	30.6	100	14.5
16	22.2	115	14.7
17	12.2	135	13.6
18	0	-	13.3
19	65.2	95	17.7

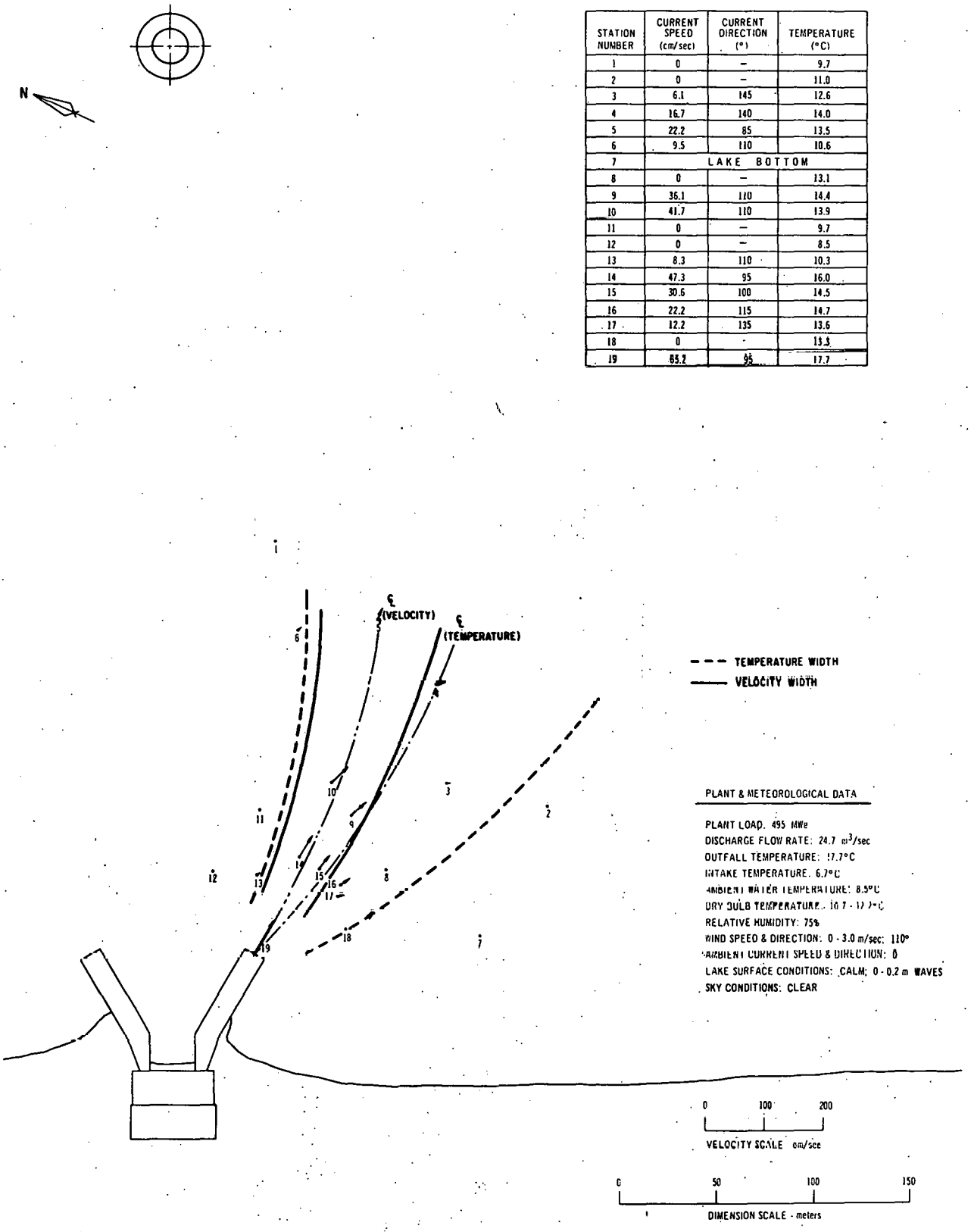

Fig. 9. Jet-regime Study for 1.0-m Depth at Point Beach Power Plant (Unit 1): May 18, 1972, 1115-1440 Hours. ANL Neg. No. 190-895.

STATION NUMBER	CURRENT SPEED (cm/sec)	CURRENT DIRECTION (°)	TEMPERATURE (°C)
1	NOT MEASURED		
2	8.9	10	10.4
3	NOT MEASURED		
4	10.6	135	13.2
5	23.9	85	12.6
6	0	–	9.7
7	LAKE BOTTOM		
8	0	–	12.1
9	33.4	115	15.0
10	29.5	100	13.4
11	NOT MEASURED		
12	0	–	8.3
13	8.3	170	8.4
14	50.0	105	16.2
15	22.2	105	15.0
16	18.3	125	14.4
17	5.6	115	13.2
18	0	–	12.5
19	62.3	95	17.7

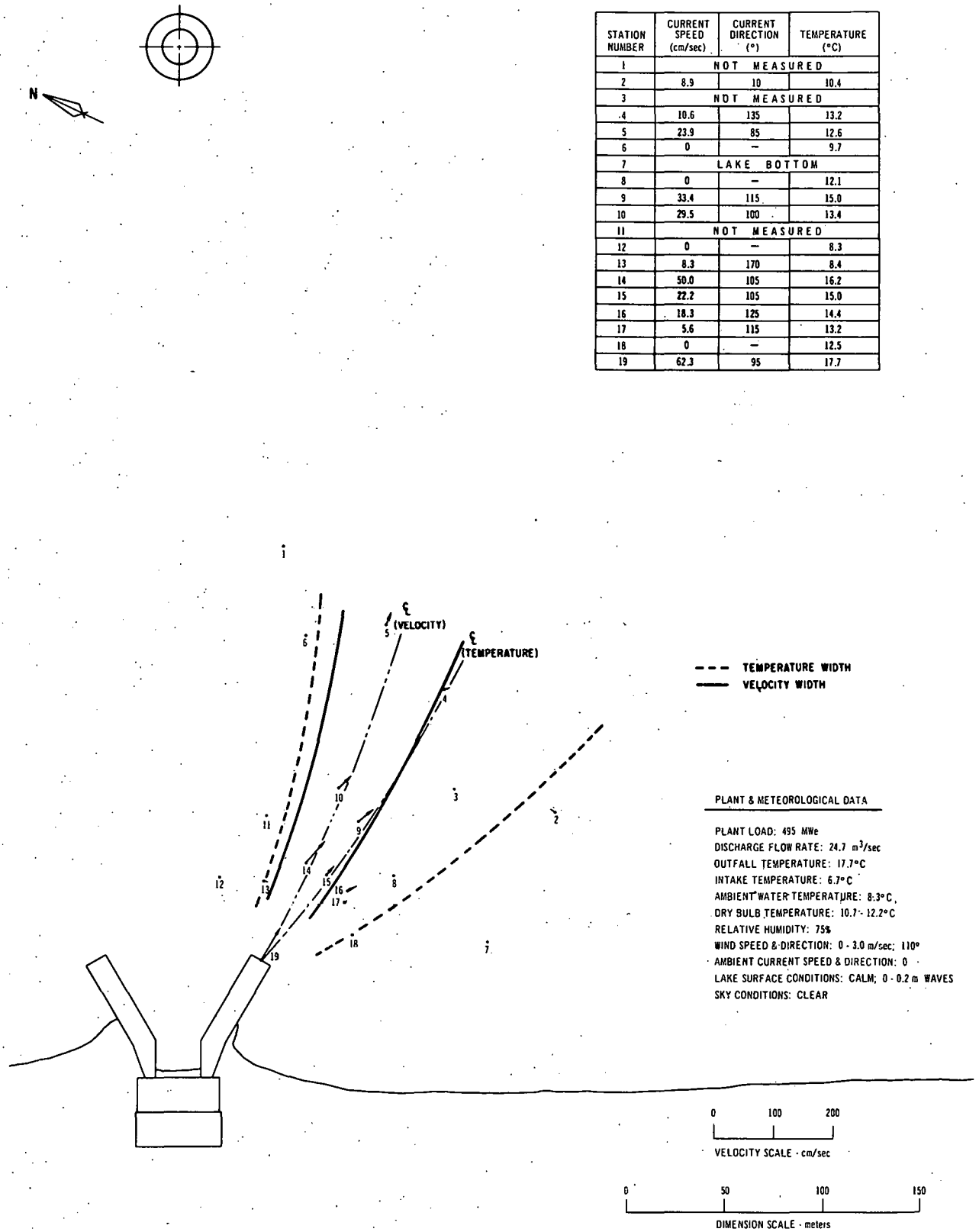

Fig. 10. Jet-regime Study for 1.5-m Depth at Point Beach Power Plant (Unit 1): May 18, 1972, 1115-1440 Hours. ANL Neg. No. 190-893.

STATION NUMBER	CURRENT SPEED (cm/sec	CURRENT DIRECTION (°:	TEMPERATURE (°C)
1	0	–	9.9
2	8.3	15	8.3
3	0	–	10.8
4	6.7	135	10.4
5	19.5	80	12.5
6	0	–	9.2
7	LAKE BOTTOM		
8	LAKE BOTTOM		
9	21.7	90	14.5
10	25.0	125	11.5
11	0	–	8.3
12	LAKE BOTTOM		
13	LAKE BOTTOM		
14	50.0	105	15.0
15	27.8	110	14.2
16	10.0	110	13.3
17	0	–	12.4
18	0	–	11.9
19	50.0	95	17.7

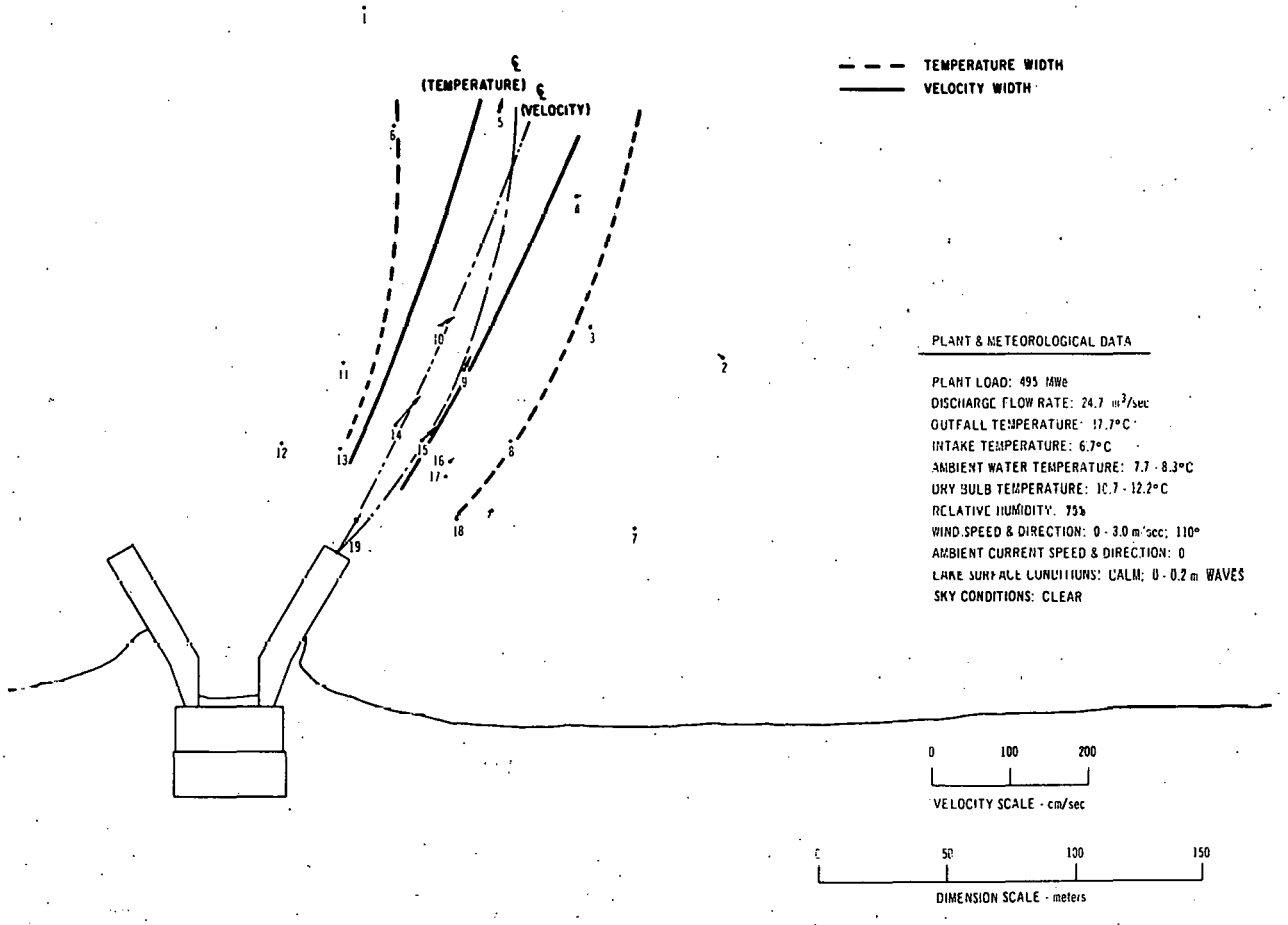

Fig. 11. Jet-regime Study for 2.0-m Depth at Point Beach Power Plant (Unit 1): May 18, 1972, 1115-1440 Hours. ANL Neg. No. 190-899.

STATION NUMBER	CURRENT SPEED (cm/sec)	CURRENT DIRECTION (°)	TEMPERATURE (°C)
1	NOT MEASURED		
2	7.8	35	7.8
3	0	–	9.0
4	0	–	12.0
5	15.6	80	11.1
6	0	–	8.8
7	LAKE BOTTOM		
8	LAKE BOTTOM		
9	16.7	95	13.2
10	17.8	130	10.0
11	LAKE BOTTOM		
12	LAKE BOTTOM		
13	LAKE BOTTOM		
14	LAKE BOTTOM		
15	LAKE BOTTOM		
16	LAKE BOTTOM		
17	6.7	45	12.8
18	LAKE BOTTOM		
19	55.6	95	17.7

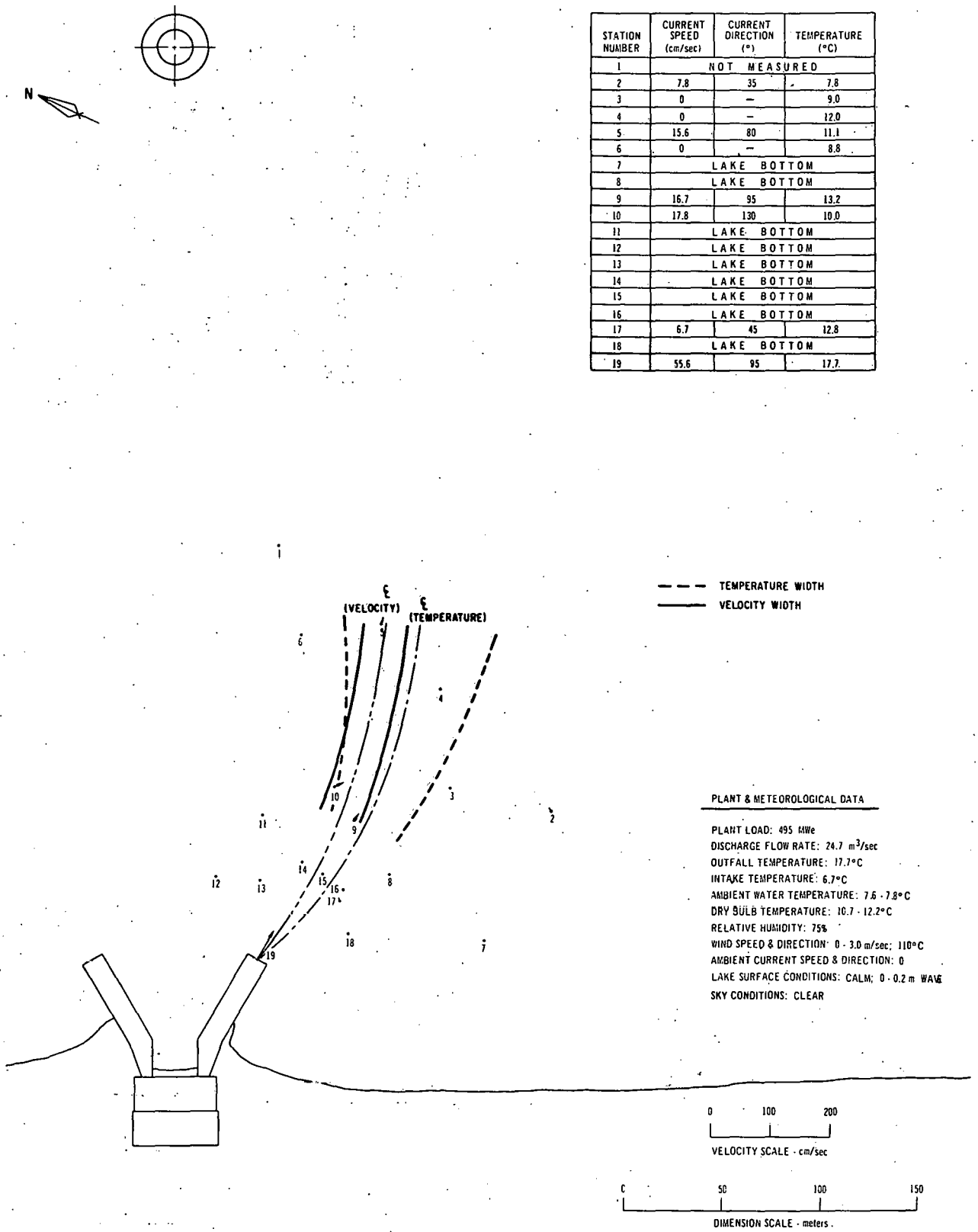

Fig. 12. Jet-regime Study for 2.5-m Depth at Point Beach Power Plant (Unit 1): May 18, 1972, 1115-1440 Hours. ANL Neg. No. 190-898.

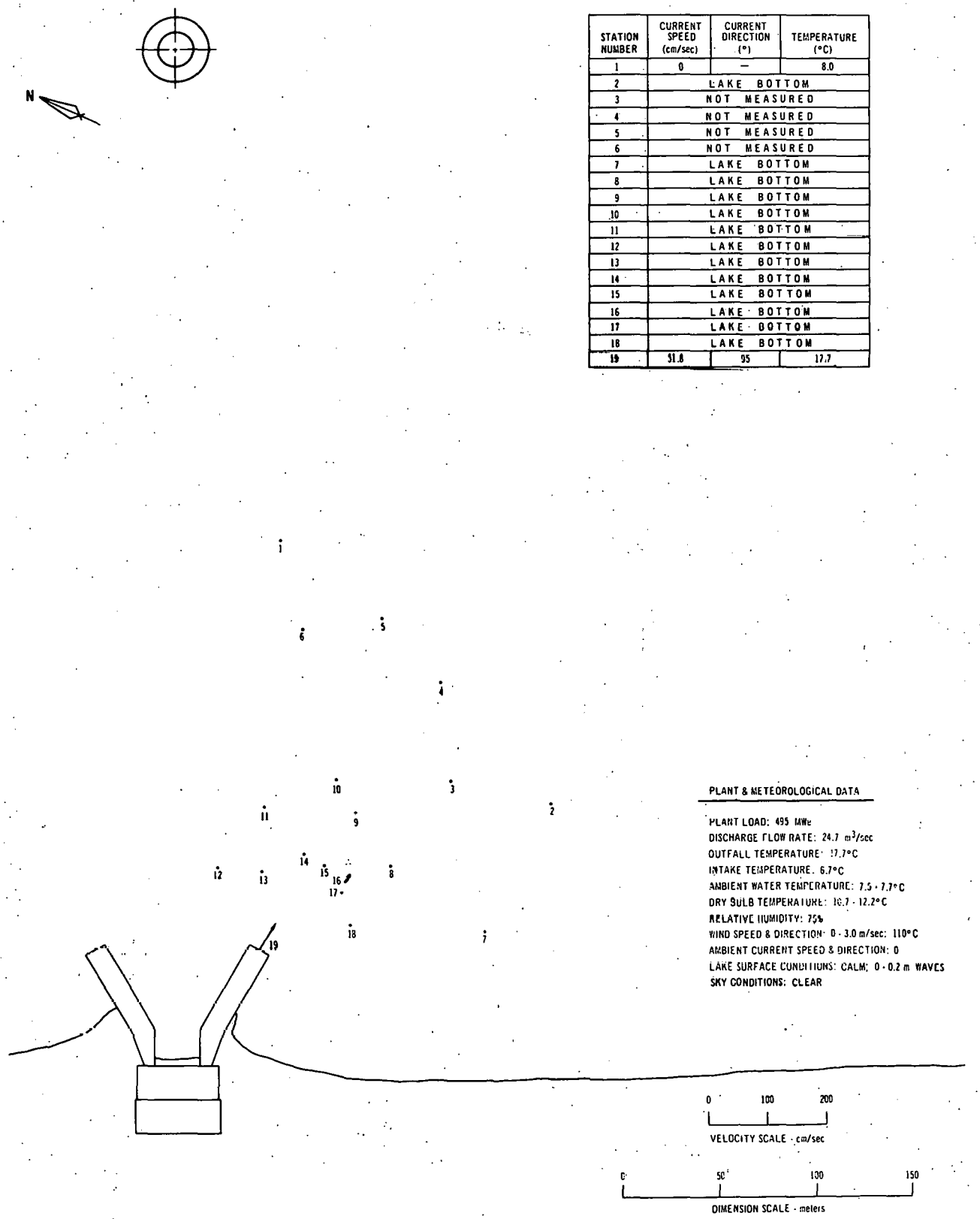

STATION NUMBER	CURRENT SPEED (cm/sec)	CURRENT DIRECTION (°)	TEMPERATURE (°C)
1	0	—	8.0
2	LAKE BOTTOM		
3	NOT MEASURED		
4	NOT MEASURED		
5	NOT MEASURED		
6	NOT MEASURED		
7	LAKE BOTTOM		
8	LAKE BOTTOM		
9	LAKE BOTTOM		
10	LAKE BOTTOM		
11	LAKE BOTTOM		
12	LAKE BOTTOM		
13	LAKE BOTTOM		
14	LAKE BOTTOM		
15	LAKE BOTTOM		
16	LAKE BOTTOM		
17	LAKE BOTTOM		
18	LAKE BOTTOM		
19	51.8	95	17.7

Fig. 13. Jet-regime Study for 3.0-m Depth at Point Beach Power Plant (Unit 1): May 18, 1972, 1115-1440 Hours. ANL Neg. No. 190-889.

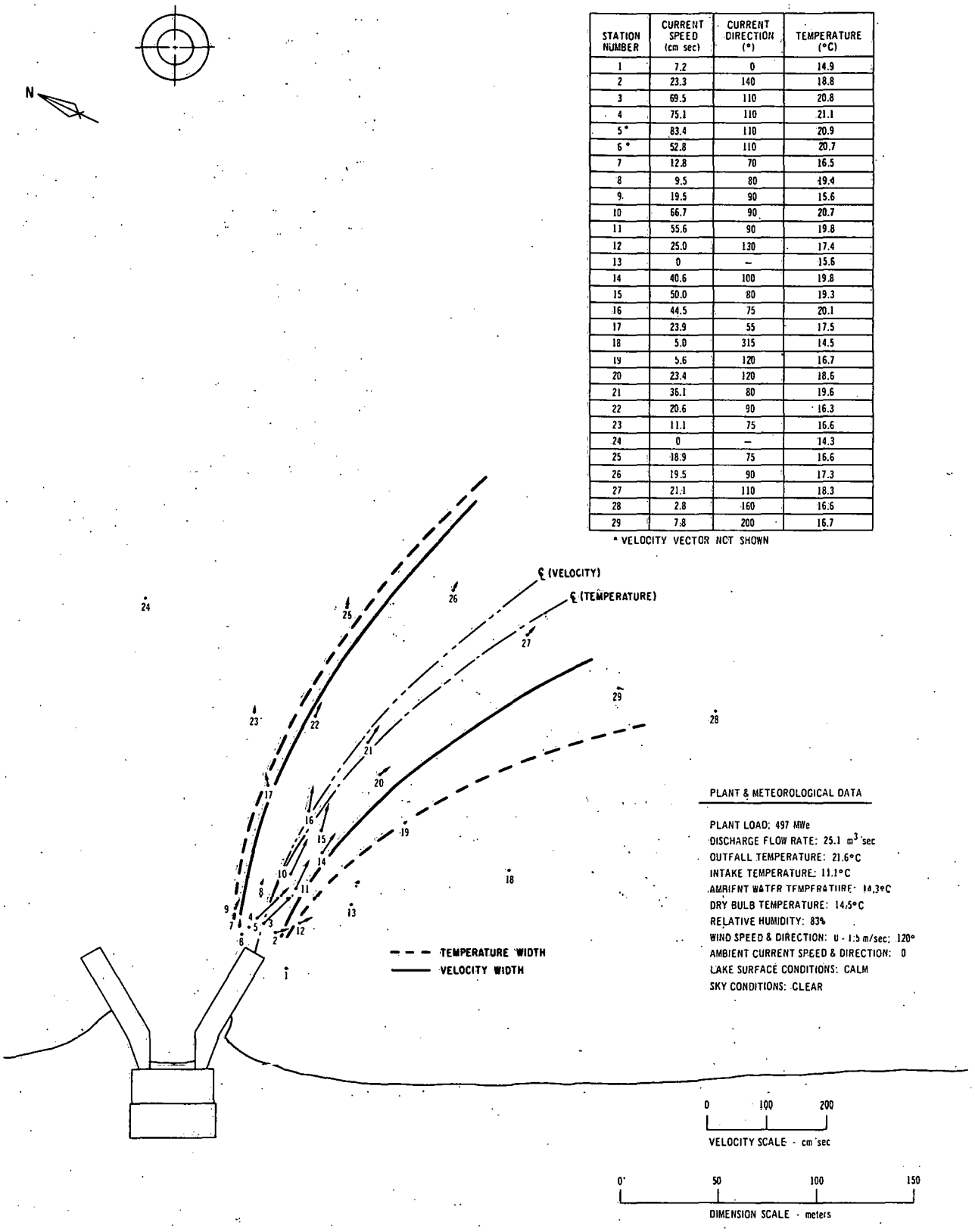

STATION NUMBER	CURRENT SPEED (cm sec)	CURRENT DIRECTION (°)	TEMPERATURE (°C)
1	7.2	0	14.9
2	23.3	140	18.8
3	69.5	110	20.8
4	75.1	110	21.1
5*	83.4	110	20.9
6*	52.8	110	20.7
7	12.8	70	16.5
8	9.5	80	19.4
9	19.5	90	15.6
10	66.7	90	20.7
11	55.6	90	19.8
12	25.0	130	17.4
13	0	–	15.6
14	40.6	100	19.8
15	50.0	80	19.3
16	44.5	75	20.1
17	23.9	55	17.5
18	5.0	315	14.5
19	5.6	120	16.7
20	23.4	120	18.6
21	36.1	80	19.6
22	20.6	90	16.3
23	11.1	75	16.6
24	0	–	14.3
25	18.9	75	16.6
26	19.5	90	17.3
27	21.1	110	18.3
28	2.8	160	16.6
29	7.8	200	16.7

* VELOCITY VECTOR NOT SHOWN

Fig. 14. Jet-regime Study for 0.5-m Depth at Point Beach Power Plant (Unit 1): May 23, 1972, 0945-1700 Hours. ANL Neg. No. 190-760 Rev. 1.

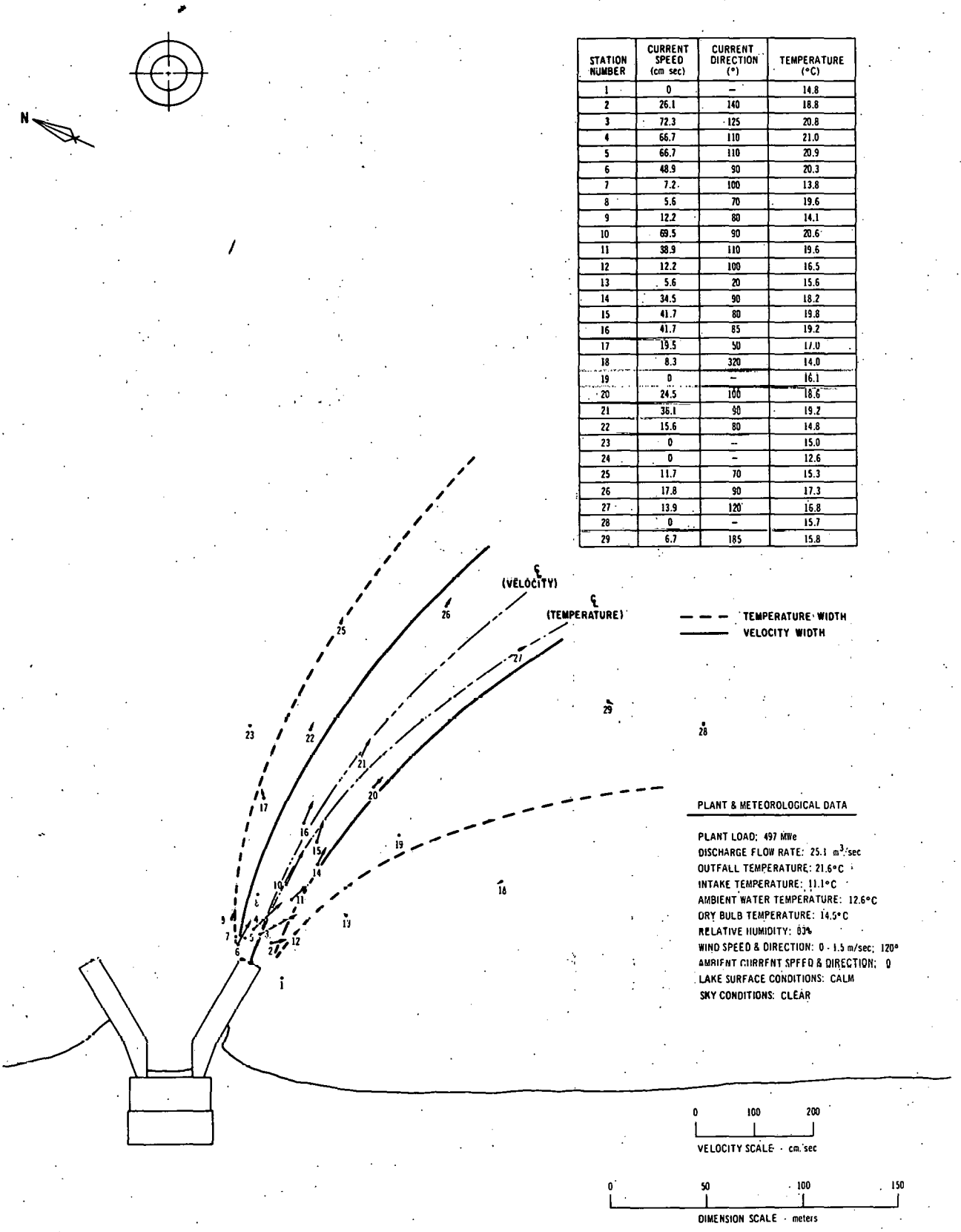

STATION NUMBER	CURRENT SPEED (cm sec)	CURRENT DIRECTION (°)	TEMPERATURE (°C)
1	0	–	14.8
2	26.1	140	18.8
3	72.3	125	20.8
4	66.7	110	21.0
5	66.7	110	20.9
6	48.9	90	20.3
7	7.2	100	13.8
8	5.6	70	19.6
9	12.2	80	14.1
10	69.5	90	20.6
11	38.9	110	19.6
12	12.2	100	16.5
13	5.6	20	15.6
14	34.5	90	18.2
15	41.7	80	19.8
16	41.7	85	19.2
17	19.5	50	17.0
18	8.3	320	14.0
19	0	–	16.1
20	24.5	100	18.6
21	36.1	90	19.2
22	15.6	80	14.8
23	0	–	15.0
24	0	–	12.6
25	11.7	70	15.3
26	17.8	90	17.3
27	13.9	120	16.8
28	0	–	15.7
29	6.7	185	15.8

Fig. 15. Jet-regime Study for 1.0-m Depth at Point Beach Power Plant (Unit 1): May 23, 1972, 0945-1700 Hours. ANL Neg. No. 190-891.

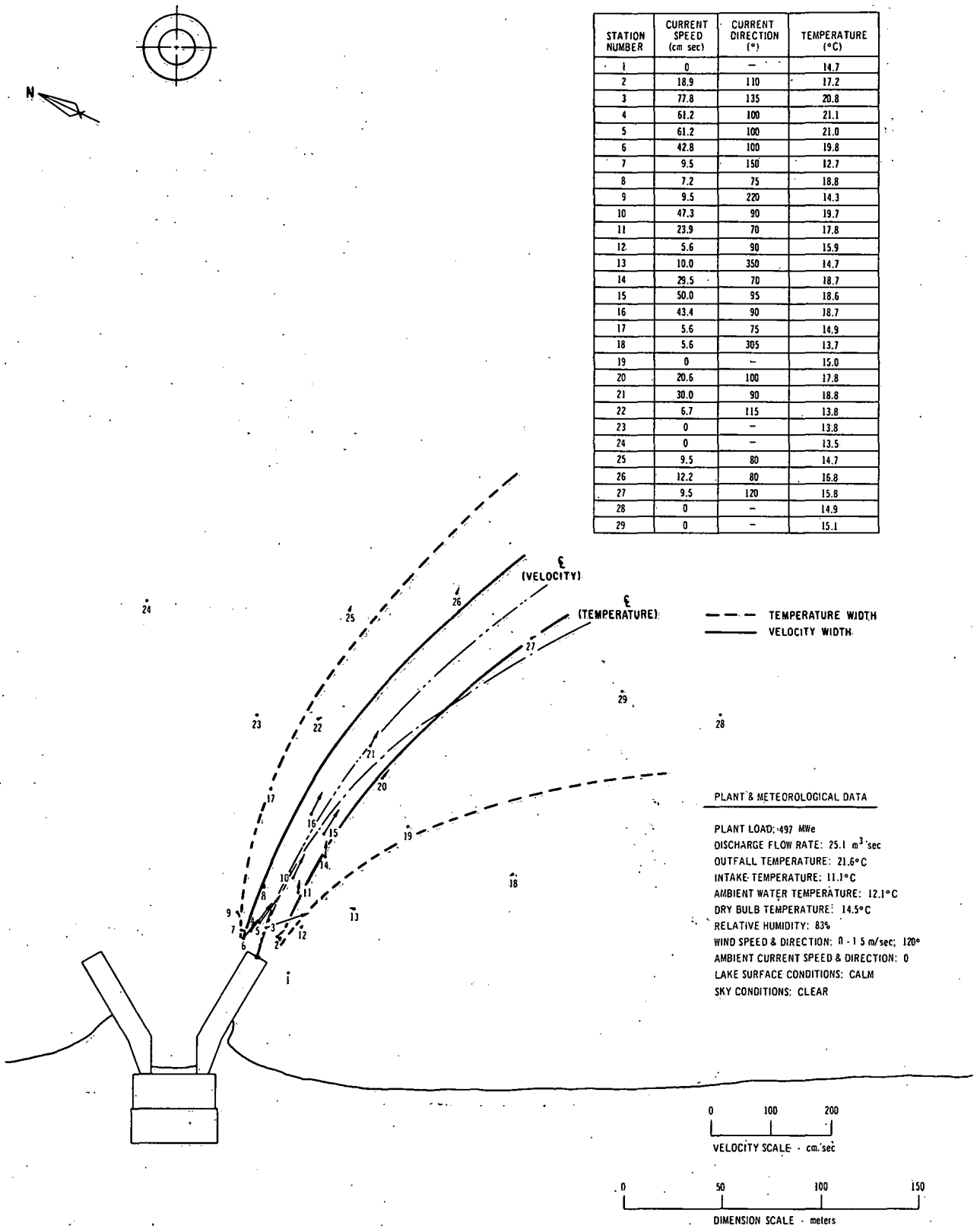

STATION NUMBER	CURRENT SPEED (cm sec)	CURRENT DIRECTION (°)	TEMPERATURE (°C)
1	0	–	14.7
2	18.9	110	17.2
3	77.8	135	20.8
4	61.2	100	21.1
5	61.2	100	21.0
6	42.8	100	19.8
7	9.5	150	12.7
8	7.2	75	18.8
9	9.5	220	14.3
10	47.3	90	19.7
11	23.9	70	17.8
12	5.6	90	15.9
13	10.0	350	14.7
14	29.5	70	18.7
15	50.0	95	18.6
16	43.4	90	18.7
17	5.6	75	14.9
18	5.6	305	13.7
19	0	–	15.0
20	20.6	100	17.8
21	30.0	90	18.8
22	6.7	115	13.8
23	0	–	13.8
24	0	–	13.5
25	9.5	80	14.7
26	12.2	80	16.8
27	9.5	120	15.8
28	0	–	14.9
29	0	–	15.1

Fig. 16. Jet-regime Study for 1.6-m Depth at Point Beach Power Plant (Unit 1): May 23, 1972, 0945-1700 Hours. ANL Neg. No. 190-906.

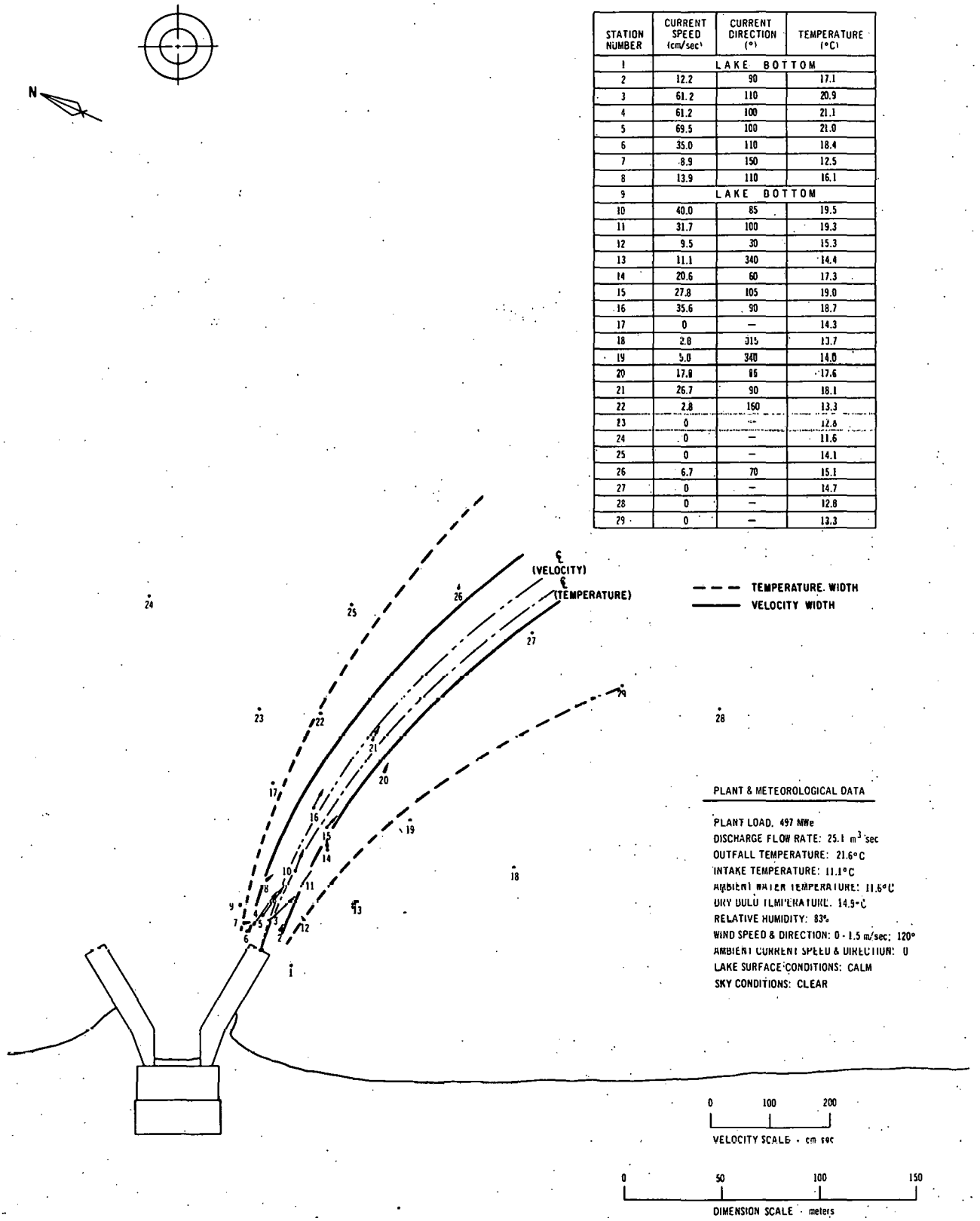

STATION NUMBER	CURRENT SPEED (cm/sec)	CURRENT DIRECTION (°)	TEMPERATURE (°C)
1	LAKE BOTTOM		
2	12.2	90	17.1
3	61.2	110	20.9
4	61.2	100	21.1
5	69.5	100	21.0
6	35.0	110	18.4
7	8.9	150	12.5
8	13.9	110	16.1
9	LAKE BOTTOM		
10	40.0	85	19.5
11	31.7	100	19.3
12	9.5	30	15.3
13	11.1	340	14.4
14	20.6	60	17.3
15	27.8	105	19.0
16	35.6	90	18.7
17	0	—	14.3
18	2.8	315	13.7
19	5.0	340	14.0
20	17.8	86	17.6
21	26.7	90	18.1
22	2.8	160	13.3
23	0	—	12.8
24	0	—	11.6
25	0	—	14.1
26	6.7	70	15.1
27	0	—	14.7
28	0	—	12.8
29	0	—	13.3

Fig. 17. Jet-regime Study for 2.0-m Depth at Point Beach Power Plant (Unit 1): May 23, 1972, 0945-1700 Hours. ANL Neg. No. 190-894.

STATION NUMBER	CURRENT SPEED (cm sec)	CURRENT DIRECTION (°)	TEMPERATURE (°C)
1	LAKE BOTTOM		
2	13.9	100	16.8
3	45.6	110	20.6
4	47.3	110	21.0
5	72.3	100	21.0
6	35.0	110	17.6
7	7.8	140	12.4
8	LAKE BOTTOM		
9	LAKE BOTTOM		
10	44.5	90	19.3
11	24.5	60	17.3
12	14.5	20	15.3
13	7.2	350	14.1
14	LAKE BOTTOM		
15	NOT MEASURED		
16	24.5	85	17.6
17	0	—	12.3
18	LAKE BOTTOM		
19	LAKE BOTTOM		
20	15.0	75	17.3
21	16.7	75	17.1
22	5.6	200	11.6
23	5.6	225	11.3
24	0	—	11.3
25	0	—	13.3
26	0	—	14.8
27	0	—	14.7
28	0	—	12.8
29	0	—	12.8

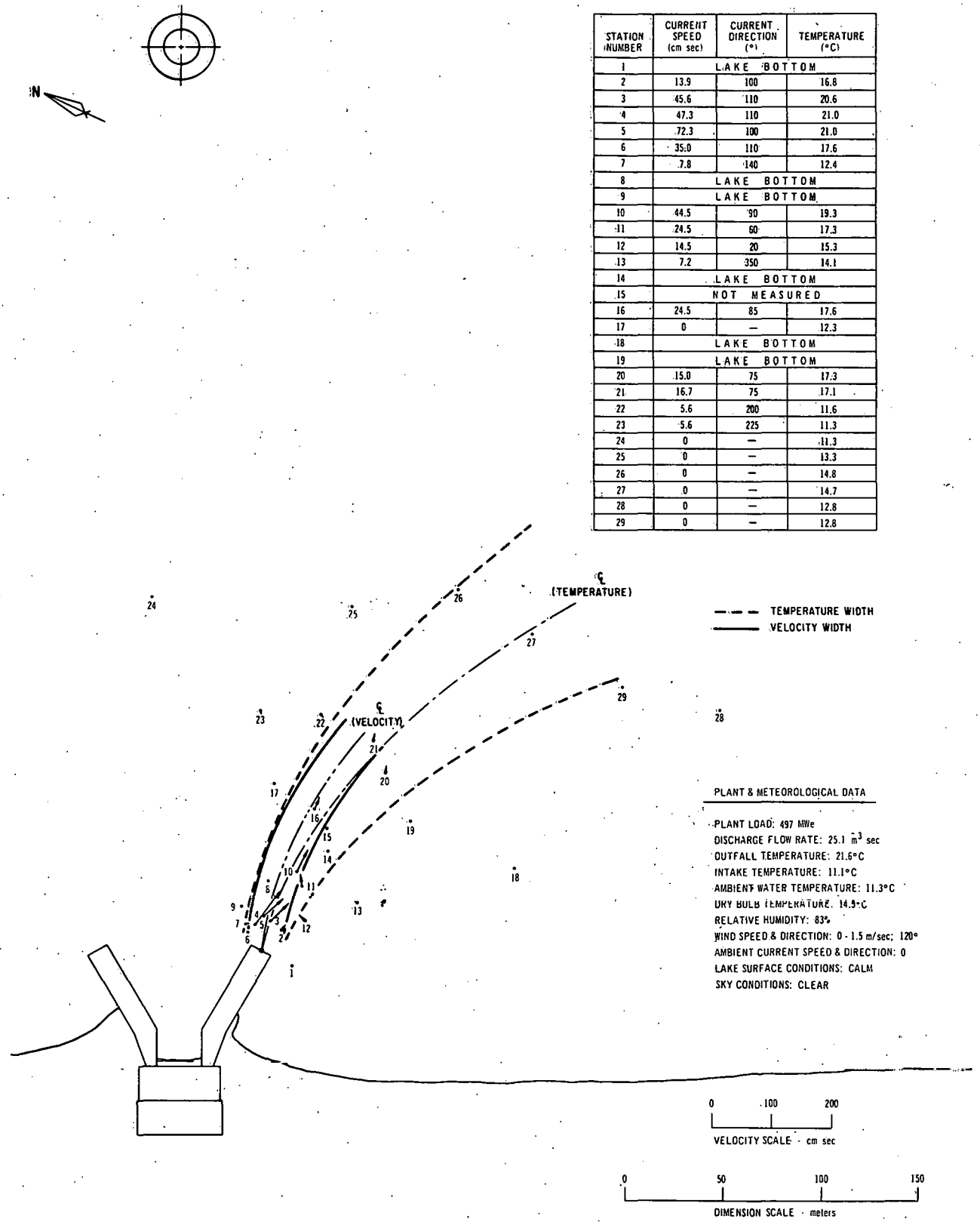

Fig. 18. Jet-regime Study for 2.5-m Depth at Point Beach Power Plant (Unit 1): May 23, 1972, 0945-1700 Hours. ANL Neg. No. 190-892.

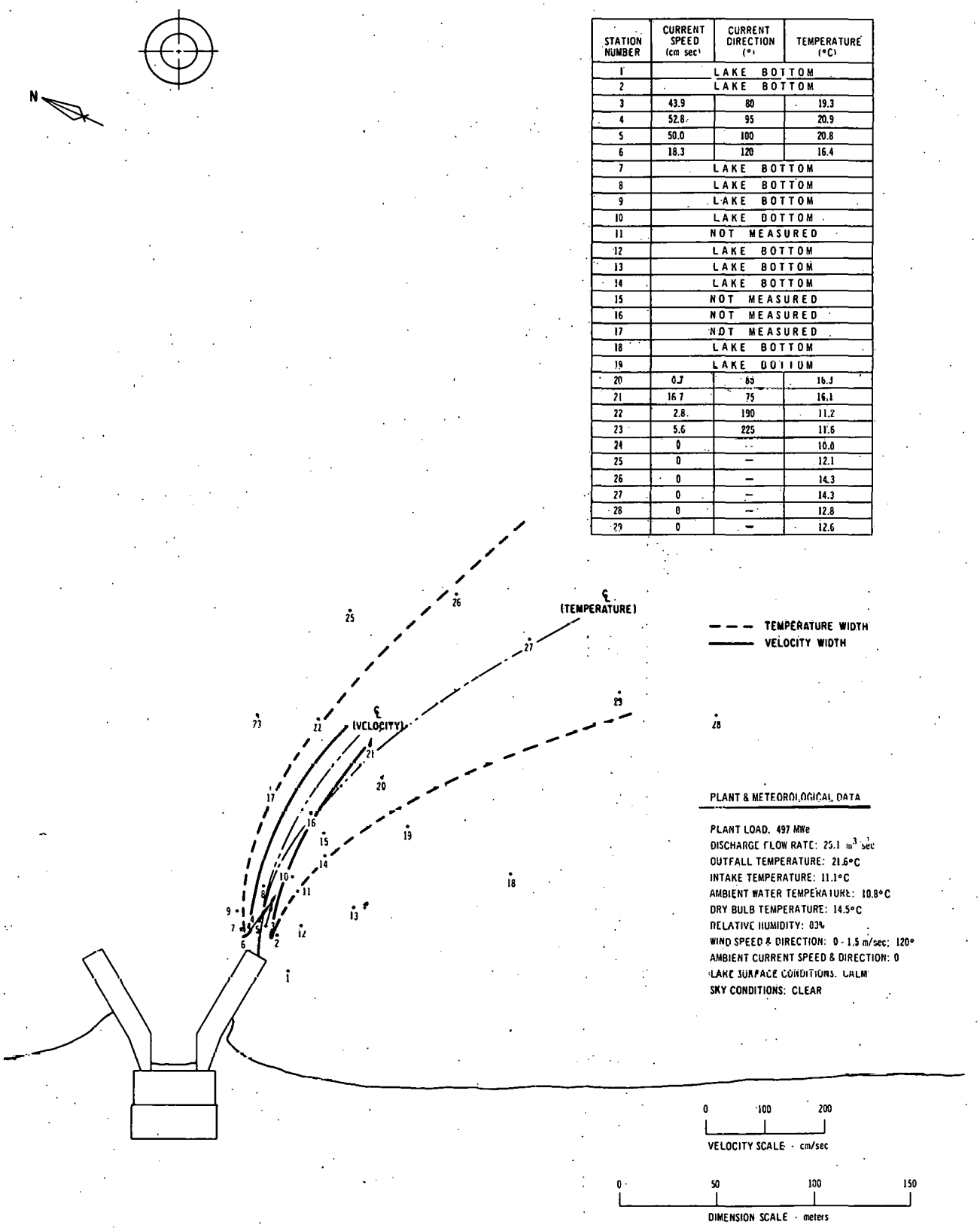

STATION NUMBER	CURRENT SPEED (cm sec⁻¹)	CURRENT DIRECTION (°)	TEMPERATURE (°C)
1	LAKE BOTTOM		
2	LAKE BOTTOM		
3	43.9	80	19.3
4	52.8	95	20.9
5	50.0	100	20.8
6	18.3	120	16.4
7	LAKE BOTTOM		
8	LAKE BOTTOM		
9	LAKE BOTTOM		
10	LAKE BOTTOM		
11	NOT MEASURED		
12	LAKE BOTTOM		
13	LAKE BOTTOM		
14	LAKE BOTTOM		
15	NOT MEASURED		
16	NOT MEASURED		
17	NOT MEASURED		
18	LAKE BOTTOM		
19	LAKE BOTTOM		
20	0.7	85	16.3
21	16.7	75	16.1
22	2.8	190	11.2
23	5.6	225	11.6
24	0	—	10.0
25	0	—	12.1
26	0	—	14.3
27	0	—	14.3
28	0	—	12.8
29	0	—	12.6

Fig. 19. Jet-regime Study for 3.0-m Depth at Point Beach Power Plant (Unit 1): May 23, 1972, 0945-1700 Hours. ANL Neg. No. 190-890.

STATION NUMBER	CURRENT SPEED (cm/sec)	CURRENT DIRECTION (°)	TEMPERATURE (°C)
1	19.5	180	17.0
2	62.3	110	19.0
3	67.8	95	20.2
4	51.1	80	18.5
5	17.8	65	16.7
6	5.6	60	16.5
7	30.0	80	16.7
8	44.5	95	18.8
9	51.1	110	19.2
10	23.4	125	17.0
11	8.9	135	17.0
12	6.7	75	15.3
13	26.1	115	16.3
14	30.0	120	16.5
15	24.4	140	16.0
16	13.9	170	15.5
17	11.1	145	15.7

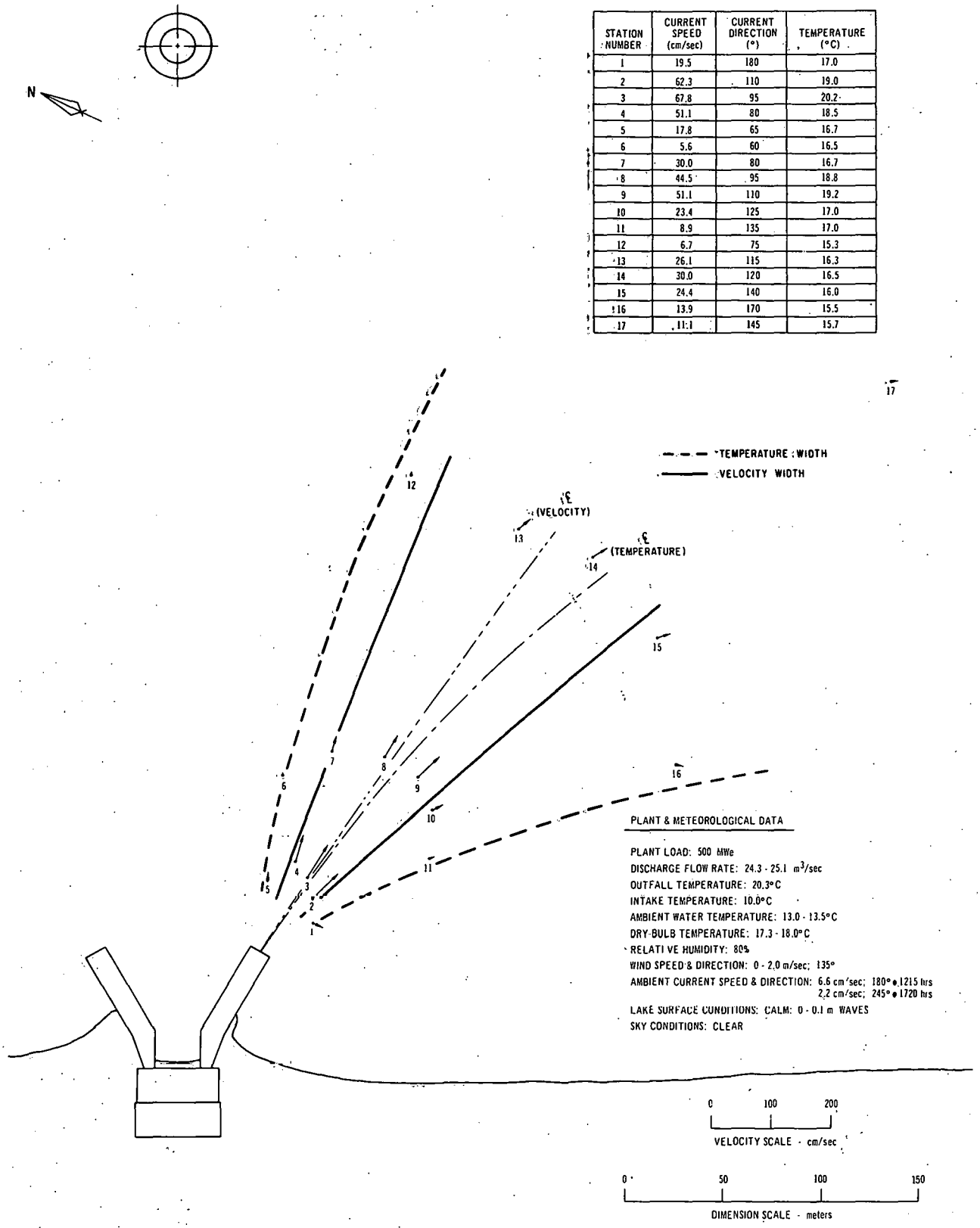

Fig. 20. Jet-regime Study for 0.5-m Depth at Point Beach Power Plant (Unit 1): July 13, 1972, 1308-1706 Hours. ANL Neg. No. 190-762 Rev. 2.

STATION NUMBER	CURRENT SPEED (cm/sec)	CURRENT DIRECTION (°)	TEMPERATURE (°C)
1	12.2	115	16.7
2	62.3	110	19.0
3	60.0	95	20.0
4	37.3	80	18.0
5	14.5	130	16.7
6	2.2	325	16.0
7	20.6	90	15.5
8	42.3	95	18.3
9	40.0	110	18.3
10	19.5	115	16.3
11	5.0	160	16.2
12	2.2	115	14.0
13	16.7	120	15.0
14	22.2	120	15.0
15	16.7	145	14.7
16	3.9	195	14.0
17	10.6	145	13.7

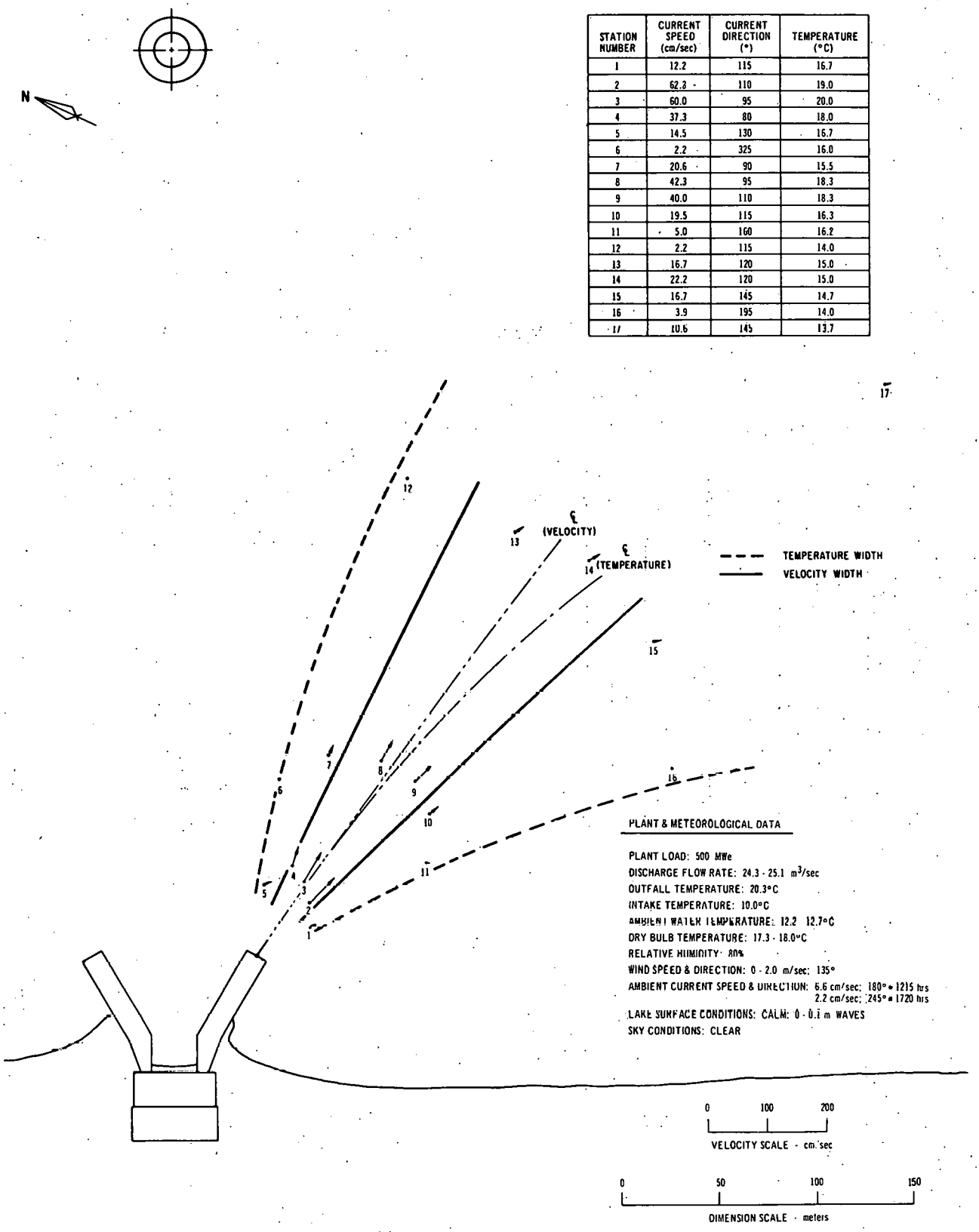

Fig. 21. Jet-regime Study for 1.0-m Depth at Point Beach Power Plant (Unit 1): July 13, 1972, 1308-1706 Hours. ANL Neg. No. 190-900 Rev. 1.

STATION NUMBER	CURRENT SPEED (cm/sec)	CURRENT DIRECTION (°)	TEMPERATURE (°C)
1	12.2	45	16.0
2	32.2	110	17.0
3	67.8	95	18.5
4	40.0	90	18.5
5	14.5	180	16.0
6	0	—	15.5
7	16.7	125	15.2
8	36.7	95	17.7
9	37.3	110	18.3
10	11.1	115	16.0
11	3.9	250	15.7
12	6.7	145	12.5
13	11.1	125	14.5
14	13.3	130	14.0
15	9.5	150	13.5
16	0	—	12.7
17	6.7	150	12.5

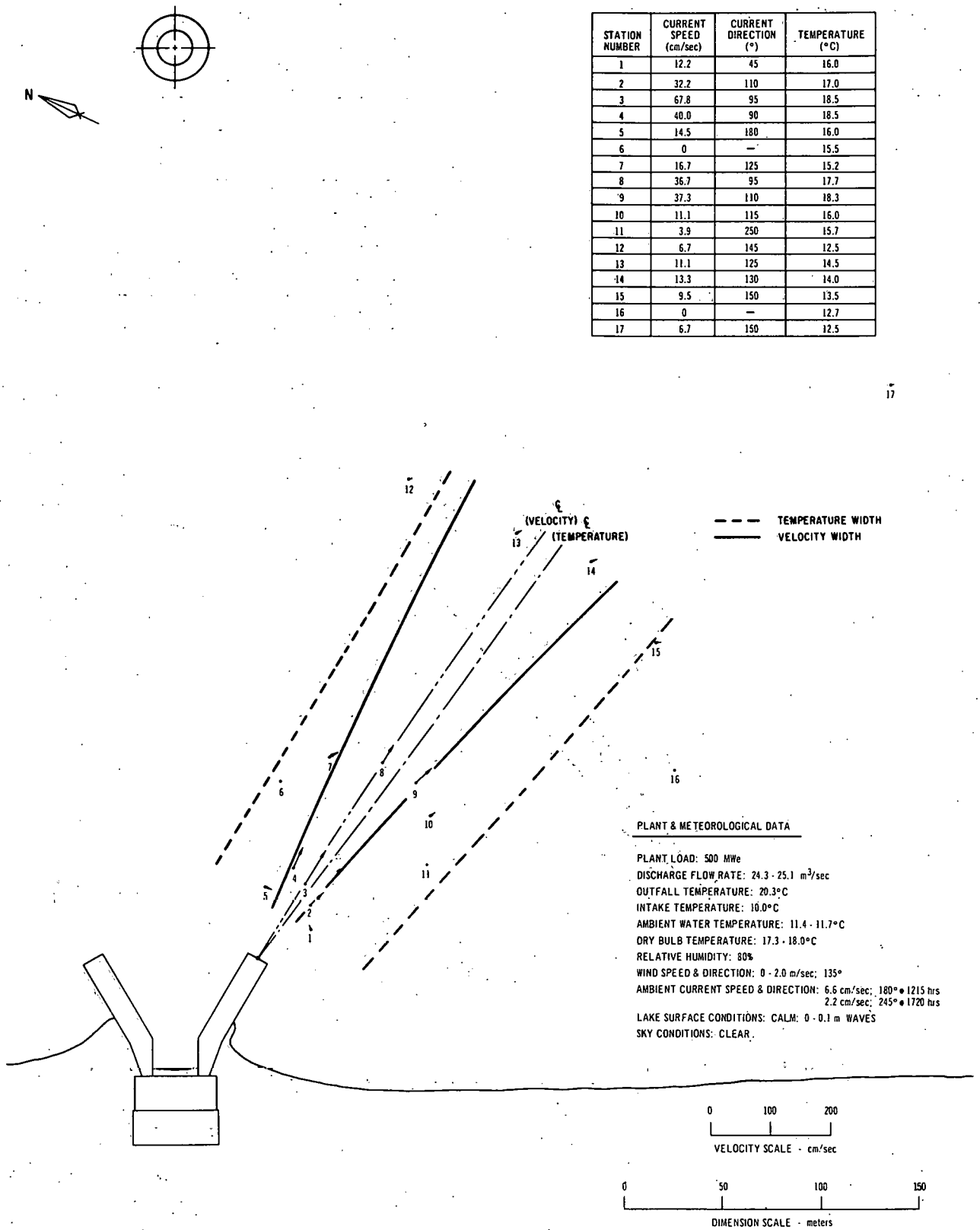

Fig. 22. Jet-regime Study for 1.5-m Depth at Point Beach Power Plant (Unit 1): July 13, 1972, 1308–1706 Hours. ANL Neg. No. 190–903 Rev. 1.

STATION NUMBER	CURRENT SPEED (cm/sec)	CURRENT DIRECTION (°)	TEMPERATURE (°C)
1	16.7	25	14.5
2	40.0	110	18.5
3	77.8	95	19.5
4	30.0	100	17.5
5	LAKE BOTTOM		
6	11.1	185	14.3
7	13.9	170	13.5
8	33.4	95	17.7
9	28.9	125	16.5
10	6.7	40	15.0
11	LAKE BOTTOM		
12	5.6	180	11.5
13	8.3	135	14.0
14	11.1	150	13.3
15	1.1	170	12.3
16	5.6	320	11.7
17	1.1	180	11.5

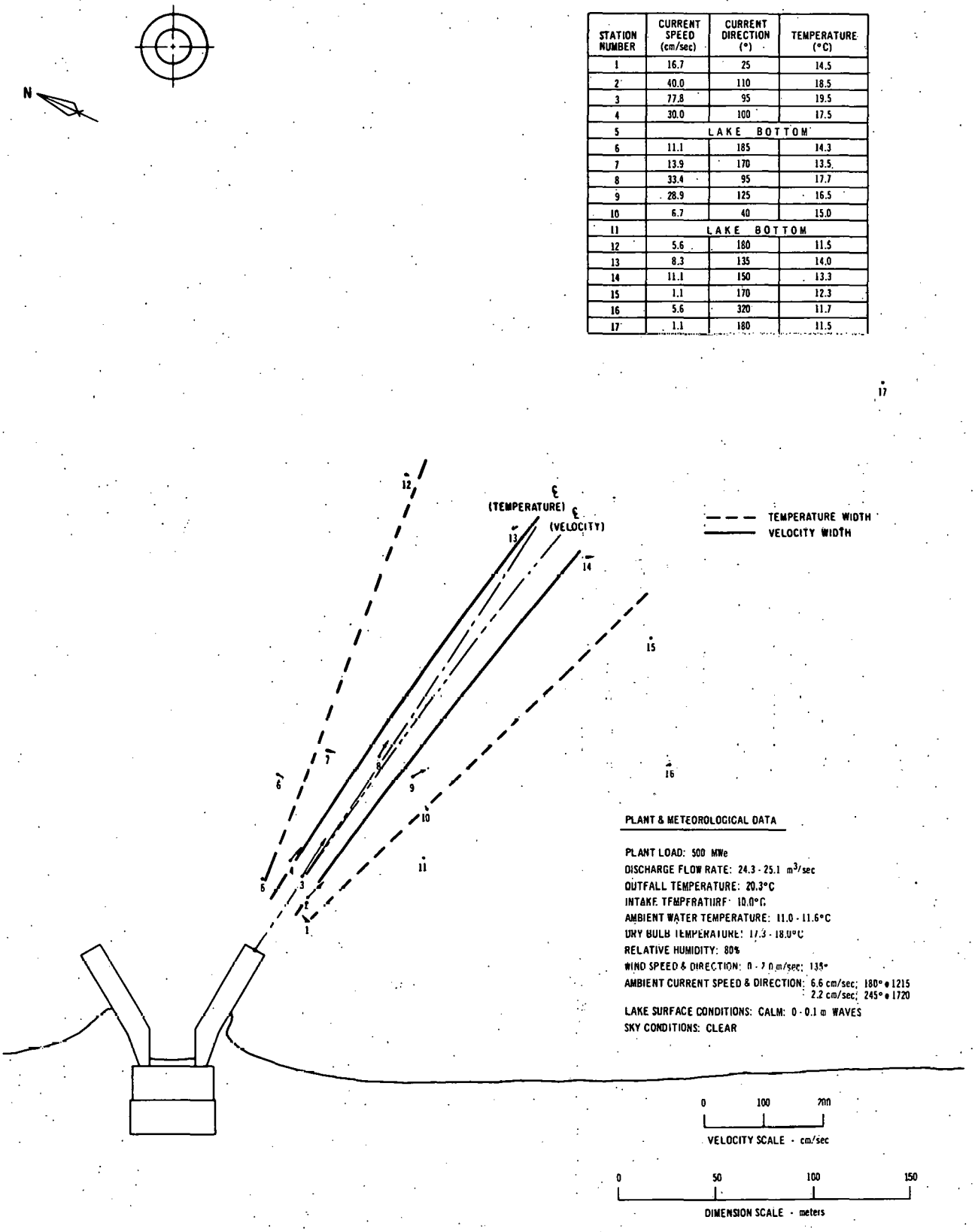

Fig. 23. Jet-regime Study for 2.0-m Depth at Point Beach Power Plant (Unit 1): July 13, 1972, 1308–1706 Hours. ANL Neg. No. 190-905 Rev. 1.

STATION NUMBER	CURRENT SPEED (cm/sec)	CURRENT DIRECTION (°)	TEMPERATURE (°C)
1	20.0	15	12.7
2	23.4	70	15.0
3	51.1	95	19.0
4	LAKE BOTTOM		
5	LAKE BOTTOM		
6	12.2	180	12.0
7	13.9	195	12.0
8	31.7	95	17.7
9	13.9	150	15.5
10	10.0	30	11.7
11	LAKE BOTTOM		
12	3.9	180	11.3
13	3.9	175	12.5
14	5.6	190	12.0
15	1.1	230	11.3
16	5.6	330	11.0
17	0	—	10.7

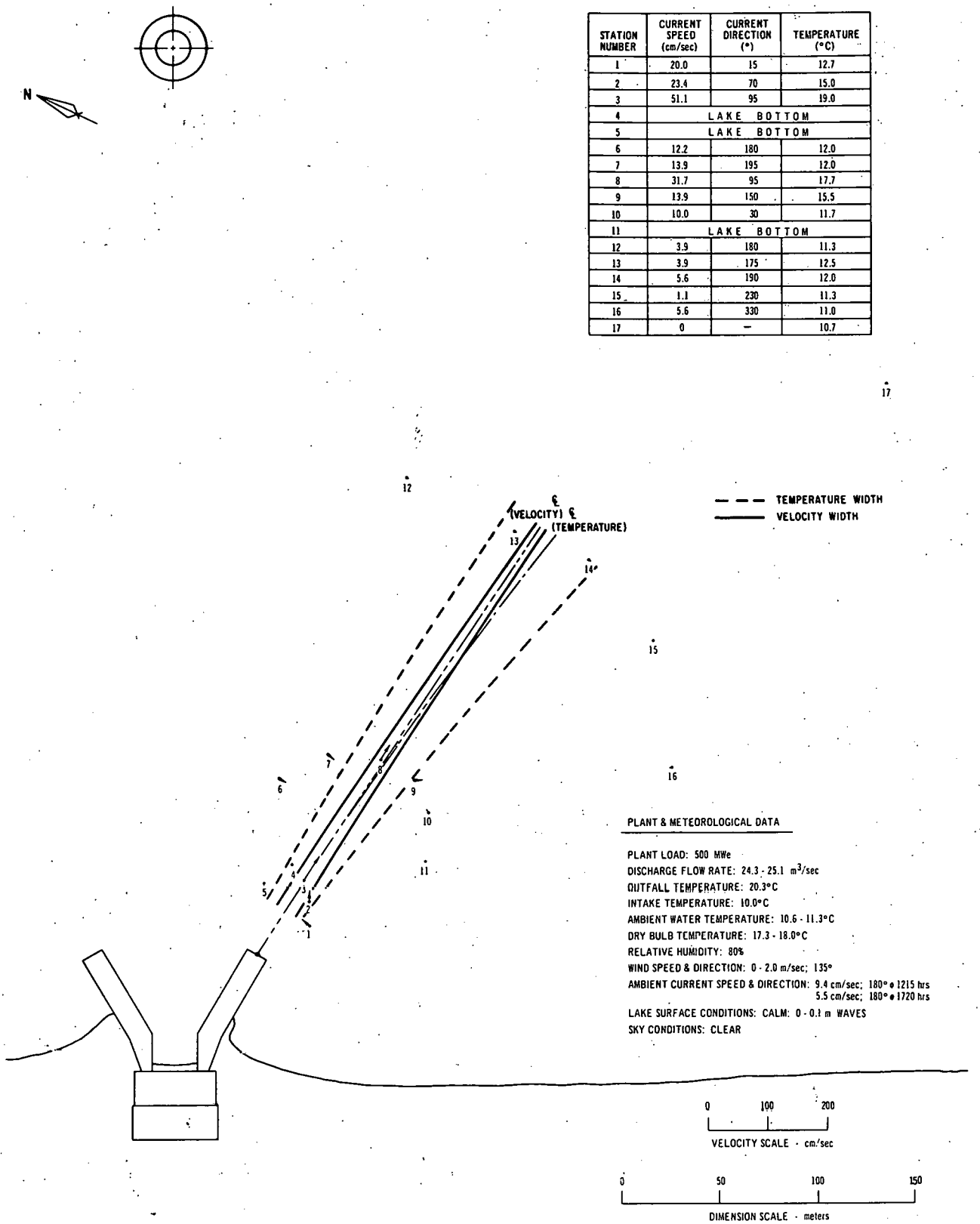

Fig. 24. Jet-regime Study for 2.5-m Depth at Point Beach Power Plant (Unit 1): July 13, 1972, 1308-1706 Hours. ANL Neg. No. 190-896 Rev. 1.

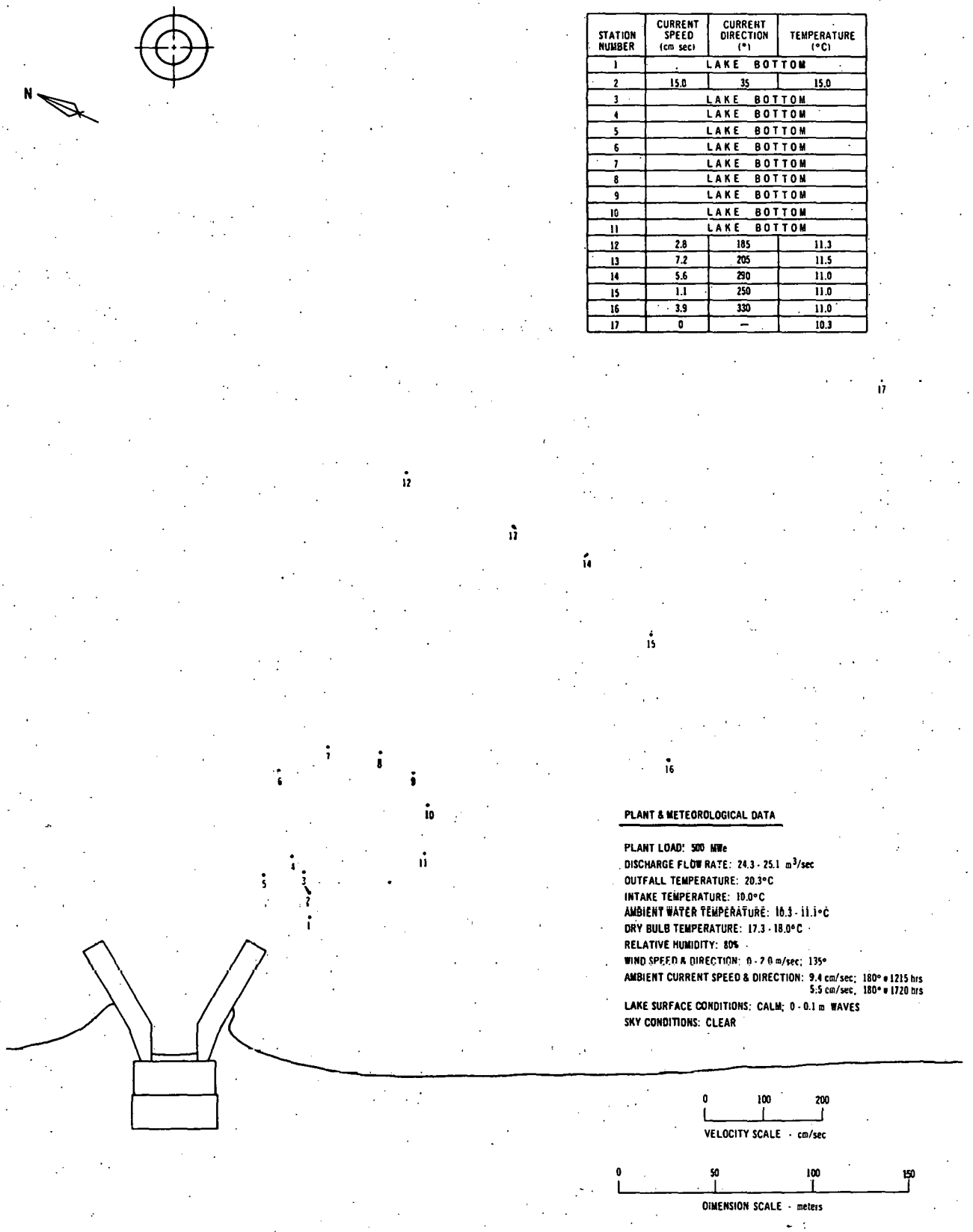

STATION NUMBER	CURRENT SPEED (cm sec)	CURRENT DIRECTION (°)	TEMPERATURE (°C)
1	LAKE BOTTOM		
2	15.0	35	15.0
3	LAKE BOTTOM		
4	LAKE BOTTOM		
5	LAKE BOTTOM		
6	LAKE BOTTOM		
7	LAKE BOTTOM		
8	LAKE BOTTOM		
9	LAKE BOTTOM		
10	LAKE BOTTOM		
11	LAKE BOTTOM		
12	2.8	185	11.3
13	7.2	205	11.5
14	5.6	290	11.0
15	1.1	250	11.0
16	3.9	330	11.0
17	0	—	10.3

Fig. 25. Jet-regime Study for 3.0-m Depth at Point Beach Power Plant (Unit 1): July 13, 1972, 1308-1706 Hours. ANL Neg. No. 190-875 Rev. 1.

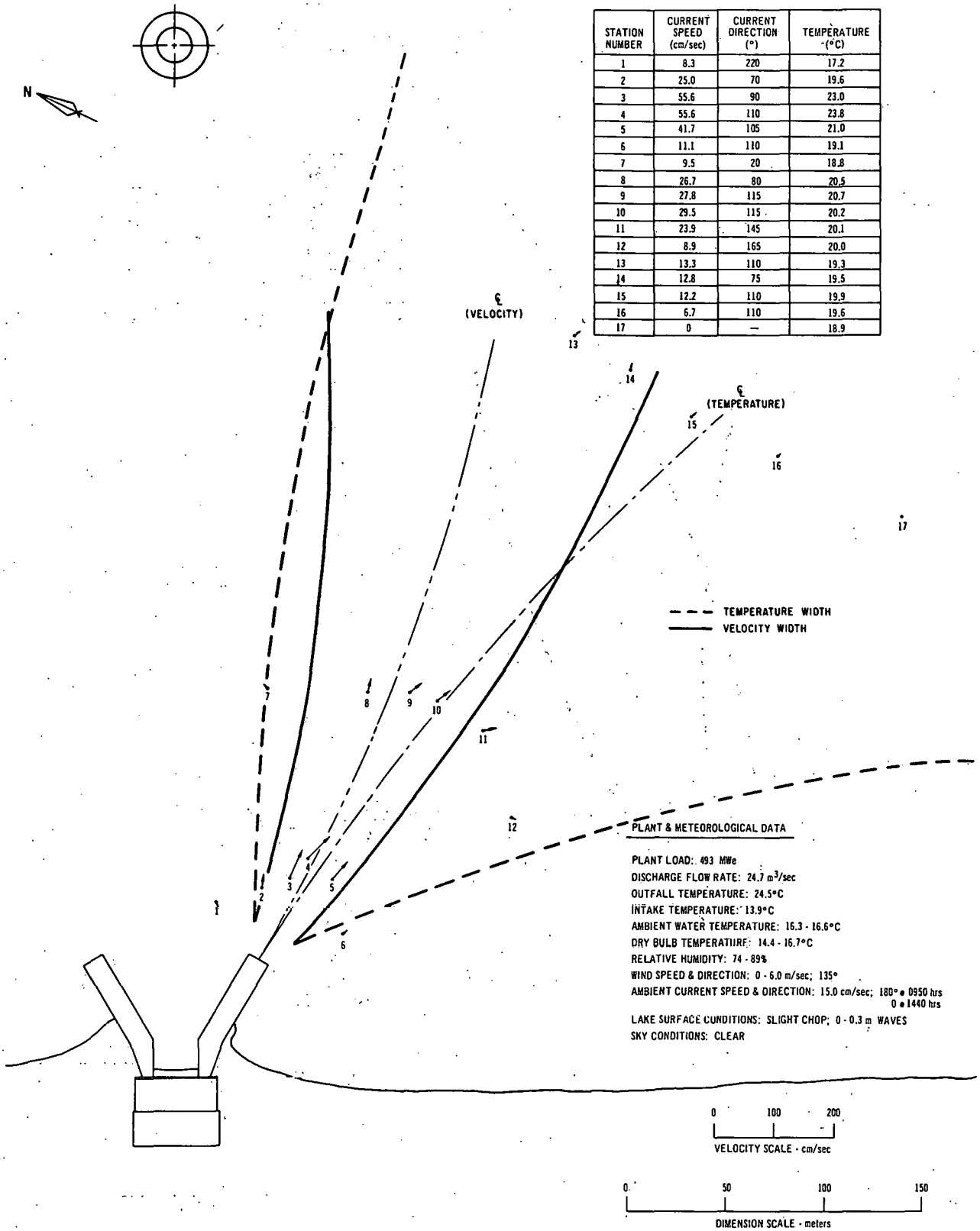

STATION NUMBER	CURRENT SPEED (cm/sec)	CURRENT DIRECTION (°)	TEMPERATURE (°C)
1	8.3	220	17.2
2	25.0	70	19.6
3	55.6	90	23.0
4	55.6	110	23.8
5	41.7	105	21.0
6	11.1	110	19.1
7	9.5	20	18.8
8	26.7	80	20.5
9	27.8	115	20.7
10	29.5	115	20.2
11	23.9	145	20.1
12	8.9	165	20.0
13	13.3	110	19.3
14	12.8	75	19.5
15	12.2	110	19.9
16	6.7	110	19.6
17	0	—	18.9

Fig. 26. Jet-regime Study for 0.5-m Depth at Point Beach Power Plant (Unit 1): September 9, 1972, 1045-1420 Hours. ANL Neg. No. 190-763 Rev. 1.

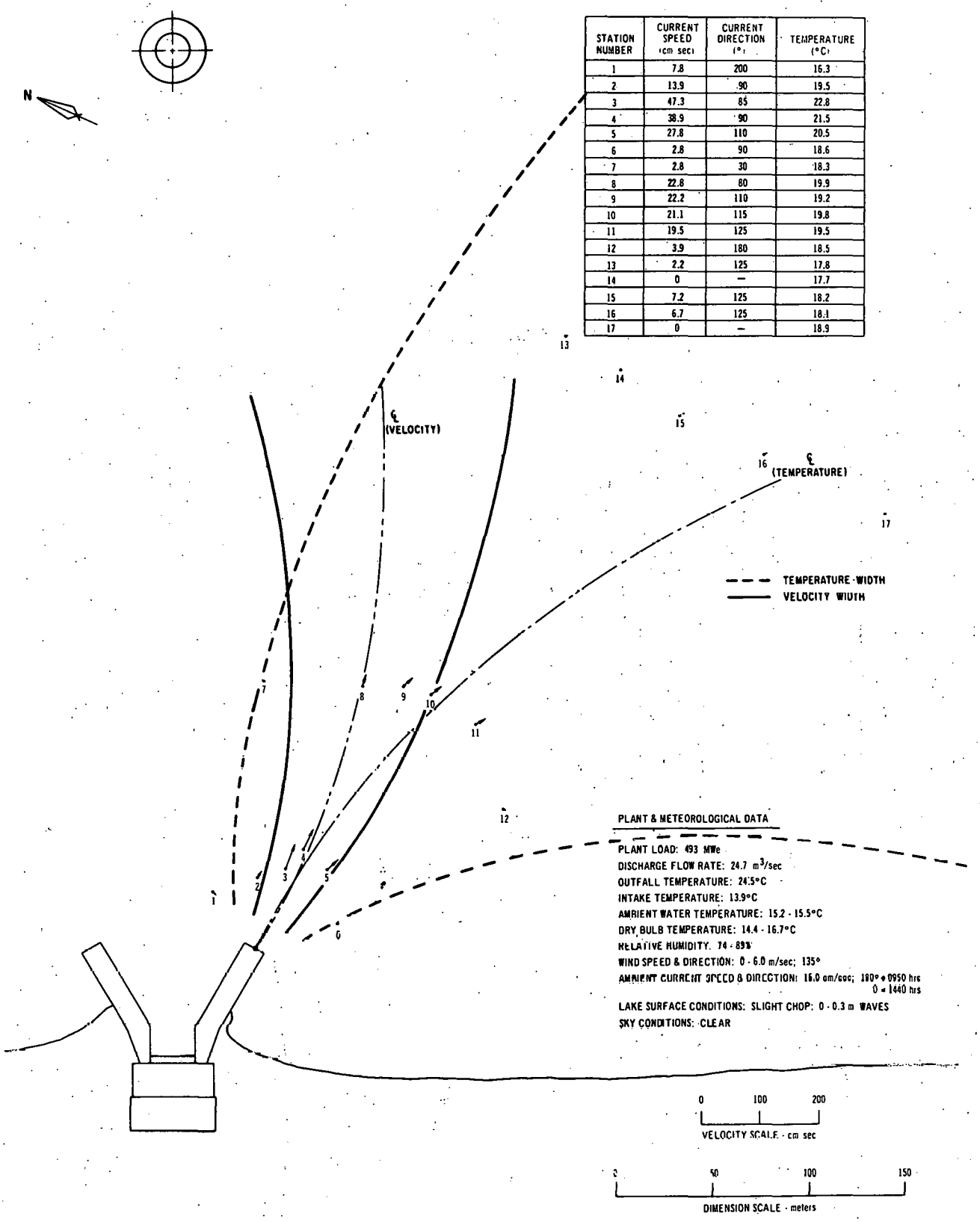

Fig. 27. Jet-regime Study for 1.0-m Depth at Point Beach Power Plant (Unit 1): September 9, 1972, 1045–1420 Hours. ANL Neg. No. 190-904.

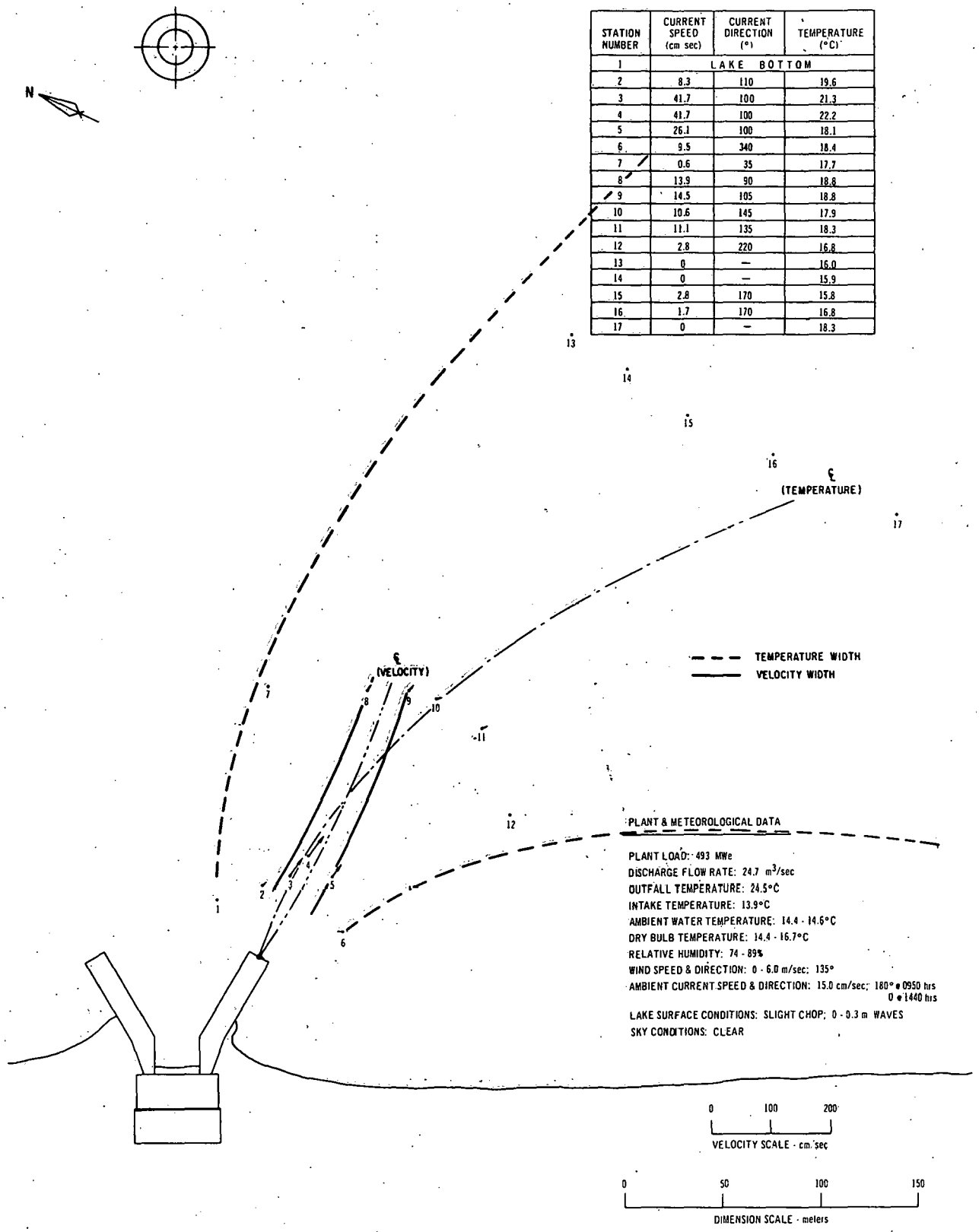

Fig. 28. Jet-regime Study for 1.5-m Depth at Point Beach Power Plant (Unit 1): September 9, 1972, 1045-1420 Hours. ANL Neg. No. 190-897.

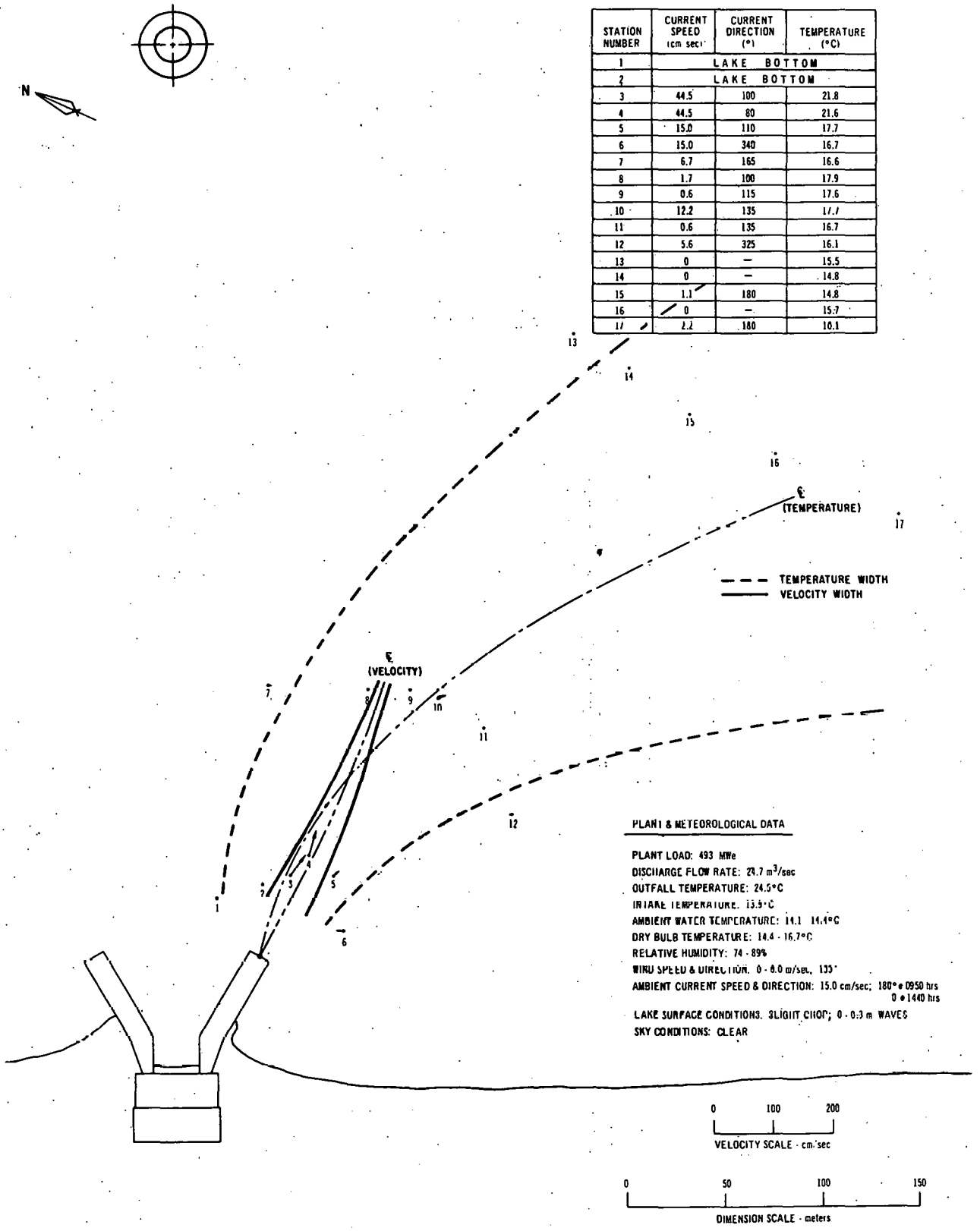

Fig. 29. Jet-regime Study for 2.0-m Depth at Point Beach Power Plant (Unit 1): September 9, 1972, 1045-1420 Hours. ANL Neg. No. 190-902.

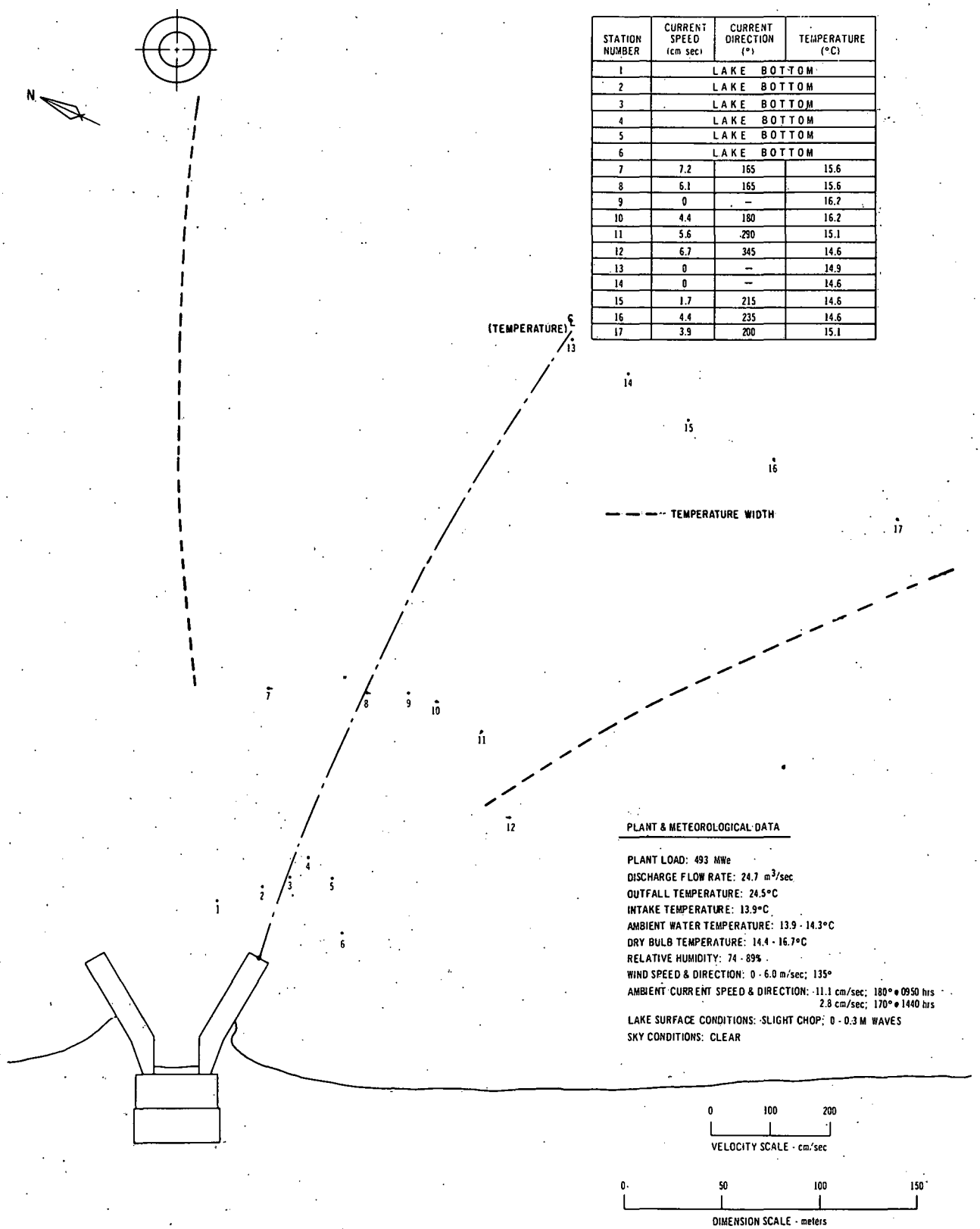

STATION NUMBER	CURRENT SPEED (cm sec)	CURRENT DIRECTION (°)	TEMPERATURE (°C)
1	LAKE BOTTOM		
2	LAKE BOTTOM		
3	LAKE BOTTOM		
4	LAKE BOTTOM		
5	LAKE BOTTOM		
6	LAKE BOTTOM		
7	7.2	165	15.6
8	6.1	165	15.6
9	0	—	16.2
10	4.4	180	16.2
11	5.6	290	15.1
12	6.7	345	14.6
13	0	—	14.9
14	0	—	14.6
15	1.7	215	14.6
16	4.4	235	14.6
17	3.9	200	15.1

Fig. 30. Jet-regime Study for 2.5-m Depth at Point Beach Power Plant (Unit 1): September 9, 1972, 1045-1420 Hours. ANL Neg. No. 190-885.

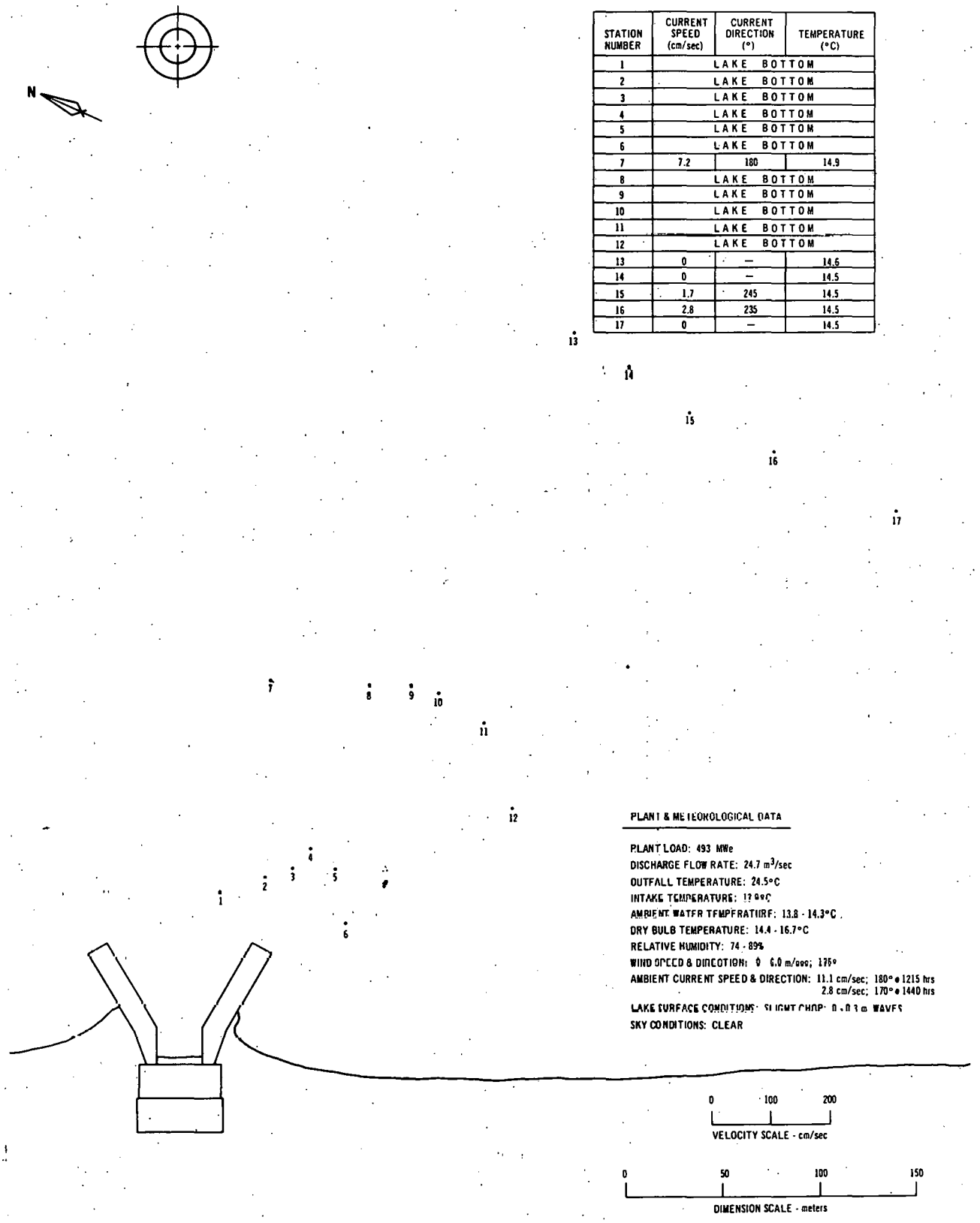

Fig. 31. Jet-regime Study for 3.0-m Depth at Point Beach Power Plant (Unit 1): September 9, 1972, 1045-1420 Hours. ANL Neg. No. 190-888.

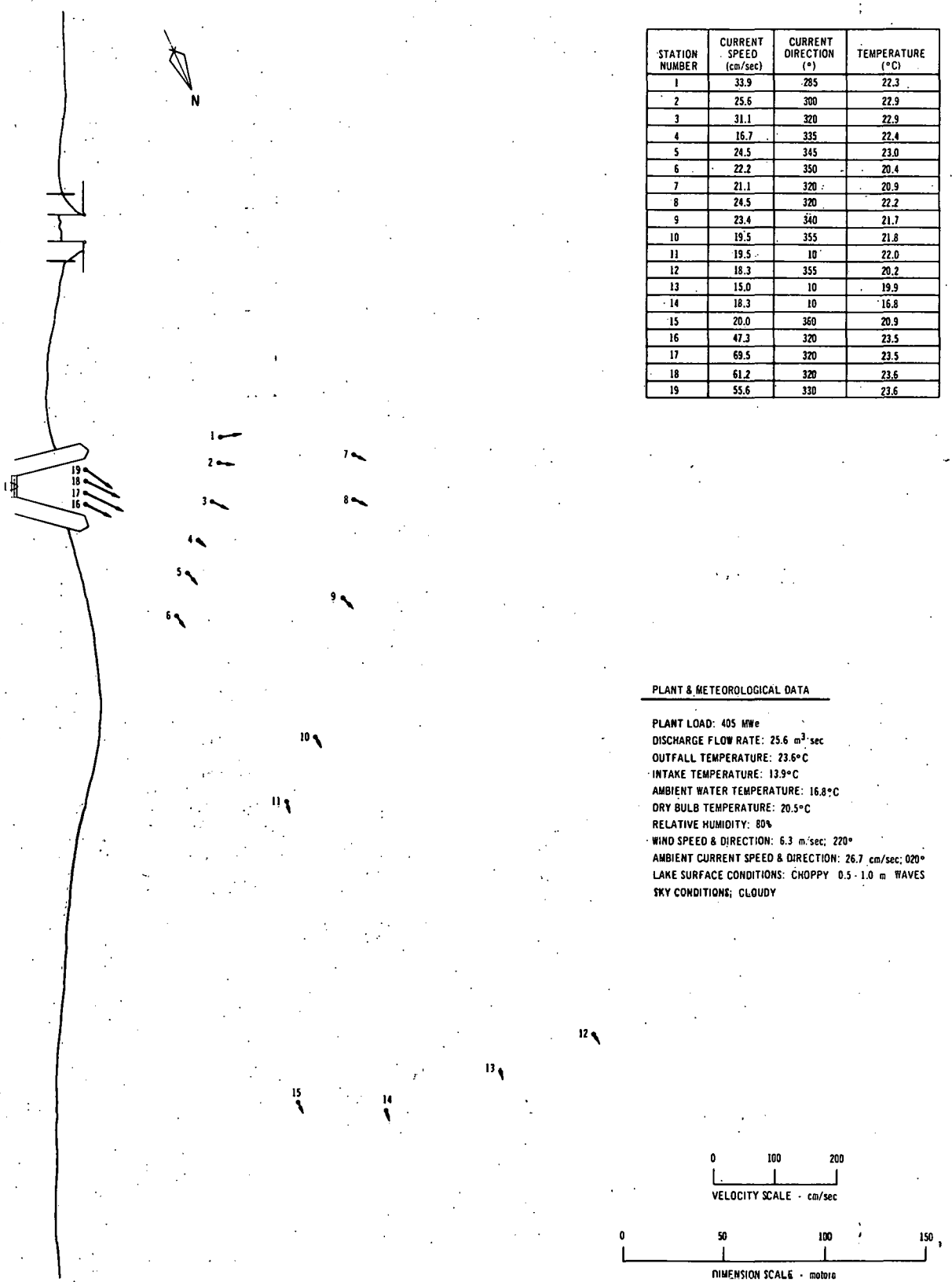

STATION NUMBER	CURRENT SPEED (cm/sec)	CURRENT DIRECTION (°)	TEMPERATURE (°C)
1	33.9	285	22.3
2	25.6	300	22.9
3	31.1	320	22.9
4	16.7	335	22.4
5	24.5	345	23.0
6	22.2	350	20.4
7	21.1	320	20.9
8	24.5	320	22.2
9	23.4	340	21.7
10	19.5	355	21.8
11	19.5	10	22.0
12	18.3	355	20.2
13	15.0	10	19.9
14	18.3	10	16.8
15	20.0	360	20.9
16	47.3	320	23.5
17	69.5	320	23.5
18	61.2	320	23.6
19	55.6	330	23.6

PLANT & METEOROLOGICAL DATA

PLANT LOAD: 405 MWe
DISCHARGE FLOW RATE: 25.6 m^3 sec
OUTFALL TEMPERATURE: 23.6°C
INTAKE TEMPERATURE: 13.9°C
AMBIENT WATER TEMPERATURE: 16.8°C
DRY BULB TEMPERATURE: 20.5°C
RELATIVE HUMIDITY: 80%
WIND SPEED & DIRECTION: 6.3 m/sec; 220°
AMBIENT CURRENT SPEED & DIRECTION: 26.7 cm/sec; 020°
LAKE SURFACE CONDITIONS: CHOPPY 0.5 - 1.0 m WAVES
SKY CONDITIONS; CLOUDY

Fig. 32. Jet-regime Study for 0.5-m Depth at Palisades Power Plant: June 14, 1972, 1000-1348 Hours: ANL Neg. No. 190-757 Rev. 1.

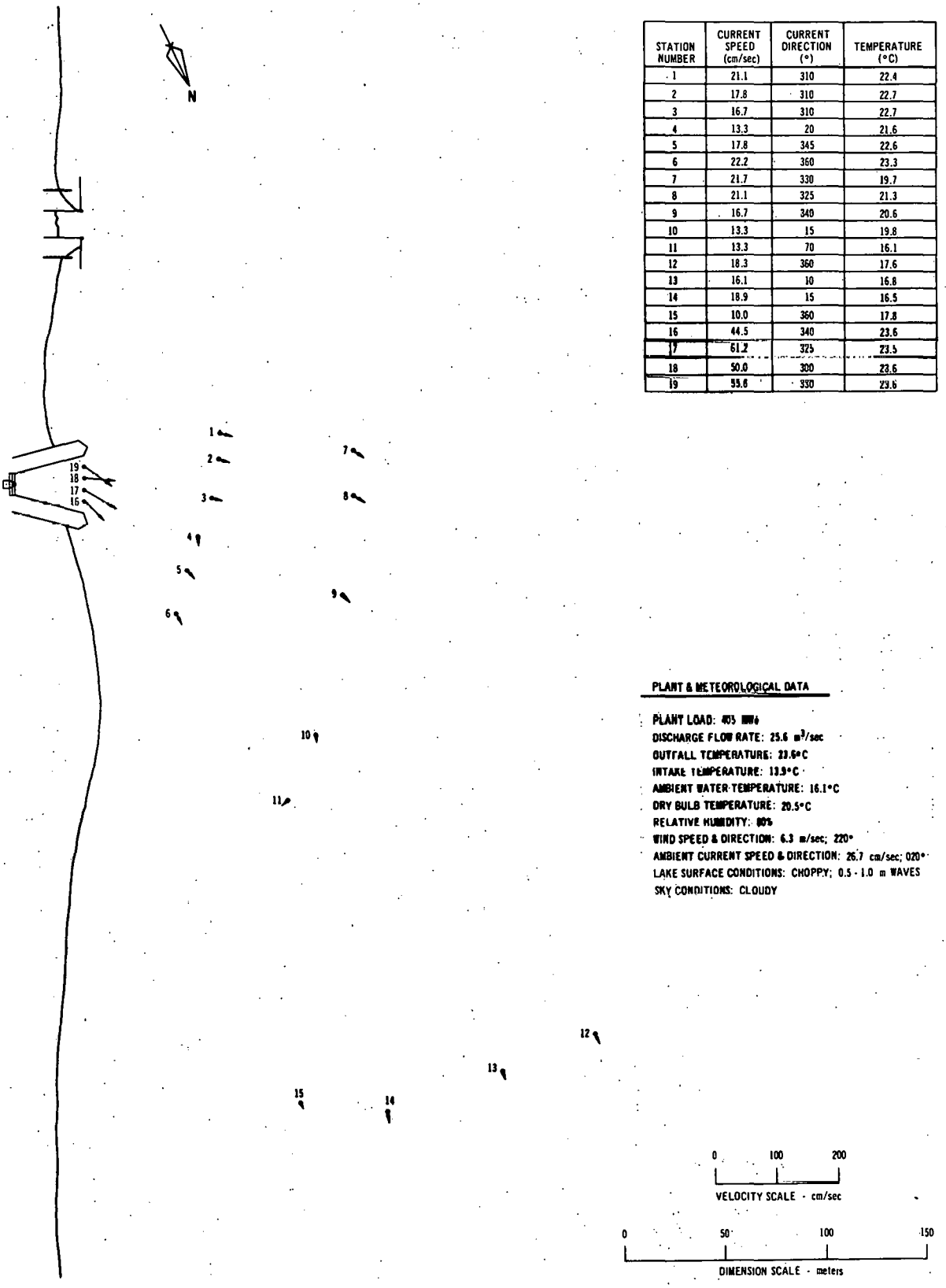

STATION NUMBER	CURRENT SPEED (cm/sec)	CURRENT DIRECTION (°)	TEMPERATURE (°C)
1	21.1	310	22.4
2	17.8	310	22.7
3	16.7	310	22.7
4	13.3	20	21.6
5	17.8	345	22.6
6	22.2	360	23.3
7	21.7	330	19.7
8	21.1	325	21.3
9	16.7	340	20.6
10	13.3	15	19.8
11	13.3	70	16.1
12	18.3	360	17.6
13	16.1	10	16.8
14	18.9	15	16.5
15	10.0	360	17.8
16	44.5	340	23.6
17	61.2	325	23.5
18	50.0	300	23.6
19	55.6	330	23.6

Fig. 33. Jet-regime Study for 1.0-m Depth at Palisades Power Plant: June 14, 1972, 1000-1348 Hours. ANL Neg. No. 190-872.

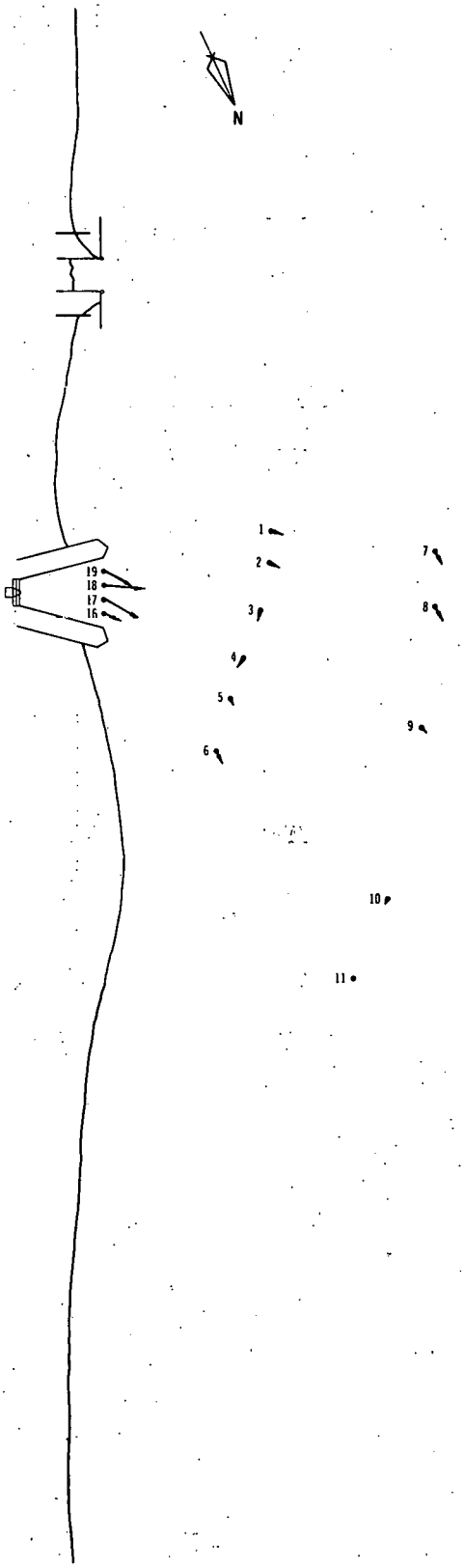

STATION NUMBER	CURRENT SPEED (cm sec)	CURRENT DIRECTION (°)	TEMPERATURE (°C)
1	18.3	315	21.7
2	16.7	325	21.8
3	14.5	35	22.2
4	15.6	55	21.3
5	11.1	360	22.6
6	20.6	360	23.3
7	22.2	355	18.3
8	22.2	355	19.1
9	11.7	345	17.3
10	9.5	45	16.0
11	LAKE BOTTOM		
12	16.7	15	16.2
13	14.5	360	16.5
14	18.9	20	16.3
15	1.1	20	16.4
16	25.0	320	23.5
17	55.6	325	23.5
18	55.6	300	23.6
19	44.5	325	23.6

PLANT & METEOROLOGICAL DATA

PLANT LOAD: 405 MWe
DISCHARGE FLOW RATE: 25.6 m^3/sec
OUTFALL TEMPERATURE: 23.6°C
INTAKE TEMPERATURE: 13.9°C
AMBIENT WATER TEMPERATURE: 16.0°C
DRY BULB TEMPERATURE: 20.5°C
RELATIVE HUMIDITY: 80%
WIND SPEED & DIRECTION: 6.3 m sec; 220°
AMBIENT CURRENT SPEED & DIRECTION: 26.7 cm/sec; 020°
LAKE SURFACE CONDITIONS: CHOPPY; 0.5 - 1.0 m WAVES
SKY CONDITIONS: CLOUDY

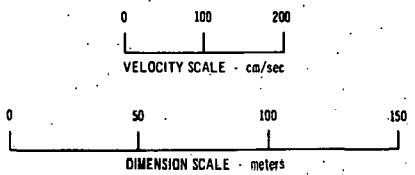

Fig. 34. Jet-regime Study for 1.5-m Depth at Palisades Power Plant: June 14, 1972, 1000-1340 Hours. ANL Neg. No. 100-879.

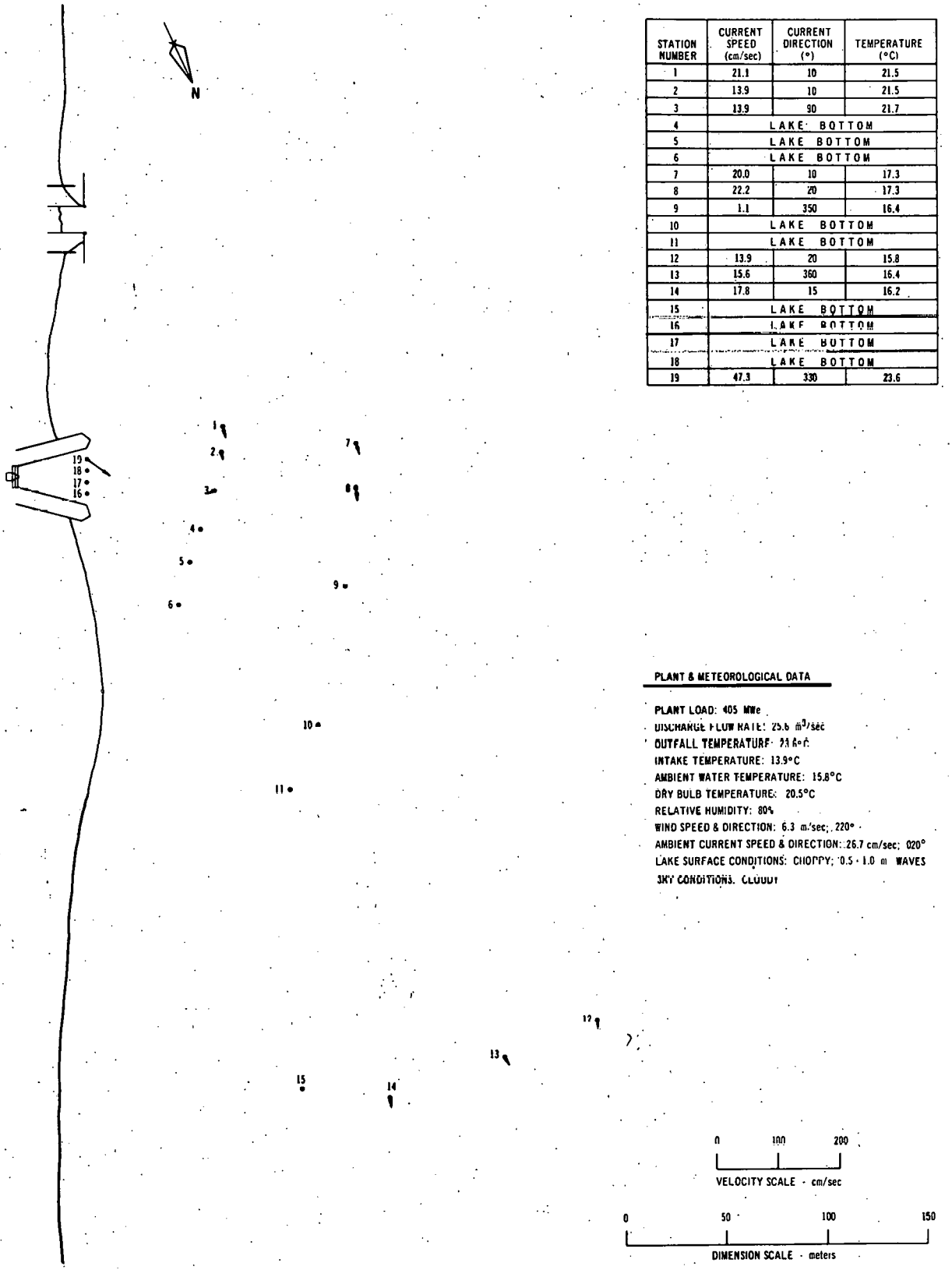

STATION NUMBER	CURRENT SPEED (cm/sec)	CURRENT DIRECTION (°)	TEMPERATURE (°C)
1	21.1	10	21.5
2	13.9	10	21.5
3	13.9	90	21.7
4	LAKE BOTTOM		
5	LAKE BOTTOM		
6	LAKE BOTTOM		
7	20.0	10	17.3
8	22.2	20	17.3
9	1.1	350	16.4
10	LAKE BOTTOM		
11	LAKE BOTTOM		
12	13.9	20	15.8
13	15.6	360	16.4
14	17.8	15	16.2
15	LAKE BOTTOM		
16	LAKE BOTTOM		
17	LAKE BOTTOM		
18	LAKE BOTTOM		
19	47.3	330	23.6

PLANT & METEOROLOGICAL DATA

PLANT LOAD: 405 MWe
DISCHARGE FLOW RATE: 25.6 m^3/sec
OUTFALL TEMPERATURE: 23.6°C
INTAKE TEMPERATURE: 13.9°C
AMBIENT WATER TEMPERATURE: 15.8°C
DRY BULB TEMPERATURE: 20.5°C
RELATIVE HUMIDITY: 80%
WIND SPEED & DIRECTION: 6.3 m/sec; 220°
AMBIENT CURRENT SPEED & DIRECTION: 26.7 cm/sec; 020°
LAKE SURFACE CONDITIONS: CHOPPY; 0.5 - 1.0 m WAVES
SKY CONDITIONS: CLOUDY

Fig. 35. Jet-regime Study for 2.0-m Depth at Palisades Power Plant: June 14, 1972, 1000–1348 Hours. ANL Neg. No. 190–877 Rev. 1.

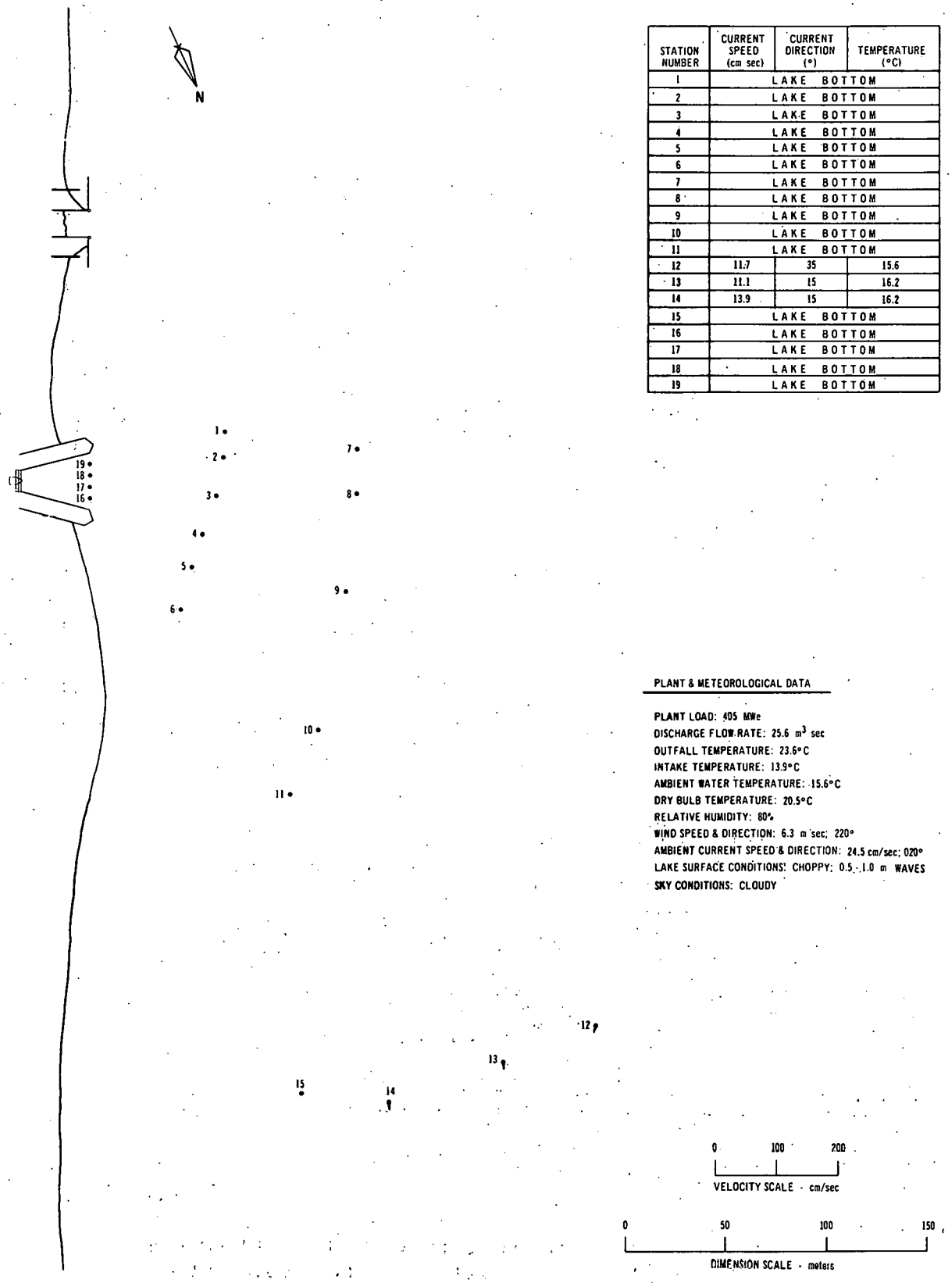

STATION NUMBER	CURRENT SPEED (cm sec)	CURRENT DIRECTION (°)	TEMPERATURE (°C)
1	LAKE BOTTOM		
2	LAKE BOTTOM		
3	LAKE BOTTOM		
4	LAKE BOTTOM		
5	LAKE BOTTOM		
6	LAKE BOTTOM		
7	LAKE BOTTOM		
8	LAKE BOTTOM		
9	LAKE BOTTOM		
10	LAKE BOTTOM		
11	LAKE BOTTOM		
12	11.7	35	15.6
13	11.1	15	16.2
14	13.9	15	16.2
15	LAKE BOTTOM		
16	LAKE BOTTOM		
17	LAKE BOTTOM		
18	LAKE BOTTOM		
19	LAKE BOTTOM		

PLANT & METEOROLOGICAL DATA

PLANT LOAD: 405 MWe
DISCHARGE FLOW RATE: 25.6 m^3 sec
OUTFALL TEMPERATURE: 23.6°C
INTAKE TEMPERATURE: 13.9°C
AMBIENT WATER TEMPERATURE: 15.6°C
DRY BULB TEMPERATURE: 20.5°C
RELATIVE HUMIDITY: 80%
WIND SPEED & DIRECTION: 6.3 m sec; 220°
AMBIENT CURRENT SPEED & DIRECTION: 24.5 cm/sec; 020°
LAKE SURFACE CONDITIONS: CHOPPY; 0.5 - 1.0 m WAVES
SKY CONDITIONS: CLOUDY

Fig. 36. Jet-regime Study for 2.5-m Depth at Palisades Power Plant: June 14, 1972, 1000-1348 Hours. ANL Neg. No. 190-887.

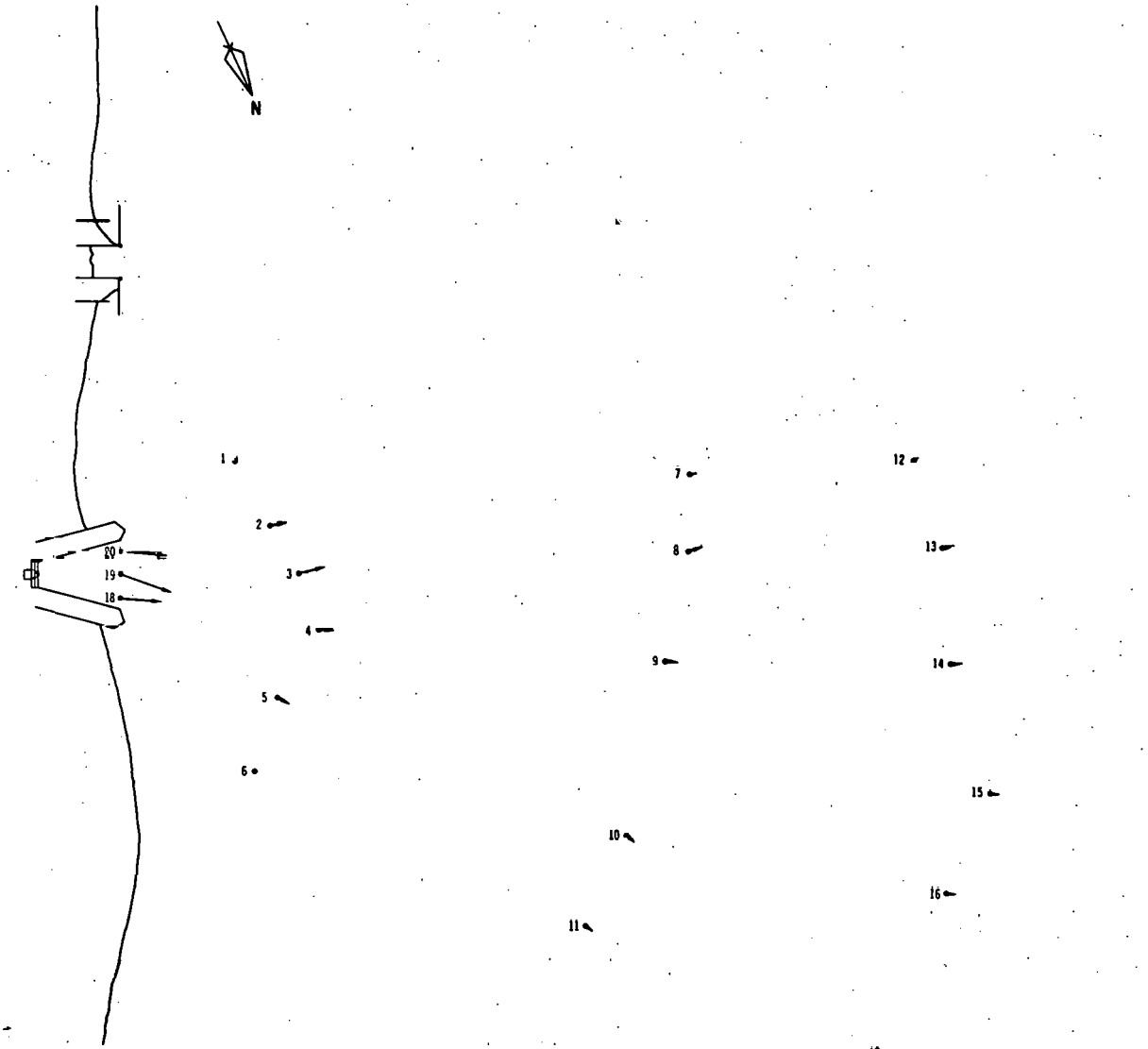

STATION NUMBER	CURRENT SPEED (cm/sec)	CURRENT DIRECTION (°)	TEMPERATURE (°C)
1	1.7	230	26.5
2	21.1	285	27.0
3	34.5	280	28.5
4	19.5	295	28.7
5	16.7	325	29.0
6	3.3	18	28.2
7	8.3	280	26.0
8	19.5	275	27.0
9	16.7	300	27.0
10	14.5	330	28.0
11	11.7	330	27.5
12	6.7	255	25.0
13	15.6	280	26.8
14	15.6	290	25.5
15	11.7	300	25.5
16	12.2	300	25.8
17	10.6	305	26.6
18	54.5	300	28.6
19	72.3	315	28.7
20	61.2	300	28.7

PLANT & METEOROLOGICAL DATA

PLANT LOAD: 420 MWe
DISCHARGE FLOW RATE: 25.6 m^3/sec
OUTFALL TEMPERATURE: 28.7°C
INTAKE TEMPERATURE: 20.0°C
AMBIENT WATER TEMPERATURE: 23.5 - 24.5°C
DRY BULB TEMPERATURE: 22.7 - 25.6°C
RELATIVE HUMIDITY: 86%
WIND SPEED & DIRECTION: 0 - 2.0 m/sec; 135°
AMBIENT CURRENT SPEED & DIRECTION: 8.6 cm/sec; 180°
LAKE SURFACE CONDITIONS: CALM
SKY CONDITIONS: CLOUDY

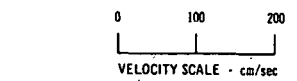

Fig. 37. Jet-regime Study for 0.5-m Depth at Palisades Power Plant: July 19, 1972, 0922-1414 Hours. ANL Neg. No. 190-758 Rev. 1.

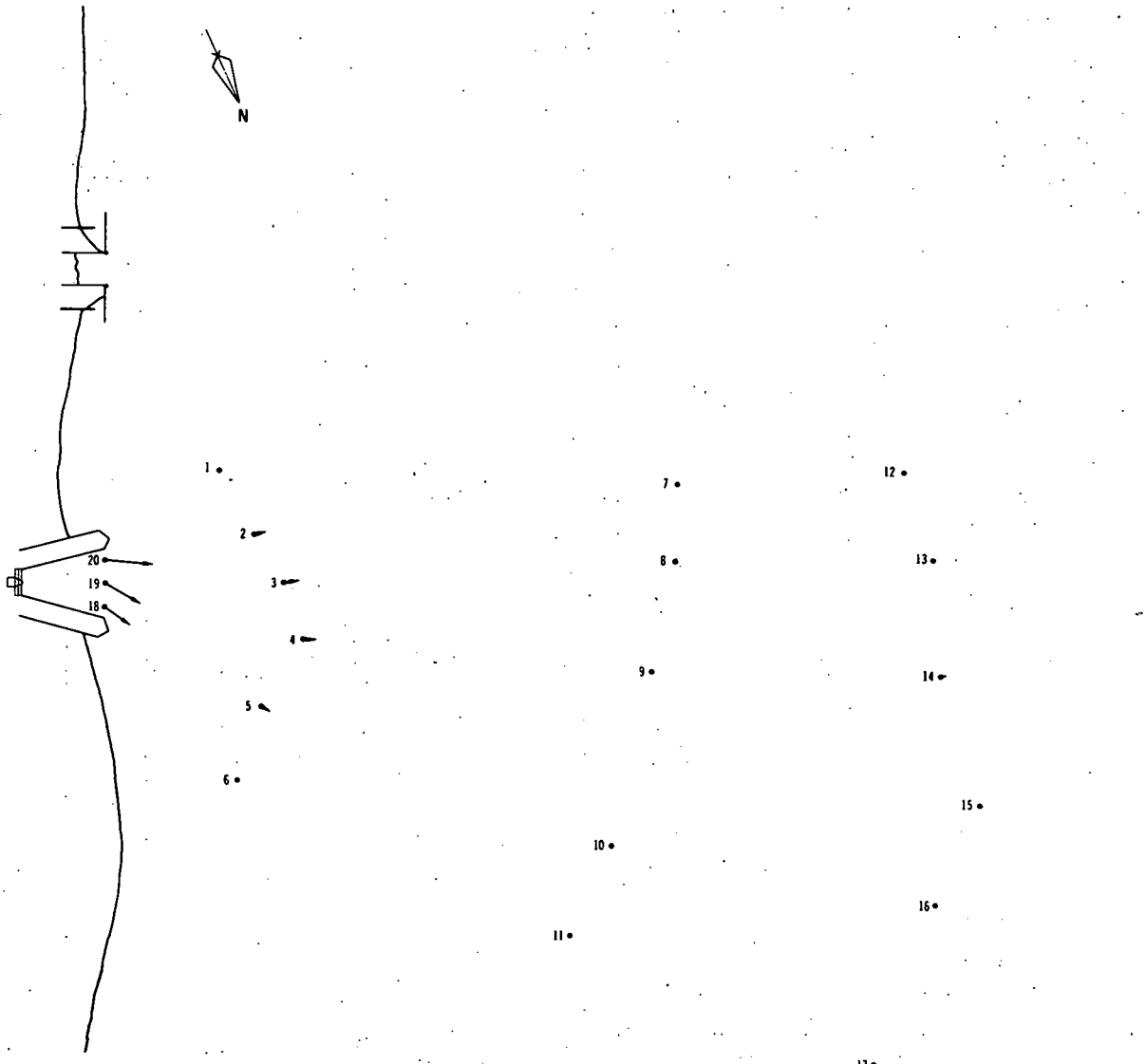

STATION NUMBER	CURRENT SPEED (cm/sec)	CURRENT DIRECTION (°)	TEMPERATURE (°C)
1	3.9	350	26.0
2	17.2	280	26.8
3	21.1	285	28.5
4	18.3	295	28.6
5	13.3	325	28.5
6	0	-	24.5
7	4.4	250	22.6
8	6.1	225	24.0
9	1.7	290	23.0
10	0	-	24.3
11	0	-	23.8
12	1.7	260	23.0
13	1.7	185	23.5
14	7.2	260	23.6
15	3.3	295	24.1
16	2.8	300	24.5
17	3.9	300	24.7
18	43.4	330	28.7
19	54.5	325	28.7
20	66.7	300	28.7

PLANT & METEOROLOGICAL DATA

PLANT LOAD: 420 MWe
DISCHARGE FLOW RATE: 25.6 m^3/sec
OUTFALL TEMPERATURE: 28.7°C
INTAKE TEMPERATURE: 20.0°C
AMBIENT WATER TEMPERATURE: 22.1 - 23.7°C
DRY BULB TEMPERATURE: 22.7 - 25.6°C
RELATIVE HUMIDITY: 86%
WIND SPEED & DIRECTION: 0 - 2.0 m/sec; 135°
AMBIENT CURRENT SPEED & DIRECTION: 8.6 cm/sec; 180°
LAKE SURFACE CONDITIONS: CALM
SKY CONDITIONS: CLOUDY

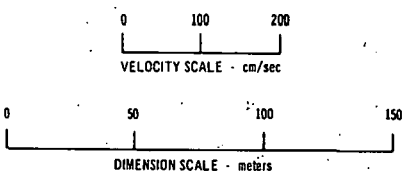

Fig. 38. Jet-regime Study for 1.0-m Depth at Palisades Power Plant: July 19, 1972, 0922-1414 Hours. ANL Neg. No. 190-873.

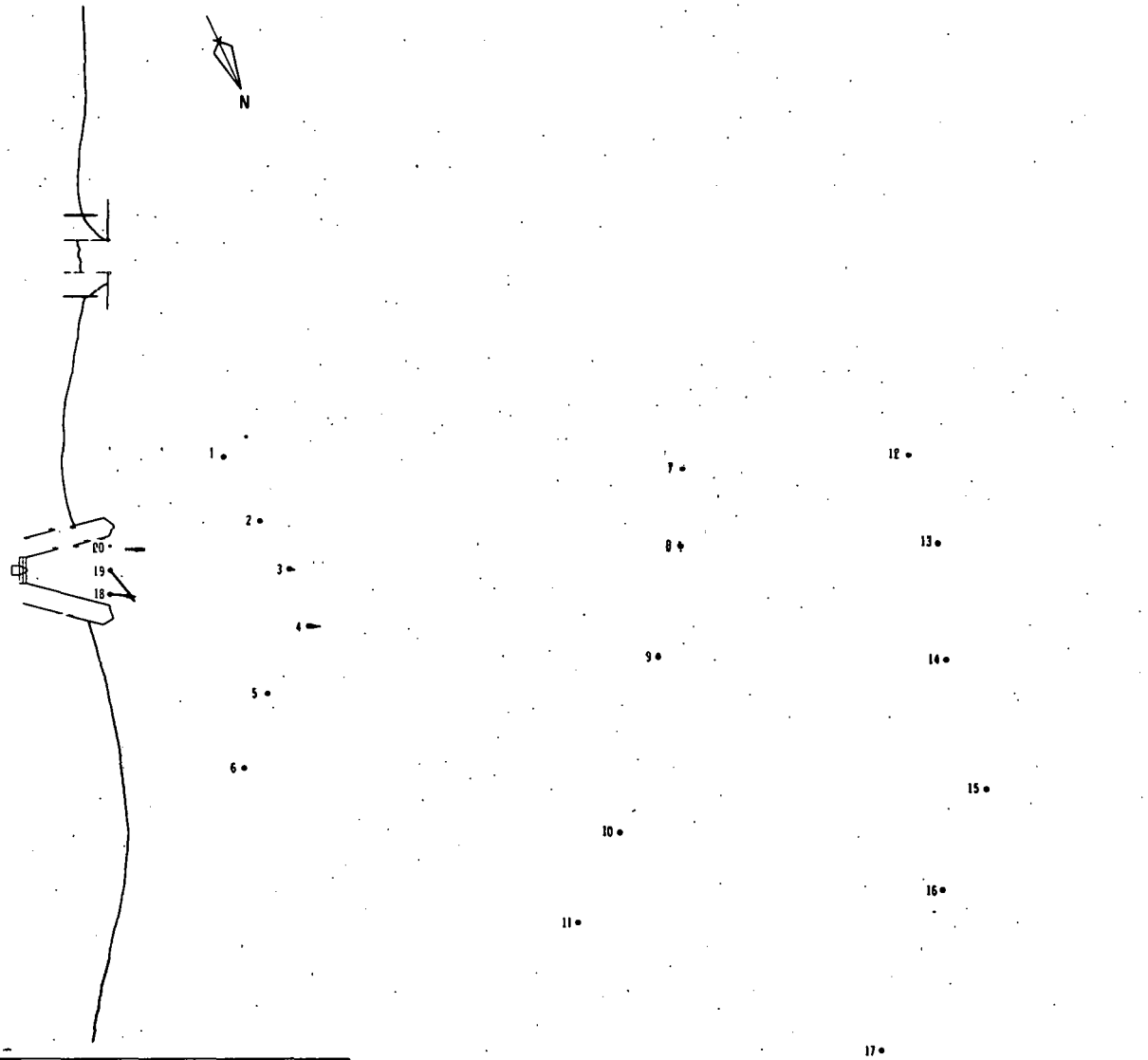

STATION NUMBER	CURRENT SPEED (cm/sec)	CURRENT DIRECTION (°)	TEMPERATURE (°C)
1	LAKE BOTTOM		
2	LAKE BOTTOM		
3	6.7	300	27.5
4	15.6	295	28.4
5	4.4	320	27.6
6	LAKE BOTTOM		
7	3.3	200	22.5
8	5.6	190	22.2
9	1.1	235	22.3
10	0.6	280	22.0
11	0	--	22.0
12	0	--	22.0
13	3.3	250	21.5
14	2.2	270	21.6
15	1.7	270	22.4
16	1.1	240	22.0
17	2.8	270	23.1
18	34.5	300	28.7
19	57.0	345	28.7
20	48.8	300	28.7

PLANT & METEOROLOGICAL DATA

PLANT LOAD: 420 MWe
DISCHARGE FLOW RATE: 25.6 m^3/sec
OUTFALL TEMPERATURE: 28.7°C
INTAKE TEMPERATURE: 20.0°C
AMBIENT WATER TEMPERATURE: 21.3 - 22.5°C
DRY BULB TEMPERATURE: 22.7 - 25.6°C
RELATIVE HUMIDITY: 86%
WIND SPEED & DIRECTION: 0 - 2.0 m/sec; 135°
AMBIENT CURRENT SPEED & DIRECTION: 8.6 cm/sec; 180°
LAKE SURFACE CONDITIONS: CALM
SKY CONDITIONS: CLOUDY

0 100 200
VELOCITY SCALE - cm/sec

0 50 100 150
DIMENSION SCALE - meters

Fig. 39. Jet-regime Study for 1.5-m Depth at Palisades Power Plant: July 19, 1972, 0922-1414 Hours. ANL Neg. No. 190-884.

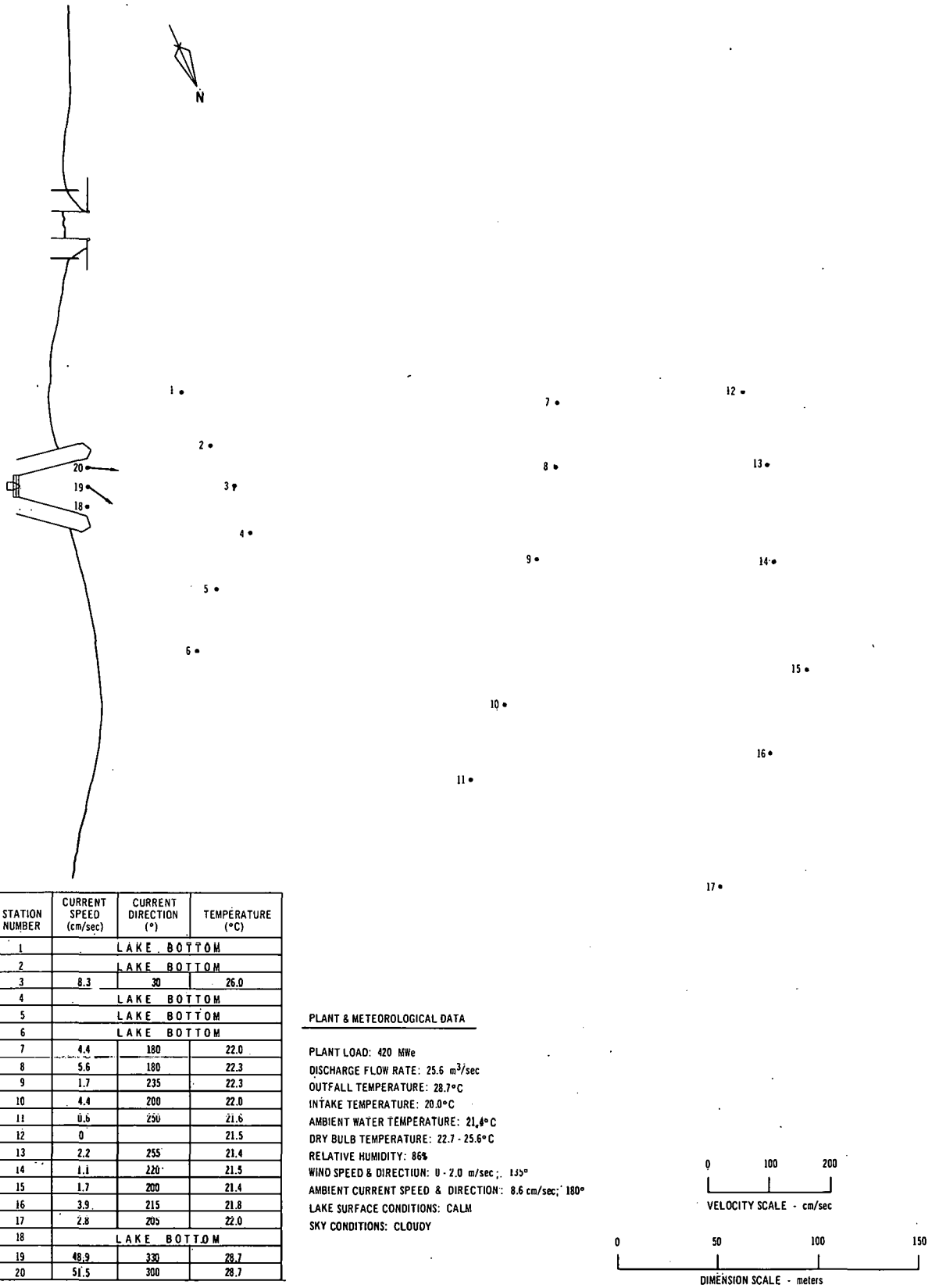

STATION NUMBER	CURRENT SPEED (cm/sec)	CURRENT DIRECTION (°)	TEMPERATURE (°C)
1	LAKE BOTTOM		
2	LAKE BOTTOM		
3	8.3	30	26.0
4	LAKE BOTTOM		
5	LAKE BOTTOM		
6	LAKE BOTTOM		
7	4.4	180	22.0
8	5.6	180	22.3
9	1.7	235	22.3
10	4.4	200	22.0
11	0.6	250	21.6
12	0		21.5
13	2.2	255	21.4
14	1.1	220	21.5
15	1.7	200	21.4
16	3.9	215	21.8
17	2.8	205	22.0
18	LAKE BOTTOM		
19	48.9	330	28.7
20	51.5	300	28.7

Fig. 40. Jet-regime Study for 2.0-m Depth at Palisades Power Plant: July 19, 1972, 0922-1414 Hours. ANL Neg. No. 190-871 Rev. 1.

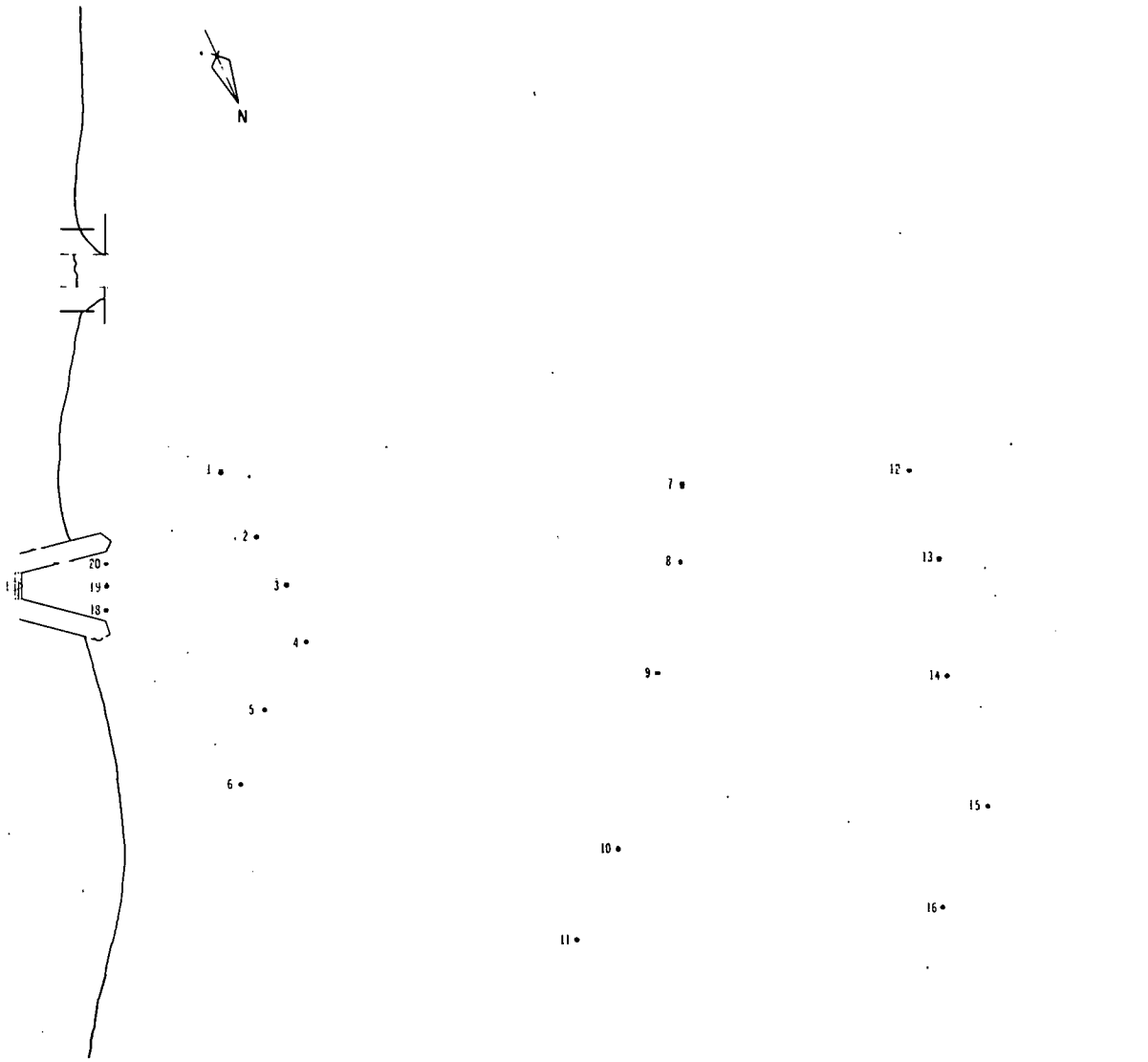

STATION NUMBER	CURRENT SPEED (cm sec)	CURRENT DIRECTION (°)	TEMPERATURE (°C)
1	LAKE BOTTOM		
2	LAKE BOTTOM		
3	LAKE BOTTOM		
4	LAKE BOTTOM		
5	LAKE BOTTOM		
6	LAKE BOTTOM		
7	LAKE BOTTOM		
8	2.2	140	21.8
9	3.3	170	22.1
10	5.6	185	22.0
11	0.6	220	21.5
12	0.6	205	21.0
13	1.1	255	21.0
14	1.1	185	21.4
15	1.1	190	21.0
16	2.8	210	21.8
17	3.3	205	21.5
18	LAKE BOTTOM		
19	LAKE BOTTOM		
20	LAKE BOTTOM		

PLANT & METEOROLOGICAL DATA

PLANT LOAD: 420 MWe
DISCHARGE FLOW RATE. 25.6 m^3 sec
OUTFALL TEMPERATURE: 28.7°C
INTAKE TEMPERATURE. 20.0°C
AMBIENT WATER TEMPERATURE 21.0°C
DRY BULB TEMPERATURE 22.7 - 25.6°C
RELATIVE HUMIDITY: 86%
WIND SPEED & DIRECTION. 0 - 2.0 m sec; - 135°
AMBIENT CURRENT SPEED & DIRECTION. 5.0 cm/sec; 200°
LAKE SURFACE CONDITIONS: CALM
SKY CONDITIONS: CLOUDY

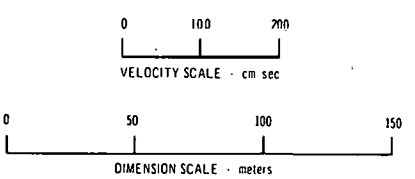

Fig. 41. Jet-regime Study for 2.5-m Depth at Palisades Power Plant: July 19, 1972, 0922-1414 Hours. ANL Neg. No. 190-881.

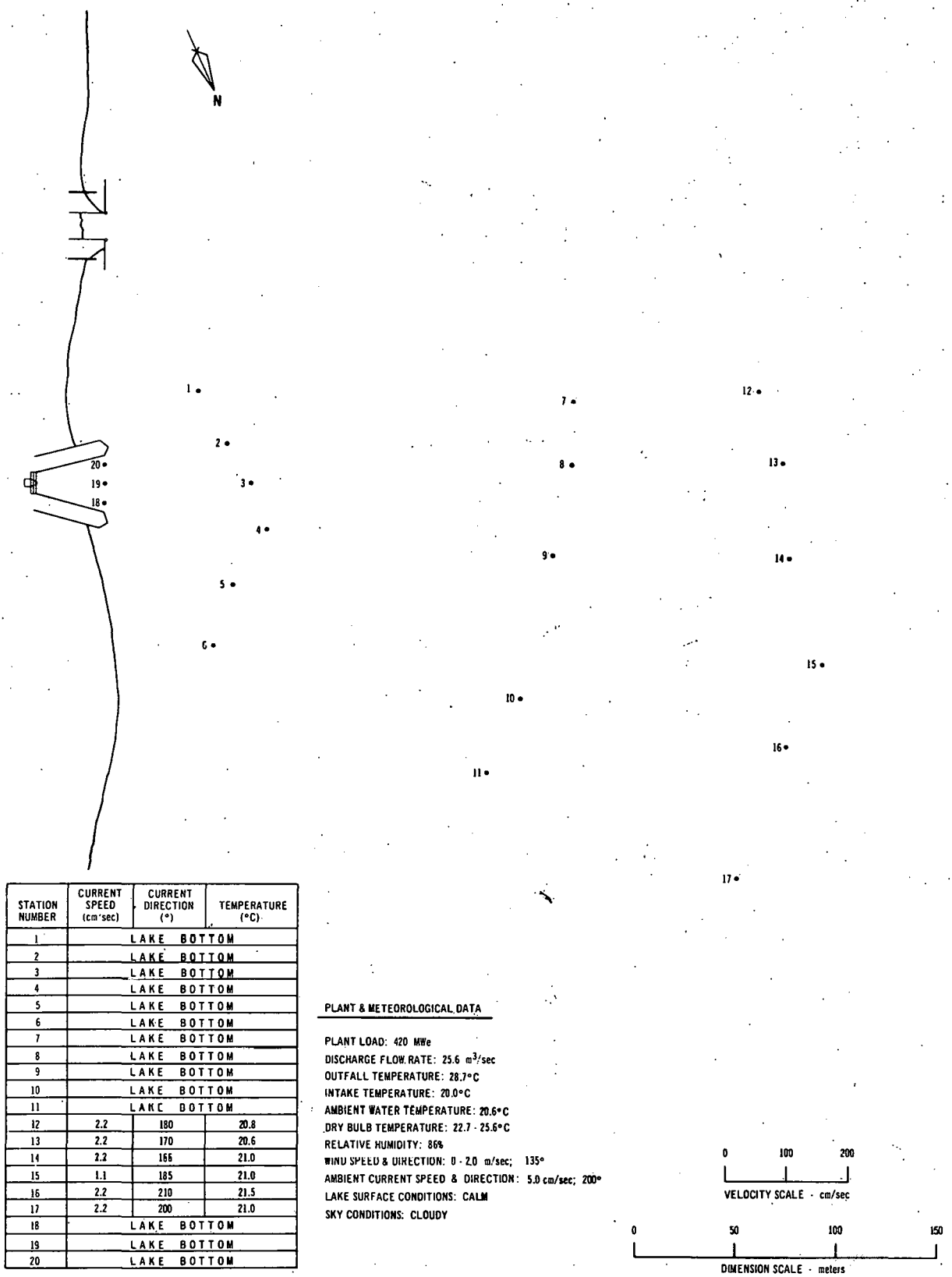

STATION NUMBER	CURRENT SPEED (cm/sec)	CURRENT DIRECTION (°)	TEMPERATURE (°C)
1	LAKE BOTTOM		
2	LAKE BOTTOM		
3	LAKE BOTTOM		
4	LAKE BOTTOM		
5	LAKE BOTTOM		
6	LAKE BOTTOM		
7	LAKE BOTTOM		
8	LAKE BOTTOM		
9	LAKE BOTTOM		
10	LAKE BOTTOM		
11	LAKE BOTTOM		
12	2.2	180	20.8
13	2.2	170	20.6
14	2.2	166	21.0
15	1.1	185	21.0
16	2.2	210	21.5
17	2.2	200	21.0
18	LAKE BOTTOM		
19	LAKE BOTTOM		
20	LAKE BOTTOM		

PLANT & METEOROLOGICAL DATA

PLANT LOAD: 420 MWe
DISCHARGE FLOW RATE: 25.6 m^3/sec
OUTFALL TEMPERATURE: 28.7°C
INTAKE TEMPERATURE: 20.0°C
AMBIENT WATER TEMPERATURE: 20.6°C
DRY BULB TEMPERATURE: 22.7 - 25.6°C
RELATIVE HUMIDITY: 86%
WIND SPEED & DIRECTION: 0 - 2.0 m/sec; 135°
AMBIENT CURRENT SPEED & DIRECTION: 5.0 cm/sec; 200°
LAKE SURFACE CONDITIONS: CALM
SKY CONDITIONS: CLOUDY

Fig. 42. Jet-regime Study for 3.0-m Depth at Palisades Power Plant: July 19, 1972, 0922-1414 Hours. ANL Neg. No. 190-882 Rev. 1.

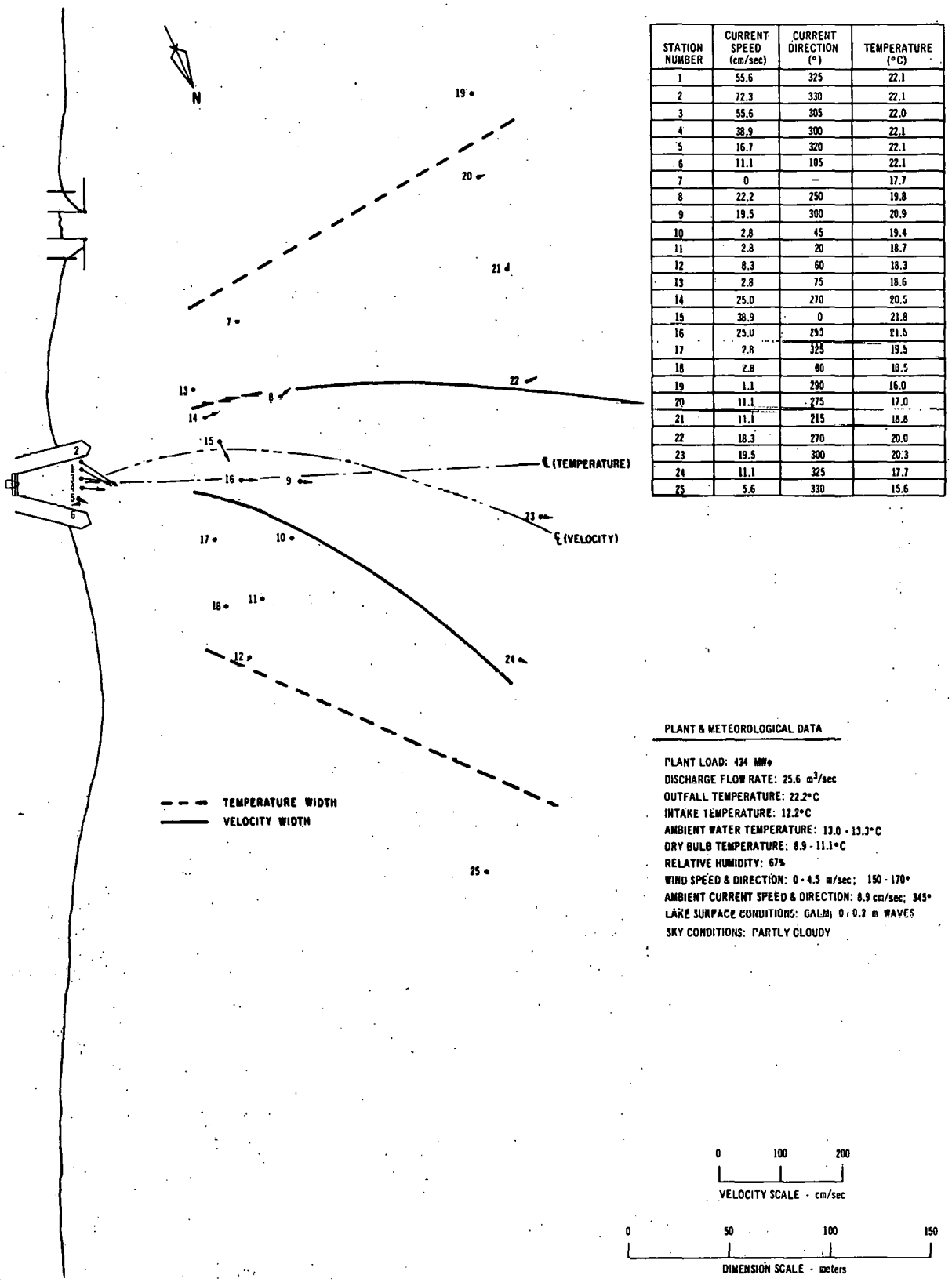

STATION NUMBER	CURRENT SPEED (cm/sec)	CURRENT DIRECTION (°)	TEMPERATURE (°C)
1	55.6	325	22.1
2	72.3	330	22.1
3	55.6	305	22.0
4	38.9	300	22.1
5	16.7	320	22.1
6	11.1	105	22.1
7	0	–	17.7
8	22.2	250	19.8
9	19.5	300	20.9
10	2.8	45	19.4
11	2.8	20	18.7
12	8.3	60	18.3
13	2.8	75	18.6
14	25.0	270	20.5
15	38.9	0	21.8
16	25.0	293	21.5
17	2.8	325	19.5
18	2.8	60	18.5
19	1.1	290	16.0
20	11.1	275	17.0
21	11.1	215	18.8
22	18.3	270	20.0
23	19.5	300	20.3
24	11.1	325	17.7
25	5.6	330	15.6

PLANT & METEOROLOGICAL DATA

PLANT LOAD: 434 MWe
DISCHARGE FLOW RATE: 25.6 m^3/sec
OUTFALL TEMPERATURE: 22.2°C
INTAKE TEMPERATURE: 12.2°C
AMBIENT WATER TEMPERATURE: 13.0 - 13.3°C
DRY BULB TEMPERATURE: 8.9 - 11.1°C
RELATIVE HUMIDITY: 67%
WIND SPEED & DIRECTION: 0 - 4.5 m/sec; 150 - 170°
AMBIENT CURRENT SPEED & DIRECTION: 8.9 cm/sec; 345°
LAKE SURFACE CONDITIONS: CALM; 0 - 0.3 m WAVES
SKY CONDITIONS: PARTLY CLOUDY

Fig. 43. Jet-regime Study for 0.5-m Depth at Palisades Power Plant: October 10, 1972, 1025-1550 Hours. ANL Neg. No. 190-759 Rev. 1.

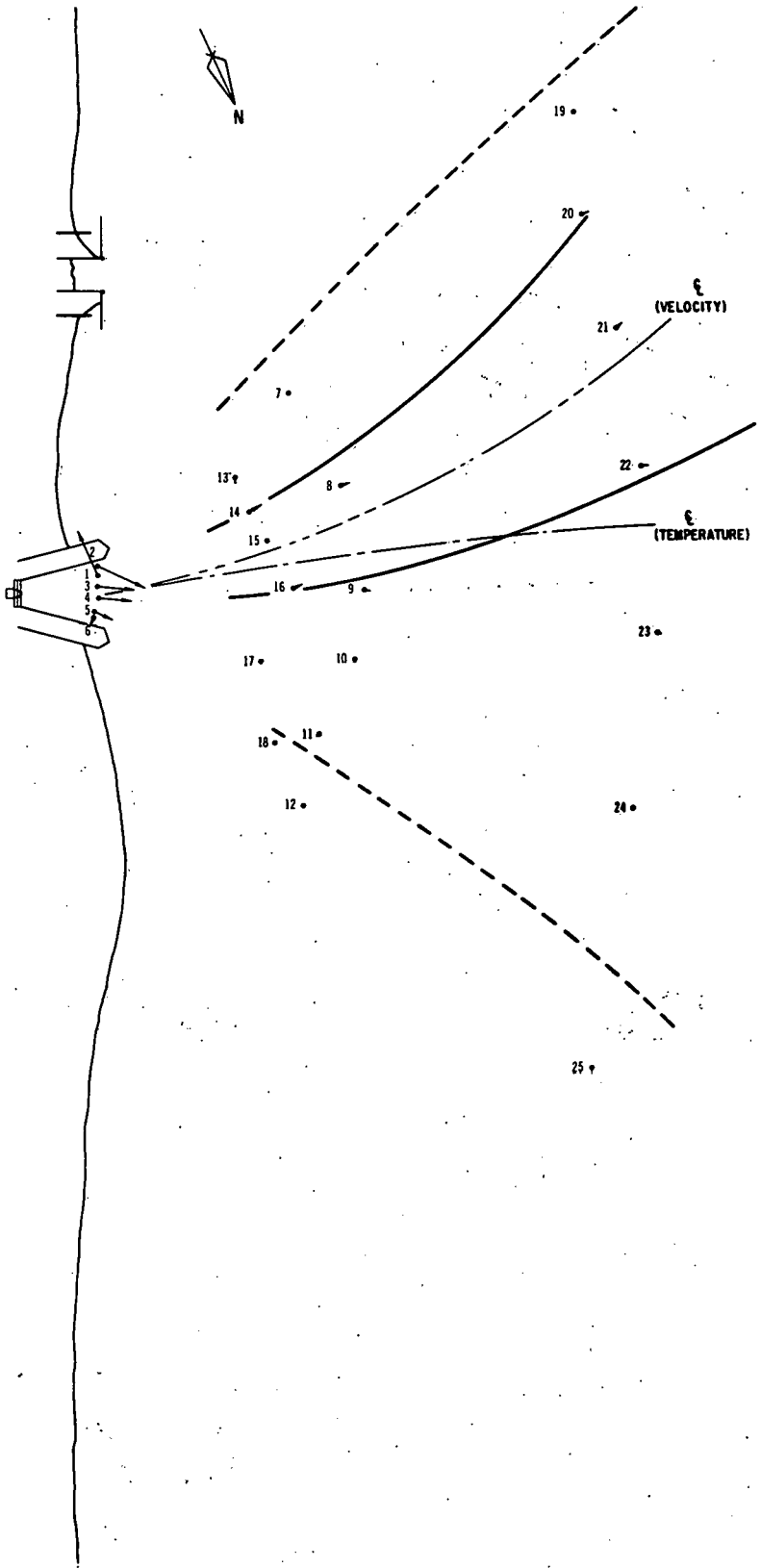

STATION NUMBER	CURRENT SPEED (cm/sec)	CURRENT DIRECTION (°)	TEMPERATURE (°C)
1	66.7	180	22.1
2	69.5	320	22.1
3	50.0	300	22.1
4	44.5	300	22.1
5	27.8	320	22.1
6	12.8	50	22.2
7	0	–	17.4
8	13.9	280	17.3
9	8.3	305	19.0
10	2.8	50	15.6
11	5.6	70	16.0
12	4.4	70	14.5
13	8.3	25	15.4
14	19.5	265	20.1
15	LAKE BOTTOM		
16	12.2	270	19.5
17	0	–	17.5
18	2.8	40	16.0
19	2.8	275	14.5
20	8.3	275	17.0
21	11.1	250	17.5
22	8.3	290	17.0
23	4.4	315	16.0
24	2.8	330	15.5
25	5.6	30	15.0

TEMPERATURE WIDTH
VELOCITY WIDTH

PLANT & METEOROLOGICAL DATA

PLANT LOAD: 434 MWe
DISCHARGE FLOW RATE: 25.6 m^3/sec
OUTFALL TEMPERATURE: 22.2°C
INTAKE TEMPERATURE: 12.2°C
AMBIENT WATER TEMPERATURE: 13.0 - 13.3°C
DRY BULB TEMPERATURE: 8.9 - 11.1°C
RELATIVE HUMIDITY: 67%
WIND SPEED & DIRECTION: 0 - 4.9 m/sec, 130 - 170°
AMBIENT CURRENT SPEED & DIRECTION: 8.9 cm/sec: 345°C
LAKE SURFACE CONDITIONS: CALM; 0 - 0.3 m WAVES
SKY CONDITIONS: PARTLY CLOUDY

0 100 200
VELOCITY SCALE - cm/sec

0 50 100 150
DIMENSION SCALE - meters

Fig. 44. Jet-regime Study for 10-m Depth at Palisades Power Plant: October 10, 1972, 1025–1550 Hours. ANL Neg. No. 190–883.

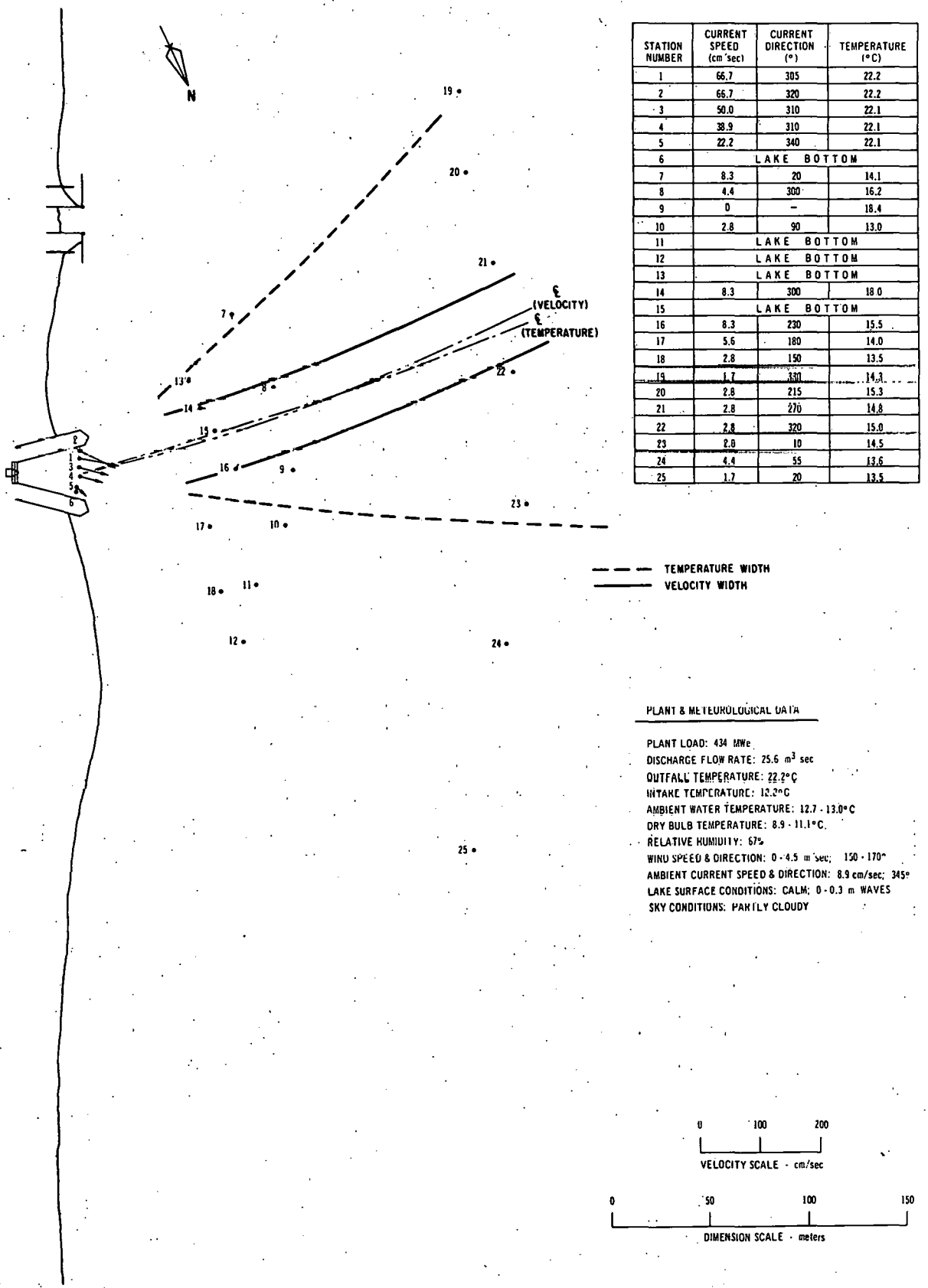

STATION NUMBER	CURRENT SPEED (cm/sec)	CURRENT DIRECTION (°)	TEMPERATURE (°C)
1	66.7	305	22.2
2	66.7	320	22.2
3	50.0	310	22.1
4	38.9	310	22.1
5	22.2	340	22.1
6	LAKE BOTTOM		
7	8.3	20	14.1
8	4.4	300	16.2
9	0	–	18.4
10	2.8	90	13.0
11	LAKE BOTTOM		
12	LAKE BOTTOM		
13	LAKE BOTTOM		
14	8.3	300	18.0
15	LAKE BOTTOM		
16	8.3	230	15.5
17	5.6	180	14.0
18	2.8	150	13.5
19	1.7	330	14.3
20	2.8	215	15.3
21	2.8	270	14.8
22	2.8	320	15.0
23	2.0	10	14.5
24	4.4	55	13.6
25	1.7	20	13.5

Fig. 45. Jet-regime Study for 1.5-m Depth at Palisades Power Plant: October 10, 1972, 1025-1550 Hours. ANL Neg. No. 190-901.

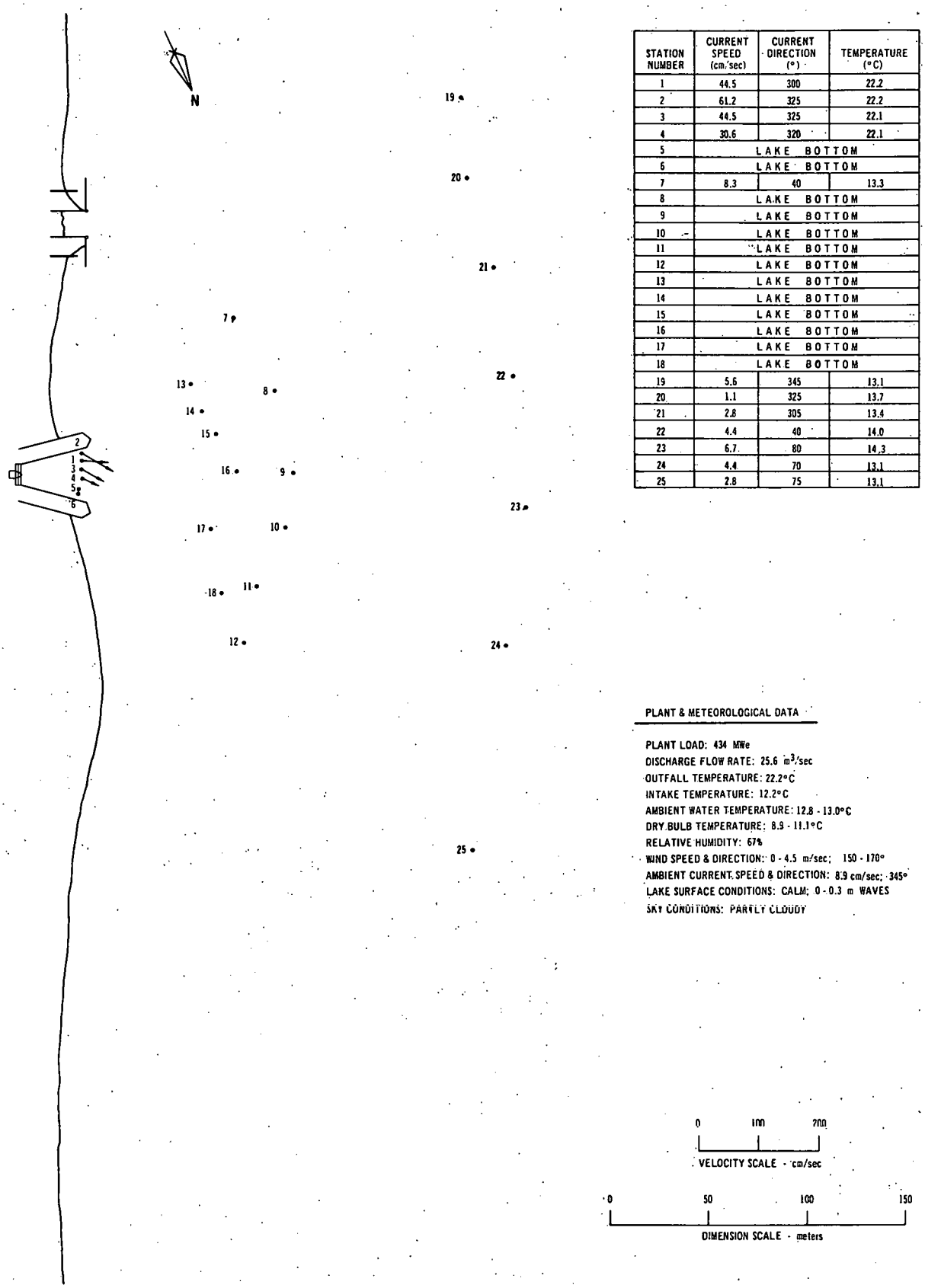

STATION NUMBER	CURRENT SPEED (cm/sec)	CURRENT DIRECTION (°)	TEMPERATURE (°C)
1	44.5	300	22.2
2	61.2	325	22.2
3	44.5	325	22.1
4	30.6	320	22.1
5	LAKE BOTTOM		
6	LAKE BOTTOM		
7	8.3	40	13.3
8	LAKE BOTTOM		
9	LAKE BOTTOM		
10	LAKE BOTTOM		
11	LAKE BOTTOM		
12	LAKE BOTTOM		
13	LAKE BOTTOM		
14	LAKE BOTTOM		
15	LAKE BOTTOM		
16	LAKE BOTTOM		
17	LAKE BOTTOM		
18	LAKE BOTTOM		
19	5.6	345	13.1
20	1.1	325	13.7
21	2.8	305	13.4
22	4.4	40	14.0
23	6.7	80	14.3
24	4.4	70	13.1
25	2.8	75	13.1

Fig. 46. Jet-regime Study for 2.0-m Depth at Palisades Power Plant: October 10, 1972, 1025-1550 Hours. ANL Neg. No. 190-876.

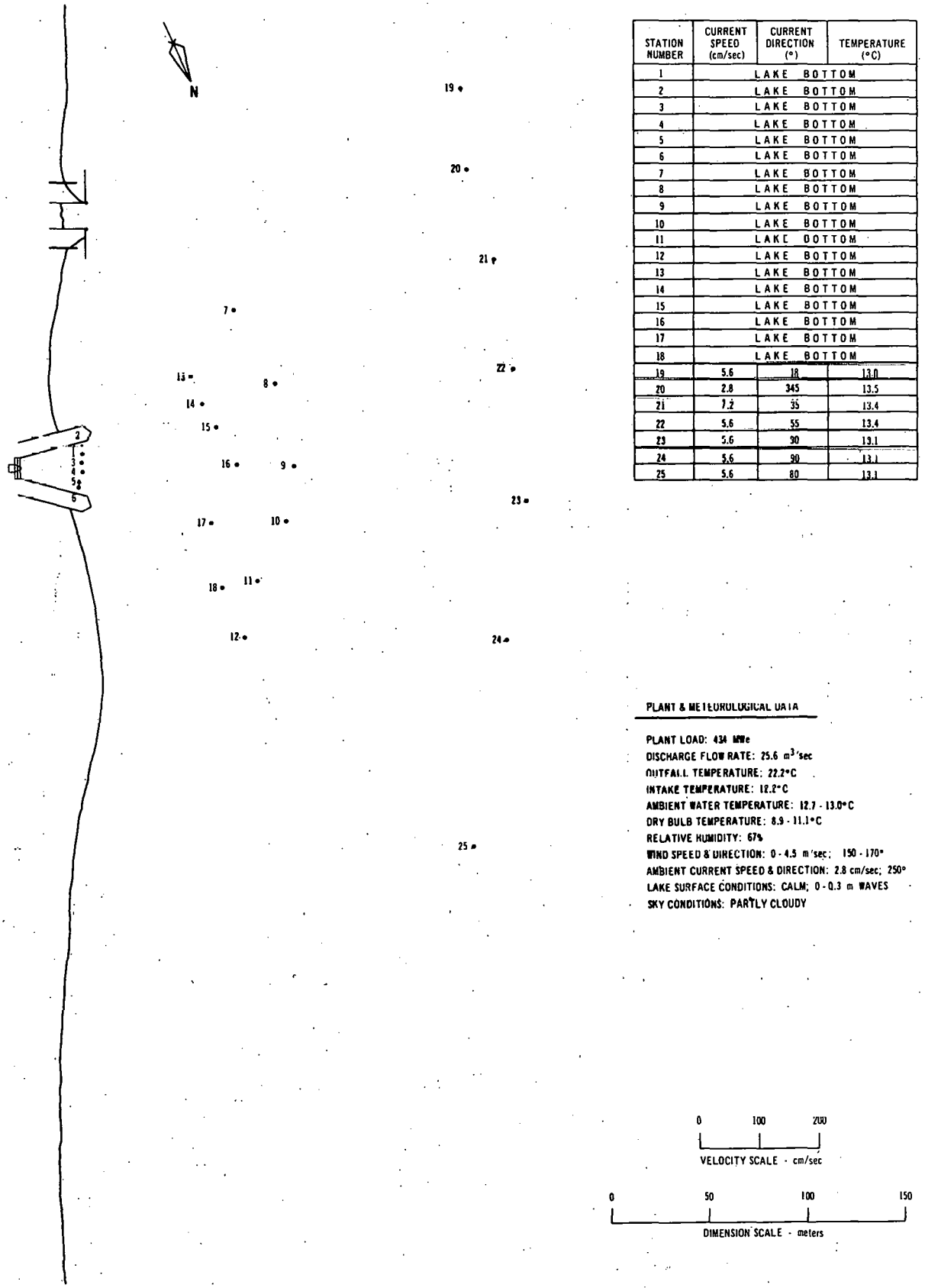

STATION NUMBER	CURRENT SPEED (cm/sec)	CURRENT DIRECTION (°)	TEMPERATURE (°C)
1	LAKE BOTTOM		
2	LAKE BOTTOM		
3	LAKE BOTTOM		
4	LAKE BOTTOM		
5	LAKE BOTTOM		
6	LAKE BOTTOM		
7	LAKE BOTTOM		
8	LAKE BOTTOM		
9	LAKE BOTTOM		
10	LAKE BOTTOM		
11	LAKE BOTTOM		
12	LAKE BOTTOM		
13	LAKE BOTTOM		
14	LAKE BOTTOM		
15	LAKE BOTTOM		
16	LAKE BOTTOM		
17	LAKE BOTTOM		
18	LAKE BOTTOM		
19	5.6	18	13.0
20	2.8	345	13.5
21	7.2	35	13.4
22	5.6	55	13.4
23	5.6	90	13.1
24	5.6	90	13.1
25	5.6	80	13.1

PLANT & METEOROLOGICAL DATA

PLANT LOAD: 434 MWe
DISCHARGE FLOW RATE: 25.6 m^3/sec
OUTFALL TEMPERATURE: 22.2°C
INTAKE TEMPERATURE: 12.2°C
AMBIENT WATER TEMPERATURE: 12.7 - 13.0°C
DRY BULB TEMPERATURE: 8.9 - 11.1°C
RELATIVE HUMIDITY: 67%
WIND SPEED & DIRECTION: 0 - 4.5 m/sec; 150 - 170°
AMBIENT CURRENT SPEED & DIRECTION: 2.8 cm/sec; 250°
LAKE SURFACE CONDITIONS: CALM; 0 - 0.3 m WAVES
SKY CONDITIONS: PARTLY CLOUDY

0 100 200
VELOCITY SCALE - cm/sec

0 50 100 150
DIMENSION SCALE - meters

Fig. 47. Jet-regime Study for 2.5-m Depth at Palisades Power Plant: October 10, 1972, 1025–1550 Hours. ANL Neg. No. 190-886.

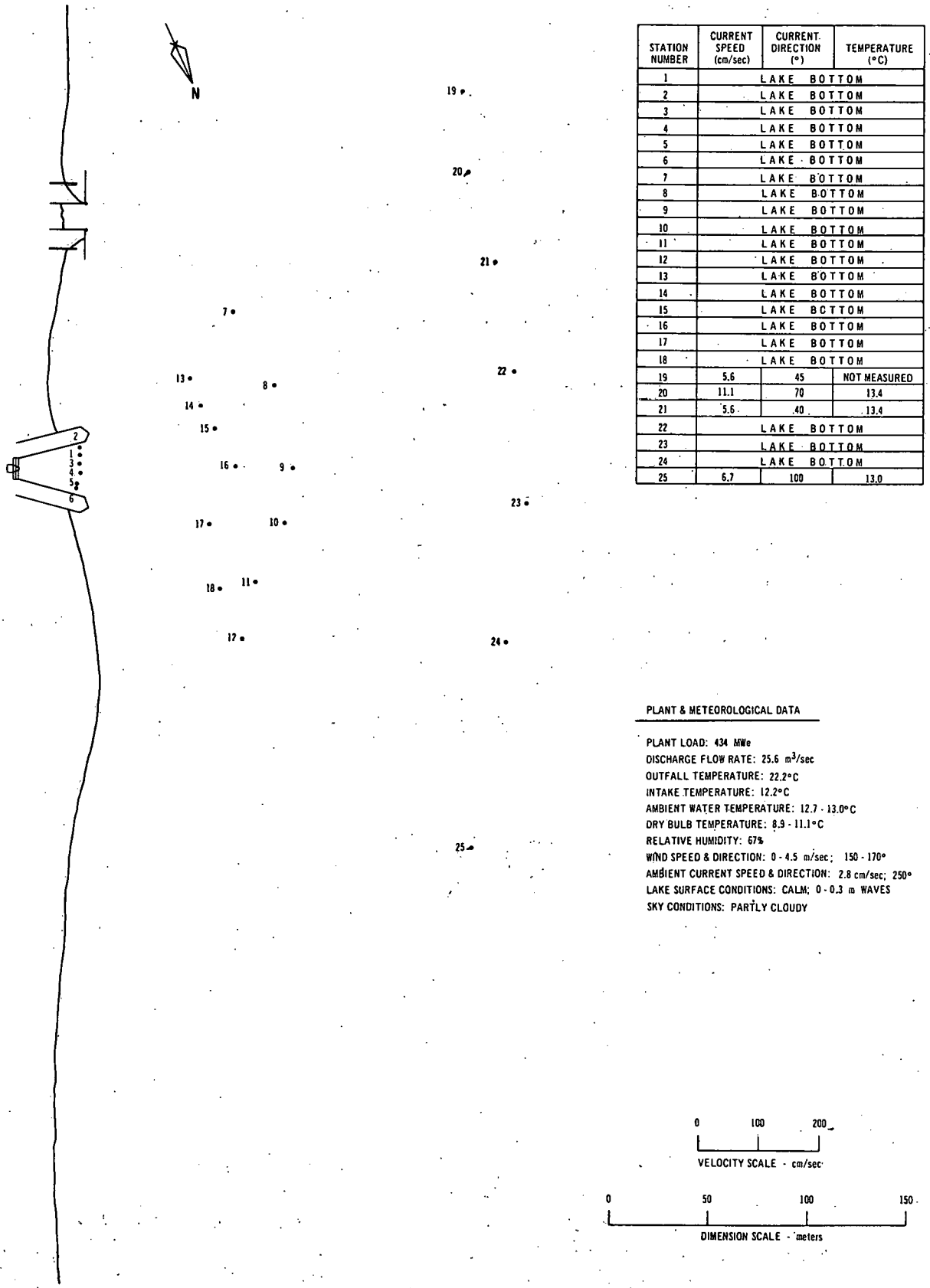

STATION NUMBER	CURRENT SPEED (cm/sec)	CURRENT DIRECTION (°)	TEMPERATURE (°C)
1	LAKE BOTTOM		
2	LAKE BOTTOM		
3	LAKE BOTTOM		
4	LAKE BOTTOM		
5	LAKE BOTTOM		
6	LAKE BOTTOM		
7	LAKE BOTTOM		
8	LAKE BOTTOM		
9	LAKE BOTTOM		
10	LAKE BOTTOM		
11	LAKE BOTTOM		
12	LAKE BOTTOM		
13	LAKE BOTTOM		
14	LAKE BOTTOM		
15	LAKE BOTTOM		
16	LAKE BOTTOM		
17	LAKE BOTTOM		
18	LAKE BOTTOM		
19	5.6	45	NOT MEASURED
20	11.1	70	13.4
21	5.6	40	13.4
22	LAKE BOTTOM		
23	LAKE BOTTOM		
24	LAKE BOTTOM		
25	6.7	100	13.0

PLANT & METEOROLOGICAL DATA

PLANT LOAD: 434 MWe
DISCHARGE FLOW RATE: 25.6 m^3/sec
OUTFALL TEMPERATURE: 22.2°C
INTAKE TEMPERATURE: 12.2°C
AMBIENT WATER TEMPERATURE: 12.7 - 13.0°C
DRY BULB TEMPERATURE: 8.9 - 11.1°C
RELATIVE HUMIDITY: 67%
WIND SPEED & DIRECTION: 0 - 4.5 m/sec; 150 - 170°
AMBIENT CURRENT SPEED & DIRECTION: 2.8 cm/sec; 250°
LAKE SURFACE CONDITIONS: CALM; 0 - 0.3 m WAVES
SKY CONDITIONS: PARTLY CLOUDY

Fig. 48. Jet-regime Study for 3.0-m Depth at Palisades Power Plant: October 10, 1972, 1025-1550 Hours. ANL Neg. No. 190-874.

V. EXTRACTION OF JET CHARACTERISTICS FROM FIELD MEASUREMENTS

In order to examine the features of the temperature and velocity distributions in the near-field region of the discharges, and additionally to facilitate comparisons with analytical-model predictions, it was decided to assume a functional form for the distributions and fit these distributions to the field measurements. The choice of the functional forms was based on preliminary examination of the Point Beach data. The functions chosen use Gaussian distributions for the lateral excess-temperature and excess-velocity profiles. The excess temperature θ is defined as the difference between the measured temperature T and the ambient temperature T_A of the lake water at that depth. The excess velocity u_E is defined as the component of the measured velocity parallel to the centerline of the jet, minus the component of the ambient current parallel to the centerline. The ambient current u_A was taken to be parallel to shore for this purpose. The widths of these profiles are assumed to grow linearly with distance from the outfall, s, as measured along the jet centerline. The centerline temperature excess θ_c and the centerline velocity excess u_{cE} are assumed to decay as the inverse of the square root of the distance from the outfall. A quadratic form was chosen for the trajectories of the centerline.

The temperature excess at a lateral distance η from the temperature centerline at a distance s from the outfall is thus given by

$$\theta(\eta,s) = \theta_c(s)\exp\{-(\ln 2)[\eta/W_T(s)]^2\} = \theta_c(s)\left(\frac{1}{2}\right)^{[\eta/W_T(s)]^2},$$

where

$$\theta_c(s) = \begin{cases} \theta_0 A & \text{for } s \le \dfrac{\alpha b_0}{A^2} \\ \theta_0\sqrt{\dfrac{\alpha b_0}{s}} & \text{for } s > \dfrac{\alpha b_0}{A^2}, \end{cases}$$

and

$$W_T(s) = Cb_0 + \gamma s.$$

In the above expression, θ_0 is the initial temperature excess at the outfall, b_0 is the width of the outfall, and W_T is the half-width of the excess temperature distribution. The half-width is defined as the lateral distance at which the excess temperature drops off to one-half the centerline value. The dimensionless parameters A, α, C, and γ are free parameters to be determined by fitting to the field data.

To specify the centerline, a coordinate system is set up with the origin at the center of the outfall. The positive y axis is perpendicular to the average shoreline in the off-shore direction, the positive z axis is vertically upward, and the positive x axis is chosen to be orthogonal to the other two so as to form a right-handed system in the conventional sense (x,y,z). The temperature centerline trajectory is most easily specified in parametric form:

$$x_{cT} = \xi \cos(R_T \beta_0) - \frac{K_T}{100 b_0} \xi^2 \sin(R_T \beta_0)$$

and

$$y_{cT} = \xi \sin(R_T \beta_0) + \frac{K_T}{100 b_0} \xi^2 \cos(R_T \beta_0)$$

for

$$\xi \geq 0.$$

The trajectory represents a parabola passing through the origin at an angle of $R_T \beta_0$ with respect to the positive x axis. The parametric variable ξ is introduced only to simplify the form of these equations. The angle of the outfall with respect to the positive x axis is β_0, and R_T and K_T are two dimensionless free parameters to be determined by fitting to the field data.

The case for which $R_T = 1.0$ and $K_T = 0.0$ corresponds to a jet centerline that is directed straight out from the outfall. Positive values of K_T correspond to the jet bending to the left, and negative values correspond to bending to the right. The quantity $R_T \beta_0$ determines the initial angle of the centerline at the origin (discharge).

The velocity excess (assumed parallel to the centerline) at a lateral distance η from the velocity centerline is given by the following expression:

$$u_E(\eta, s) = u_{CE}(s) \left(\frac{1}{2}\right)^{[\eta / W_u(s)]^2},$$

where

$$u_{cE}(s) = \begin{cases} u_0 R & \text{for } s \leq \dfrac{\beta b_0}{B^2} \\ u_0 \sqrt{\dfrac{\beta b_0}{s}} & \text{for } s > \dfrac{\beta b_0}{B^2}, \end{cases}$$

and

$$W_u(s) = D b_0 + \delta s.$$

These velocity-excess equations have the same form as the expressions for the temperature excess, except that u_0 is the outfall velocity averaged over the entire outfall. The velocity centerline has a form analogous to that for the temperature centerline:

$$x_{cu} = \xi \cos(R_u \beta_0) - \frac{K_u}{100 b_0} \xi^2 \sin(R_u \beta_0)$$

and

$$y_{cu} = \xi \sin(R_u \beta_0) + \frac{K_u}{100 b_0} \xi^2 \cos(R_u \beta_0).$$

The parameters B, β, D, δ, R_u, and K_u are determined by fitting to the data.

The temperature and velocity functions described above, each with only six free parameters, are fairly restrictive. However, due to the limited amount of data available, it was felt that more general functions with more free parameters would be unwarranted. As a consequence, only the general trends of the resulting fitted function can be considered significant. The details are artifacts of the functions chosen.

The fitting procedure was carried out on the computer by a minimization technique. The root-mean-square deviations of the functions from the data are defined as follows:

$$(\sigma_T; A, \alpha, C, \gamma, R_T, K_T) = \left[\sum_{i=1}^{N} \frac{(\theta_{Di} - \theta_{Fi})^2}{N - 6} \right]^{1/2}$$

and

$$(\sigma_u; B, \beta, D, \delta, R_u, K_u) = \left[\sum_{i=1}^{N} \frac{(u_{Di} - u_{Fi})^2}{N - 6} \right]^{1/2},$$

where N is the number of data points, θ_{Di} is the measured temperature excess at the ith data point, θ_{Fi} is the temperature excess calculated from the function, u_{Di} is the component of the measured velocity excess parallel to the velocity centerline, and u_{Fi} is the velocity excess calculated from the function. The 6 in the denominator is introduced to account for the six degrees of freedom associated with the six free parameters of the fitting function. The final values of the parameters were then chosen to be those values that minimize σ_T and σ_u. The FORTRAN program JETFIT used for this fitting procedure is listed in Appendix C.

The sets of measurements taken during the four jet studies at the Point Beach outfall and one of the studies at the Palisades outfall (October 10, 1972) were each fitted independently. The measurements of the

other two Palisades surveys did not lend themselves to this fitting procedure because the limited number of data points did not appear to characterize a major portion of the jet region; i.e., the jet seems to be significantly wider than the region surveyed.

The parameters resulting from the fitting procedure and a tabulation of the deviations of the fitted functions from the measurements are included in Appendix D. The average deviation of the function from the data varied from about 0.2 to 1.1C°, with an overall average deviation for all five studies of 0.7C°. The average velocity deviation varied from 1 to 8 cm/sec, with an overall average deviation of 4 cm/sec. These overall average deviations correspond to about 7% of the average initial temperature excess and outfall velocity, respectively. Figures 8-48 show the temperature and velocity centerlines and the temperature and velocity half-widths resulting from this fitting procedure, along with the actual field measurements. Note that the field measurements were made in groups corresponding approximately to perpendicular transects of the jet. Some of the fitting results for the Point Beach studies are shown together in Figs. 49-52 so that they may be compared with each other. The circles on the curves of θ_c/θ_0, plotted as a function of distance from the outfalls (Fig. 49), indicate the approximate location of the measurement groupings. The results for the one Palisades case are presented in Sec. VII along with the model comparisons.

Figure 49 shows the centerline temperature and velocity decays resulting from the fits to the measurements taken at a depth of 0.5 m for all four Point Beach dates. The drop-off rates are approximately the same for each survey and for both temperature and velocity, except for the velocity results of July 13, 1972. This difference is presently unexplained. Indeed, the differences shown in the figures, with that one exception, are probably within the errors associated with the experimental measurements and the fitting procedure. On all four dates, the power plant was operating at essentially the same power level and discharge flow rate. The temperature distribution across the outfall has been measured and found to be quite uniform. Therefore, the excess temperature ratio θ_c/θ_0 plotted in the upper half of Fig. 49 must be 1.0 at s = 0. This restriction was not placed on the fitting function, and so not much significance should be attached to the details contained in the first 100 m of the fitting results. The initial velocity distribution at the Point Beach outfall has also been measured.* It was not found to be uniform. In fact, velocities as much as 60% above the average outfall velocity were observed. This fact shows up in the lower half of Fig. 49, where the velocity ratio exceeds 1.0 for small values of s. Again, not much significance should be attached to the details of the results in this initial 100-m region.

Figure 50 presents the corresponding temperature and velocity half-widths for the same four dates. It is evident that the temperature distribution is wider than the velocity distribution. Indeed, on the average, it is approximately twice as wide.

*A typical outfall velocity distribution for Point Beach appears in ANL/ES-16 (Ref. 19 of Appendix A). Measurements on several other dates exist and will be published in the future.

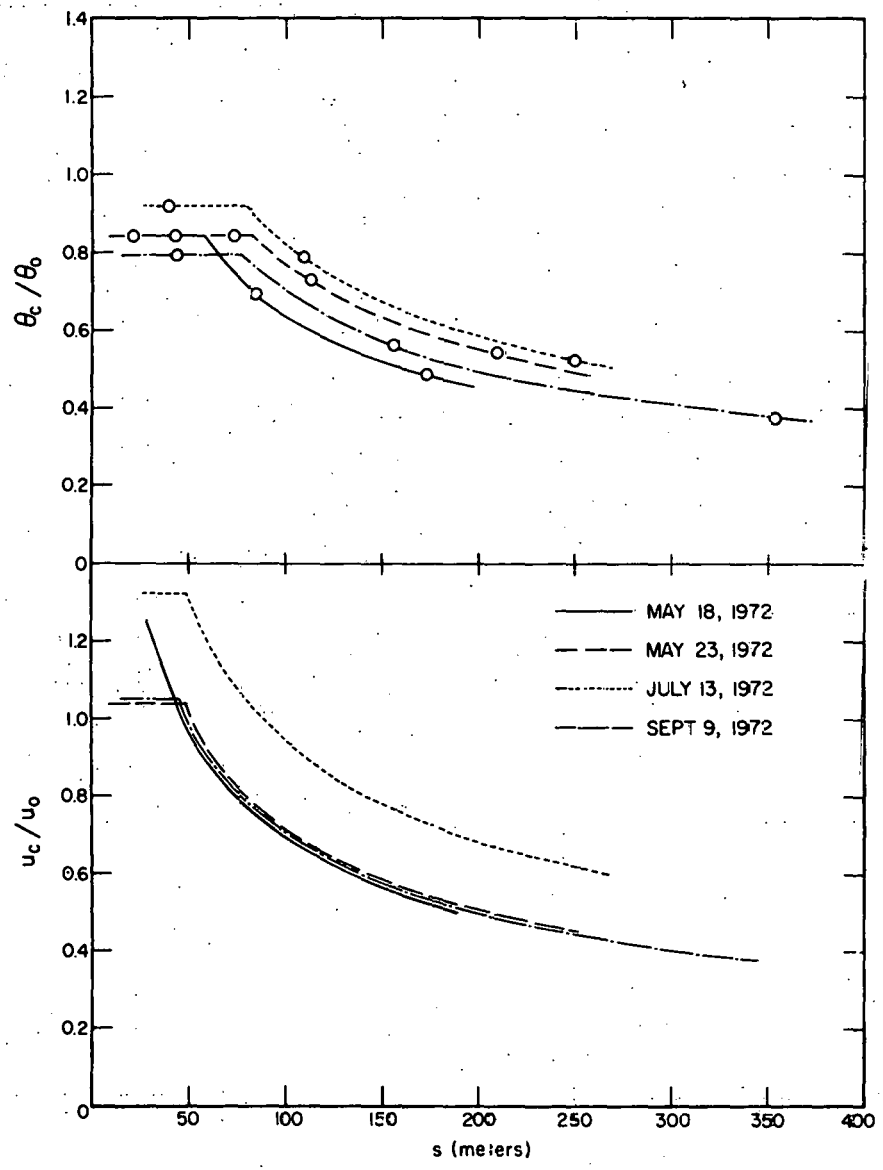

Fig. 49. Centerline Excess-temperature and -velocity Decays Resulting from Fits to Point Beach Jet Data at 0.5-m Depth. ANL Neg. No. 190-950.

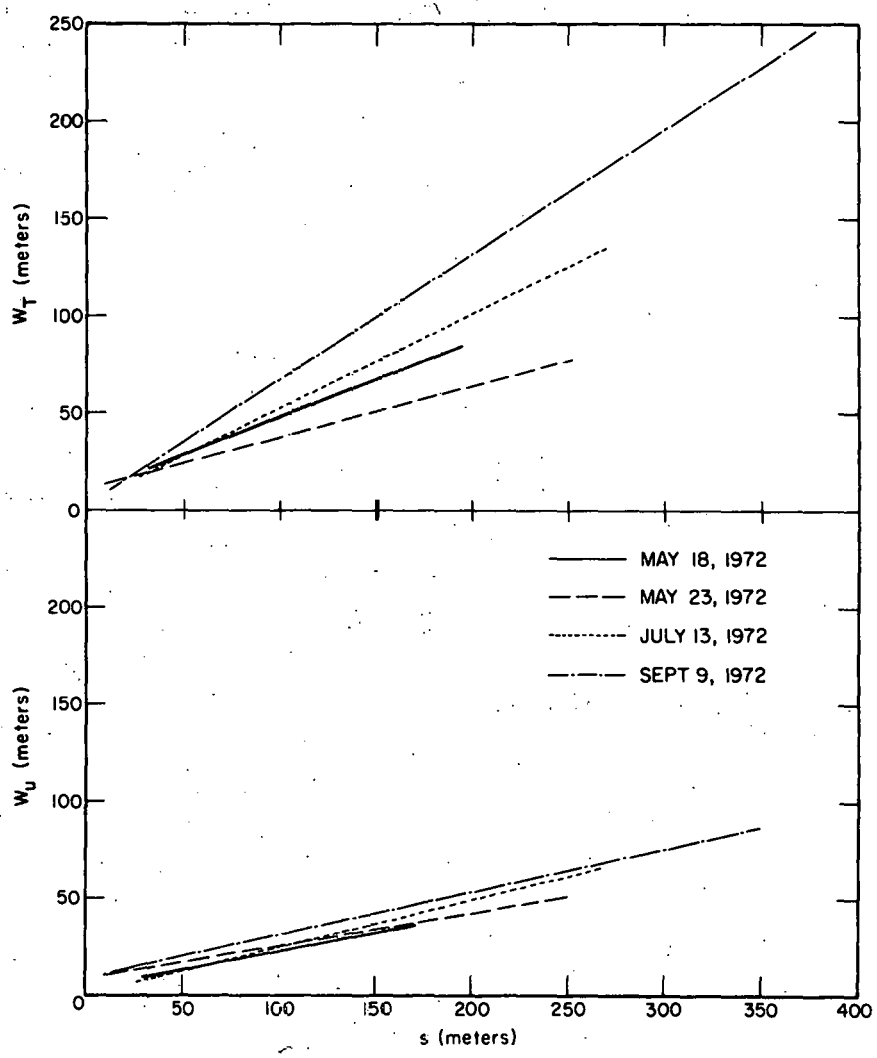

Fig. 50. Half-widths of Temperature and Velocity Distributions Resulting from Fits to Point Beach Jet Data at 0.5-m Depth. ANL Neg. No. 190-961.

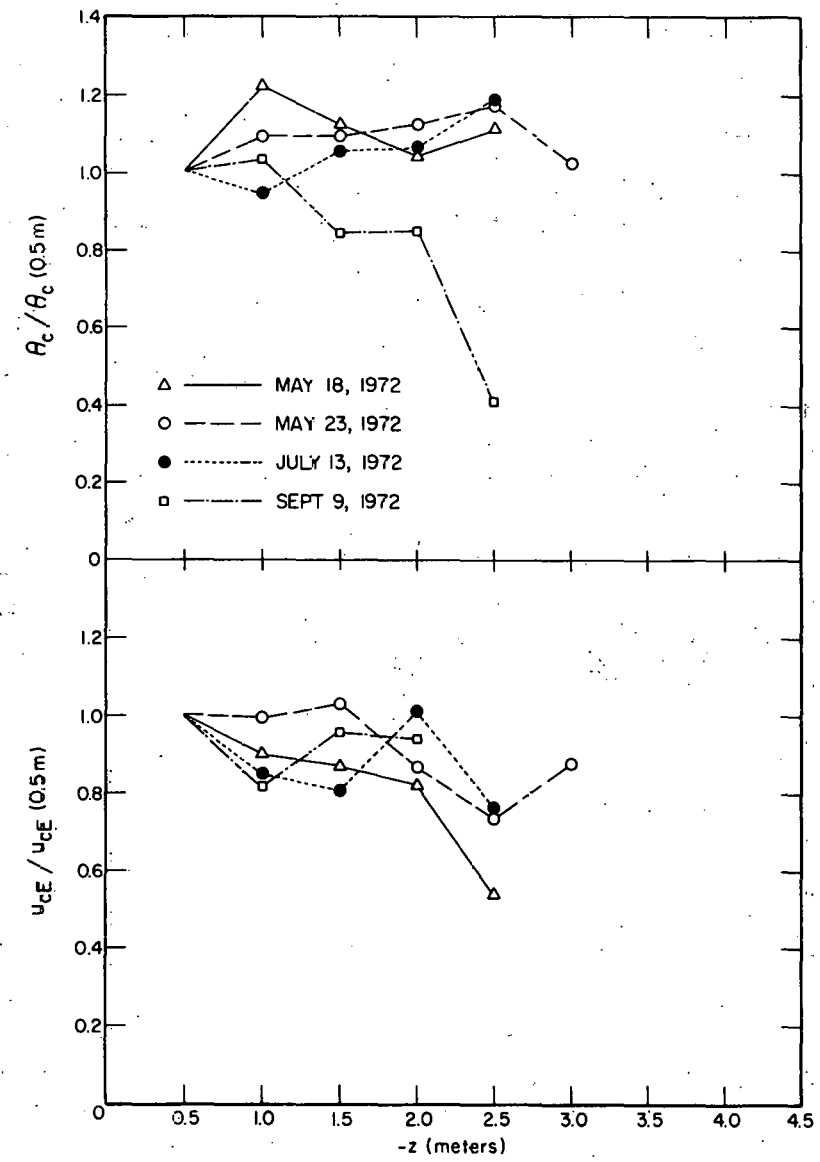

Fig. 51. Centerline Temperature Excess and Velocity Excess as a Function of Depth Resulting from Fits to Point Beach Jet Data (normalized to the 0.5-m results). ANL Neg. No. 190-953.

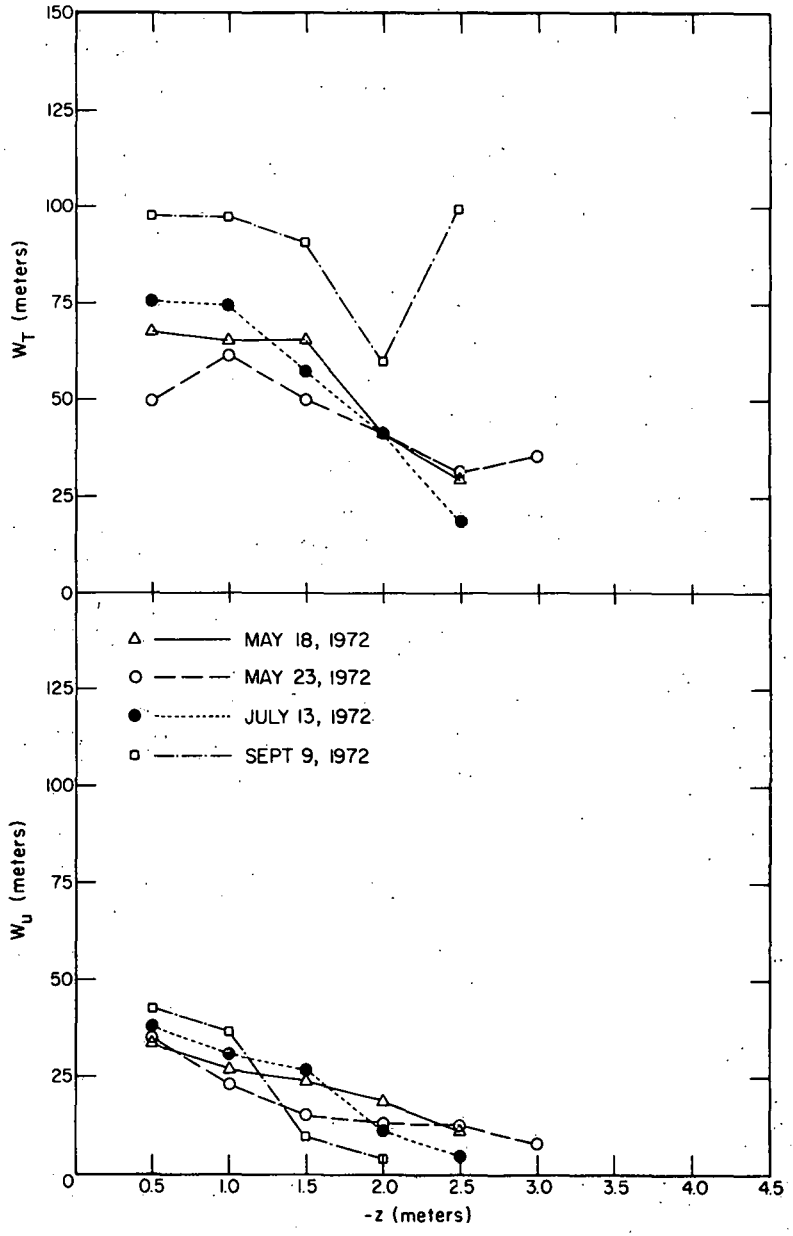

Fig. 52. Half-widths of Temperature and Velocity Distributions as a Function of Depth at s = 150 m, Resulting from Fits to Point Beach Jet Data. ANL Neg. No. 190-945.

Figure 51 shows the centerline temperature and velocity excesses as a function of depth relative to the 0.5-m results. Because of the nature of the functional form chosen, these quantities are independent of distance from the outfall after the initial region, which was always less than about 100 m. Within the accuracy of these results, the excesses are fairly constant with depth. However, the temperature data of September 9, 1972, do show an exception. Because there is no clear drop-off with depth, a characteristic depth of the jet could not be extracted from the JETFIT results.

Figure 52 shows the widths as a function of depth at a distance of 150 m from the outfall. This distance was chosen because it lies approximately in the middle of the range for which measurements were made. These widths show a decreasing trend, tending toward zero at a depth of 2.5-3.0 m. The temperature widths are approximately constant for the first 1.0-1.5 m and then decrease while the velocity widths decrease more uniformly.

In summary, the Point Beach jet studies indicate that the centerline excess temperature and excess velocity ratios decay at about the same rate, with jet longitudinal distance, for all four dates and for depths down to 2 m or more. This decay, beyond about the first 50 m, is characterized by

$$\frac{\theta_c}{\theta_0} \approx \frac{u_{cE}}{u_0} \approx \sqrt{\frac{4.2 b_0}{s}}.$$

In the above expression, 4.2 is the average value of α and β for all cases except for the 0.5-m velocity results of July 13, 1972, and the 1.5-, 2.0-, and 2.5-m temperature results of September 9, 1972. The average deviation of the actual values of α and β from this value of 4.2 is 0.7. The temperature half-widths at the 0.5-m depth grow at a rate of 3-6 m for each 10 m from the outfall; the velocity half-widths grow at only about 2 m per 10 m. Both these rates decrease with depth, tending toward zero at about 2.5-3.0 m.

VI. MATHEMATICAL MODELING OF NEAR-FIELD REGION OF SURFACE THERMAL DISCHARGES

The utility of analytical near-field, surface-discharge models is primarily centered around three considerations. The first of these is a desire to assess, and therefore avoid, possible recirculation of heated water into the plant intake. The second is the necessity to develop an appropriate discharge design to satisfy temperature standards. The third is a desire to help predict possible biological effects relating to changes in the physical and chemical properties of the water.

Most presently operating power plants use a surface channel or canal to discharge their heated condenser-cooling water, and many new plants still plan for similar discharge designs. Since thermal discharges of cooling water from power plants will undoubtedly increase greatly in both magnitude and number during the next decade, the adequacy of predictive models for such discharges becomes an important factor in design.

Table II summarizes the basic characteristics of 15 near-field analytical models[1-15] for surface thermal discharges presently available in the literature. Table III summarizes those complete-field models[16-24] that have separate jet-regime analyses. Due to limitations of time and space, the field of 24 models had to be narrowed down considerably. Considered in this report and compared with the Point Beach Unit 1 and Palisades data are the more promising and widely used models of Pritchard (Model No. 1), Motz and Benedict, Stolzenbach and Harleman, and Prych. Some of the reasons for not including comparisons with the other models are as follows:

1. Hoopes et al.: model too sensitive to the main parameter, wind speed; generally unsatisfactory comparison with earlier data taken at Point Beach (Ref. 21 of Appendix A).

2. Hayashi and Shuto: mainly historical nature of model; no jet entrainment simulated in this model.

3. Wada (Model No. 1): computer program unavailable.

4. Carter: mainly historical nature of model; jet model based on hydraulic data taken in too small a basin; improved data appeared recently in Ref. 25.

5. Koh and Fan (2D Model): no lateral entrainment simulated in this two-dimensional (longitudinal, vertical) model; as with the Wada Model No. 2, it is basically a tool to develop greater physical insight.

6. Koh and Fan (axisymmetric model): discharge outfall assumed in this model is circular, not rectangular as exists at Point Beach and Palisades.

7. Barry and Hoffman: model authors prefer to make changes in model development before further application.

8. McLay et al.: modification on Hoopes et al. model which includes a region of flow establishment and a constant spreading rate; not used because of generally unsatisfactory experience with computer code.

9. Stefan: no region of flow establishment, which severely restricts application of model; also, model comparison with Stefan's tank data not satisfactory (possibly due also to stratification of ambient water in tank).

10. Paul and Lick: new model with computer code incomplete at time of present study.

11. Engelund and Pedersen: model applicable only for surface discharges having large initial densimetric Froude numbers.

12. Waldrop and Farmer: model is of too recent an origin.

13. Wada (Model No. 2): no computer code available; no lateral entrainment simulated in this two-dimensional (longitudinal, vertical) model.

14. Sundaram et al.: mainly historical nature of model; jet-trajectory formulas not applicable until reasonably distant from outfall.

15. Elliott and Harkness: model authors are presently improving their near-field analysis.

16. Giles et al.: model authors will be making further (though minor) modifications in the model; the hybrid computer required for model application is too large for Argonne facilities.

17. Loziuk et al.: model authors are presently modifying the hydraulics of their jet analysis; computer code presently unavailable.

18. Brady and Geyer: model is of too recent an origin for application in this report.

19. Till: model is of too recent an origin.

20. Pritchard (Model No. 2): model is of too recent an origin.

The four analytical models to be considered in this report and compared with the present field data are summarized next.

A. Motz-Benedict Model

Motz and Benedict have developed a two-dimensional model for the velocity and temperature distribution of a heated surface jet.[5] Ambient receiving-water turbulence and buoyancy are assumed to be of minimal influence with regard to plume dynamics and heat transfer within the jet regime. The authors built their integral analysis upon the framework established primarily by Morton,[26] Fan,[27] Hoopes et al.,[1] and Carter.[4] Conservation equations of mass, x and y momentum, and energy, along with two equations of jet bending, lead to a system of six ordinary differential equations which must be solved numerically to yield the jet trajectory, centerline temperature and velocity, and profile width. The Motz-Benedict model assumes that only two factors affect the flux of momentum at any

TABLE II. Summary of Characteristics of Jet Models (ANL Neg. No. 190-990 Rev. 1)

		DIRECTION OF TEMPERATURE VARIATION			INITIAL MIXING (JET REGIME)	AMBIENT TURBULENCE (FAR-FIELD REGION)	MATHEMATICAL APPROACH				TIME DEPENDENT SOLUTION	BUOYANCY	CROSS FLOW	BOTTOM SLOPE	SURFACE HEAT LOSS	DISCHARGE GEOMETRY	PROVIDES FOR FLOW ESTABLISHMENT	AMBIENT STRATIFICATION INTERACTION	DIRECT WIND STRESS EFFECTS	RECIRCULATION OF PLUME WATER	COMPARED OR FITTED WITH		COMPUTER PROGRAM
		LONGITUDINAL	LATERAL	VERTICAL			NUMERICAL	INTEGRAL	CLOSED FORM	SEMI-EMPIRICAL											FIELD DATA	TANK DATA	
1.	HOOPES ET AL.	YES	YES	NO	YES	NO	NO	YES	NO[a]	YES	NO	NO	YES	NO[b]	YES	YES	NO[b]	NO	YES	NO	YES	NO	YES[j]
2.	HAYASHI AND SHUTO	YES	YES	YES	YES	NO	NO	YES	YES	YES	NO	YES	NO	NO	YES	YES	NO	NO	NO	NO	NO	YES	NO[k]
3.	WADA (MODEL NO. 1)	YES	YES	YES[c]	YES	NO	YES	NO	NO	YES	YES	YES	NO	YES	YES	YES	NO	NO	NO	YES	UNKNOWN	UNKNOWN	YES[t]
4.	CARTER	YES	YES	NO	YES	NO	NO	YES	NO	YES	NO	NO	YES	NO	NO	YES	YES	NO	NO	NO	NO	YES	YES[m]
5.	MOTT AND BENEDICT	YES	YES	NO	YES	NO	NO	YES	NO[d]	YES	NO	NO	YES	NO	YES	YES	YES	NO	NO	NO	YES	YES	YES[j]
6.	KOH AND FAN (2D MODEL)	YES	NO	YES	YES	NO	NO	YES	NO	YES	NO	YES	NO	NO	YES	YES	NO	NO	NO[e]	NO	NO	NO	YES[j]
7.	KOH AND FAN (AXISYMMETRIC MODEL)	YES	YES	YES	YES	NO	NO	YES	NO	YES	NO	YES	NO	NO	YES	YES	NO	NO	NO	NO	NO	NO	YES[j]
8.	BARRY AND HOFFMAN	YES	YES	YES	YES	NO	YES	NO	NO	YES	NO	YES	YES	YES	YES	YES	NO	NO	NO	NO	YES	NO	YES[t]
9.	STOLZENBACH AND HARLEMAN	YES	YES	YES	YES	NO	NO	YES	NO	YES	NO	YES	YES	NO	YES	YES	YES	NO	NO	NO	NO	YES	YES[j]
10.	McLAY ET AL.	YES	YES	YES	YES	NO	YES[f]	YES[f]	NO[g]	YES	NO	NO	YES	NO	YES	YES	YES	NO	NO[e]	NO	YES	NO	YES[j]
11.	STEFAN	YES	YES	YES	YES	NO	NO	YES	NO	YES	NO	YES	YES	NO	YES	YES	NO	NO	YES	NO	NO	YES	YES[j]
12.	PRYCH	YES	YES	YES	YES	NO	NO	YES	NO	YES	NO	YES	YES	NO	YES	YES	YES	NO	NO	NO	YES	YES	YES[j]
13.	PAUL AND LICK[h]	YES	YES	YES	YES	NO	YES	NO	NO	YES	YES	YES	NO	YES[i]	YES	YES	YES	NO	NO	YES	NO	NO	YES[j]
14.	EGGELUND AND PEDERSEN	YES	YES	YES	YES	NO	NO	YES	YES	YES	YES	NO	YES	NO	NO	NO	YES	NO	NO	NO	NO	YES	NO[k]
15.	NALUROP AND FARMER[h]	YES	YES	YES	YES	NO	YES	NO	NO	YES	YES	YES	YES	YES	YES	YES	YES	YES	YES	YES	YES	YES	YES[j]

[a] A CLOSED-FORM SOLUTION HAS BEEN DERIVED FOR THE CASE OF ZERO WIND STRESS.

[b] FLOW DEVELOPMENT AND BOTTOM EFFECTS WERE CONSIDERED INDIRECTLY VIA WIND SPEED-CORRELATIONS.

[c] THE MODEL IS ACTUALLY QUASI THREE-DIMENSIONAL WITHIN A SEMI-INFINITE SYSTEM HAVING TWO-LAYER FLOW. FLUID PROPERTIES ARE "AVERAGED" VERTICALLY WITH-IN EACH LAYER.

[d] A CLOSED-FORM SOLUTION CAN BE DERIVED FOR THE CASE OF ZERO AMBIENT CURRENT.

[e] MODEL EQUATIONS ARE DERIVED WITH DIRECT WIND STRESS INCLUDED: IN THE FINAL ANALYSIS, HOWEVER, WIND EFFECTS ARE NEGLECTED.

[f] THE ZONE OF FLOW ESTABLISHMENT IS HANDLED NUMERICALLY: THE ESTABLISHED-FLOW REGION IS TREATED BY INTEGRAL METHODS.

[g] A CLOSED-FORM SOLUTION HAS BEEN DERIVED FOR THE ESTABLISHED-FLOW REGIME FOR THE CASE OF ZERO WIND STRESS.

[h] THIS NUMERICAL MODEL MAY ALSO BE USED FOR FAR- AND COMPLETE-FIELD APPLICATIONS.

[i] A HORIZONTAL BOTTOM IS SIMULATED AT A DEPTH EQUAL TO THAT OF THE DISCHARGE. IN THE PRESENT FORM OF THE MODEL, THE POSSIBILITY OF A SLOPING BOTTOM IS NOT TREATED.

[j] COMPUTER PROGRAM INCLUDED WITH MODEL OR AVAILABLE FROM AUTHORS.

[k] COMPUTER CODE DOES NOT EXIST, YET MAY BE EASILY WRITTEN FROM MODEL EQUATIONS.

[t] COMPUTER CODE EXISTS, BUT IS PRESENTLY UNAVAILABLE FROM AUTHORS.

[m] COMPUTER PROGRAM WRITTEN AND AVAILABLE AT ARGONNE NATIONAL LABORATORY.

TABLE III. Summary of Characteristics of Complete-field Models
(ANL Neg. No. 190-989 Rev. 1)

		DIRECTION OF TEMPERATURE VARIATION			INITIAL MIXING (JET REGIME)	AMBIENT TURBULENCE (FAR-FIELD REGION)	MATHEMATICAL APPROACH				TIME DEPENDENT SOLUTION	BUOYANCY	CROSS FLOW	BOTTOM SLOPE	SURFACE HEAT LOSS	DISCHARGE GEOMETRY	PROVIDES FOR FLOW ESTABLISHMENT	AMBIENT STRATIFICATION INTERACTION	DIRECT WIND STRESS EFFECTS	RECIRCULATION OF PLUME WATER	COMPARED WITH FITTED WITH		COMPUTER PROGRAM
		LONGITUDINAL	LATERAL	VERTICAL			NUMERICAL	INTEGRAL	CLOSED FORM	SEMI-EMPIRICAL											FIELD DATA	TANK DATA	
16.	NADA (MODEL NO. 2)	YES	NO	YES	YES	YES	YES	NO	NC	YES	NO	YES	NO	YES	YES	YES	YES	NO	NO	YES	UNKNOWN	UNKNOWN	YES[a]
17.	PRITCHARD (MODEL NO. 1)	YES	YES	YES	YES	YES	NO	YES	YES	YES	NO	NO	NO	NO	YES	YES	YES	NO	NO	YES	YES	YES	YES[b]
18.	SUNDARAM ET AL.	YES	YES	NC	YES	YES	NO	NO	YES	YES	NO	NO	YES	NO	YES[c]	YES	NC	NO	NO	NO	YES	NO	YES[b]
19.	ELLIOTT AND HARKNESS[d]	YES	YES	NC	YES	YES	NO	YES	NC	YES	NO	NO[e]	YES	NO	NO	YES	NO	NO	NO	NO	YES	NO	YES[a]
20.	GILES ET AL.	YES	YES	YES	YES	YES	YES	YES	NC	YES	NO	NO	YES	YES	YES	YES	NO	NO	YES	YES	YES	NO	YES[f]
21.	LOZIUK ET AL.	YES	YES	NC	YES	YES	YES	NO	NC	YES	NO	NO	YES	NO	YES	YES	NO	NO	NO	NO	YES	YES	YES[a]
22.	BRADY AND GEYER	YES	YES	YES	YES	YES	YES	NO	NC	YES	YES	YES	YES	YES	YES	YES	YES	YES	YES	YES	NO	NO	YES[f]
23.	TILL	YES	YES	YES	YES	YES	YES	NO	NC	YES	NO	YES	YES	YES	YES	YES	YES	NO	NO	YES	YES	NO	YES[f]
24.	PRITCHARD[d] (MODEL NO. 2)	YES	YES	YES	YES	YES	NO	NO	YES	YES	NO	YES[e]	YES	YES	YES	YES	YES	NO	NO	NO	YES	YES	YES[b]

[a] COMPUTER PROGRAM EXISTS BUT IS PRESENTLY UNAVAILABLE FROM AUTHORS.

[b] COMPUTER CODE WRITTEN AND AVAILABLE AT ARGONNE NATIONAL LABORATORY.

[c] SURFACE HEAT LOSS WAS CONSIDERED ONLY IN THE FAR-FIELD REGIME.

[d] FACTORS SUCH AS BUOYANCY, BOTTOM SLOPE, SURFACE HEAT LOSS, FLOW-ESTABLISHMENT REGION, AMBIENT STRATIFICATION, WIND EFFECTS, AND PLUME RECIRCULATION ARE IMPLICIT IN THE EMPIRICAL DATA UTILIZED FOR MODEL DEVELOPMENT BUT ARE NOT SPECIFICALLY MODELED. THIS ALSO HOLDS TRUE FOR CROSS FLOW AND DISCHARGE GEOMETRY CONSIDERATIONS WITH REFERENCE TO PRITCHARD (MODEL NO. 2).

[e] DENSIMETRIC FROUDE NUMBER DEPENDENCY IS INCLUDED IN THIS MODEL ALTHOUGH BUOYANCY IS NOT SPECIFICALLY MODELED.

[f] COMPUTER PROGRAM INCLUDED WITH MODEL OR AVAILABLE FROM AUTHORS.

lateral slice of the jet: The first is the entrainment of lateral crossflow momentum, and the second is a net pressure force caused by eddying of the ambient fluid in the lee of the jet and by distortion of the jet boundaries. Explicit expressions must be assumed for both the entrainment function (to determine mass and momentum conservation) and the drag force per unit length (to determine momentum conservation). The assumed form of the entrainment velocity is

$$v_i = E(U - U_a \cos \beta),$$

where

v_i = inflow velocity (of entrainment),

U = local jet centerline velocity,

U_a = ambient current velocity,

β = local angle between jet centerline and ambient current,

and

E = entrainment coefficient.

The form of the assumed drag force is

$$F_D = \rho \frac{C_D U_a^2 z \sin \beta}{2},$$

where

F_D = drag force operating normal to jet axis,

C_D = experimentally determined drag coefficient,

and

z = jet depth.

This form for F_D is based on the assumption that the interaction of the jet with the ambient current can be treated as if the jet were a solid body and the resulting pressure gradients can be represented by a drag force. Utilization of the model requires the specification of the drag and entrainment coefficients, C_D and E, respectively.

In the region of established flow, the authors make similarity assumptions for velocity and temperature:

$$u(s,\eta) = U(s) \exp(-\eta^2/b^2)$$

and

$$T'(s,\eta) = T(s) \exp(-\eta^2/b^2),$$

where

u = local jet velocity,

T' = local jet temperature,

U = jet centerline velocity,

T = jet centerline temperature,

s = distance along jet centerline,

η = lateral distance from jet centerline,

and

b = characteristic width of lateral profiles.

The assumed forms for u, T', v_i, and F_D are used in the integral equations of conservation to yield the jet characteristics in the established flow regime.

To account for the zone of flow establishment, Motz and Benedict have developed phenomenological relationships for the length of the region of flow establishment (s_e') and the initial angle of the jet at the end of the region of flow establishment (β_0). These relationships are based on a series of laboratory hydraulic studies. No details of the temperature and velocity distribution in the region of flow establishment were determined, only its length and final angle with the shore. These studies yielded values for s_e', β_0, C_D, and E in terms of the ratio A of ambient to initial jet velocity and the actual initial angle of the jet with respect to shore, β_0'. (The authors, however, recommend a value for C_D of 0.5 be used for most cases.) Also needed is the width of the jet at the end of the region of flow establishment, $2b_0$. The authors suggest a value calculated by equating the heat flux at the point of discharge with the heat flux at the end of flow establishment. The actual width at the point of discharge is denoted by $2b_0'$.

B. Stolzenbach-Harleman Model

The mathematical model of Stolzenbach and Harleman[9] predicts the distributions of temperature and velocity within a completely determined jet structure for a near-field region, defined by the predominance of initial jet momentum over the effects of ambient lake turbulence.

Wherever possible, the model synthesizes previous knowledge of buoyant and nonbuoyant jets. The heated discharge is assumed to be structured in its physical characteristics as well as its assumed velocity and temperature distribution, basically like a classical, turbulent, nonbuoyant jet. Just as for nonbuoyant jets, the authors assume an initial core region void of shear followed by the main turbulent region. The basic jet structure assumed by Stolzenbach and Harleman appears in Fig. 53.

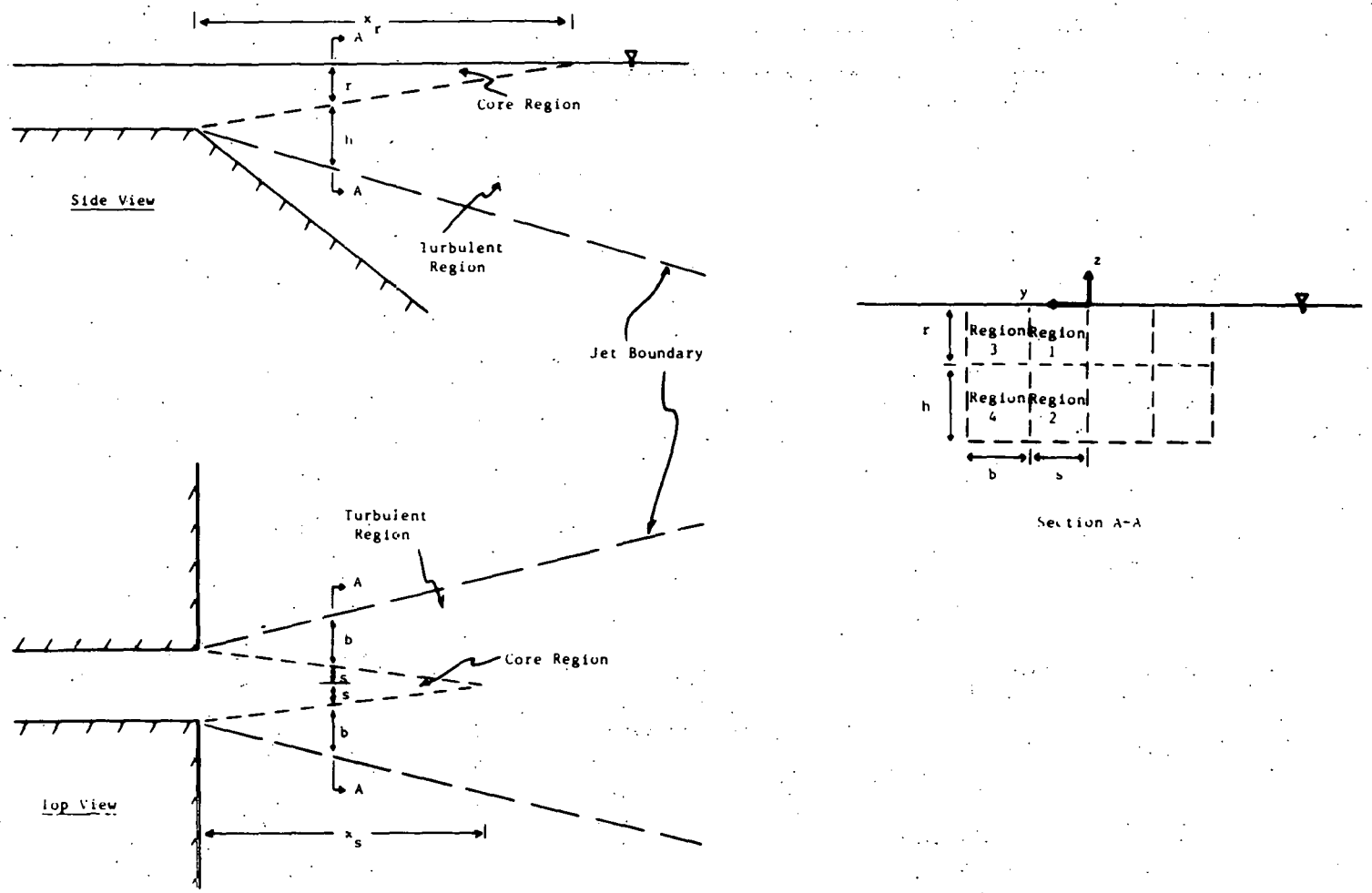

Fig. 53. Geometrical Characteristics of Jet Assumed in Stolzenbach-Harleman Model

Using an integral method as in most jet analyses, velocities and temperatures at each longitudinal cross section are presumed to be related to centerline values by similarity profiles. Figure 54 illustrates the similarity profiles assumed. These are represented mathematically by

$$u = u_c(x)F_y(y)F_z(z) - V \cos \theta$$

and

$$\Delta T = \Delta T_c(x)T_y(y)T_z(z),$$

where

$u, \Delta T$ - local value of velocity and temperature excess,

x,y,z = longitudinal, lateral, and vertical coordinates,

$V \cos \theta$ = component of ambient velocity normal to jet,

$$F_y = T_y = 1.0, \qquad 0 < |y| < s,$$

$$F_y = f(\zeta_y), \quad T_y = t(\zeta_y), \qquad s < |y| < b + s, \quad \zeta_y = \frac{|y| - s}{b},$$

$$F_y = T_y = 0, \qquad b + s < |y|,$$

$$F_z = T_z = 1.0, \qquad -r < z < 0,$$

$$F_z = f(\zeta_z), \quad T_z = t(\zeta_z), \qquad -r - h < z < -r, \quad \zeta_z = \frac{-z - r}{h},$$

$$F_z = T_z = 0, \qquad z < -h - r.$$

The form of the similarity functions (from Abramovich[28]) are

$$f = (1 - \zeta^{3/2})^2,$$

and

$$t = \sqrt{f} = 1 - \zeta^{3/2}.$$

The variables b, s, h, and r are defined in Figs. 53 and 54.

Horizontal and vertical entrainment of ambient fluid is related to the jet centerline velocity by appropriate entrainment coefficients. The lateral-entrainment coefficient is determined by nonbuoyant jet theory alone and is constant; the vertical-entrainment coefficient is related to the local temperature gradient by the local Richardson number, using the experimental results of Ellison and Turner,[29] and is chosen to reduce to the nonbuoyant value when no density gradients exist.

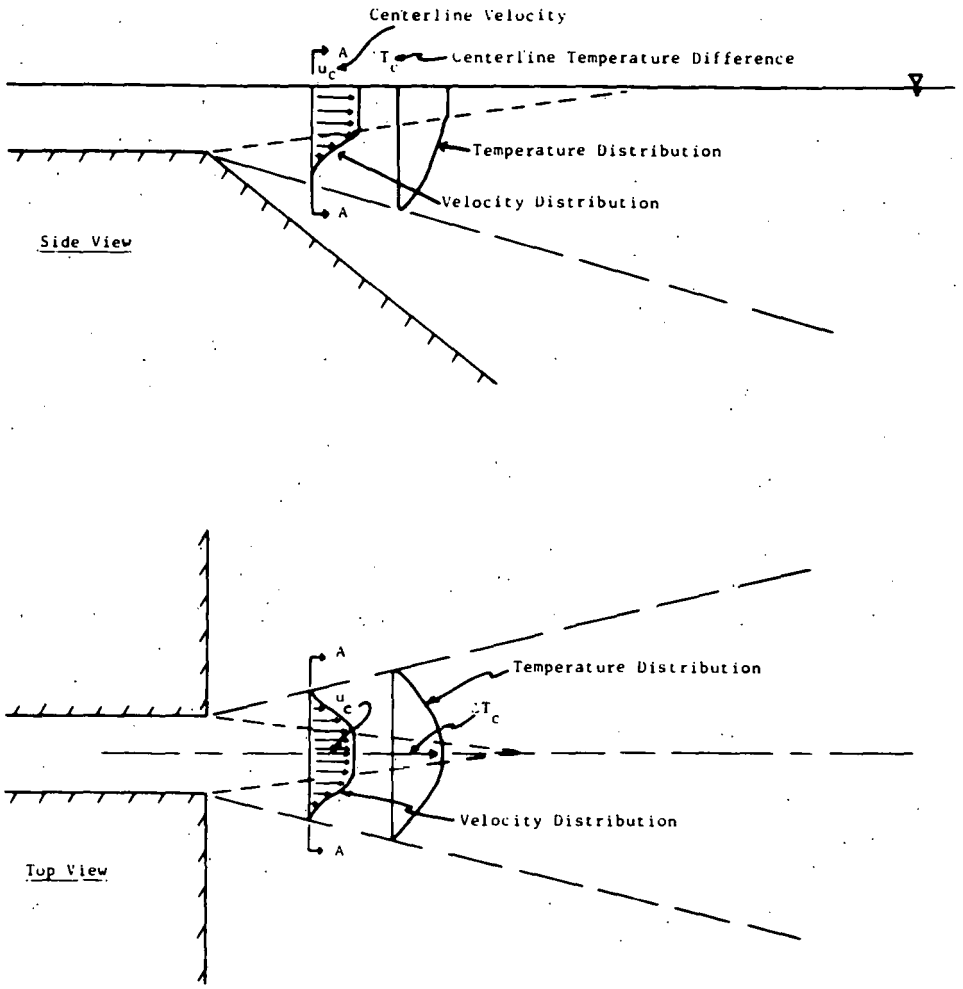

Fig. 54. Velocity and Temperature Characteristics of Jet Assumed in Stolzenbach-Harleman Model

Buoyant convection is incorporated through the pressure-gradient terms in the equations of motion and through the vertical-entrainment coefficient. Buoyancy effects generally reduce vertical entrainment and enhance lateral spreading.

To treat the interaction of these complex phenomena encompassing jet momentum, entrainment, buoyancy, and ambient crosscurrent, the authors developed their model from the steady, time-averaged differential equations of mass, momentum, and conservation of heat energy by dropping negligible terms, assuming a form for some of the unknown variables, and finally integrating the simplified equations over the four assumed regions of the jet longitudinal cross section.

Boundary conditions for the differential equations of mass, momentum, and energy (along with jet geometry) required assumptions for the boundary values of heat and mass fluxes as well as for internal lateral and vertical velocity distributions.

The set of conservation differential equations for a buoyant deflected jet are integrated over the jet cross section. The continuity and x-momentum equations are each integrated over all of the four regions defined in Fig. 53, yielding eight equations. The y-momentum equation is integrated over half the (symmetric) cross section to yield the ninth equation. The tenth is a jet-bending equation obtained from equating the rate of entrainment of lateral momentum to the rate of jet deflection. (No drag force on the jet is assumed.)

In this manner, the coupled flow and energy equations reduce to a system of simultaneous, first-order, nonlinear ordinary differential equations in the single variable x (longitudinal distance along jet centerline from the outfall), which are then solved numerically. The solution to the model equations yields three-dimensional temperature and velocity predictions as well as the jet physical characteristics.

The complete solution may be written in nondimensional form as

$$\left.\begin{aligned} \frac{T - T_a}{T_0 - T_a} &= \\ \frac{u}{u_0} &= \\ \text{jet characteristics} &= \end{aligned}\right\} \text{functions}\left(\mathbb{F}_0,\ A,\ \frac{K}{\rho c_p u_0},\ \frac{V}{u_0},\ \text{and } \alpha_0\right),$$

where

$$\mathbb{F}_0 = \frac{u_0}{\sqrt{\frac{\Delta\rho_0}{\rho_a} g h_0}} = \text{discharge densimetric Froude Number,}$$

$A = h_0/b_0$ = discharge-channel aspect ratio,

$\frac{K}{\rho c_p u_0}$ = surface-heat-loss parameter,

V = ambient crossflow velocity (possibly a function of offshore distance),

u_0 = channel outlet velocity,

α_0 = angle of discharge with respect to shoreline,

T_a = uniform lake water temperature,

T_0 = initial discharge temperature,

$\Delta\rho_0$ = density difference between discharged and ambient water,

ρ_a = density of ambient lake water,

g = acceleration due to gravity,

$2b_0$ = width of discharge canal,

h_0 = depth of discharge canal,

K = surface-heat-transfer coefficient,

ρ = density of water,

and

c_p = specific heat of water.

Thus the only site-dependent input parameters required are:

$$\mathbb{F}_0,\ A,\ \frac{K}{\rho c_p u_0},\ \frac{V}{u_0},\ \text{and}\ \alpha_0.$$

C. Prych Model

The Prych model[12] is based on a three-dimensional integral analysis of a turbulent, buoyant, horizontal, surface jet into a large, deep, uniform, turbulent flowing receiving water. Integral equations of conservation are written for mass, horizontal x and y momentum, and energy, as well as equations for the jet trajectory. Figure 55 illustrates the coordinate systems and the jet region. The model uses Gaussian similarity assumptions for temperature and velocity:

$$t(s,n,z) = T'(s) \exp[-n^2/B^2(s)] \exp[-z^2/H^2(s)]$$

$$u(s,n,z) = U(s) \exp[-n^2/B^2(s)] \exp[-z^2/H^2(s)] + V \cos\theta(s),$$

where

t, u = local values of temperature excess and velocity,

s, n = curvilinear coordinates along jet centerline parallel and perpendicular to the jet trajectory, respectively,

z = vertical distance from receiving-water surface,

$T'(s)$, $U(s)$ = centerline values of excess temperature and excess velocity,

$B(s)$, $H(s)$ = local characteristic width and depth of jet,

and

$V \cos\theta$ = component of ambient velocity parallel to jet trajectory.

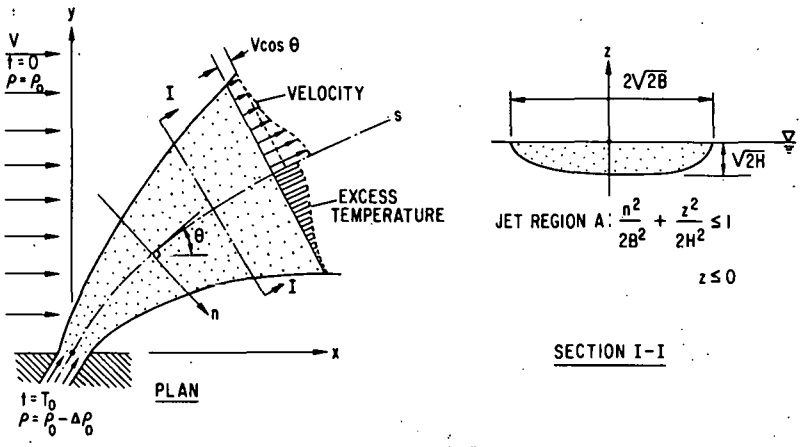

Fig. 55. Definition Sketch for Coordinate System and Jet Region Assumed in Prych Model. ANL Neg. No. 190-1045.

The rate of increase of the local jet flow due to incorporation of ambient water is included in the model by simulating entrainment due to jet mixing and also entrainment caused by turbulence in the ambient fluid. Horizontal and vertical rates of entrainment are calculated separately for both processes and are then summed. Prych computes jet entrainment in a manner similar to Stolzenbach and Harleman. Most notable is the requirement that the entrainment coefficient decreases with increasing fluid stability in the density-stratified jet. Prych calculates the contribution of ambient mixing to horizontal and vertical entrainment as $3.5\epsilon/\sigma$, where ϵ is the ambient turbulent diffusion coefficient (horizontal or vertical) and σ is the standard deviation of the lateral distribution of a tracer (excess temperature) in a two-dimensional jet. Prych assumes $\sigma = 2\sqrt{H}$ for the vertical direction.

Four force terms appear in the x- and y-momentum equations:

1. Ambient momentum flux in the direction of the ambient current.

2. Pressures due to the density differential between the fluid in the jet region and the ambient fluid. This force is assumed hydrostatic and is calculated by integrating the excess pressure force:

$$\int_{-\infty}^{z} g \frac{\Delta\rho_0}{T_0}(s,n,z')\,dz' \text{ over each vertical cross-sectional face.}$$

3. A form drag on the jet due to the pressure difference between offshore and lee sides of the jet, represented by

$$F_D = \tfrac{1}{2} C_D \sqrt{2} HV|V| \sin^2\theta,$$

where C_D = form-drag coefficient.

This force is computed in the same way one computes form drag on a solid body.

4. Interfacial shear stress between the jet fluid and the underlying ambient fluid. Prych approximates this force by modifying an expression for the shear stress at the base of a turbulent boundary layer on a smooth, flat, solid surface.

Once the basic conservation equations are integrated over the jet cross section using the above assumptions, a system of ordinary differential equations results that are solved for jet trajectory, jet width, jet depth, and jet-centerline temperature and velocity. A separate region of flow establishment is included with the same forces simulated as described previously.

The basic input parameters to the model are:

Q_0 - discharge flow rate from the outfall,

T_0 = excess temperature of jet (above ambient) at the outfall,

θ_0 = angle of discharge velocity vector with positive x axis,

$2b_0$ = width of outfall,

h_0 = depth of outfall,

V = ambient-current velocity (assumed constant),

$\Delta\rho_0$ = difference in density between ambient water and water from outlet,

K = surface-heat-transfer coefficient,

E_0 = jet-entrainment coefficient (horizontal),

C_D = form-drag coefficient,

and

C_F = (interfacial) shear-stress coefficient.

D. Pritchard Model

Pritchard's model[17] is basically a synthesis of previous theoretical- and physical-modeling results for buoyant and nonbuoyant jets, complemented by results the author has gleaned from field data obtained from existing power plants sited on bays, estuaries, and large lakes.

The model is simple and considers plume dispersion to be governed solely by momentum-jet entrainment, turbulent diffusion, and surface heat loss. An integral technique is used in which the plume velocity and excess temperature (above ambient) are assumed to have, at each longitudinal position, a "tophat" distribution laterally and vertically. Buoyancy-induced convective motions are not explicitly considered. No ambient current is assumed to exist in the theoretical development; yet, the author expects that the predicted centerline-temperature decay and areas within isotherms

will still be accurate in the presence of a current less than 10% of the initial discharge velocity. In the model, environmental changes are reflected solely in the surface-heat-transfer coefficient, K. Entrainment is accounted for by the specification of a fixed inverse spreading-rate parameter, n, normally taken to be about 6. The lake bottom is assumed to have no effect other than upon the author's choice of a plume depth and, when necessary, upon the length and depth of an initial region of vertical entrainment.

The model handles both the jet and far-field regions; it predicts a two-dimensional temperature field and areas within isotherms down to a 0.56C° (1.0F°) temperature excess. The parameters required for the application of this model are:

b_0 = width of rectangular outfall,

h_0 = depth of rectangular outfall,

Q_H* = excess heat-rejection rate of power plant based on θ_0,

θ_0 = initial excess temperature of the jet,

and

K = surface-heat-loss coefficient.

In spite of the simplifications made in the model development, the author claims the model to be conservative in many respects and simple to apply.

The author's theoretical development is carried out in four consecutive stages:

1. Horizontal spreading is considered, neglecting vertical diffusion and surface heat loss to the atmosphere. A two-dimensional temperature field is determined for the jet and far-field regions by the integral equations of conservation. Centerline temperature and velocity is found to drop off as $1/\sqrt{s}$ in the jet regime, where s is the distance along the centerline after a constant region of flow establishment of length $6b_0$. For the far-field region, excess temperature is assumed to drop off as $1/s$.

2. Vertical entrainment is then considered independent of horizontal spreading and surface heat loss. The depth is assumed constant, except possibly for a small region in the vicinity of the outfall, where the depth grows slowly in a linear fashion. When vertical spreading is assumed to occur, a correction of the two-dimensional temperature field is made to account for the additional dilution. For Lake Michigan, Pritchard suggests that vertical

---

*Q_H would be identically equal to the total condenser heat-rejection rate if the condenser intake temperature were identically equal to the ambient temperature.

spreading be allowed for until the plume depth reaches 3.05 m (10 ft). For a greater initial depth, the jet is assumed to remain at that constant depth throughout the complete field.

3. A second correction of the temperature field may be needed, depending on the temperature of the water entrained into the plume. Due to possible recirculation of condenser cooling water, the diluting water mixed into the plume may have an excess temperature above ambient. Once this additional correction on the temperature field is made, the areas within isotherms can then be calculated for the condition of mixing alone.

4. Surface heat losses are then included in the analysis as a correction to the areas derived in stage 3. This surface-heat-loss correction yields the final two-dimensional temperature field and the isotherm areas.

VII. MODEL COMPARISONS TO DATA

Table IV summarizes the basic discharge and environmental parameters required for application of the analytical models to the four Point Beach cases and the single Palisades case. Parameters such as entrainment and drag coefficients were chosen, based upon the recommendations of the model authors. In some cases (especially with the Motz-Benedict model), no clear-cut choice exists for some of the required parameters. This problem is discussed in more detail in Sec. VIII.C.2 below.

The data, JETFIT-smoothed results and model predictions are discussed and compared with respect to some of the major jet characteristics in the following paragraphs.

A. Jet Trajectories

Figures 56-60 show the jet trajectories resulting from JETFIT and the four model predictions. Before the analytical models are compared to the jet trajectory data, a few comments should be made regarding the JETFIT trajectories themselves. Figure 56 shows the jet centerline to bend gradually toward the north-shore direction (negative x direction). In a similar fashion, Fig. 57 shows the jet to bend gradually toward the south-shore direction (positive x direction). In both cases, the ambient current has been assigned a nominal value of zero, based on field measurements. Possible causes of the seemingly anomalous behavior may be combinations of the following:

1. A small but undetectable ambient current, directed north on May 18 and south on May 23, may have been present. The threshold of the instrument used for measuring ambient current is about 3.0 cm/sec; consequently, any current below or near this value is virtually undetectable. Further, the ambient-current conditions were measured at a limited number of specific locations. A small current could possibly have been detected at some other location, since near-shore current measurements are known to be spatially and temporally unsteady.

2. Local gyres might exist in the region of the outfall. The intrusion of the 33-m discharge structure into a small ambient-current field will cause local eddies and gyres to form in the vicinity of the discharge. Data taken near the outfall may be influenced by them. Also, a return current on the lee side of the jet (when an ambient current exists) or on both sides of the jet (when no ambient current is present) is required to provide water to the jet as it disperses due to jet entrainment and ambient mixing. When an ambient current exists, the region between the outer boundary of the jet on the lee side and the shoreline will be likely to contain eddies of continually recirculating water.

3. Lake-bottom irregularities in the vicinity of the discharge might influence the jet trajectory. The contours in Fig. 6 represent average values

TABLE IV. Data and Parameters Used for Model Calculations for Point Beach and Palisades
(ANL Neg. No. 190-956 Rev. 1)

General Data and Parameters	Point Beach Unit No. 1				Palisades
	May 18	May 23	July 13	September 9	October 10
Ambient Water Temperature (0.5-meter depth)	9.2°C	14.3°C	13.0°C	16.3°C	13.0°C
Ambient Current Speed	0	0	5.7 cm/sec	2.2 cm/sec	0
Average Wind Speed	1.9 m/sec	1.0 m/sec	1.5 m/sec	3.7 m/sec	2.0 m/sec
Width of Outfall	10.7 m	10.7 m	10.7 m	10.7 m	28.3 m
Depth of Outfall (average)	4.2 m	4.2 m	4.2 m	4.2 m	2.1 m
Angle of Outfall with Shore	60°	60°	60°	60°	90°
Discharge Flow Rate	24.7 m^3/sec	25.1 m^3/sec	24.7 m^3/sec	24.7 m^3/sec	25.6 m^3/sec
Outfall Temperature	17.7°C	21.6°C	20.3°C	24.5°C	22.2°C
Average Outfall Velocity	54.7 cm/sec	55.5 cm/sec	54.7 cm/sec	54.7 cm/sec	42.3 cm/sec
Initial Froude Number	2.57	2.37	2.42	2.06	2.27
Surface-heat-transfer Coefficient	242 kcal/m^2-day-C°	197 kcal/m^2-day-C°	166 kcal/m^2-day-C°	459 kcal/m^2-day-C°	281 kcal/m^2-day-C°
Additional Parameters for Pritchard Model					
Inverse Spreading Rate	6.0	6.0	6.0	6.0	6.0
Critical Mixing Depth	4.2 m	4.2 m	4.2 m	4.2 m	3.0 m
Temperature Excess of Recirculated Water	0	0	0	0	0
Additional Parameters for Motz-Benedict Model					
Length of Flow-establishment Region	55.5 m	55.5 m	30.4 m	45.3 m	147.2 m
Angle at End of Flow-establishment Region	60°	60°	49.9°	52.3°	90°
Width at End of Flow-establishment Region	8.5 m	8.5 m	8.5 m	8.5 m	22.6 m
Entrainment Coefficient	0.05	0.05	0.307	0.126	0.04
Drag Coefficient	0.5	0.5	0.5	0.5	0.5
Additional Parameters for Stolzenbach-Harleman Model					
Aspect Ratio	0.79	0.79	0.79	0.79	0.151
Additional Parameters for Prych Model					
Entrainment Coefficient	0.1	0.1	0.1	0.1	0.1
Drag Coefficient	0.2	0.2	0.2	0.2	0.2
Interfacial-shear-stress Coefficient	0.5	0.5	0.5	0.5	0.5

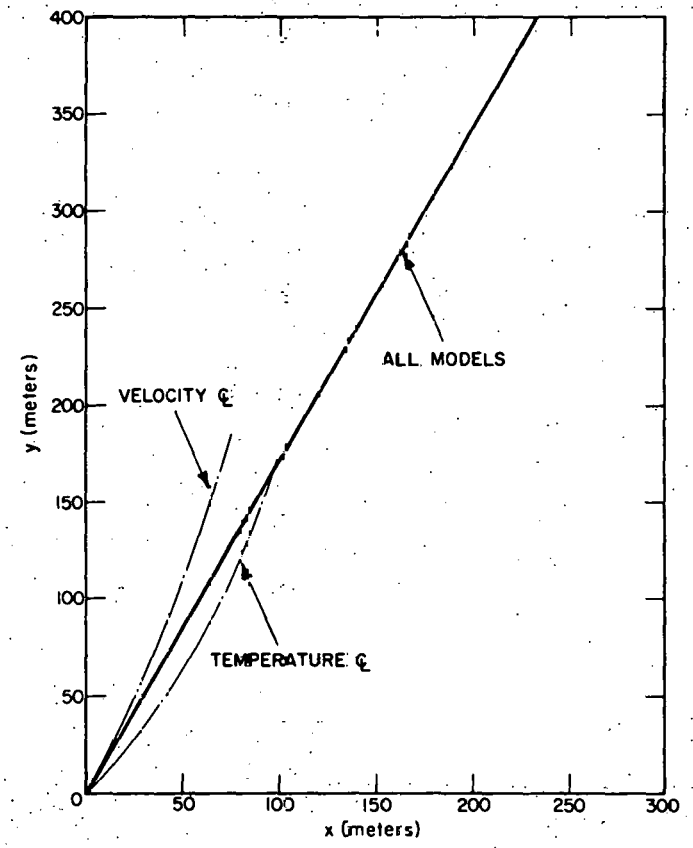

Fig. 56. Centerline Trajectories Resulting from the Fitting Procedure and Model Calculations for Point Beach: May 18, 1972. ANL Neg. No. 190-935.

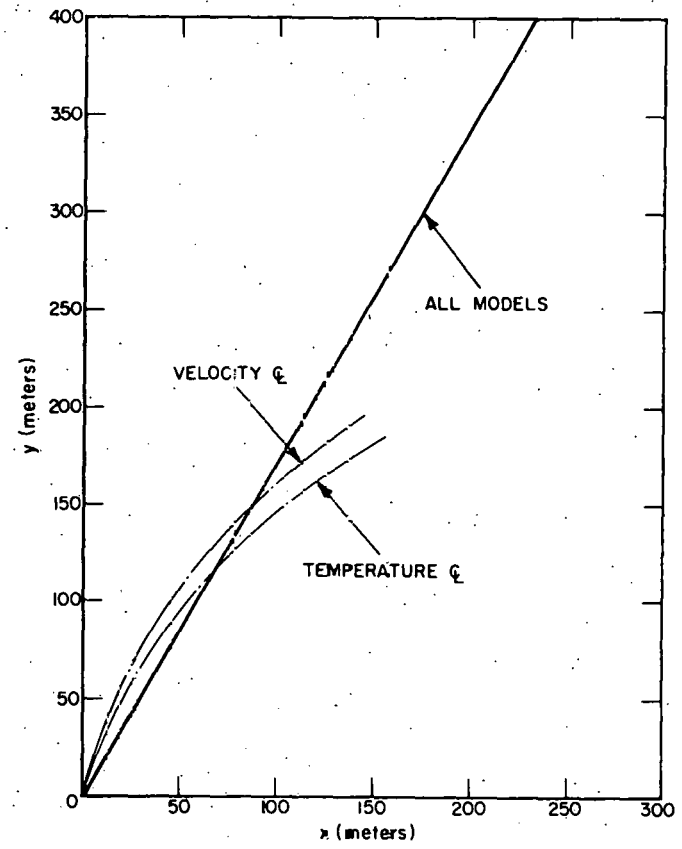

Fig. 57. Centerline Trajectories Resulting from the Fitting Procedure and Model Calculations for Point Beach: May 23, 1972. ANL Neg. No. 190-936.

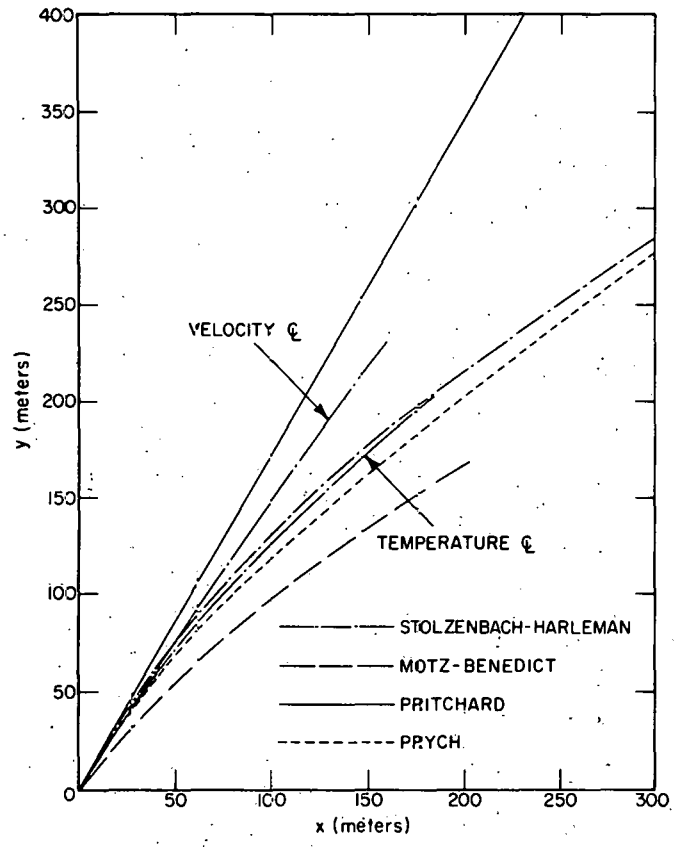

Fig. 58. Centerline Trajectories Resulting from the Fitting Procedure and Model Calculations for Point Beach: July 13, 1972. ANL Neg. No. 190-940.

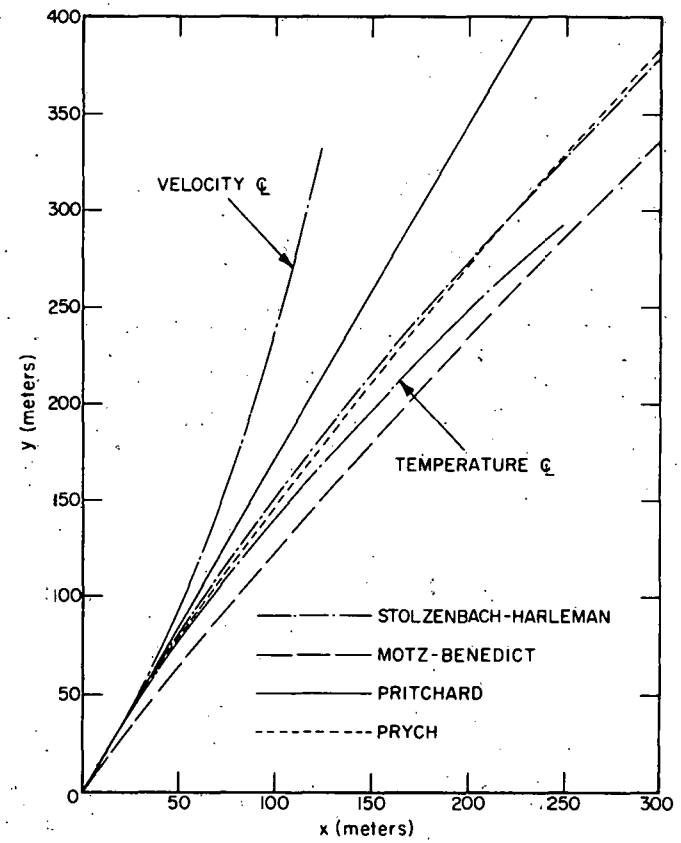

Fig. 59. Centerline Trajectories Resulting from the Fitting Procedure and Model Calculations for Point Beach: September 9, 1972. ANL Neg. No. 190-948.

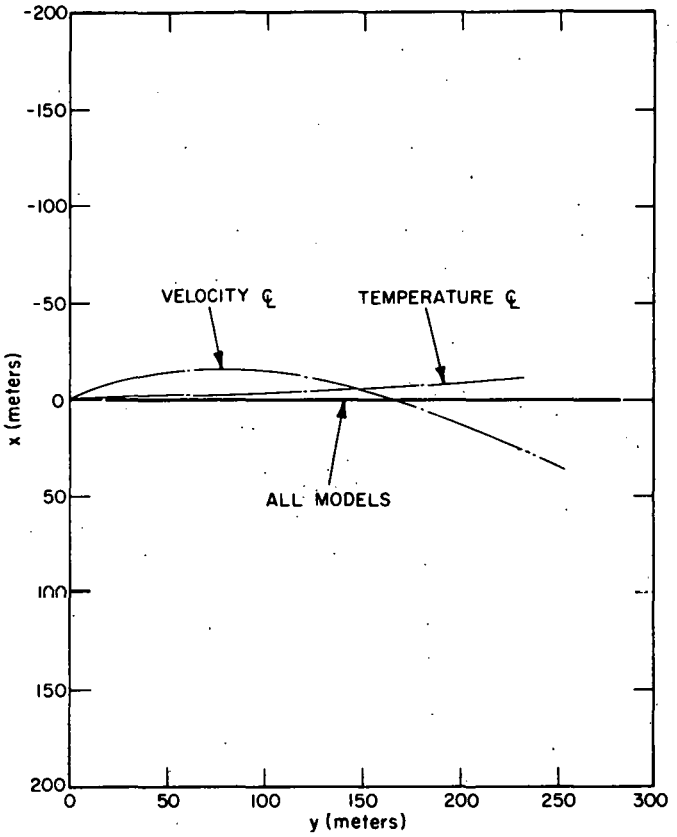

Fig. 60. Centerline Trajectories Resulting from the Fitting Procedure and Model Calculations for Palisades: October 10, 1972. ANL Neg. No. 190-957.

of bottom soundings taken at several different dates in 1972. Continual operation of the Point Beach Unit 1 discharge has apparently dug out a small channel directly off the discharge. A small ridge appears north of the discharge canal, as well as a small bar just south of the outfall. Changes in the local bottom contours are possible, due to occasional storms in the area and daily variation in both ambient current and discharge conditions.

4. The fitting of symmetric profiles of temperature and velocity, as used in JETFIT, to distributions that are probably unsymmetric when an ambient current exists, may influence the apparent location of the centerline. Figure 61 illustrates a somewhat more realistic profile of centerline excess temperature θ/θ_0 and jet-centerline-velocity ratio u/u_0 (in the lateral direction) for a bent jet near the outfall. The profiles are based on hydraulic-model measurements by Carter[25] for an outfall angle β_0 of 60° and a ratio of outfall to ambient current, R, of 2.0. The JETFIT data discussed here are for R = 10 to ∞ (i.e., weak currents), which should reduce but not eliminate the asymmetry of the velocity and temperature profiles shown in the figure. Any asymmetry due to an ambient current should bias the centerline fit to the

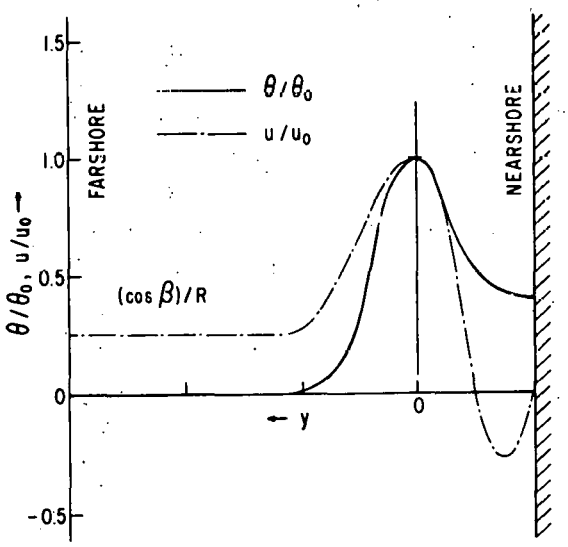

Fig. 61

Idealized Surface Profile of Excess Temperature θ/θ_0, and Velocity u/u_0 across (y direction) Bent Jet near Orifice (based on measurements). R = 2 (nominal) and β_0 = 60° (Ref. 25).

lee direction for the temperature centerline and to the offshore direction for the velocity centerline. This might explain the relative orientation of velocity and temperature centerlines for May 23, July 13, and September 9 Point Beach data (Figs. 57-59). The velocity centerline is also upstream of the temperature centerline for the fitting results at the other depths on these dates; discrepancies when occurring were very small and could, however, just as easily have been caused by insufficient data. Far-field temperature measurements taken several hours later at 1645-1751 hours on May 18 (not presented here) indicate a southerly directed plume under the influence of a small ambient current. The results of May 18 seem to be largely biased by data measurements at Station No. 5, where the plume appears to be directed northward. There is the possibility of a small wind-induced current directed north existing near the third transect offshore in opposition to a southerly moving ambient current. Also, note that Station No. 7 with zero velocity was eliminated from the JETFIT calculation, since it was not thought to be a point in the thermal plume. This would bias the velocity centerline in a southerly direction on May 18. More data are necessary to more accurately define the centerlines in this case.

5. Uncertainties in the data (up to ±0.5C° for temperature, ±20% for velocity magnitude, ±12° of velocity direction) and the limited amount of data available clearly influence the fitting results. The temperatures recorded were averaged over 1- to 2-min time intervals; thermal fronts have been observed (Ref. 30) that can change the plume temperature at a fixed point at Point Beach up to 3C° in 1-2 sec. The appearance and frequency of such fronts (estimated to be from 30 sec to several minutes) will be important in any given averaged measurement. Determination of ambient temperatures and currents is also important to the analysis, yet are difficult to determine in the field.

Several of the general comments given in paragraphs 2-5 above also apply to the jet data of July 13 and September 9. On September 9, Unit 2 at Point Beach was operating at 12% power with only one of the two available pumps. This corresponds to a flow rate of about 14 m^3/sec with a temperature excess above ambient of about 2C°. Clearly, the velocity distribution should be affected by this second discharge, with the temperature field perturbed only slightly. The nonlinear interaction of flow and temperature fields complicates any further evaluation of resultant effects.

Analytical model predictions for May 18 and May 23 at Point Beach were based on a zero-ambient-current value. Consequently, a straight-line trajectory was predicted by all models. The JETFIT results for these dates yielded only slight differences from a straight-line trajectory, probably due to the reasons given previously. Models will be compared to the temperature centerline of the jet, since it is generally of greater interest than the velocity centerline.

The Stolzenbach-Harleman model and the Prych model appear most accurate for the dates with a measured ambient current. Prych predicts greater bending than Stolzenbach and Harleman for both dates. The Pritchard model suggests only a small change in trajectory from a straight line for situations in which a small ambient current exists. Consequently, a straight-line trajectory is shown for Pritchard in Figs. 58 and 59. The Motz-Benedict model overpredicts jet bending for both dates. As stated above, the model is very sensitive to the value of the entrainment coefficient chosen.

Interpreting the Palisades results is difficult for several reasons. First, the lake bottom in the vicinity of the discharge is very shallow, as may be seen in Fig. 7. This may inhibit any significant vertical entrainment. For the first 100 m, the lake bottom is at approximately the depth of the outfall. At the north end (positive y-direction) of the diverging Palisades outfall, lake water occasionally enters the discharge channel. The discharge cross section is highly irregular, as sketched in Fig. 62. The discharge width, b_0, was chosen as 28.3 m, since it is the channel width at the lake opening. The discharge depth h_0 was chosen to be

$$h_0 = \frac{\text{discharge area}}{b_0};$$

the calculated h_0 was then averaged for the three dates shown in Fig. 62.

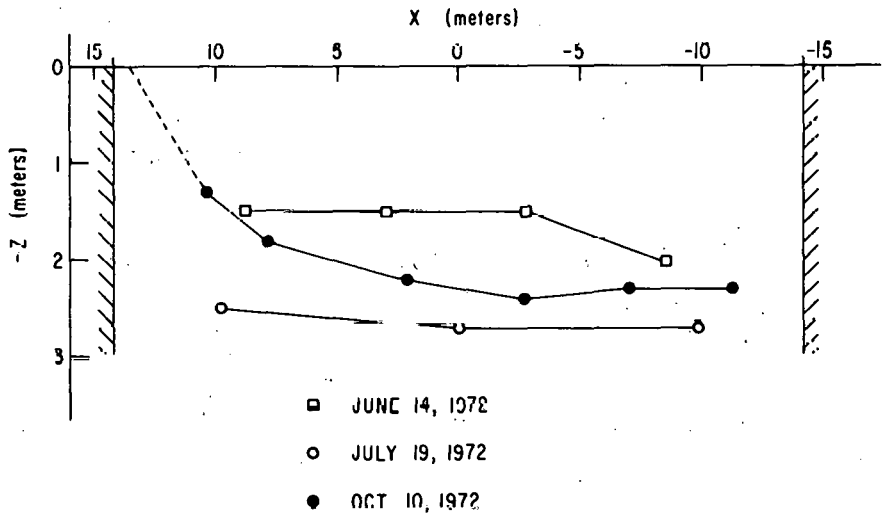

Fig. 62. Bottom Depth at Palisades Outfall for Three Dates of Jet Studies

Considering the significant bottom interaction that undoubtedly occurs in this case, all model predictions will be considered qualitatively only. Zero ambient current on October 10 clearly implies no bending for model predictions; JETFIT results indicate little deviation from this position (see Fig. 60).

B. Centerline Temperature Decay and Temperature Half-widths

The centerline excess temperatures resulting from JETFIT and the four model predictions are shown in Figs. 63-67. The assumed parametric temperature profile to which the jet data was fitted with JETFIT is again

$$\theta(\eta,s) = \theta_c(s)\left(\frac{1}{2}\right)^{[\eta/W_T(s)]^2},$$

where

$$\theta_c(s) = \theta_0 A \qquad \text{for } s \le \frac{\alpha b_0}{A^2}$$

$$= \theta_0 \sqrt{\frac{\alpha b_0}{s}} \qquad \text{for } s > \frac{\alpha b_0}{A^2},$$

$$W_T(s) = Cb_0 + \gamma s,$$

and A, α, C, and γ are fitted parameters. It is clear from Figs. 63-67 that the temperature excess near the outfall from the data-smoothing procedure can be different from θ_0. This corresponds to $A \neq 1$.

The values of A, α, and length of region of flow establishment $s_0 = \alpha/A^2$ (in units of the outfall width) for the four Point Beach dates considered are:

	May 18	May 23	July 13	September 9
A	0.84	0.84	0.92	0.79
α	3.8	5.6	6.2	4.5
s_0	5.38	7.95	7.32	7.22

The values of s_0 do compare with values in the range from 5 to 7 usually quoted in the literature. However, the above Point Beach numbers certainly reflect insufficiencies in the data and inadequacies in the fitting procedure; consequently, much significance should not be attached to them.

Since $\theta \neq \theta_0$ (i.e., $A \neq 1$) at the outfall, one should not place much significance on the results of the fitting procedure for the first 50-100 m. It may have been more profitable to have A fixed at 1.0 and introduce a new parameter ϵ as the power of $\alpha b_0/s$ in the formula for $\theta_c(s)$. (The present formulation restricts ϵ to a value of 1/2.) The fit would then involve α, ϵ, C, and γ. It is not expected, however, that the present JETFIT results would be altered significantly if such changes were implemented in the fitting function. One further comment: The results of JETFIT for the jet characteristics most generally agreed with what one would expect from visual examination of the data along each transect of the jet. This gives additional confidence to the JETFIT results.

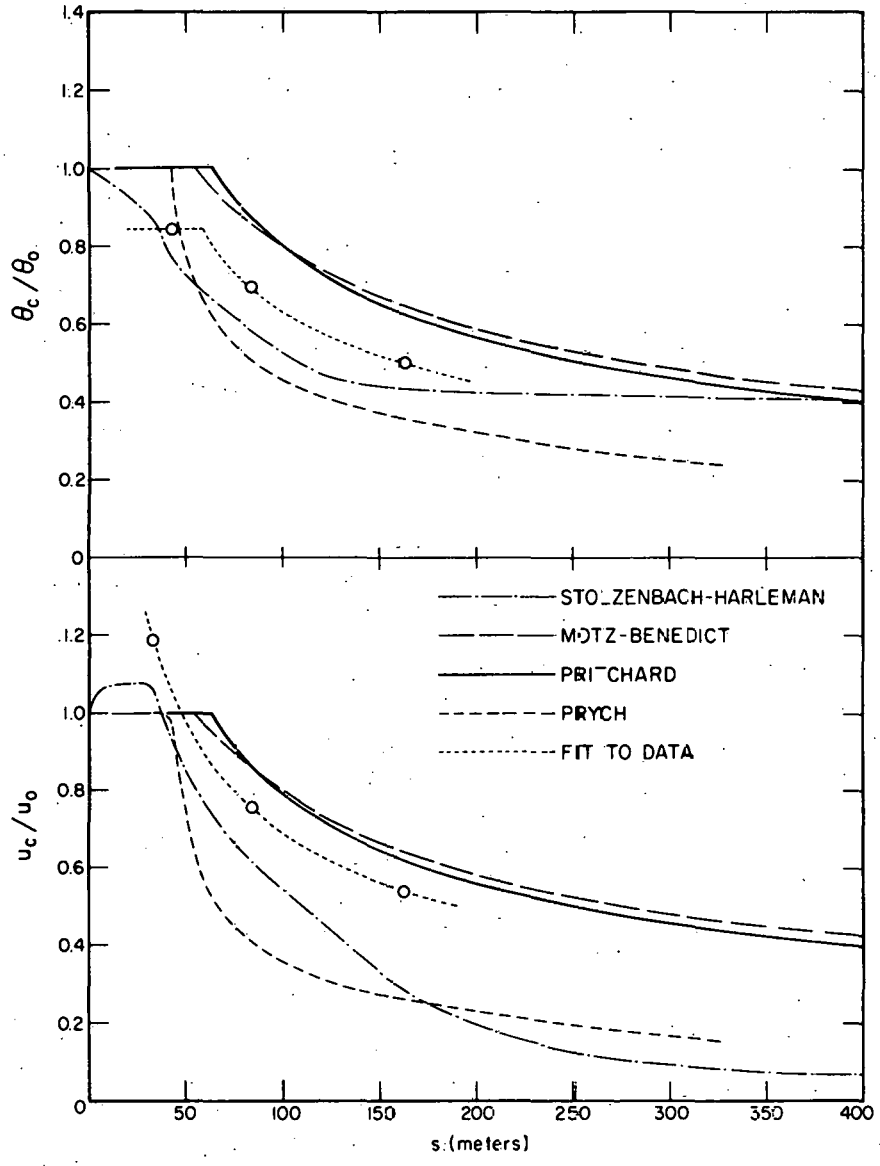

Fig. 63. Centerline Temperature Excess and Velocity Decays Resulting from the Fitting Procedure and Model Calculations for Point Beach: May 18, 1972. ANL Neg. No. 190-952.

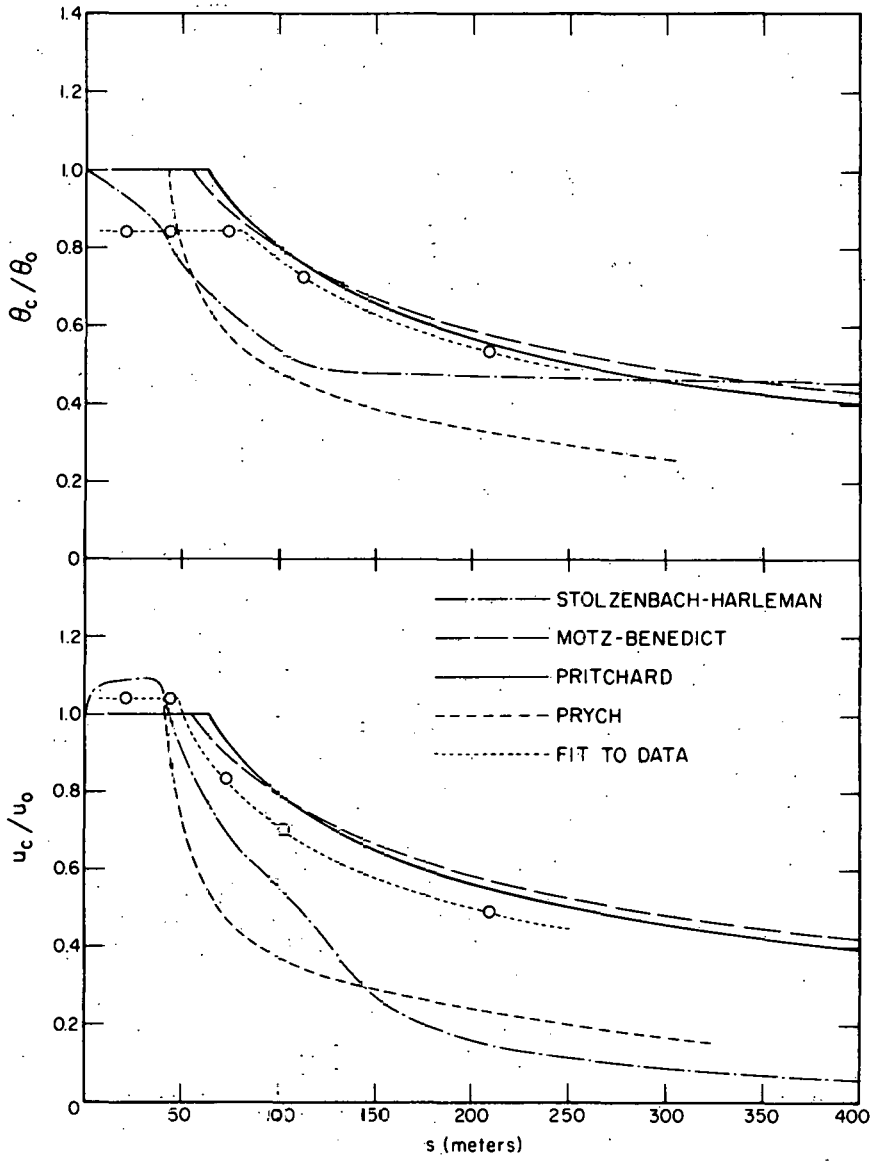

Fig. 64. Centerline Temperature Excess and Velocity Decays Resulting from the Fitting Procedure and Model Calculations for Point Beach: May 23, 1972. ANL Neg. No. 190-949.

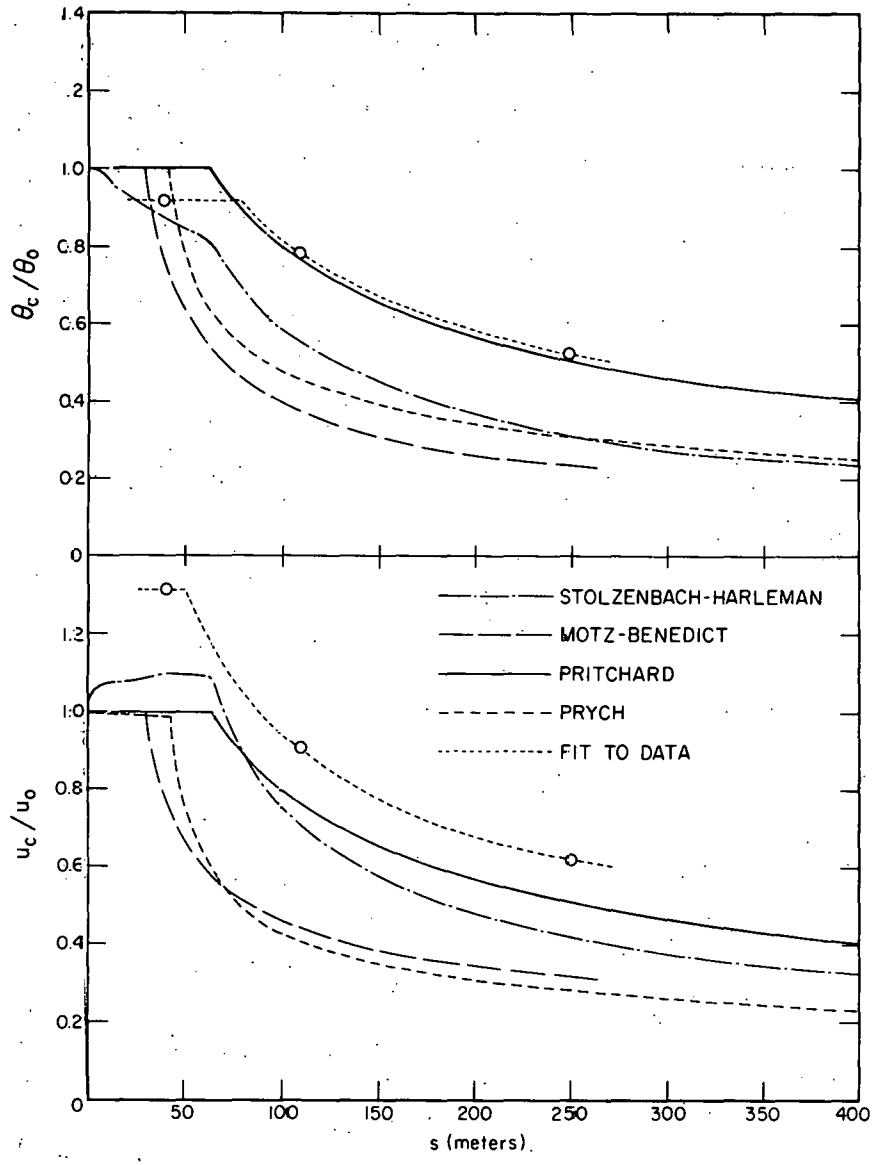

Fig. 65. Centerline Temperature Excess and Velocity Decays Resulting from the Fitting Procedure and Model Calculations for Point Beach: July 13, 1972. ANL Neg. No. 190-958.

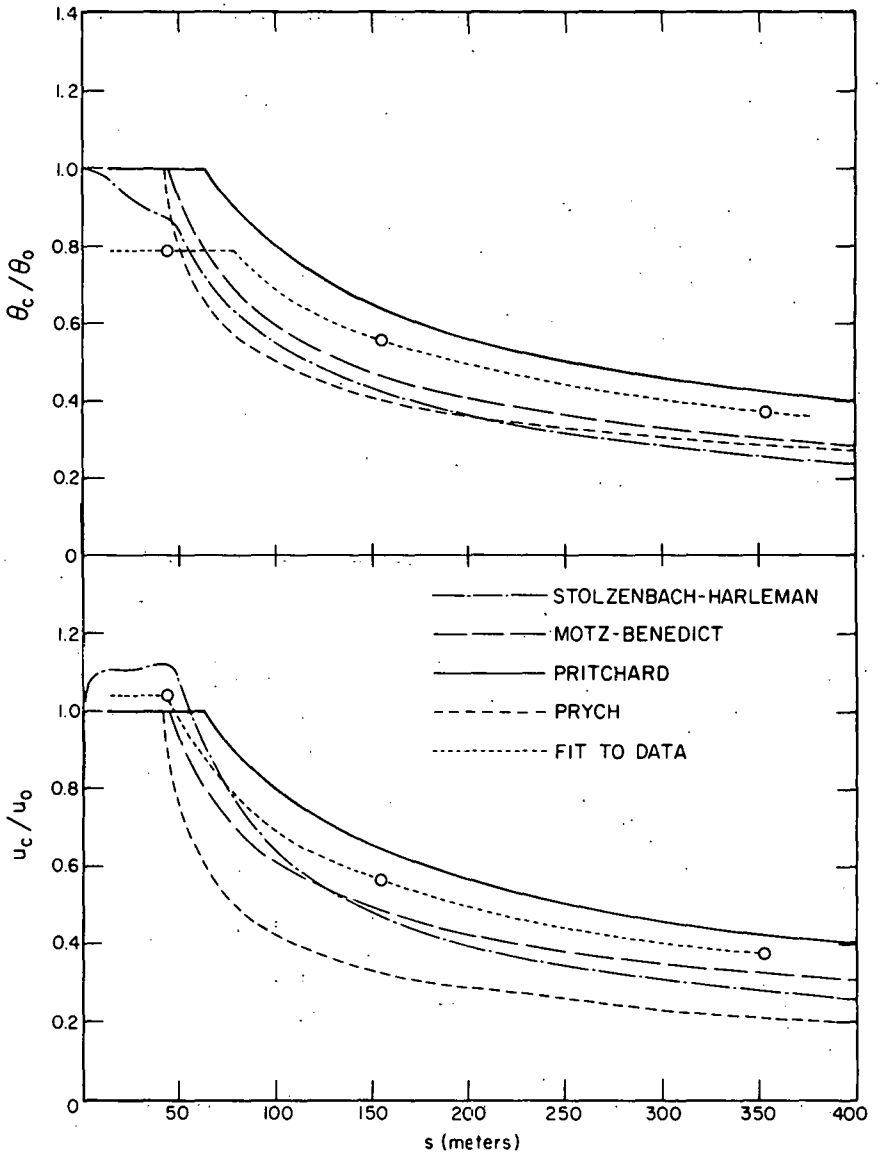

Fig. 66. Centerline Temperature Excess and Velocity Decays Resulting from the Fitting Procedure and Model Calculations for Point Beach: September 9, 1972. ANL Neg. No. 190-951.

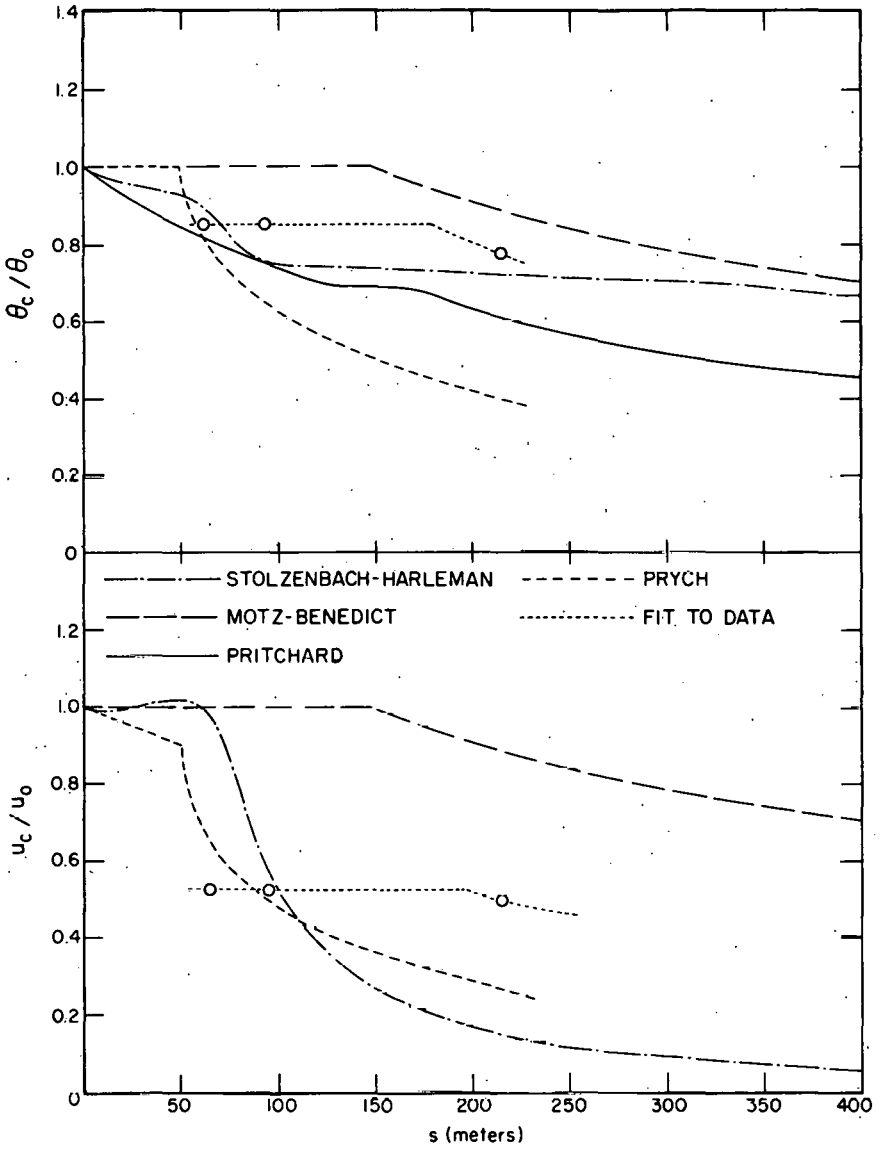

Fig. 67. Centerline Temperature Excess and Velocity Decays Resulting from the Fitting Procedure and Model Calculations for Palisades: October 10, 1972. ANL Neg. No. 190-960.

The Pritchard model appears most accurate and also conservative for the four Point Beach cases of Figs. 63-66. Both JETFIT and the Pritchard model have centerline temperature decay rates proportional to the -1/2 power of the centerline distance; hence, both curves become parallel as s increases. The Motz-Benedict model gives reasonably conservative predictions for the no-current cases of May 18 and May 23 where the entrainment coefficient was chosen to be 0.05. (Benedict recommends 0.04 for a 90° outfall and suggests a slight increase for an off-90° discharge.) The model does poorly on July 13 and September 9, apparently due to the choice of entrainment coefficient. The authors' recommendation for the value of the entrainment coefficient for cases with ambient current less than $0.2u_0$ is not clear. The model overpredicts temperature decay for both these cases. The Stolzenbach-Harleman and Prych models both predict a much greater temperature decay than the data indicate. When no current exists, the Stolzenbach-Harleman decay is initially very abrupt,

yet tends to level off after about 125 m; the centerline temperature data eventually drop below the model results. For the current cases of July 13 and September 9, the centerline decay of Stolzenbach and Harleman is more regular, yet is too rapid. The Prych model predicts too great a temperature decay, yet does so at a rather regular rate of decrease, seemingly independent of an ambient current. Moreover, Prych predicts lower temperatures than Stolzenbach and Harleman, at least within the first 200-250 m from the outfall. Beyond this point, the two models run nearly parallel.

Figures 68-72 show the widths W_T of the excess temperature distributions resulting from JETFIT and the model calculation. (Note that the linearity of the JETFIT results is a consequence of the linear form assumed in the fitting function.) A very rapid rate of lateral spreading is apparent for the Prych and Stolzenbach-Harleman models. Both models require an assumed form for a lateral spreading velocity that is instrumental in determining the

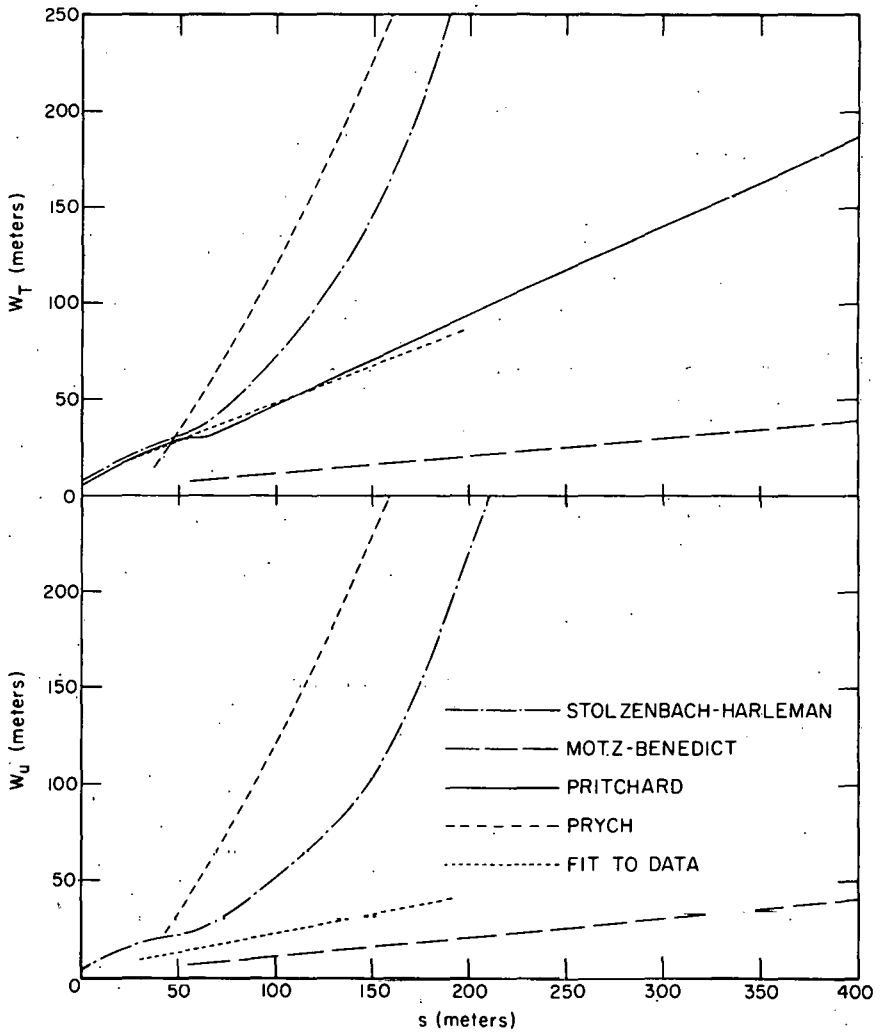

Fig. 68. Half-widths of Temperature and Velocity Distributions Resulting from the Fitting Procedure and Model Calculations for Point Beach: May 18, 1972. ANL Neg. No. 190-947.

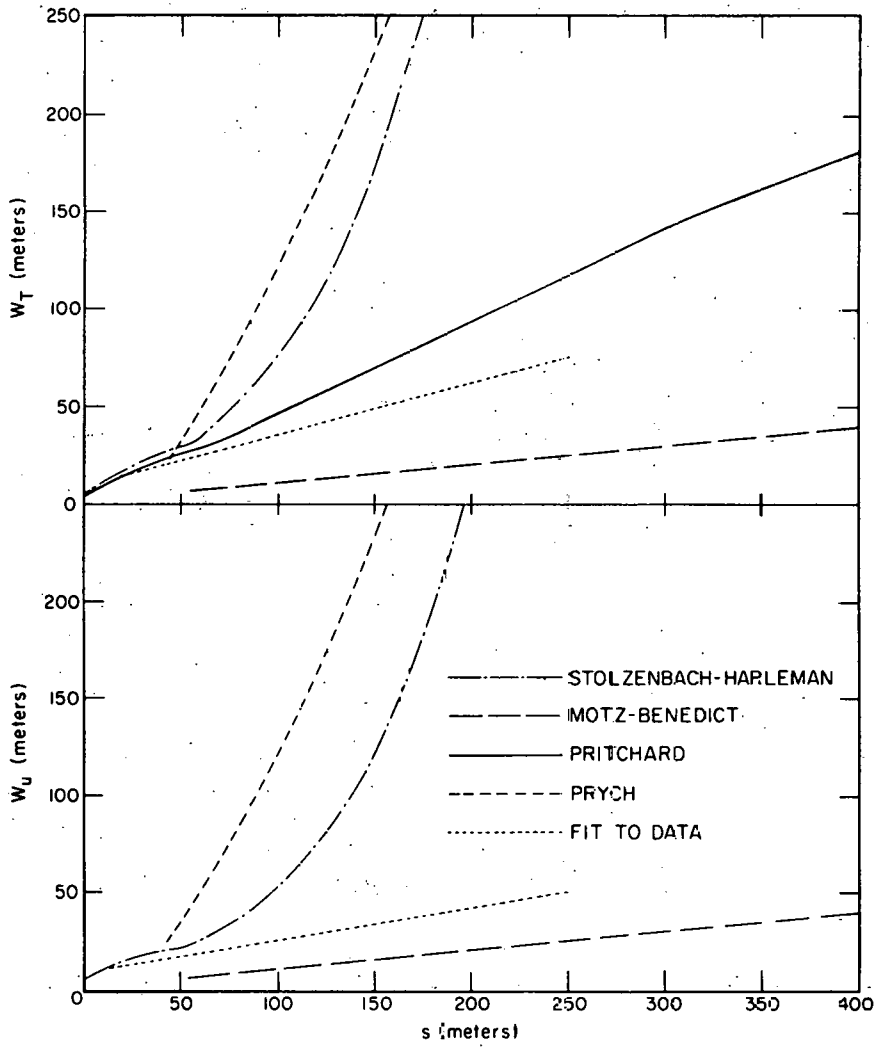

Fig. 69. Half-widths of Temperature and Velocity Distributions Resulting from the Fitting Procedure and Model Calculations for Point Beach: May 23, 1972. ANL Neg. No. 190-946.

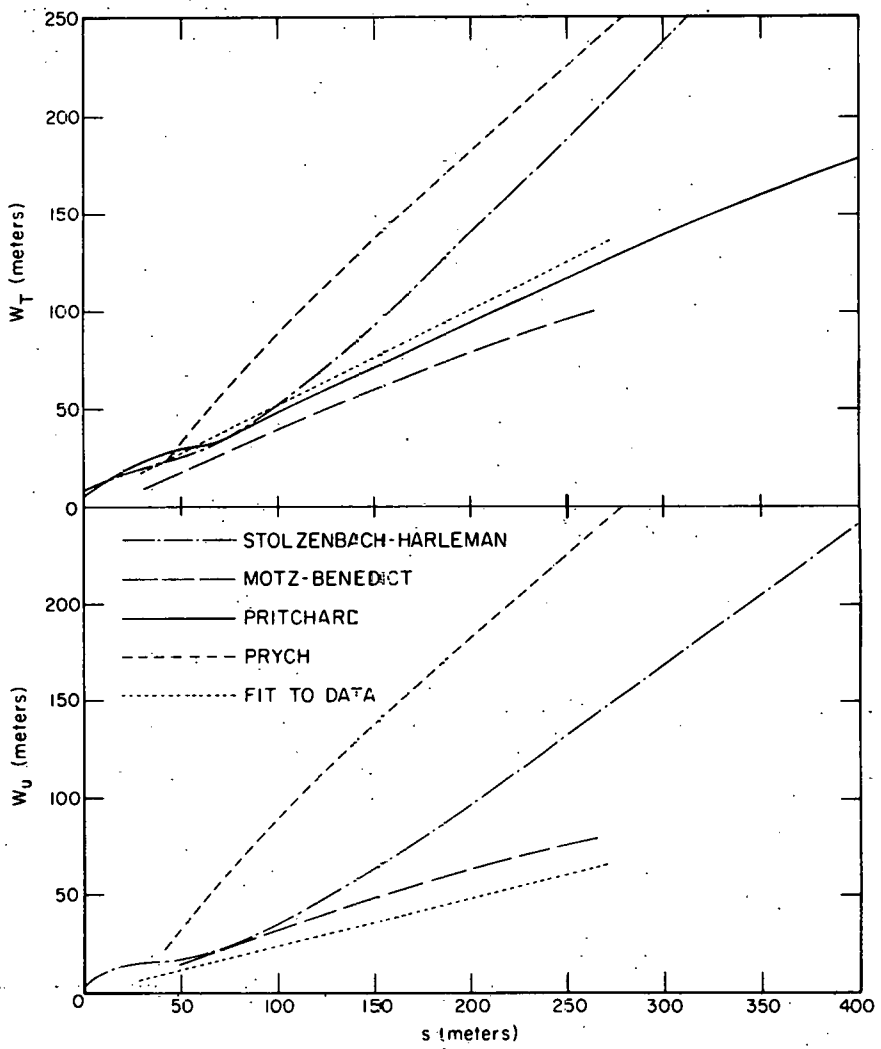

Fig. 70. Half-widths of Temperature and Velocity Distributions Resulting from the Fitting Procedure and Model Calculations for Point Beach: July 13, 1972. ANL Neg. No. 190-942.

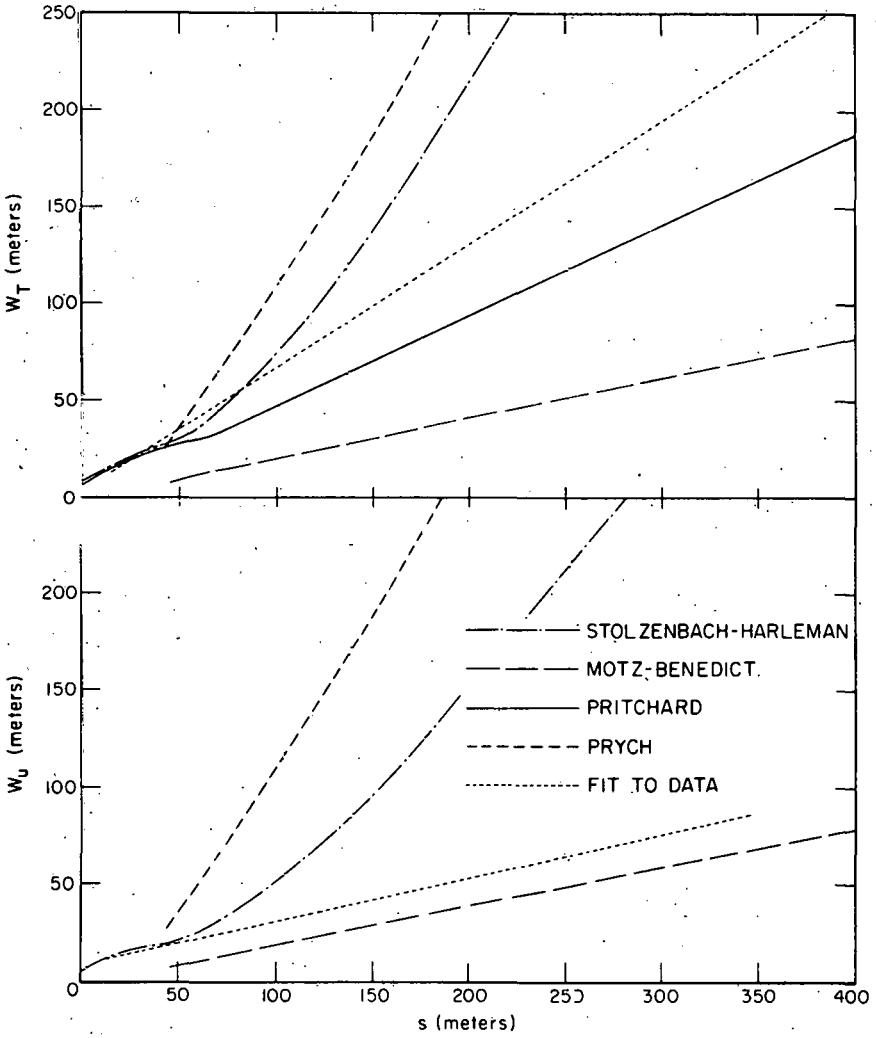

Fig. 71. Half-widths of Temperature and Velocity Distributions Resulting from the Fitting Procedure and Model Calculations for Point Beach: September 9, 1972. ANL Neg. No. 190-941.

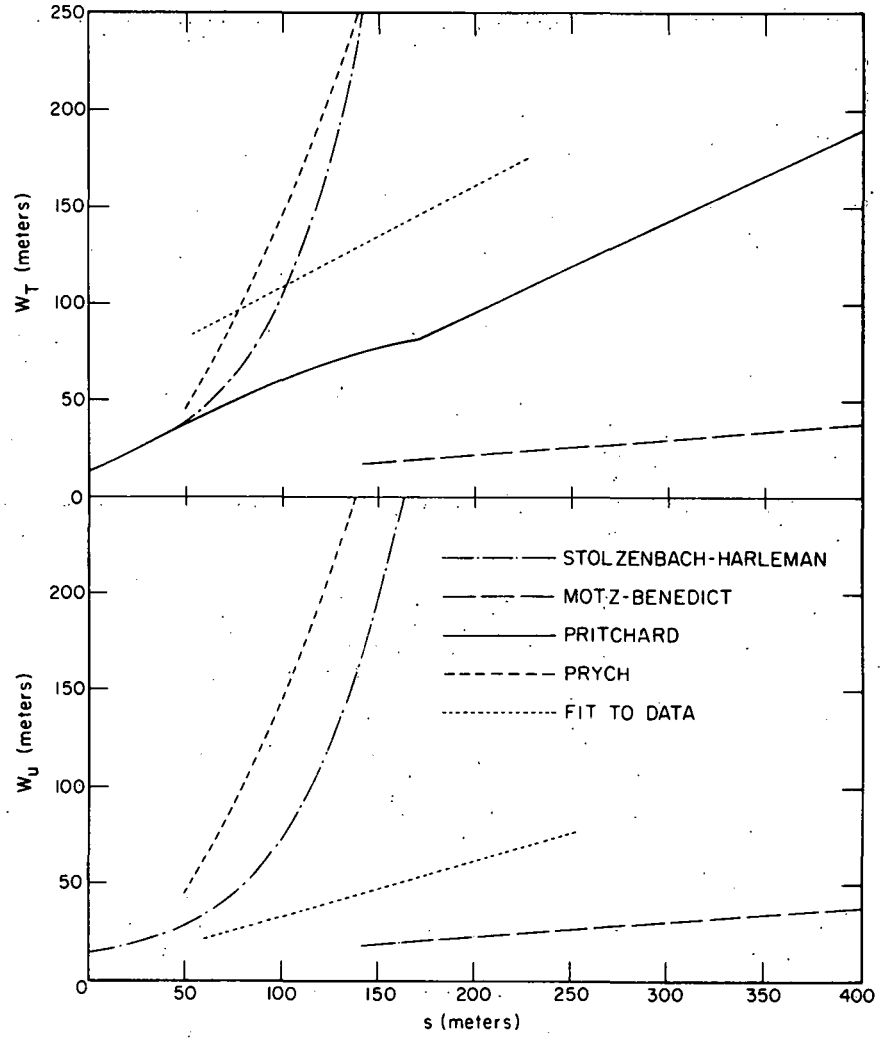

Fig. 72. Half-widths of Temperature and Velocity Distributions Resulting from the Fitting Procedure and Model Calculations for Palisades: October 10, 1972. ANL Neg. No. 190-959.

lateral extent of the jet. Both models, on the basis of present results, used assumptions that were apparently too theoretical in nature and apparently require calibration with some empirical data to yield more accurate results. The overextended lateral spread of these two jet solutions is a probable cause of the extremely rapid centerline temperature decay required by energy conservation at each jet cross section.

The Motz-Benedict model predicts a jet that is by far too narrow for all four Point Beach cases. The model is very sensitive to the particular choice for the value of some of the input parameters, in particular, the entrainment coefficient and the jet width at the end of the region of flow establishment. A more judicious choice for these parameters would undoubtedly improve the comparisons. However, when this model is used as a predictive tool, it is difficult, at present, to know what values to choose other than those recommended by the authors of the model.

Pritchard predicts rather accurate temperature decays and widths, except for the temperature width on September 9. The wider width of the data might well be due to the second unit operating at 12% power on that date, adding to the temperature excesses on the offshore side of the plume.

The Palisades results are quite interesting (Figs. 67 and 72). As expected, the temperature does not drop off until about 175 m downstream, due to the larger region of flow establishment resulting from the wider outfall at Palisades. Again, Prych and Stolzenbach and Harleman are still too optimistic in their temperature-decay predictions and too wide in their lateral jet spreading. Pritchard predicts too great a temperature decrease and too narrow a jet. This is probably due to his method of handling vertical entrainment, which is very sensitive to the difference between the outfall depth and the critical mixing depth of the lake. Vertical entrainment is not a factor in Pritchard's predictions for Point Beach. Motz and Benedict are conservative in temperature decay for Palisades due to the large region of flow establishment (5.2 times the full width of the outfall). Lateral widths are again very much underpredicted.

C. Centerline Velocity Decay and Velocity Half-widths

Figures 63-67, for u_c/u_0 derived from JETFIT, indicate a significant deviation of the initial jet velocity from the calculated average channel velocity. For July 13, velocity measurements near the channel outlet indeed verified a velocity greater than u_0 for the first meter depth. Other measurements, on different dates, all showed values greater than u_0.

The Stolzenbach-Harleman and Prych models predict too rapid a velocity-centerline decay. In each case, the Stolzenbach-Harleman model predicts an increase in velocity after the jet leaves the outlet up to 60 m along the centerline. This is possible for discharges having very low densimetric Froude numbers. A light fluid, discharged over a heavier fluid,

accelerates laterally as well as longitudinally due to hydrostatic pressure gradients. For low densimetric Froude numbers (near 1.0) such buoyant accelerations become dominant. Although increases in velocity are possible, increases in temperature are never realistic. If such hydrostatic pressure gradients were removed or neglected in the model, a momentum jet would occur. For discharges having high densimetric Froude numbers, lateral accelerations greatly dominate longitudinal ones and consequently allows such longitudinal gradients to be neglected. The densimetric Froude numbers for the four Point Beach cases are about 2.4, which may be a little large for the above floating-plume phenomenon to occur. For the stagnant-lake cases of Figs. 63 and 64, the Prych model has a sharp decrease in velocity within 125 m of the outfall and then tends to level off. The Stolzenbach-Harleman model is more regular in its rapid velocity decline, crossing the Prych curve for u_c/u_0 at about 170 m from the outfall. The ambient-current cases realize a more regular velocity decline, with the Prych model giving consistently lower velocities.

The Motz-Benedict and Pritchard models appear adequate for both stagnant-lake cases of May 18 and May 23, and the current case of September 9. The data of July 13 reveal higher velocities than predicted by any of the models. An apparent defect in the Motz-Benedict model is the assumption of decay of lateral velocity to zero, even where an ambient current exists. A more realistic assumption would require a decay superimposed on $U_a \cos \beta$ (the component of the ambient current parallel to the local jet centerline).

Velocity widths as predicted by the Prych and Stolzenbach-Harleman models are much too large for the four Point Beach dates (Figs. 68-71). This again reflects on their assumptions of lateral spreading velocity. The Prych predictions are consistently larger than those of Stolzenbach and Harleman. The Stolzenbach-Harleman predictions appear too sensitive to ambient current; the Prych predictions seem very insensitive. Pritchard has no predictions for velocity width. Examining the data reveals that the temperature width is approximately twice the size of the velocity width for any fixed date at Point Beach.

The Palisades data indicate a very slow velocity decline after a rather rapid drop in the first 50 m (see Fig. 67). This rapid drop might be due to the long, diverging discharge channel. Irregularities in the velocity distribution across the channel (lake water entering the channel at the north end combined with significant channel-depth irregularities) may be a contributing factor. No model for velocity decay appears adequate for Palisades on October 10. Velocity widths of Prych and Stolzenbach and Harleman are again too large, and the Motz-Benedict predictions, although more reasonable, are too small (see Fig. 72). Due to site-dependent irregularities (diverging outfall, shallow bottom), Palisades is not the ideal site to evaluate near-field models, albeit a real site.

D. Temperature and Velocity Half-depth

Figures 73-76 compare the predictive models with respect to half-depth. The half-depth is the vertical distance at which the excess temperature and/or excess velocity drop to one-half the local surface-centerline value. Also shown is an indication of the location of the lake bottom. No data are plotted, since the vertical profile information was insufficient to define a half-depth in most cases. Either the 3.0-m limit or the lake bottom was reached before the half-depth or the temperature or velocity distribution was reached.

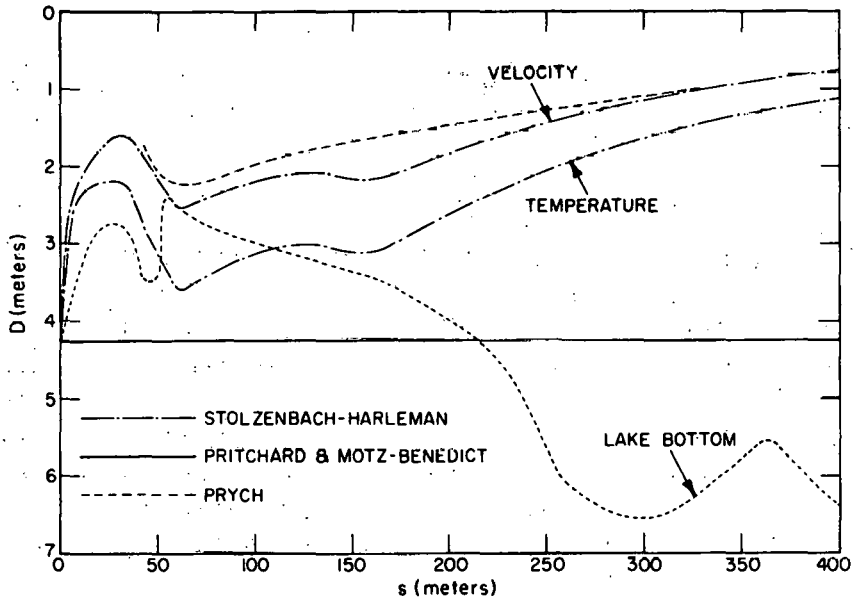

Fig. 73. Half-depths of Temperature and Velocity Distributions Resulting from Model Calculations for Point Beach: May 18, 1972

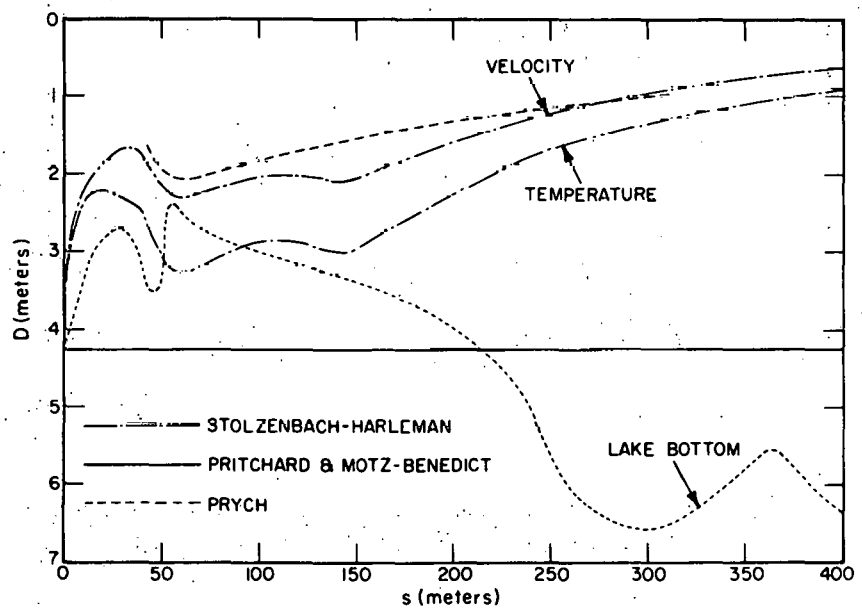

Fig. 74. Half-depths of Temperature and Velocity Distributions Resulting from Model Calculations for Point Beach: May 23, 1972

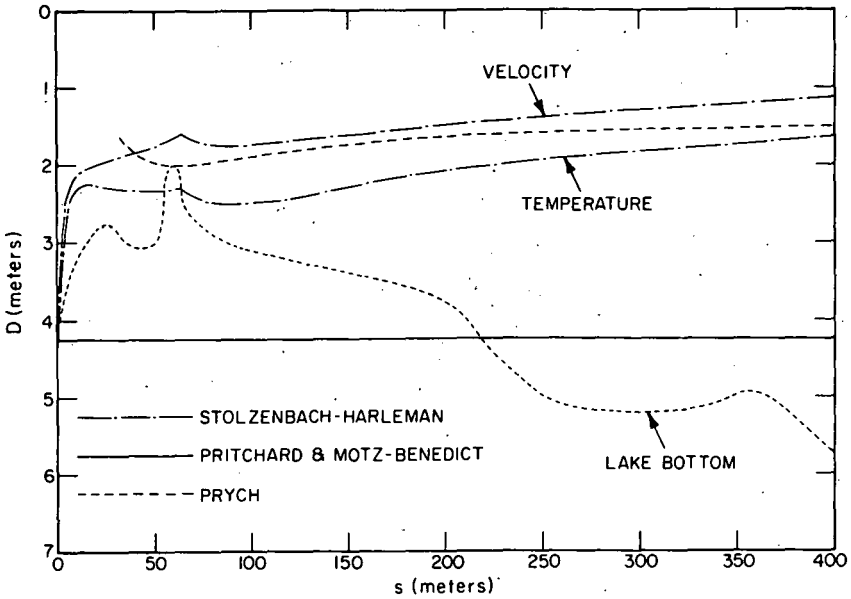

Fig. 75. Half-depths of Temperature and Velocity Distributions Resulting from Model Calculations for Point Beach: July 13, 1972

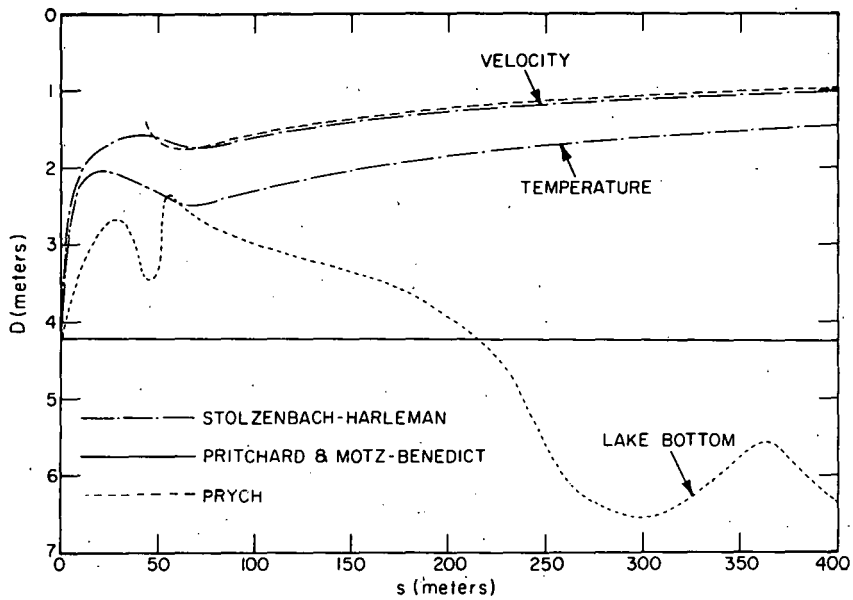

Fig. 76. Half-depths of Temperature and Velocity Distributions Resulting from Model Calculations for Point Beach: September 9, 1972

The Motz-Benedict and Pritchard models, being two-dimensional, naturally predict constant-depth jets. However, Prych and Stolzenbach and Harleman predict a buoyant jet that spreads into a thin layer (typically 1.0 to 1.5 m thick), after brief contact with the lake bottom for a distance of about 100 m. The Stolzenbach-Harleman model predicts several small ridges in the jet-depth contour that do not appear reasonable. The sharp decrease in jet-depth within the first 75 m might be associated with the increase in velocity above the channel velocity

near the outfall predicted by Stolzenbach and Harleman. The Prych model contains no mechanism to allow for a difference in the vertical temperature and velocity spreading; Stolzenbach and Harleman employ different velocity and temperature similarity functions. Note also that Prych consistently predicts thinner plumes for the four Point Beach cases. Bottom interaction, as predicted by the above three-dimensional models, appears less than was actually determined by field measurements. Tables V-IX summarize the vertical distributions of excess temperature and excess velocity on a location-by-location basis for the four dates at Point Beach and one at Palisades. The jet appears to be influenced by bottom interaction in the vicinity of the outfall, followed by stratification at the final transect. Changes in temperature and velocity excess with depth tend to indicate a lens-shaped plume, with a greater vertical spread of heat than momentum. Estimates of the plume velocity and temperature half-depths as the plume stratifies are given in the tables. At Point Beach, the plume tends to stratify to a temperature depth of 2 m from an initial temperature depth of 4.2 m; the velocity spreading is to approximately 1.5 m. The Palisades plume is thinner: It reaches an asymptotic temperature and velocity depth of about 0.5-1.5 m from an initial discharge depth of 2.1 m. The data are not sufficiently refined to permit more than just a gross estimate. Irregularities in the decay of temperature and velocity excess from an expected monotonic profile are due perhaps to:

1. Different ambient values of temperature and velocity at each depth.
2. The transient thermal-front phenomenon, which complicates the concept of a steady-state temperature at a single location.

This irregular behavior is real and cannot be ignored; it reflects on the transient nature of the jet discharge as well as a discharge into a stratified ambient environment.

As is evident from the data, bottom interaction should imply greater lateral spread, since vertical entrainment is reduced; even the observed spread was not nearly as great as Prych and Stolzenbach-Harleman predict for no interaction. The bottom influence appears to be most significant for the first 150 m offshore for the four Point Beach cases with an asymptotic approach to a half-depth of temperature and velocity of 1.0-1.5 m.

Figure 77 compares model predictions for plume half-depth along the jet centerline with actual lake-bottom depths to assist in determining bottom interaction for October 10 at Palisades. Again, each model prediction in Fig. 77 represents the half-depth along the centerline predicted by that model. Predicted model centerlines do not coincide, but are sufficiently close for the present discussion. The lake-bottom depth shown in Fig. 77 is along a line straight out from the outfall.

As can be seen in the figure, the lake depth is about 2 m to a distance of 125 m from the outfall; then the bottom drops away rather sharply. The

TABLE V. DETERMINATION OF TEMPERATURE AND VELOCITY HALF-DEPTHS AT EACH STATION LOCATION FROM THE POINT BEACH DATA OF MAY 18, 1972

STATION NUMBER

	1	2	3	4	5	6	7	8	9	10	11	12	13	14	15	16	17	18
Temperature Excess at Each Depth Level Measured																		
0.5 m	1.8	2.0	NM	4.8	5.3	1.9	0.0	4.1	5.3	3.8	1.3	1.4	1.8	7.5	6.8	6.8	4.6	4.2
1.0 m	1.2	2.5	4.1	5.5	5.0	2.1	LB	4.6	5.9	5.4	1.2	0.0	1.8	7.5	6.0	6.2	5.1	4.8
1.5 m	NM	2.1	NM	4.9	4.3	1.4	LB	3.8	6.7	5.1	NM	0.0	0.1	7.9	6.7	6.1	4.9	4.2
2.0 m	2.2	0.6	3.1	2.7	4.8	1.5	LB	LB	6.8	3.8	0.6	LB	LB	7.3	6.5	5.6	4.7	4.2
2.5 m	NM	0.2	1.4	4.4	3.5	1.2	LB	LB	5.6	2.4	LB	LB	LB	LB	LB	LB	5.2	LB
3.0 m	LB	LB	NM	NM	NM	NM	LB	LB	LB	LB	LB	LB	LB	LB	LB	LB	LB	LB
Velocity Excess at Each Depth Level Measured																		
0.5 m	0.0	0.0	NM	17.9	26.1	15.5	0.0	0.0	32.3	37.3	0.0	0.0	9.5	56.3	29.4	17.8	7.4	7.9
1.0 m	0.0	0.0	2.8	7.6	21.8	7.8	LB	0.0	33.0	37.6	0.0	0.0	7.9	47.1	30.2	20.2	8.8	0.0
1.5 m	NM	2.3	NM	6.5	23.9	0.0	LB	0.0	29.7	28.8	NM	0.0	1.6	48.3	21.5	15.0	5.1	0.0
2.0 m	0.0	2.5	0.0	4.4	19.4	0.0	LB	LB	21.7	20.1	0.0	LB	LB	48.4	26.2	9.4	0.0	0.0
2.5 m	NM	5.4	0.0	0.0	15.4	0.0	LB	LB	16.5	12.4	LB	LB	LB	LB	LB	LB	4.4	LB
3.0 m	LB	LB	NM	NM	NM	NM	LB	LB	LB	LB	LB	LB	LB	LB	LB	LB	LB	LB

LB = LAKE BOTTOM INTERFERENCE
NM = NOT MEASURED

POINTS OF IRREGULAR VERTICAL EXCESS-TEMPERATURE VARIATION: 1, 4-6, 8-10, and 14-16.
FROM POINTS 2, 3, 7, 11-13, THE TEMPERATURE HALF-DEPTH OF THE JET MAY BE ESTIMATED TO BE ABOUT 2 METERS.

POINTS OF IRREGULAR VERTICAL EXCESS-VELOCITY VARIATION: 2, 5, 9, 14, 15, 16, AND 17.
FROM POINTS 1, 3, 4, 6-8, 10-13, AND 18, THE VELOCITY HALF-DEPTH OF THE JET MAY BE ESTIMATED AS 1.5 METERS.

TABLE VI. DETERMINATION OF TEMPERATURE AND VELOCITY HALF-DEPTHS AT EACH STATION LOCATION FROM THE POINT BEACH DATA OF MAY 23, 1972

	STATION NUMBER																											
	1	2	3	4	5	6	7	8	9	10	11	12	13	14	15	16	17	18	19	20	21	22	23	24	25	26	27	28	29
Temperature Excess at Each Depth Level Measured																													
0.5 m	0.6	4.5	6.5	6.8	6.6	6.4	2.2	5.1	1.3	6.4	5.5	5.1	1.3	5.5	5.0	5.8	3.2	0.2	2.4	4.3	5.5	2.0	2.3	0.0	2.3	3.0	4.0	2.3	2.4
1.0 m	2.2	6.2	8.2	8.4	8.3	7.7	1.2	7.0	1.5	8.0	7.0	5.9	3.0	5.6	7.2	6.6	4.4	1.4	3.5	6.0	5.6	2.2	2.4	0.0	2.7	5.0	4.2	3.1	3.2
1.5 m	2.5	5.1	8.7	9.0	8.9	7.7	0.6	6.7	2.2	7.6	5.7	3.8	2.6	5.6	6.5	6.6	2.8	1.6	2.9	5.7	5.7	1.7	1.7	1.4	2.6	5.0	3.7	2.8	3.0
2.0 m	LB	5.5	9.3	9.5	9.4	6.8	0.9	4.5	LB	7.9	7.7	3.7	2.8	5.7	7.4	7.1	2.7	2.1	2.4	6.0	5.5	1.7	1.2	0.0	2.5	4.0	3.1	1.2	1.7
2.5 m	LB	5.5	9.3	9.7	9.7	6.3	1.1	LB	LB	8.0	6.0	4.0	2.8	LB	NM	6.3	1.0	LB	LB	6.0	5.3	0.3	0.0	0.0	2.0	4.0	3.4	1.5	1.5
3.0 m	LB	LB	8.5	10.1	10.0	5.6	LB	LB	LB	LB	NM	LB	LB	LB	NM	NM	NM	LB	LB	5.5	5.3	0.4	0.8	0.0	1.3	4.0	3.5	2.0	1.8
Velocity Excess at Each Depth Level Measured																													
0.5 m	1.5	11.9	61.0	66.2	72.6	45.6	12.6	9.5	13.3	66.7	55.5	17.0	0.0	40.2	48.6	41.8	18.2	-4.2	5.2	22.2	35.1	20.1	10.1	0.0	15.5	18.0	21.0	2.2	1.3
1.0 m	0.0	14.2	54.1	59.8	59.3	48.4	6.9	9.4	13.2	69.5	36.0	11.8	2.1	34.5	40.5	41.1	13.8	-6.4	0.0	24.5	35.3	14.5	0.0	0.0	9.1	16.3	13.9	0.0	2.5
1.5 m	0.0	16.9	48.5	58.8	58.4	40.7	3.6	7.0	6.8	47.3	22.7	5.6	-1.6	27.2	50.0	43.2	5.2	-5.2	0.0	20.6	29.1	6.6	0.0	0.0	8.2	10.0	9.5	0.0	0.0
2.0 m	LB	12.1	53.9	58.2	65.6	30.3	3.1	12.7	LB	40.0	31.0	5.7	-3.3	17.6	27.3	35.5	0.0	-2.3	-2.4	17.1	26.0	1.5	0.0	0.0	0.0	5.0	0.0	0.0	0.0
2.5 m	LB	12.9	38.2	39.9	66.0	28.5	3.4	LB	LB	44.4	22.4	7.6	-0.5	LB	NM	24.2	0.0	LB	LB	13.3	14.5	-0.6	-3.2	0.0	0.0	0.0	0.0	0.0	0.0
3.0 m	LB	LB	43.5	49.1	43.8	11.7	LB	LB	LB	LB	NM	LB	LB	LB	NM	NM	NM	LB	LB	6.3	14.3	0.3	-3.1	0.0	0.0	0.0	0.0	0.0	0.0

LB = LAKE BOTTOM INTERFERENCE
NM = NOT MEASURED

NO POINTS HAVE A MONOTONIC EXCESS-TEMPERATURE VARIATION WITH DEPTH FROM WHICH A TEMPERATURE HALF-DEPTH OF THE STRATIFIED JET CAN BE DETERMINED. TEMPERATURES DO NOT VARY SIGNIFICANTLY WITH DEPTH FOR 0.5-2.0 METERS.

POINTS OF IRREGULAR VERTICAL EXCESS-VELOCITY VARIATION: 2-8, 10-13, 15, 18, 20-22, AND 29.
FROM POINTS 1, 9, 14, 16, 17, 19, AND 23-28, THE VELOCITY HALF-DEPTH OF THE STRATIFIED JET MAY BE ESTIMATED AS 1.5-2.0 METERS.

TABLE VII. DETERMINATION OF TEMPERATURE AND VELOCITY HALF-DEPTHS AT EACH STATION LOCATION FROM THE POINT BEACH DATA OF JULY 13, 1972

	STATION NUMBER																
	1	2	3	4	5	6	7	8	9	10	11	12	13	14	15	16	17
Temperature Excess at Each Depth Level Measured																	
0.5 m	4.0	6.0	7.2	5.5	3.7	3.5	3.7	5.8	6.2	4.0	4.0	2.3	3.3	3.5	3.0	2.5	2.7
1.0 m	4.5	6.8	7.8	5.8	4.5	3.8	3.3	6.1	6.1	4.1	4.0	1.8	2.8	2.8	2.5	1.8	1.5
1.5 m	4.6	5.6	7.1	7.1	4.6	4.1	3.8	6.3	6.9	4.6	4.3	1.1	3.1	2.6	2.1	1.3	1.1
2.0 m	3.5	7.5	8.5	6.5	LB	3.3	2.5	6.7	5.5	4.0	LB	0.5	3.0	2.3	1.3	0.7	0.5
2.5 m	2.1	4.4	8.4	LB	LB	1.4	1.4	7.1	4.9	1.1	LB	0.7	1.9	1.4	0.7	0.4	0.1
Velocity Excess at Each Depth Level Measured																	
0.5 m	-0.3	57.9	64.5	45.2	11.7	1.2	25.1	41.1	47.0	17.9	4.0	2.7	22.0	25.0	15.6	1.5	4.7
1.0 m	8.5	58.0	56.6	31.9	9.3	-4.8	17.0	38.8	36.1	15.6	-0.8	-1.3	12.5	17.7	8.8	-3.6	4.4
1.5 m	4.6	28.3	64.8	36.7	-1.3	-3.1	11.8	33.5	33.4	7.5	-6.5	1.5	6.8	8.3	2.9	-3.3	1.1
2.0 m	1.8	36.9	74.5	26.9	LB	-2.4	1.5	30.0	23.0	0.1	LB	-2.2	3.5	4.1	-3.1	7.9	-3.6
2.5 m	-0.4	17.7	48.0	LB	LB	-1.4	-4.8	28.5	5.5	0.6	LB	-2.6	-2.3	-3.3	-3.9	-6.7	-3.3

LB = LAKE BOTTOM INTERFERENCE

POINTS OF IRREGULAR VERTICAL EXCESS-TEMPERATURE VARIATION: 1-11 and 13.
FROM POINTS 12 AND 14-17, THE TEMPERATURE HALF-DEPTH OF THE STRATIFIED JET MAY BE ESTIMATED TO BE ABOUT 2.0-2.5 METERS.

POINTS OF IRREGULAR VERTICAL EXCESS-VELOCITY VARIATION: 1-4, 6, 12, 16, and 17.
FROM POINTS 5, 7-11, AND 13-15, THE VELOCITY HALF-DEPTH OF THE STRATIFIED JET MAY BE ESTIMATED AS 1.0-1.5 METERS.

TABLE VIII. DETERMINATION OF TEMPERATURE AND VELOCITY HALF-DEPTHS AT EACH STATION LOCATION FROM THE POINT BEACH DATA OF SEPTEMBER 9, 1972

	STATION NUMBER																
	1	2	3	4	5	6	7	8	9	10	11	12	13	14	15	16	17
Temperature Excess at Each Depth Level Measured																	
0.5 m	0.9	3.3	6.7	7.5	4.7	2.8	2.5	4.2	4.4	3.9	3.8	3.7	3.0	3.2	3.6	3.3	2.6
1.0 m	1.1	4.3	7.6	6.3	5.3	3.4	3.1	4.7	4.0	4.6	4.3	3.3	2.6	2.5	3.0	2.9	3.7
1.5 m	LB	5.2	6.9	7.8	3.7	4.0	3.3	4.4	4.4	3.5	3.9	2.4	1.6	1.5	1.4	2.4	3.9
2.0 m	LB	LB	7.7	7.5	3.5	2.6	2.5	3.8	3.5	3.6	2.6	2.0	1.4	0.7	0.7	1.6	2.0
2.5 m	LB	LB	LB	LB	LB	LB	1.7	1.7	2.3	2.3	1.2	0.7	1.0	0.7	0.7	0.7	1.2
Velocity Excess at Each Depth Level Measured																	
0.5 m	-5.9	21.8	54.5	52.0	39.7	9.6	2.8	25.7	23.6	25.0	11.7	1.2	10.5	12.4	9.8	5.2	-0.5
1.0 m	-3.2	12.9	46.2	38.0	25.0	1.8	1.4	22.3	18.1	16.1	13.0	-1.2	1.1	0.1	3.5	3.4	-0.1
1.5 m	LB	6.9	40.4	40.3	25.0	-5.0	-0.4	13.1	12.8	4.4	6.3	-2.7	-0.2	-0.2	-0.7	-0.5	-0.4
2.0 m	LB	LB	43.0	43.0	13.2	-6.7	0.5	0.9	-0.2	7.0	-0.4	-3.8	-0.3	-0.3	-0.7	-0.4	-1.0
2.5 m	LB	LB	LB	LB	LB	LB	0.4	0.2	-0.7	-1.2	-5.7	-2.1	-0.2	-0.2	-1.6	-4.5	-2.7

LB = LAKE BOTTOM INTERFERENCE

POINTS OF IRREGULAR VERTICAL EXCESS-TEMPERATURE VARIATION: 1-11 AND 17.
FROM POINTS 12-16, THE TEMPERATURE HALF-DEPTH OF THE STRATIFIED JET MAY BE ESTIMATED TO BE ABOUT 2.0 METERS.

POINTS OF IRREGULAR VERTICAL EXCESS-VELOCITY VARIATION: 1, 7, 10, 11, 12, and 17.
FROM POINTS 2-6, 8-9, AND 13-16, THE VELOCITY HALF-DEPTH OF THE STRATIFIED JET MAY BE ESTIMATED AS 1.0 METER.

TABLE IX. DETERMINATION OF TEMPERATURE AND VELOCITY HALF-DEPTHS AT EACH STATION LOCATION FROM THE PALISADES DATA OF OCTOBER 10, 1972

	STATION NUMBER																		
	7	8	9	10	11	12	13	14	15	16	17	18	19	20	21	22	23	24	25
Temperature Excess at Each Depth Level Measured																			
0.5 m	4.7	6.8	7.9	6.4	5.7	5.3	5.6	7.5	8.8	8.5	6.5	5.5	3.0	4.0	5.8	7.0	7.3	4.7	2.6
1.0 m	4.4	4.3	6.0	2.6	3.0	1.5	2.4	7.1	LB	6.5	4.5	3.0	1.5	4.0	4.5	4.0	3.0	2.5	2.0
1.5 m	1.4	3.5	5.7	0.3	LB	LB	LB	5.3	LB	2.8	1.3	0.8	1.6	2.6	2.1	2.3	1.8	0.9	0.8
2.0 m	0.5	LB	LB	LB	LB	LB	LB	LB	LB	LB	LB	LB	0.3	0.9	0.6	1.2	1.5	0.3	0.3
2.5 m	LB	LB	LB	LB	LB	LB	LB	LB	LB	LB	LB	LB	0.3	0.8	0.7	0.7	0.4	0.4	0.4
3.0 m	LB	LB	LB	LB	LB	LB	LB	LB	LB	LB	LB	LB	-13.7	0.7	0.7	LB	LB	LB	0.3
Velocity Excess at Each Depth Level Measured																			
0.5 m	0.0	14.8	19.5	-0.7	0.4	-4.7	-2.3	23.5	14.2	25.0	2.3	-1.8	1.1	9.1	-1.4	12.8	18.5	11.1	5.6
1.0 m	0.0	13.7	6.9	-2.1	-5.1	-3.9	-2.9	19.2	LB	12.2	0.0	-1.5	2.6	7.8	11.0	7.1	2.6	1.2	-2.8
1.5 m	-2.2	4.0	0.0	-2.8	LB	LB	LB	7.6	LB	5.8	-0.7	-1.7	0.8	1.7	2.8	1.8	-0.5	-3.5	-0.5
2.0 m	-2.3	LB	LB	LB	LB	LB	LB	LB	LB	LB	LB	LB	3.5	1.0	2.8	-1.2	-5.5	-3.2	-2.2
2.5 m	LB	LB	LB	LB	LB	LB	LB	LB	LB	LB	LB	LB	0.6	1.8	-1.4	2.9	-5.1	-5.1	-4.6
3.0 m	LB	LB	LB	LB	LB	LB	LB	LB	LB	LB	LB	LB	-2.0	-8.0	-1.5	LB	LB	LB	-6.5

LB = LAKE BOTTOM INTERFERENCE
NM = NOT MEASURED

POINT OF IRREGULAR VERTICAL EXCESS-TEMPERATURE VARIATION: NONE.
FROM POINTS 7-25, THE TEMPERATURE HALF-DEPTH OF THE STRATIFIED JET MAY BE ESTIMATED TO BE ABOUT 0.5-1.5 METERS.

POINTS OF IRREGULAR VERTICAL EXCESS-VELOCITY VARIATION: 18-25.
FROM POINTS 7-17, THE VELOCITY HALF-DEPTH OF THE STRATIFIED JET MAY BE ESTIMATED AS 0.5-1.5 METERS.

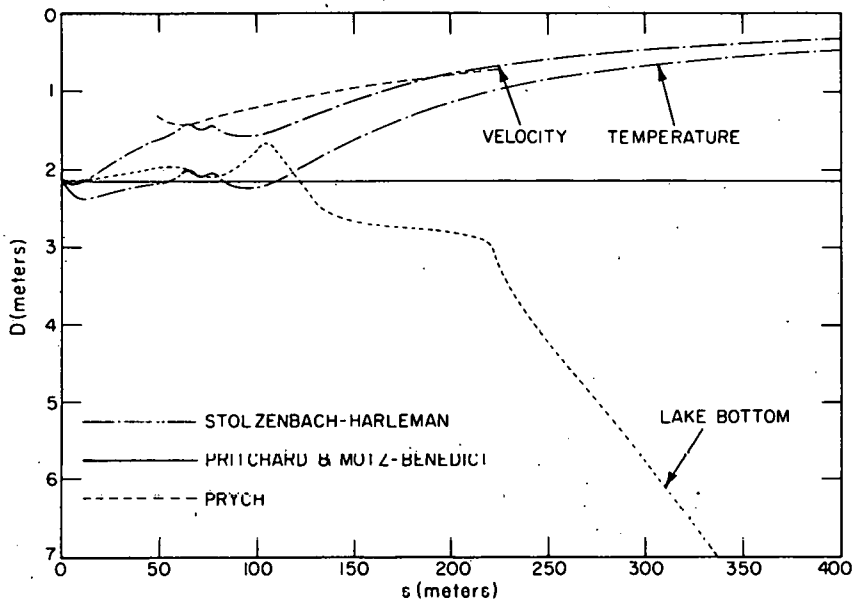

Fig. 77. Half-depths of Temperature and Velocity Distributions Resulting from Model Calculations for Palisades: October 10, 1972

three-dimensional Prych and Stolzenbach-Harleman models predict a buoyant surface jet, with only the Stolzenbach-Harleman temperature half-depth reaching the bottom. On a point-by-point basis (see Figs. 43-48), the temperatures at Stations 9, 11, 14, and 15 do not decline to half their near-surface values before the lake bottom is reached. All other points indicate a 1.0- to 1.5-m temperature half-depth. It is inferred from the data that the jet hugs the bottom for the first 125 m and then rises to a 1.0- to 1.5-m half-depth as the bottom drops away and jet buoyancy becomes predominant. A point-by-point analysis of the velocity data indicates no real trend. The bottom was usually encountered on the first two transects before the half-depth was reached. The velocity half-depth appears to be 1.0-1.5 m otherwise. The variation of velocity data with depth at Palisades is just too erratic for any consistent conclusions. This also was true for the Palisades data of June 14 and July 19.

E. Isotherm Areas

Isotherm areas were calculated based upon the temperature-distribution function resulting from the fit to the data by JETFIT. The data were not sufficiently detailed to contour isotherms and determine areas directly. Consequently, the JETFIT area calculations should be used with caution. It is encouraging, however, to note that isotherm areas for the four dates at Point Beach are approximately the same; this is to be expected, since plant conditions were nearly the same and ambient currents were weak, if present at all. These isotherm areas, along with the model predictions, are presented in Figs. 78-82.

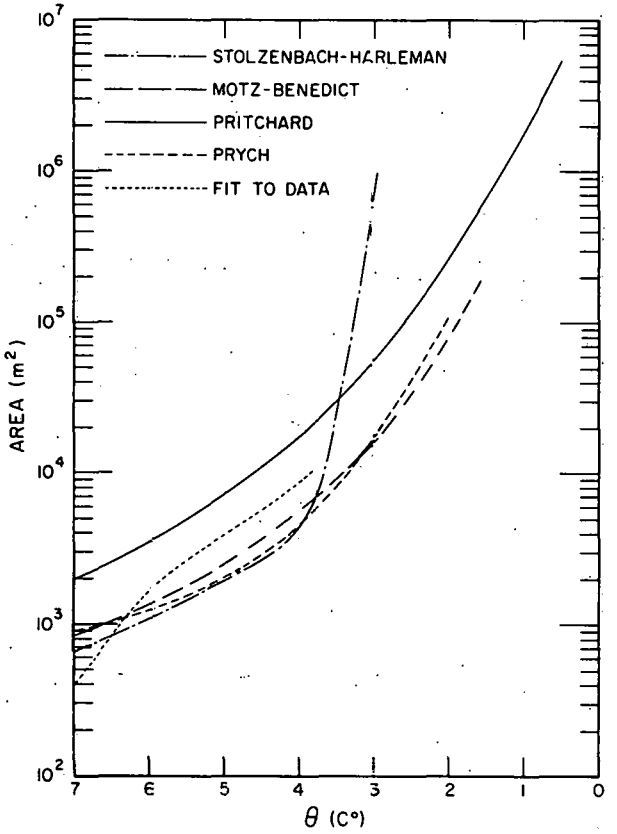

Fig. 78. Isotherm Areas Resulting from the Fitting Procedure and Model Calculations for Point Beach: May 18, 1972. ANL Neg. No. 190-939.

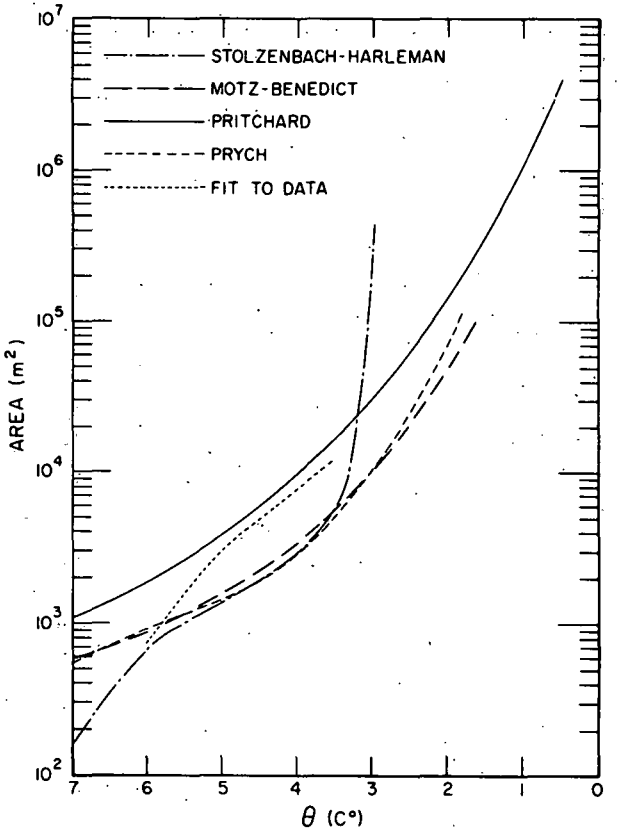

Fig. 79. Isotherm Areas Resulting from the Fitting Procedure and Model Calculations for Point Beach: May 23, 1972. ANL Neg. No. 190-938.

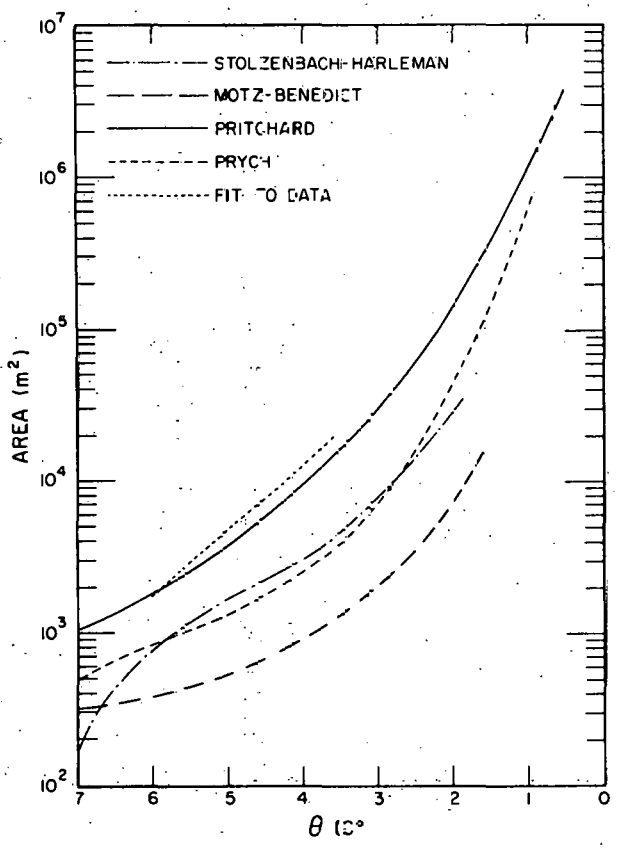

Fig. 80. Isotherm Areas Resulting from the Fitting Procedure and Model Calculations for Point Beach: July 13, 1972. ANL Neg. No. 190-943.

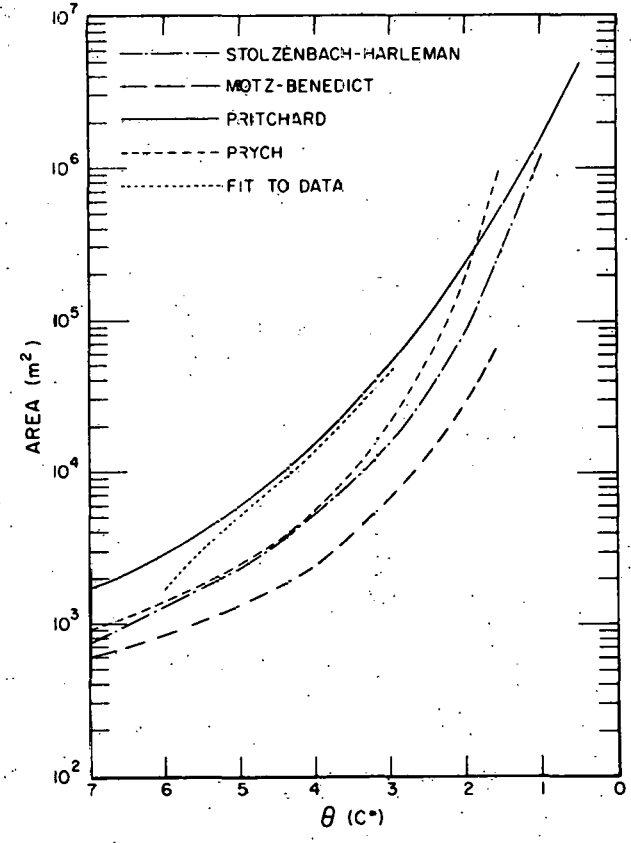

Fig. 81. Isotherm Areas Resulting from the Fitting Procedure and Model Calculations for Point Beach: September 9, 1972. ANL Neg. No. 190-955.

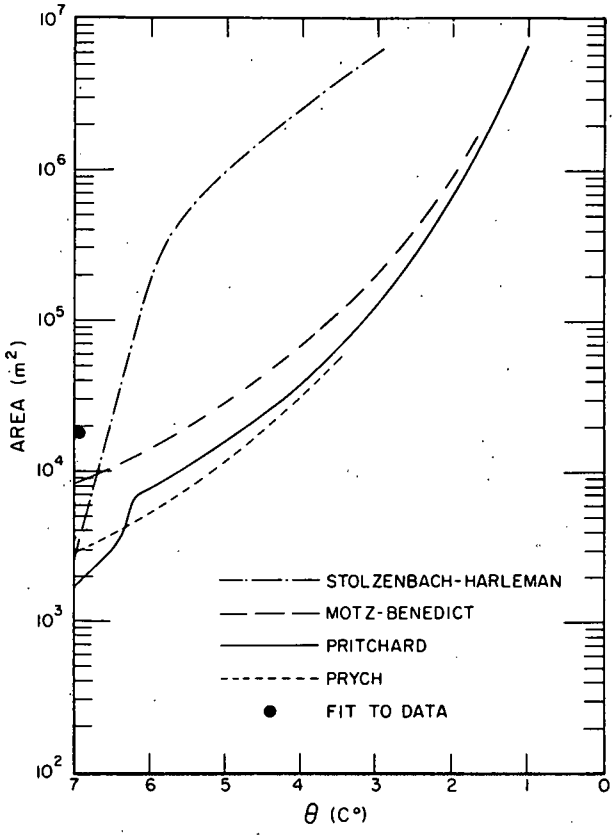

Fig. 82. Isotherm Areas Resulting from the Fitting Procedure and Model Calculations for Palisades: October 10, 1972. ANL Neg. No. 190-937.

The Pritchard model appears to be most accurate in area predictions for the four Point Beach dates. Any discrepancies appear to be on the conservative side. For the no-current cases (Figs. 78, 79, and 82), the areas predicted by Stolzenbach and Harleman are reasonable but optimistic for the region in which data were taken (to 3-4C° isotherm). Beyond the data, however, the model predicts sharply increasing areas, perhaps due to the large lateral spreading predicted. The current cases of July 13 and September 9 reveal a less steep increase in areas with decreasing temperature excess; the model for those dates tends to underpredict areas for the region in which data exist. Too sharp a distinction between the no-current and weak-current cases appears in the area predictions. The Stolzenbach-Harleman model as derived is too complex to allow any speculation as to possible reasons for that behavior.

The Prych model gives reasonable areas, but they are consistently lower than the data. Also, the predictions are nearly the same for all dates. This is to be expected, since the plant and environmental conditions varied only slightly from date to date at Point Beach. Motz-Benedict predictions are consistently lower on all dates. A different choice of parameters in this regard could affect these results greatly.

The Palisades area calculations are difficult to evaluate. Most of the jet data taken appears to be in the region of flow establishment. Although the actual excess temperature was 9.2C°, the data fit indicated a temperature excess of 7.8C° for a good 200 m offshore. The models all underpredict areas at the 7C° isotherm shown by the dot on Fig. 82; little can be said beyond that isotherm, since no data exist. The Pritchard curve has a sharp increase in area at approximately the 6C° isotherm due to Pritchard's method of halting vertical entrainment when a predicted plume depth of 3.05 m (10 ft) is reached.

F. Decay of Centerline Temperature and Velocity with Depth

Observation of the Point Beach field measurements with depth reveals an approximate constancy of temperature and velocity for the depths measured

(to a depth of 2.5-3.0 m). It is expected that, beyond the 2.5-3.0 m of uniform profile, there exists a vertical region for which temperature and velocity excesses decrease to zero (see Fig. 83). These vertical distributions are perhaps reminiscent of fully developed turbulent flow in pipes, which consists of a large uniform temperature and velocity core, combined with a sharp approach to the boundary value (wall of pipe, or here, the lake bottom).

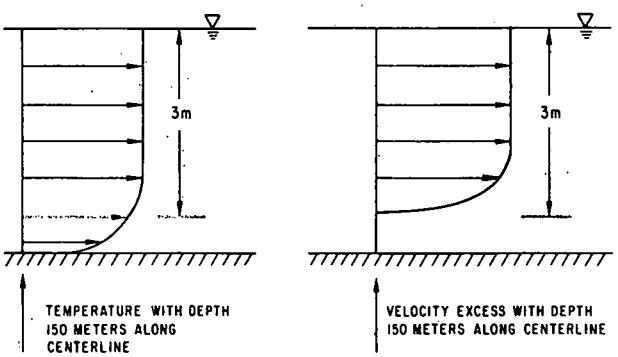

Fig. 83. Idealized Decay of Temperature Excess and Velocity Excess with Depth

The results of the data-fitting procedure for Point Beach appear in Figs. 84-87. The points in these four figures are the centerline temperature and velocity excesses from the fitting procedure at 150 m from the outfall along the centerline. Model predictions of temperatures and velocities with depth at 150 m are also plotted. The lake depth at this distance is about 3.0-3.5 m.

The chosen distance of 150 m is about two to three times the length of the region of flow establishment; only the two-dimensional models predict uniformity of vertical profiles at that distance. Although predictions of the Prych and Stolzenbach-Harleman models look poor, their predictions for the centerline values are too low, biasing the entire vertical-distribution predictions. More accurate centerline predictions would perhaps have yielded better agreement with the data. The three-dimensional models evaluated here predict too rapid a temperature and velocity decay with depth. The flow-establishment assumptions for vertical temperature decay of Stolzenbach and Harleman (constant-temperature vertical core, with small, turbulent boundary layer below it) also appear to be appropriate in the region of established flow. The Stolzenbach-Harleman decay with depth beyond the region of flow establishment is essentially parabolic, with no jet effects beyond a certain depth. The Prych decay is Gaussian in the vertical direction. The Pritchard and Motz-Benedict models, being two-dimensional, predict no change in behavior with depth.

The Palisades data are more of an enigma (see Fig. 88). The centerline distance of 150 m is expected to border the end of the region of flow establishment, yet the vertical temperature and velocity decay appears quite sharp. The depth of constant temperature, if any, is quite small. Complicating factors here are the irregular shallow bottom, approximately 2 m in depth, a diverging surface outfall structure, and a nonuniform velocity distribution. More detailed data would be required before further conclusions could be drawn.

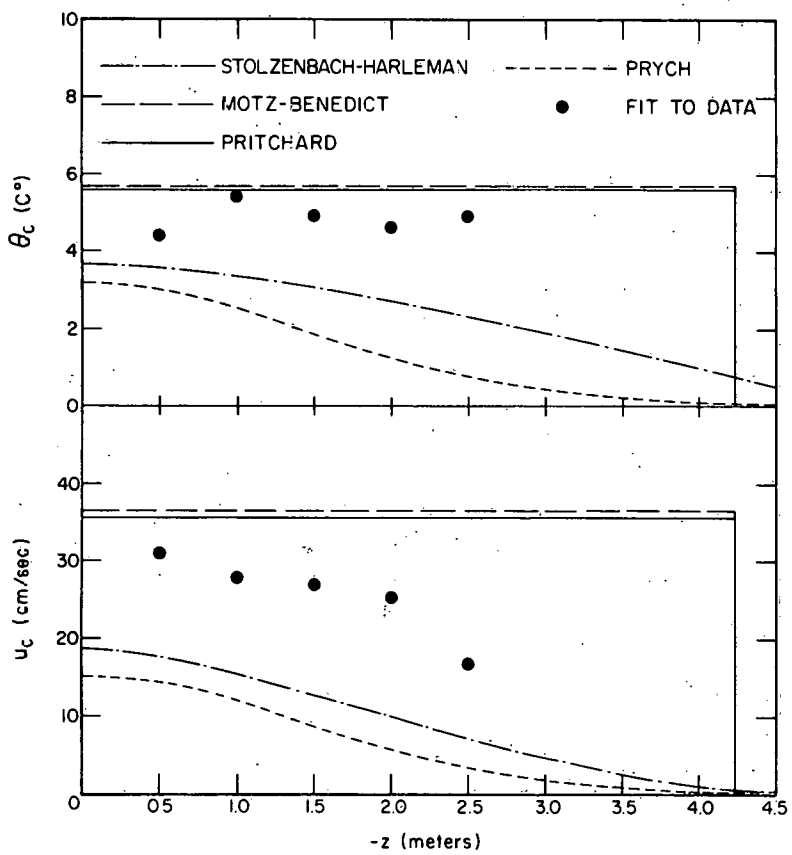

Fig. 84. Centerline Temperature Excess and Velocity Excess as a Function of Depth at 150 m from Outfall Resulting from the Fitting Procedure and Model Calculations for Point Beach: May 18, 1972

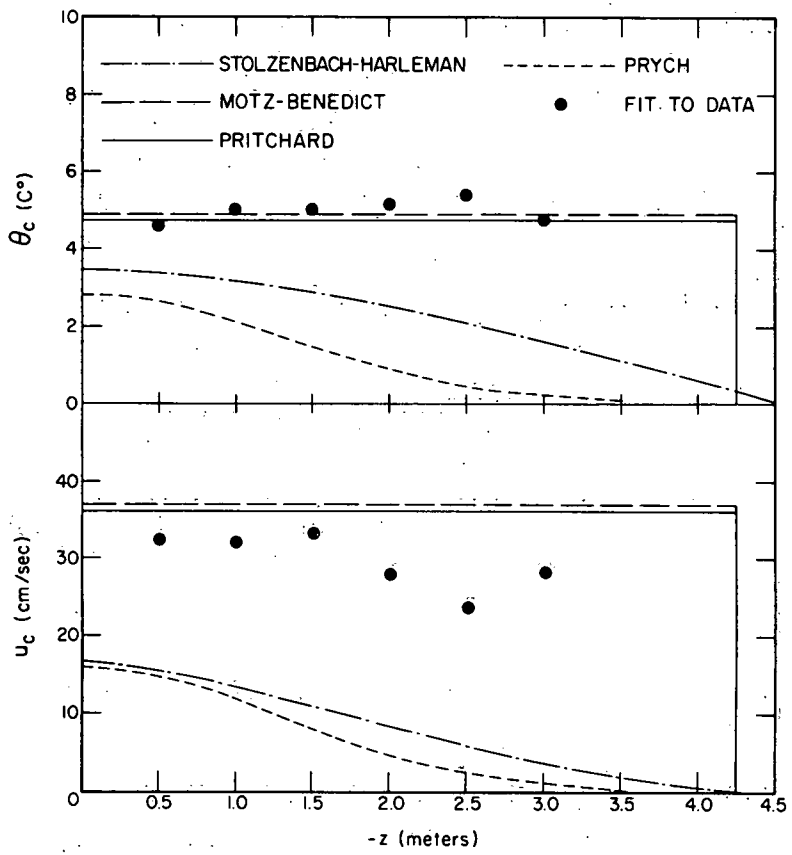

Fig. 85. Centerline Temperature Excess and Velocity Excess as a Function of Depth at 150 m from Outfall Resulting from the Fitting Procedure and Model Calculations for Point Beach: May 23, 1972

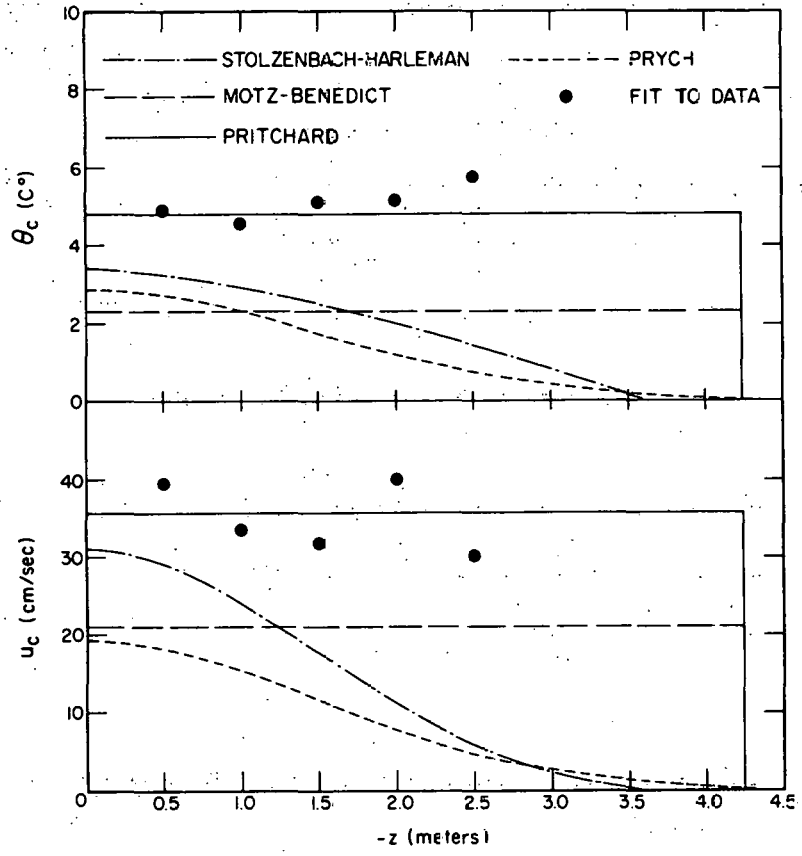

Fig. 86. Centerline Temperature Excess and Velocity Excess as a Function of Depth at 150 m from Outfall Resulting from the Fitting Procedure and Model Calculations for Point Beach: July 13, 1972

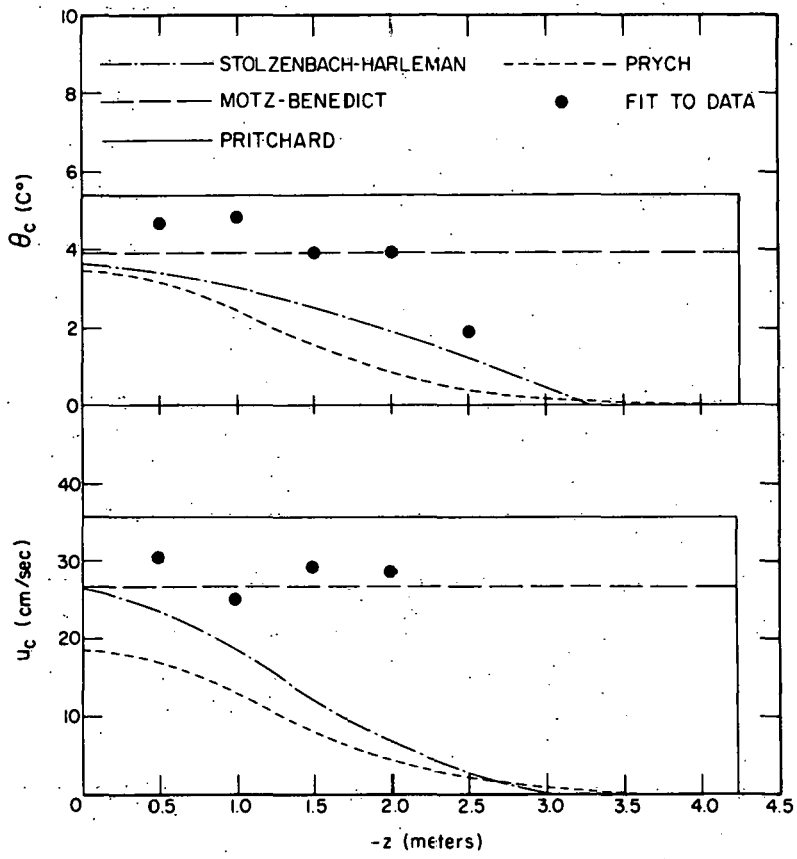

Fig. 87. Centerline Temperature Excess and Velocity Excess as a Function of Depth at 150 m from Outfall Resulting from the Fitting Procedure and Model Calculations for Point Beach: September 9, 1972

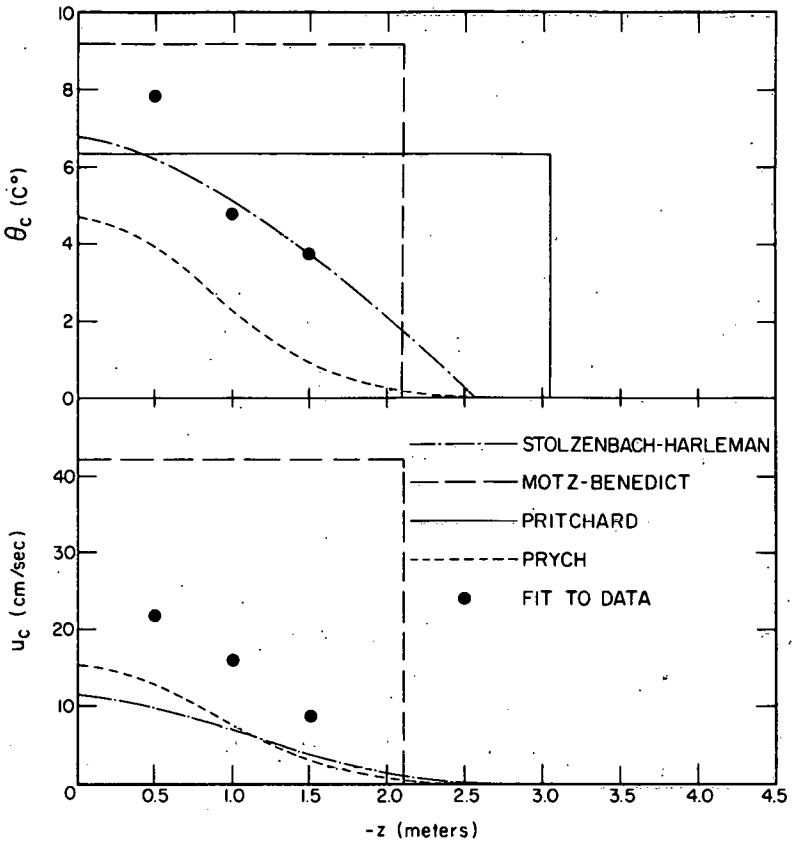

Fig. 88. Centerline Temperature Excess and Velocity Excess as a Function of Depth at 150 m from Outfall Resulting from the Fitting Procedure and Model Calculations for Palisades: October 10, 1972

G. Variation of Temperature and Velocity Width with Depth

Each mathematical model predicts a constant velocity and temperature width with depth. The two-dimensional models do so by the nature of their two-dimensionality, the three-dimensional models by definition of their lateral and vertical profiles. The Stolzenbach-Harleman and Prych models assume, for any cross section of the jet normal to the centerline, the same decay laterally independent of depth, as well as identical decay vertically, irrespective of lateral distance. Consequently, the widths must maintain a constant value with depth.

The data, however, show a more lens-shaped profile, indicating that the temperature and velocity widths decrease with depth (see Figs. 89-92). The local centerlines (with depth) do not coincide, yet are sufficiently close to indicate that such vertical profile results may be meaningful. From the figures, the temperature width appears to be uniform with depth for about 1.5 m and then decreases abruptly; the velocity width appears constant for a shorter depth distance (0.5-1 m) before decreasing toward zero.

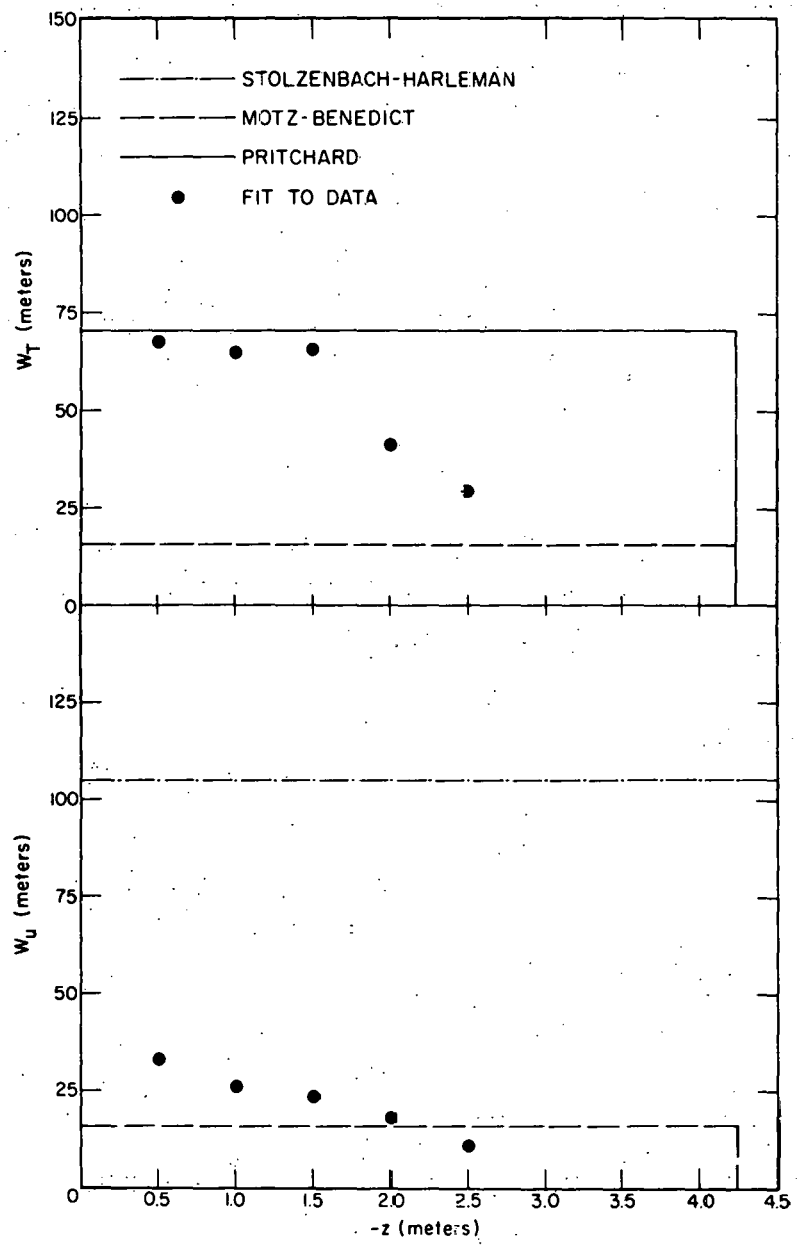

Fig. 89. Half-widths of Temperature and Velocity Distributions as a Function of Depth at 150 m from Outfall Resulting from the Fitting Procedure Model Calculations for Point Beach: May 18, 1972

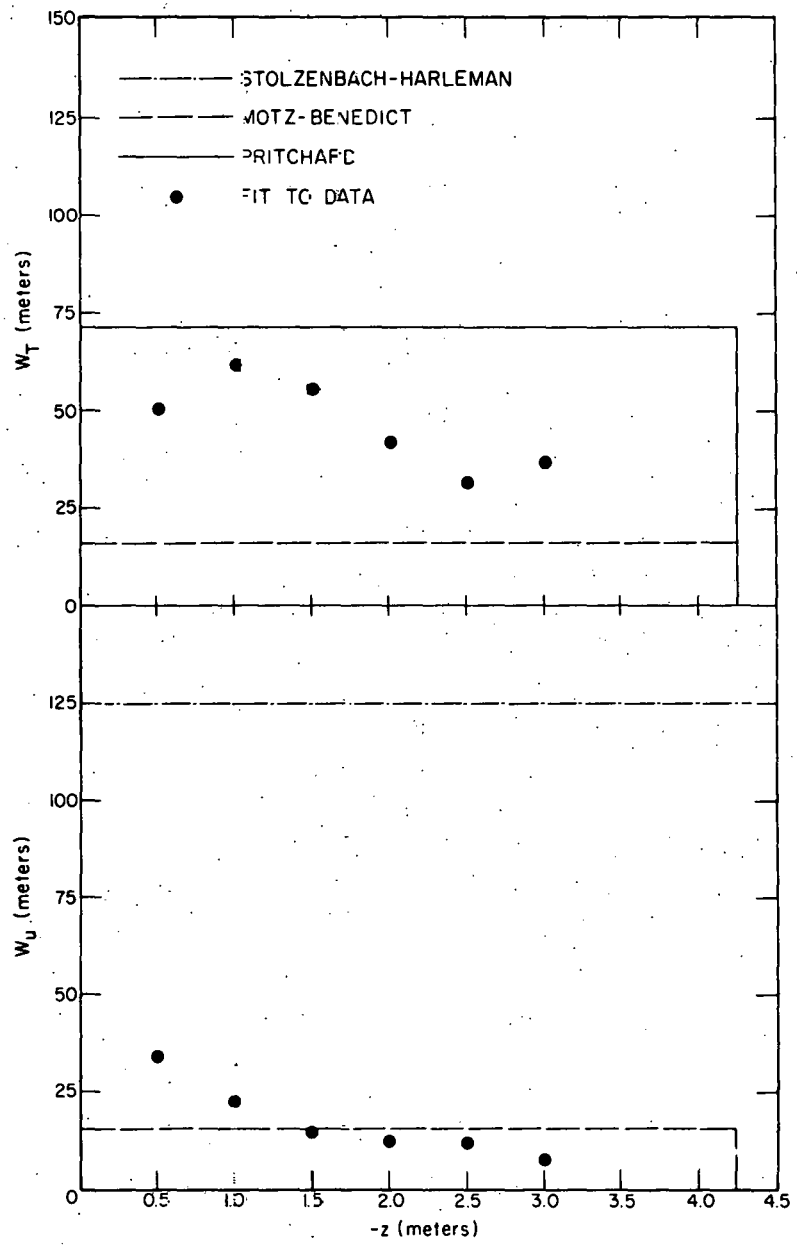

Fig. 90. Half-widths of Temperature and Velocity Distributions as a Function of Depth at 150 m from Outfall Resulting from the Fitting Procedure and Model Calculations for Point Beach: May 23, 1972

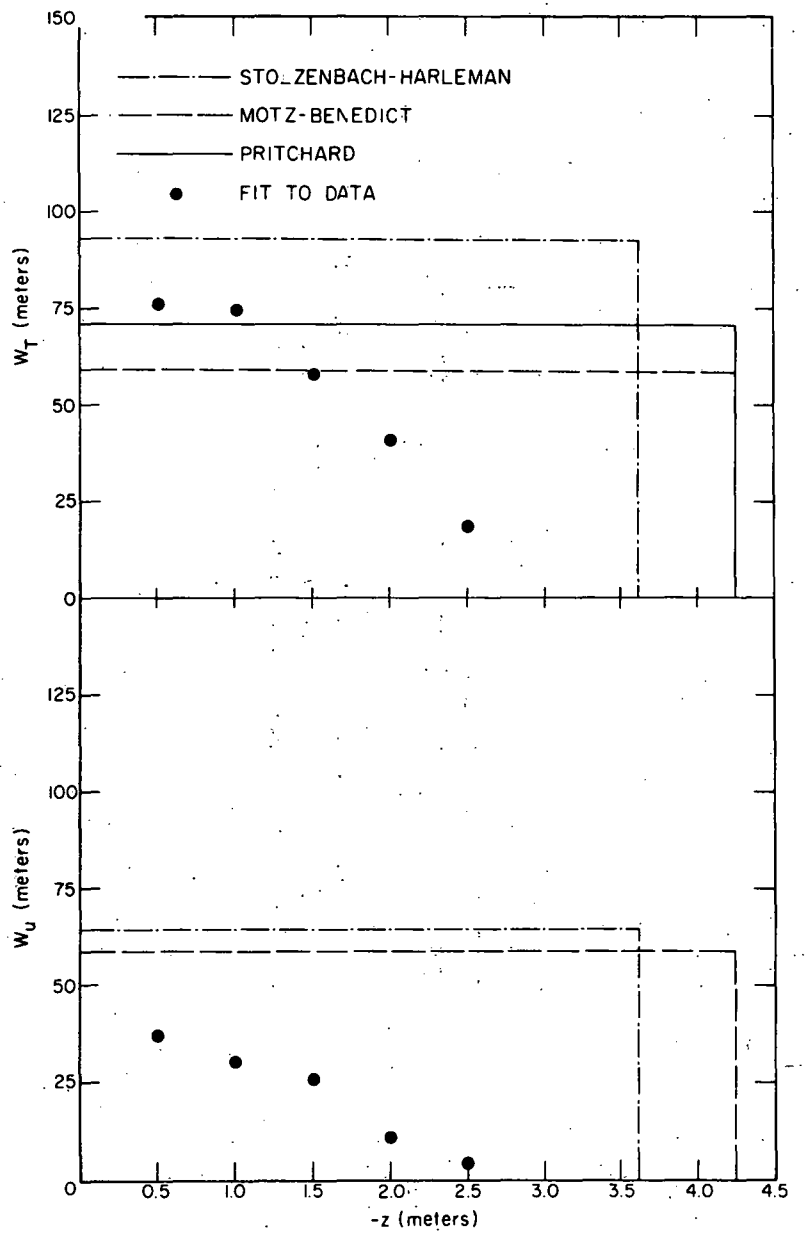

Fig. 91. Half-widths of Temperature and Velocity Distributions as a Function of Depth at 150 m from Outfall Resulting from the Fitting Procedure and Model Calculations for Point Beach: July 13, 1972

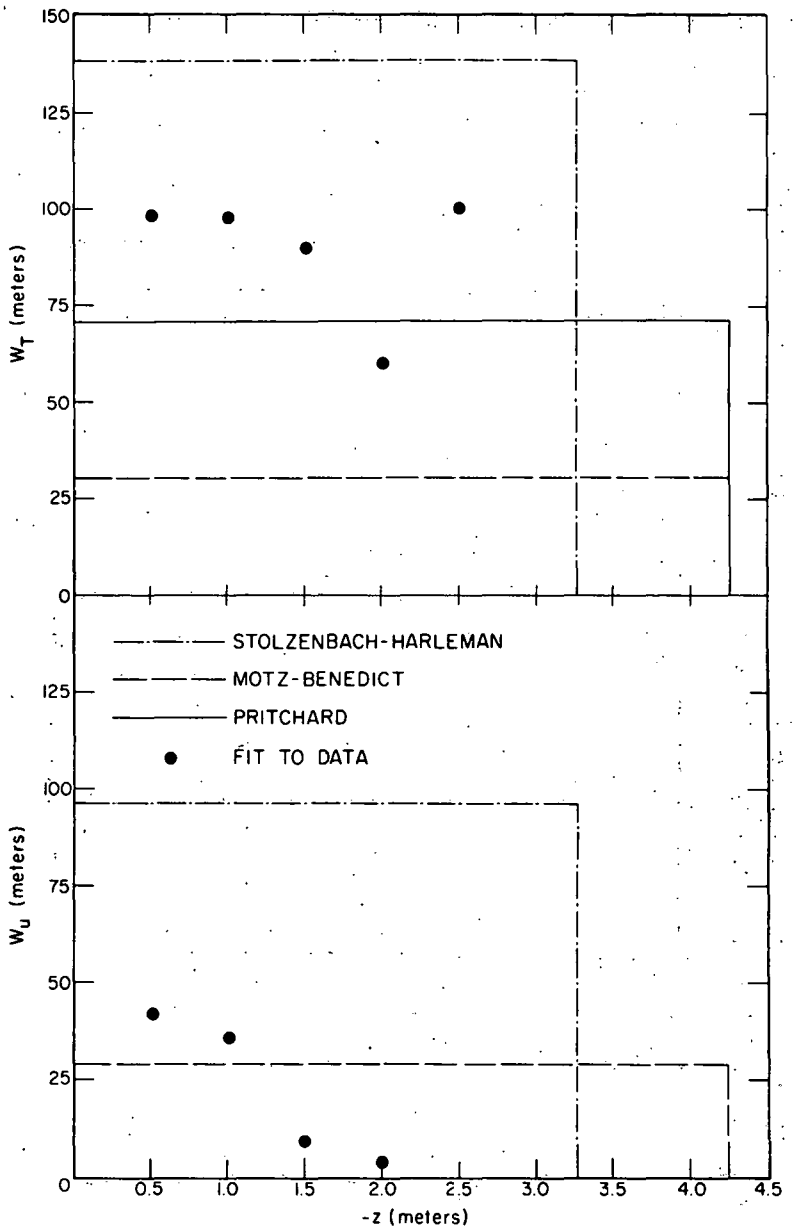

Fig. 92. Half-widths of Temperature and Velocity Distributions as a Function of Depth at 150 m from Outfall Resulting from the Fitting Procedure and Model Calculations for Point Beach: September 9, 1972

The Palisades data (see Fig. 93) are insufficient and irregular, due again perhaps to the shallow lake depths in the discharge vicinity as well as the nonuniformity of the diverging discharge.

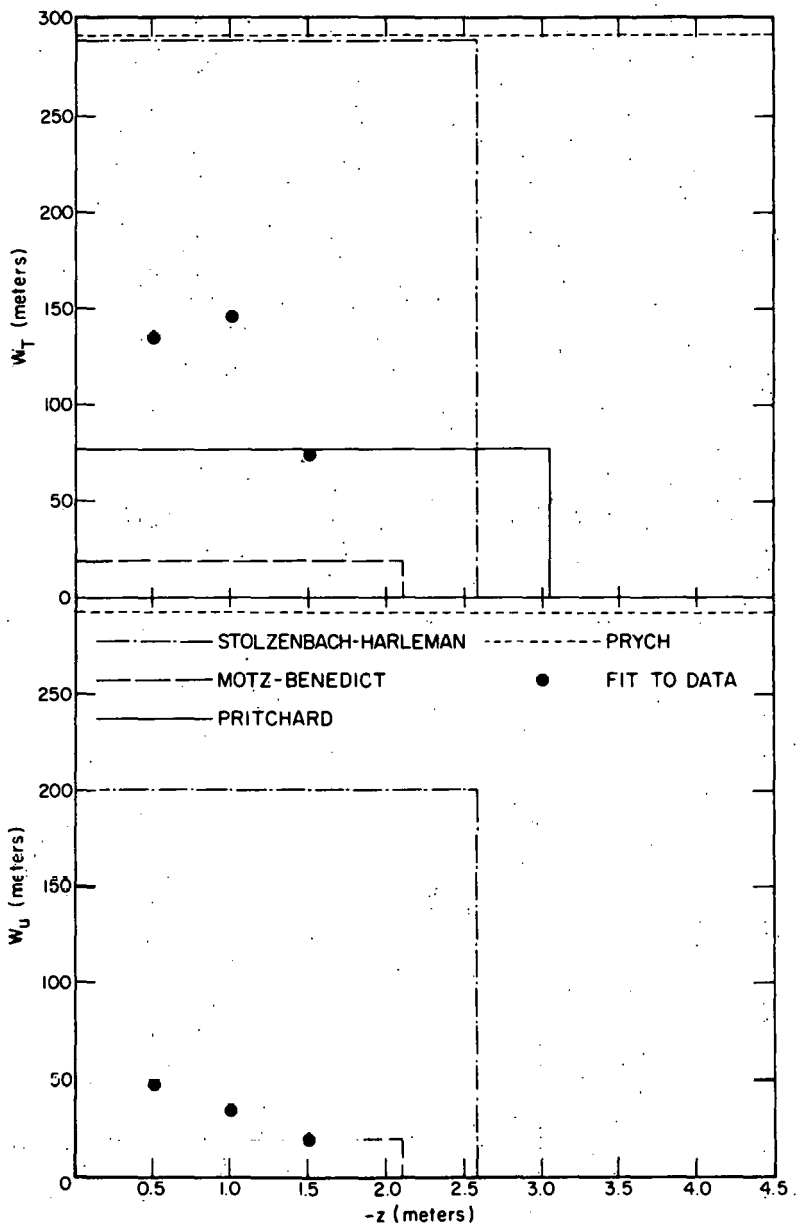

Fig. 93. Half-widths of Temperature and Velocity Distributions as a Function of Depth at 150 m from Outfall Resulting from the Fitting Procedure and Model Calculations for Palisades: October 10, 1972

VIII. SUMMARY AND CONCLUSIONS

A. Field-data Acquisition

The experimental technique described in Sec. II for making measurements in the jet regime represents a compromise between speed and completeness. More data in a shorter period of time are needed for a more accurate comparison with model predictions. Given the manpower and equipment limitations under which the work was done, the technique reported on in this report gives reasonable results in terms of number of data points versus time of measurement. The data obtained in this manner reflect the gross features of the jet regime, but have two limitations:

1. Since the temperature and velocity at a point in the jet are not constant, a single measured value of each may not accurately define these parameters at a point.

2. The measurements are not made simultaneously. Typically, they are collected over a period of 3-7 hr during which time factors affecting the jet may change.

B. Data-smoothing Technique

The fitting procedure described in Sec. V was used to extract the gross features of the temperature and velocity distributions from the field measurements. Some procedure of this type is necessary because the data consist of measurements at isolated points in the temperature and velocity fields. The functional forms used in this study were chosen for several reasons. One reason is their similarity to the forms resulting from the simple yet fairly widely used jet analyses of Pritchard[17] and Motz and Benedict.[5] Another reason is that preliminary examination of the Point Beach data indicated that such forms might represent the available data fairly well. Finally, it was thought that for this initial attempt at data fitting, simple forms with limited numbers of free parameters would be appropriate. Clearly, unless the actual functional forms are known, any fitting procedure of this type will have limitations and biases.

The results of the present fitting procedure can be considered to be a successful first attempt. It is difficult to assess the goodness of fit in a meaningful, quantitative way; therefore a point-by-point tabulation has been included in Appendix D. The average deviations of the fitted function from the data for any particular set of measurements never exceeded 1.1C° for temperature and 8 cm/sec for velocity. These values correspond to 12 and 14% of the initial excess temperature and average outfall velocity, respectively. Certainly at least the gross behavior of the near-field temperature and velocity distributions has been accounted for with the present fitting procedure.

C. Analytical Model; Field-data Comparisons

The results of the model-data comparisons are summarized here for each model evaluated.

1. Pritchard Model

The Pritchard model compared best with the Point Beach Unit 1 and Palisades jet data presented in this report. Model-data discrepancies usually indicated conservative predictions on the part of the model. The success of Pritchard's model for these cases is due in part to the persistent efforts of the author in calibrating the model with field and hydraulic data. Also, the field data used by Pritchard in the development of his model were generally from plants with similar discharge and environmental characteristics to Point Beach and Palisades.

This basically empirical or phenomenological model is not expected to perform well when buoyancy is significant (initial densimetric Froude number less than about 2) or when the dilution capacity of the receiving water is significantly restricted by lateral or bottom boundaries. The model is also weak in its treatment of vertical mixing; the model has scarcely been tested for prototype situations in which vertical entrainment is significant.

Although the model is too simplistic to handle the major complications that may be important in certain field cases (buoyancy, cross currents, etc.), it might well give good results for cases of the higher-velocity discharges (i.e., larger densimetric Froude number problems) for the critical case of a stagnant lake. Further verification work for this model is desirable at different sites describing a variety of geometric, kinematic, and dynamic conditions.

2. Motz-Benedict Model

The Motz-Benedict recommendations for the choice of entrainment coefficient E apparently vary over too large a range for the data observed at Point Beach and Palisades. The recommended value of 0.05 for the stagnant-lake case gave a reasonably good approximation for centerline temperature and velocity decay. Values of E for A (ratio of ambient velocity to initial jet velocity) between 0 and 0.2 were determined by a linear interpolation from the known values of 0.05 (A = 0) and 0.4 (A = 0.2). This appeared to us to be as good an approximation for E as any in the presence of the wide scatter in the Motz-Benedict data from which E is to be determined. The results indicate that smaller values of E for the cases of nonzero ambient crosscurrents would have been more appropriate. Temperature and velocity decays would not have been as rapid and plume widths would have been larger. The most sensitive parameters are E and $r = b_0/b'_0$. Data for the determination

of E have much scatter; data for r have not been determined. The inadequacies of this simple, two-dimensional model are briefly summarized as follows:

a. Buoyant forces, as well as vertical entrainment, are ignored in the model development. For densimetric Froude numbers less than about 2, buoyant spreading is quite important; for densimetric Froude numbers exceeding about 5, a substantial amount of vertical entrainment may be expected. Consequently, the types of discharges for which the model may be used is limited. The entrainment coefficient, determined from data fitting, must actually account for spreading due to buoyancy as well as from jet entrainment.

b. The choice of a coefficient of entrainment must be based on inconsistent data as expressed above. Data presented by Motz and Benedict show considerable variation in the value of entrainment coefficient from situation to situation. Particularly for lake data, the value of E is shown to be extremely small, ~0.04, in relation to riverine situations where E is about an order of magnitude larger. A particularly interesting contrast is afforded when one compares[5] the Motz-Benedict laboratory data for a 90° discharge to the Romberg-Ayres lake data. Although most of the initial conditions are similar, the entrainment coefficients are different by about a factor of 10. Part of the problem probably lies with the fact that Motz and Benedict analyzed lake data from locations in which prominences (breakwaters, for example) were present. A second difficulty is that the limited field results indicated that the entrainment coefficient remained essentially constant at a particular location with changing values of A; this behavior is consistent with the laboratory findings showing $\bar{E}$ to be relatively independent of A for each site. Here, turbulent intensity of the ambient current (see item e below) may be a significant factor that was ignored.

c. We believe the model is actually restricted to small ambient currents. The simulation assumes that the jet velocity approaches zero at large distances normal to the jet centerline. The assumption of Gaussian profiles for temperature and velocity and the assumption of equal rates of entrainment on offshore and lee sides of the jet are not valid for ambient currents that are not very small.

d. The model does not simulate unequal rates of spread for momentum and heat, as has been observed to be significant in the Point Beach and Palisades data. The Prych and Pritchard models also do not distinguish between these rates of spread.

e. The model does not treat turbulent intensity in the crossflow, due to the assumption that such turbulence and its effect on mixing are negligible. Although some account of this effect may be made in the choice of entrainment coefficient, any such treatment would be only qualitative in nature. The other models do not treat this phenomenon adequately either; the Prych model does include ambient turbulence in terms of a horizontal and vertical ambient eddy-thermal diffusivity.

Deficiencies a and b could eventually be fatal to the model. Improved predictions might be obtained by determining the free parameters

E = entrainment coefficient,

$r = b_0/b_0'$

and

s = ratio of lateral spread of heat to that of momentum

for each set of data available, with the hope that a consistent trend (or correlation) might develop as the initial densimetric Froude number, initial angle of jet discharge with the current, velocity ratio A, and w (ambient stream width/discharge width) vary.

3. Stolzenbach-Harleman Model

The Stolzenbach-Harleman model generally compared poorly with the jet data of Point Beach and Palisades. Centerline temperature and velocity decay were predicted to be too rapid; the lateral spread of the jet was much too great. The model does not consider jet interaction with the lake bottom, which does occur to some degree near the outfall. Such interaction should provide some increase in lateral spread due to restricted dilution at the jet-lake bottom interface. The predicted lateral spread, however, greatly exceeded the observed spread, even with bottom effects assisting that lateral growth. Surprisingly, the model tends to underpredict lateral spread in the region of flow establishment. These poor comparisons of model to data may be traced, in part, to the model assumption on lateral-spreading velocity, which was based more on physical intuition than on any data.

A second major fault of the model lies in the presumed jet structure based upon nonbuoyant jet theory. First, the four-zone, rectangular jet structure may not be valid for buoyant jets. In particular, the cross section of a buoyant jet is normally taken to be lens-shaped rather than rectangular, as supposed by the model. The assumed division of the jet into four distinct regions necessitates that interregional velocities be specified. The forms of these velocities are unknown and therefore must be guessed. Stolzenbach and Harleman also require that no turbulent momentum transfer occurs between regions of the jet or between the jet and ambient water. This is tantamount to dropping the Reynolds stress terms in the equations of motion or, equivalently, dropping the turbulent-diffusion mechanism. As a consequence, turbulent jet diffusion had to be artificially simulated through the entrainment coefficient and similarity forms for temperature and velocity. In any case, some calibration of the model to actual field and hydraulic data might have provided better predictions.

Aside from the largely theoretical criticisms of the model, there are practical difficulties in actually obtaining a numerical solution to the set

of ordinary differential equations. Due to the complexity of the set, derivatives must be found by solving a linear set of algebraic equations before applying a Runge-Kutta scheme. For many cases, the matrix, which must be reduced, is nearly singular and much precision is lost in solving for the derivatives. Among the problems that may be encountered in using the code are:

a. Width predictions may decrease by as much as 50% with each order-of-magnitude reduction in the error criteria until the program finally fails!

b. The program may not run for cases of

(1) Low initial densimetric Froude number.
(2) Low aspect ratio.
(3) Initial angles greater than 90°.

c. Numerical underflows must be suppressed for successful completion of many runs.

d. Differences in machine precision due either to differences in word structure or to differences in the operating system may cause differences of up to 5%.

4. Prych Model

The Prych predictions have the same problems as those of Stolzenbach and Harleman:

a. Too rapid a decay in centerline temperature and velocity.

b. Too great a lateral spread.

The Prych model also compares poorly with the Point Beach and Palisades data.

We suspect that a major difficulty with the theoretical development is in the assumption for a lateral-spreading velocity based upon the analogy to the celerity of a density front of a uniform depth with a uniform density difference. This model for lateral spreading is apparently incorrect as simulated. Also, the hydrostatic pressure force is simulated to act in the longitudinal direction only. Pressure forces in reality act longitudinally and laterally, with an approximate hydrostatic distribution vertically. The assumption of a fictitious lateral-spreading velocity was made to remedy that omission. The adequacy of the Prych simulation of ambient turbulence and shear stresses has not been verified. Calibration of the model and its empirical coefficients with hydraulic or prototype data might have improved predictions.

As with the Stolzenbach-Harleman model, the Prych model is applicable for small or zero ambient currents due to the assumption of similarity for temperature and velocity profiles, as well as equal entrainment on offshore and lee sides of the jet. The computer code developed by Prych operates well (model equations are simpler than those of Stolzenbach and Harleman); this makes it easier for future alteration, manipulation, and calibration of the model.

IX. RECOMMENDATIONS FOR FUTURE RESEARCH

A. Field-data Acquisition

Other techniques, such as fixed instrument arrays, aerial photography and aerial infrared imagery, and nonstationary measurement systems, may prove worthwhile in future measurements in the jet regime. These techniques or combinations of techniques may make it possible to overcome the limitations inherent in the fixed-boat method described here, but will probably also result in increased complexity of the measurement and significant monetary commitment.

B. Data-smoothing Technique

To extract as much information as possible from the data, the most general functional forms practicable should be used. This would require more free parameters and a more involved and lengthy fitting process. Future attempts to extend this method of data analysis might include some of the following:

1. Instead of Gaussian lateral profiles, a function that allows for a flat region near the jet centerline might be chosen. This could then simulate the core region included in the Stolzenbach-Harleman analysis.

2. The form of the centerline temperature excess should be such as to require that it extrapolate to the measured excess at the outfall ($s = 0$). The present form does not have this property.

3. In the present procedure, the rate of dropoff of the centerline temperature and velocity excesses is fixed as being inversely proportional to the one-half power of s, the distance from the outfall. Instead of this being restricted to the one-half power, it could be left as a free parameter to be determined by fitting to the data. The more recent phenomenological model by Pritchard[24] has employed this form for centerline decay of temperature.

4. Additional parameters could be added to the expressions for the widths to allow them to vary quadratically with s instead of linearly. The alternatives are limitless, and only through repeated attempts at a fitting procedure can it be determined whether significant improvements are possible.

C. Analytical Model; Field-data Comparisons

1. An attempt should be made to calibrate the Motz-Benedict, Stolzenbach-Harleman, and Prych models to field and hydraulic data.* The Pritchard model (No. 1) should be further tested with field data from other sites as well as available data from physical hydraulic models. The new numerical models of Brady and Geyer, Paul and Lick, and Waldrop and Farmer

*Work is presently underway by Dr. M. Shirazi at the Pacific Northwest Environmental Research Laboratory at Corvallis to improve the Stolzenbach-Harleman and Prych models by calibration with data. At this writing, a successful modification and calibration of the Prych model appears imminent.

look promising, and attempts should be made at verification with prototype field data. The new phenomenological model of Pritchard (No. 2), based upon 52 sets of model and prototype data, also looks promising and should be verified.

2. Considerably more data are required from more ideal or classical types of discharge structures for verification. The Palisades data had too many irregularities (rough shallow bottom and diverging discharge channel) for adequate model evaluation for those integral-type models studied in this report. Data are required for model verification (for both integral and numerical models), which include a wide range of densimetric Froude numbers, aspect ratios, bottom slopes, angle of discharge, ambient currents, etc., to provide a fair and wide variety of test situations for the models. Only when this large body of data (physical model or preferably prototype field data) becomes available will it be possible to fully and fairly evaluate and improve, or develop, better models.

From our verification efforts supplemented by the work done by Dr. M. Shirazi at the Pacific Northwest Water Laboratory of the EPA, we recommend that:

1. The Stolzenbach-Harleman and Prych models not be used as they exist in their present form for those cases when significant bottom interaction is expected. However, the vast majority of prototype situations do have some bottom interaction.
2. The Motz-Benedict model be used for stagnant ambient water case only (with an entrainment coefficient on the order of 0.04)
3. The Pritchard model be used for stagnant receiving water only.

Further analytical work is necessary to modify the Prych and Stolzenbach-Harleman models so they can be used for shallow water surface discharges. Additional work in model calibration is necessary before a viable form of the Motz-Benedict model can be achieved for ambient currents. More verification work on the Motz-Benedict (no current) and Pritchard models would be useful.

APPENDIX A

Previous Program Reports

1. J. G. Asbury, Effects of Thermal Discharges on the Mass/Energy Balance of Lake Michigan, ANL/ES-1 (July 1970).
2. E. Silberman and H. Stefan, Physical (Hydraulic) Modeling of Heat Dispersion in Large Lakes: A Review of the State of the Art, ANL/ES-2 (Aug 17, 1970).
3. J. G. Asbury, R. E. Grench, D. M. Nelson, W. Prepejchal, E. P. Romberg, and P. Siebold, A Photographic Method for Determining Velocity Distributions within Thermal Plumes, ANL/ES-4 (Feb 1971).
4. J. G. Asbury and A. A. Frigo, A Phenomenological Relationship for Predicting the Surface Areas of Thermal Plumes in Lakes, ANL/ES-5 (Apr 1971).
5. I. K. Abu-Shumays, D. L. Phillips, and S. M. Prastein, "Thermal Plume Data Acquisition, Documentation and Initial Analysis," Proceedings of the 14th Conference of the International Association of Great Lakes Research, Toronto, Ontario, April 19-21, 1971, p. 495.
6. G. P. Romberg, W. Prepejchal, and D. M. Nelson, "Thermal Plume Measurements," Proceedings of the 14th Conference of the International Association of Great Lakes Research, Toronto, Ontario, April 19-21, 1971, p. 625.
7. G. E. Birchfield, Wind-driven Currents in a Large Lake or Sea, ANL/ES-6 (July 1971).
8. J. V. Tokar, Thermal Plumes in Lakes: Compilations of Field Experience, ANL/ES-3 (Aug 1971).
9. R. E. Nakatani, D. Miller, and J. V. Tokar, "Thermal Effects and Nuclear Power Stations in the U.S.A.," International Atomic Energy Agency Transactions, Vienna, 1971, IAEA-SM-146/30, p. 561.
10. J. G. Asbury and A. A. Frigo, "A Phenomenological Relationship for Predicting the Surface Area of Thermal Plumes in Lakes," Transactions of the American Nuclear Society, 1971 Winter Meeting, October 17-21, 1971, Volume 14, No. 2, p. 461.
11. B. M. Hoglund, D. Nelson, and S. Spigarelli, "The Anatomy of a Thermal Plume and its Biological Implications," Transactions of the American Nuclear Society, 1971 Winter Meeting, October 17-21, 1971, Volume 14, No. 2, p. 462.
12. A. J. Policastro and J. V. Tokar, Heated Effluent Dispersion in Large Lakes: State-of-the-Art of Analytical Modeling: Part 1. Critique of Model Formulations, ANL/ES-11 (Jan 1972).

13. T. H. Hughes and G. E. Birchfield, A Compilation of the Average Depths of Lake Michigan and Lake Ontario on a Two-minute Grid, ANL/ES-10, (Jan 1972).

14. J. E. Draley, The Treatment of Cooling Waters with Chlorine, ANL/ES-12 (Feb 1972).

15. A. A. Frigo, "Prediction of Surface Plume Areas Associated with Heated Discharges into Large Lakes--A Phenomenological Model," Proceedings of the 15th Conference of the International Association of Great Lakes Research, Madison, Wisconsin, April 5-7, 1972, p. 583.

16. B. M. Hoglund and S. A. Spigarelli, "Studies of the Sinking Plume Phenomenon," Proceedings of the 15th Conference of the International Association of Great Lakes Research, Madison, Wisconsin, April 5-7, 1972, p. 614.

17. A. J. Policastro, "State-of-the-Art of Analytical Modeling of Heated Effluent Dispersion in Large Lakes," Proceedings of the 15th Conference of the International Association of Great Lakes Research, Madison, Wisconsin, April 5-7, 1972, p. 652.

18. Center for Environmental Studies and Environmental Statement Project, Summary of Recent Technical Information Concerning Thermal Discharges into Lake Michigan, Argonne National Laboratory for the Environmental Protection Agency Region V, Enforcement Branch, Contract Report 72-1 (Aug 1972).

19. A. A. Frigo and D. E. Frye, Physical Measurements of Thermal Discharges into Lake Michigan: 1971, ANL/ES-16 (Oct 1972).

20. A. J. Policastro, "Heated Effluent Dispersion in Large Lakes: State-of-the-Art of Analytical Modeling, Surface and Submerged Discharges," paper presented and published in Session Notes of the Topical Conference, Water Quality Considerations: Siting and Operating of Nuclear Power Plants, Atomic Industrial Forum, Inc. (Oct 1972).

21. A. J. Policastro and R. A. Paddock, Analytical Modeling of Heated Surface Discharges with Comparisons to Experimental Data, paper presented at the 1972 Annual Meeting of AIChE, November 26-30, 1972, to be published (Heat Transfer Symposium Series, 1973).

22. A. J. Policastro, Thermal Discharges into Lakes and Cooling Ponds, paper presented at ASCE Water Resources Conference, Washington, D.C. (Feb 1973).

23. R. A. Paddock, J. V. Tokar, and A. J. Policastro, "Analysis of Data Taken in the Near-Field Region of a Surface Thermal Discharge with Comparisons to Analytical Model Predictions," paper presented at 16th Conference of the International Association of Great Lakes Research, Huron, Ohio (Apr 1973).

24. D. E. Frye, A. A. Frigo, and B. M. Hoglund, "Data Collection and Reduction Techniques Used for Investigating Thermal Discharges," paper presented at 16th Conference of the International Association of Great Lakes Research, Huron, Ohio (Apr 1973).

25. A. A. Frigo, D. E. Frye, and P. Siebold, "Temperature and Velocity Measurements in the Near-Field Region of Thermal Plumes," paper presented at 16th Conference of the International Association of Great Lakes Research, Huron, Ohio (Apr 1973).

26. A. J. Policastro and W. Dunn, Chapter 13: "Heated Surface Discharges--Mathematical Models and Similarity Principles," Chapter 14: "Heated Surface Discharges--Application and Verification of State-of-the-Art Near-Field Models," Heat Disposal in Power Plant Siting, Joint Center for Graduate Study, Richland, Wash., August 20-24, 1973.

APPENDIX B

Preliminary Feasibility Study

On November 3, 1971, a preliminary feasibility study of the technique for studying the temperature and velocity profiles was made near the outfall of the Point Beach Nuclear Power Plant (Unit 1). A three-point mooring system was used to hold the boat steady while simultaneous temperature and velocity measurements were obtained in the near-field region. Anchors were located on either side of the plume and attached to the stern cleats of the boat, and a bowline was attached to the center of the outfall. Transects across the plume centerline were then made at about 8, 27, and 73 m from the outfall by pulling the boat from one side anchor to the other. The position of the boat was held relatively constant, and transits were used to obtain the location of each station. (Station locations for this jet study are shown in Fig. 94.) A Bendix Q-15 current meter with a YSI thermistor attached was used to measure current velocity and water temperature. The meter was lowered over the side and suspended at 2-ft intervals to a depth of 10 ft or to the bottom. The lake depth was 4.1 m at the outfall and decreased in depth to 2.1 m at a point 73 m from the outfall.

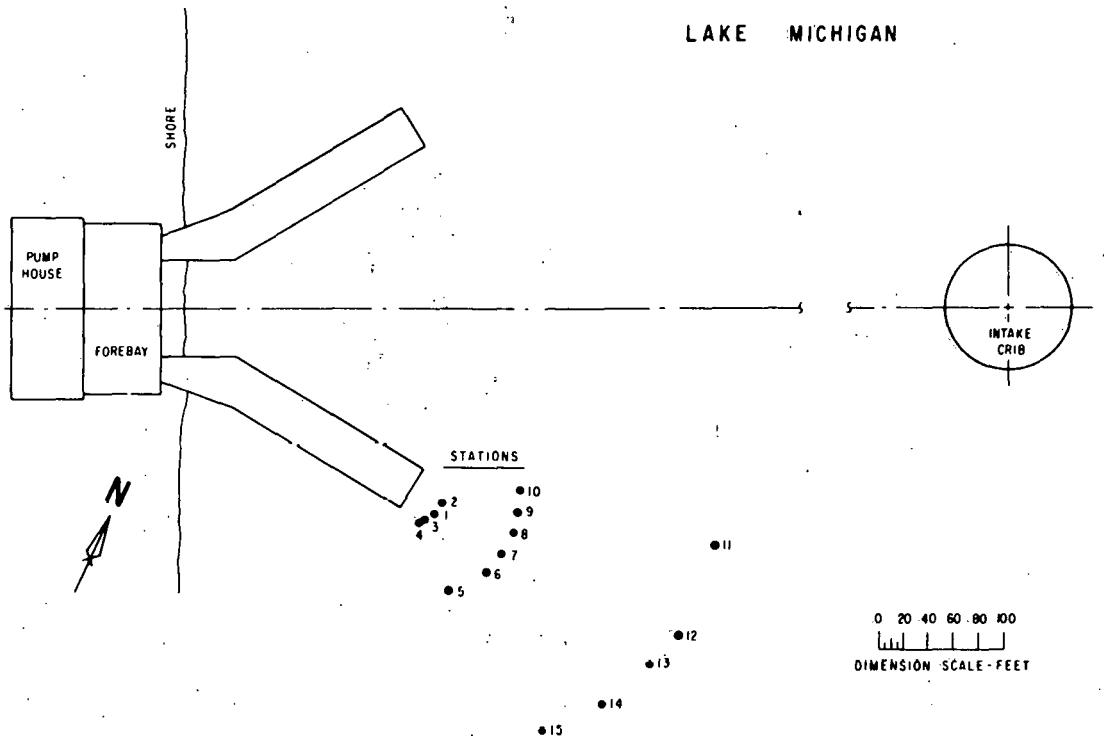

Fig. 94. Station Locations for Jet-regime Study: November 3, 1971, 1245-1605 Hours. ANL Neg. No. 190-573.

The data with the range of variability are plotted in Figs. 95-97 for three different depths. Drawings for the 8- and 10-ft depths were not made because data were not available at all stations. The temperature at a given

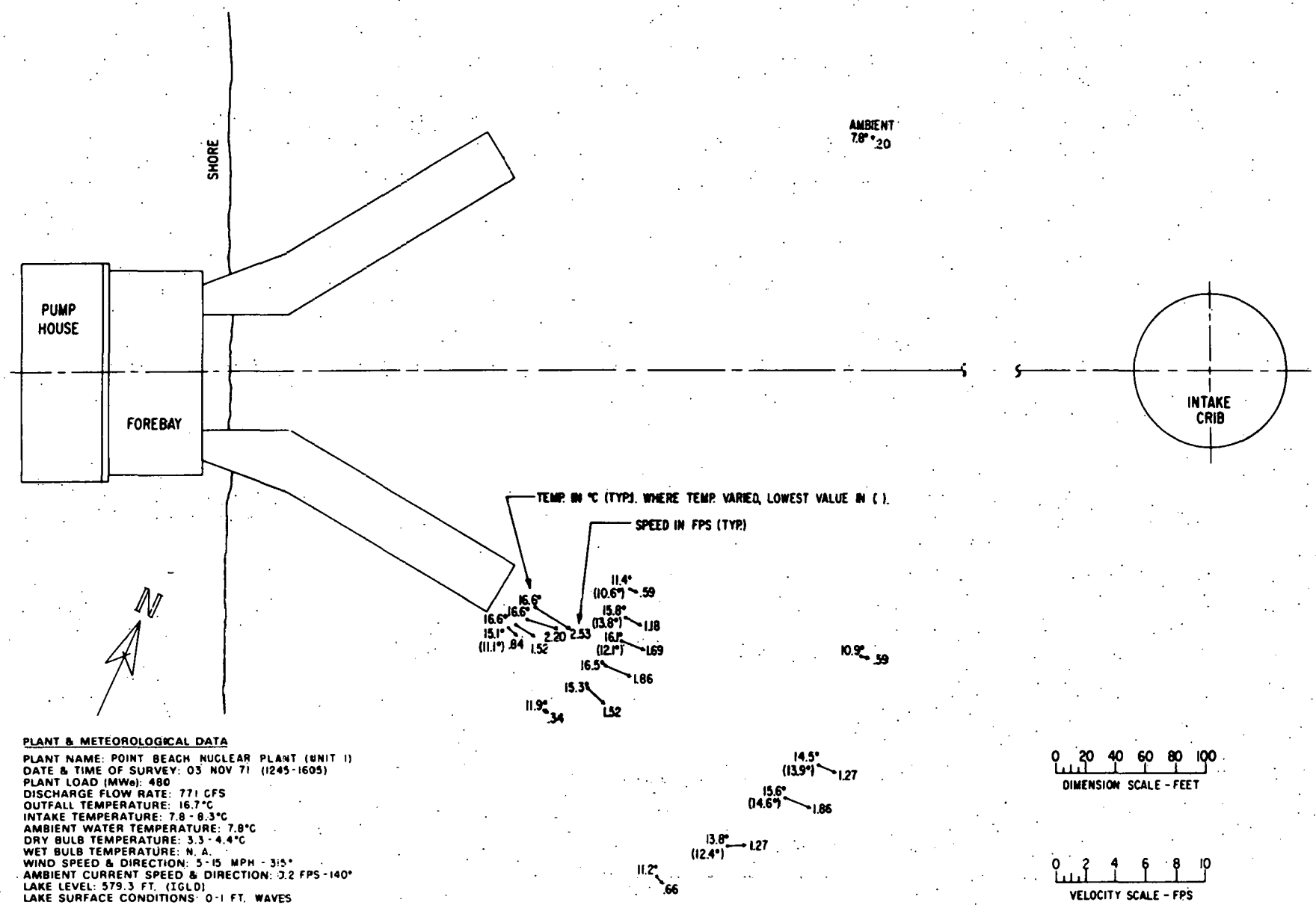

PLANT & METEOROLOGICAL DATA

PLANT NAME: POINT BEACH NUCLEAR PLANT (UNIT 1)
DATE & TIME OF SURVEY: 03 NOV 71 (1245-1605)
PLANT LOAD (MWe): 480
DISCHARGE FLOW RATE: 771 CFS
OUTFALL TEMPERATURE: 16.7°C
INTAKE TEMPERATURE: 7.8 - 8.3°C
AMBIENT WATER TEMPERATURE: 7.8°C
DRY BULB TEMPERATURE: 3.3 - 4.4°C
WET BULB TEMPERATURE: N. A.
WIND SPEED & DIRECTION: 5 - 15 MPH - 315°
AMBIENT CURRENT SPEED & DIRECTION: 0.2 FPS - 140°
LAKE LEVEL: 579.3 FT. (IGLD)
LAKE SURFACE CONDITIONS: 0-1 FT. WAVES

Fig. 95. Jet-regime Study for 2-ft Depth at Point Beach Power Plant (Unit 1): November 3, 1971, 1245–1605 Hours. ANL Neg. No. 190-410.

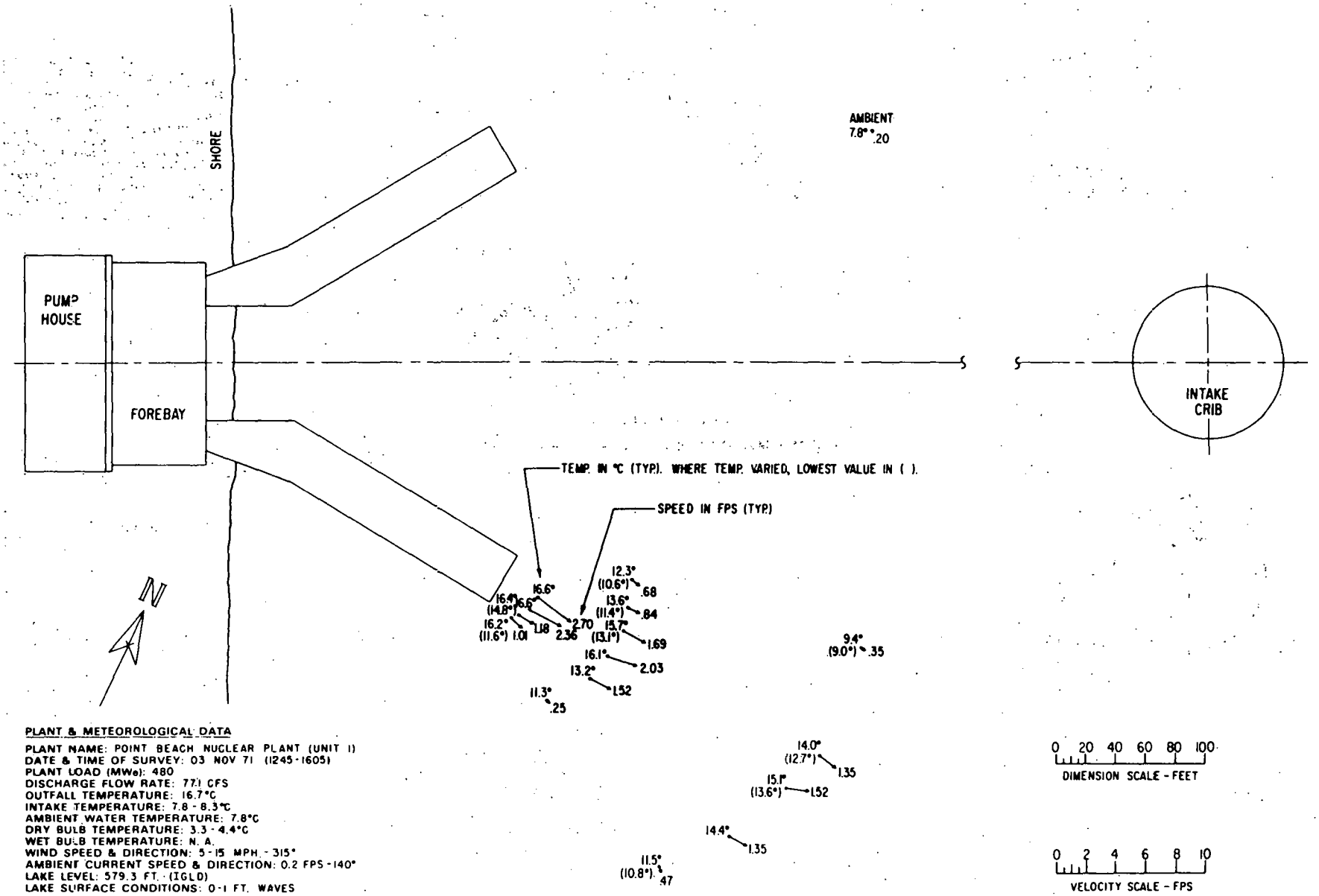

PLANT & METEOROLOGICAL DATA

PLANT NAME: POINT BEACH NUCLEAR PLANT (UNIT 1)
DATE & TIME OF SURVEY: 03 NOV 71 (1245-1605)
PLANT LOAD (MWe): 480
DISCHARGE FLOW RATE: 77.1 CFS
OUTFALL TEMPERATURE: 16.7°C
INTAKE TEMPERATURE: 7.8 - 8.3°C
AMBIENT WATER TEMPERATURE: 7.8°C
DRY BULB TEMPERATURE: 3.3 - 4.4°C
WET BULB TEMPERATURE: N. A.
WIND SPEED & DIRECTION: 5 - 15 MPH. - 315°
AMBIENT CURRENT SPEED & DIRECTION: 0.2 FPS - 140°
LAKE LEVEL: 579.3 FT. - (IGLD)
LAKE SURFACE CONDITIONS: 0-1 FT. WAVES

Fig. 96. Jet-regime Study for 4-ft Depth at Point Beach Power Plant (Unit 1): November 3, 1971, 1245-1605 Hours. ANL Neg. No. 190-411.

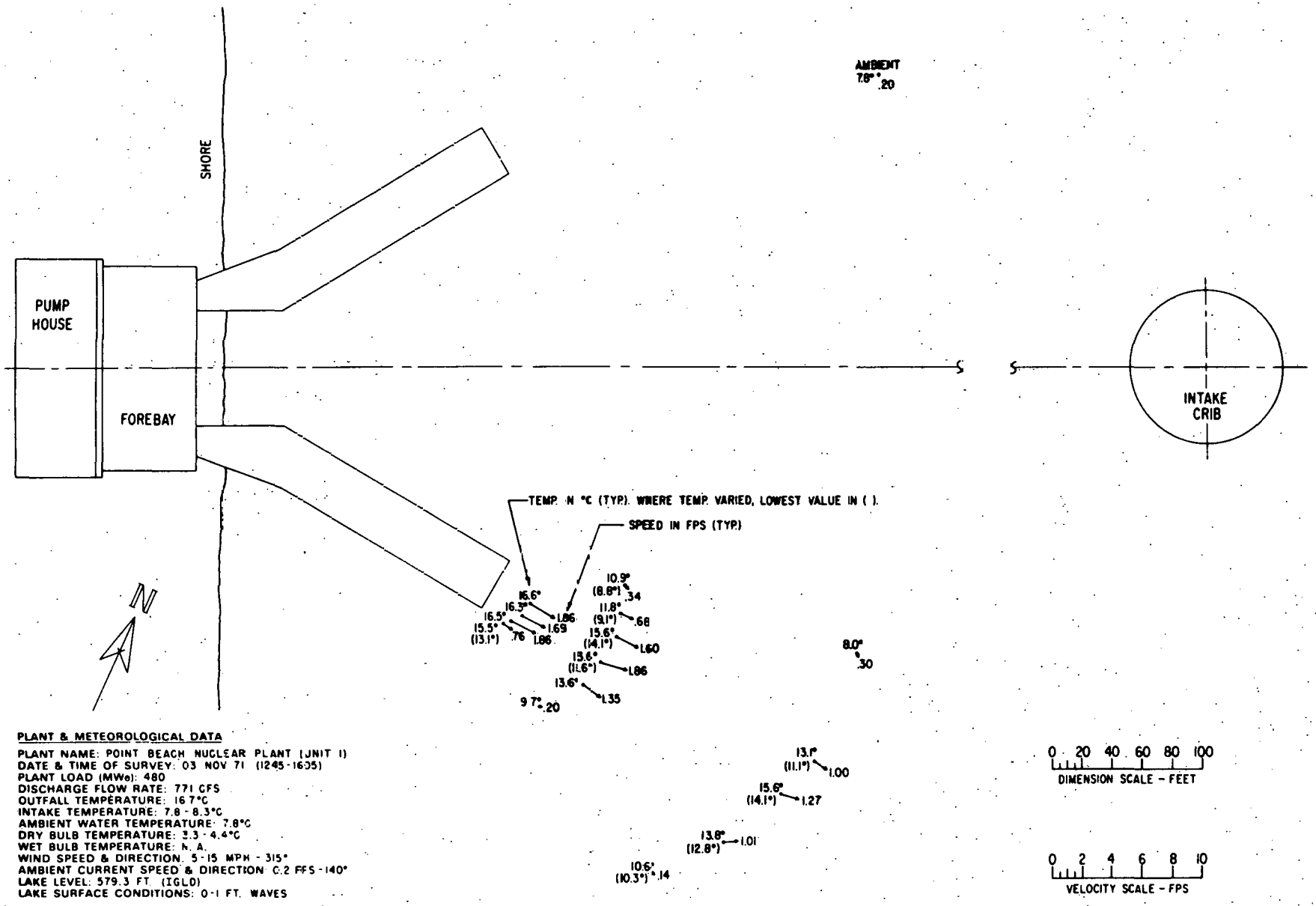

Fig. 97. Jet-regime Study for 6-ft Depth at Point Beach Power Plant (Unit 1): November 3, 1971, 1245-1605 Hours. ANL Neg. No. 190-412.

depth and location exhibited greater variability than expected, even near the plume centerline. As a result, temperature ranges are presented in the figures with the lowest temperature in parentheses. Each measurement was made over a period of about 1 min, which is indicative of the rapid variability of the temperature. Variations in the velocity were not as easily observed, because of the current-meter time constant. The lengths of the arrows in the figures are proportional to current magnitude, and their directions indicate current directions.

A more complete discussion of this jet-regime study appears in Ref. 19 of Appendix A. The results of this preliminary study are presented here only for completeness and were not used in the analysis discussed. In fact, since all the data were collected within 75 m of the outfall, the data are more representative of the flow-establishment region than of the established flow regime of the jet.

APPENDIX C

FORTRAN Listing for Fitting Procedure

The FORTRAN listing of the computer code JETFIT used for the jet data fitting procedure appears below.

```
C*************************************************************************C
C                                                                         C
C      PROGRAM JETFIT                                                     C
C                                                                         C
C*************************************************************************C
C
C      PROGRAM FITS A FUNCTION (CALLED 'JET-FUNCTION') WITH 12
C      PARAMETERS TO JET STUDY DATA.  THE FUNCTION YIELDS TEMPERATURE
C      AND VELOCITY CENTERLINES, CENTERLINE DECAYS AND WIDTHS(1/2).  THE
C      FUNCTION 'JET-FUNCTION' USES GAUSSIAN PROFILES, A QUADRATIC FORM
C      FOR THE CENTERLINE TRAJECTORIES, A CENTERLINE DECAY OF TEMPERATURE
C      AND VELOCITY THAT FALLS OFF AS THE INVERSE OF THE SQUARE ROOT OF
C      THE DISTANCE FROM THE OUTFALL, AND WIDTHS WHICH INCREASE LINEARLY
C      WITH DISTANCE.
C
C      INPUT -----
C
C      CARD 1 (20A4)
C           TITLE
C
C      CARD 2 (2I5,5F10.5)
C           NPTS = NO. OF DATA POINTS (STATIONS) (<=60)
C           NLEVEL = NO. OF LEVELS (DEPTHS) AT WHICH DATA WAS TAKEN (<=6)
C           ANGN = ANGLE OF NORTH W.R.T. +X-AXIS (DEG.)
C           BO = FULL WIDTH OF OUTFALL (FT.)
C           BETAO = ANGLE OF OUTFALL W.R.T. +X-AXIS (DEG.)
C           TO = OUTFALL TEMPERATURE (DEG.-C)
C           UO = AVERAGE OUTFALL SPEED (CM./SEC.)
C
C      CARD 3 (6F10.5)
C           AMTEMP(1 TO NLEVEL) = AMBIENT TEMPERATURE AT EACH LEVEL
C                                                        (DEG.-C)
C
C      CARD 4 (6F10.5)
C           AMCUR(1 TO NLEVEL) - AMBIENT CURRENT (CM./SEC.) (ASSUMED TO
C                BE PARALLEL TO THE +X-AXIS)
C
C      CARD 5 (6F10.5)
C           CON(1 TO NLEVEL) = FACTOR WHICH SETS THE CONVERGENCE
C                CRITERION FOR THE SEARCH TYPE FIT BASED ON THE DELTA'S
C                FOR EACH OF THE 12 PARAMETERS TO BE ENTERED BELOW.
C                CONVERGENCE IS  ASSUMED TO HAVE OCCURRED WHEN CHANGES
C                IN THE PARAMETERS ARE ALL LESS THAN
C                                        CON*DELTA(PARAMETER) .
C
C      CARD 6 (6F10.5)
C           ALIMT(1 TO NLEVEL) = MAXIMUM NUMBER OF ITERATIONS IN FITTING
C                THE TEMPERATURE PART OF 'JET-FUNCTION' (STEPS ARE
C                PRINTED OUT IF ALIMT < 0.0).
C
C      CARD 7 (6F10.5)
C           ALIMV(1 TO NLEVEL) = SAME AS ABOVE BUT FOR THE VELOCITY PART
C                OF THE FUNCTION.
C
C      CARD 8 (6F10.5)
```

```
C          P(1,1 TO NLEVEL) = FIRST GUESS AT FIRST PARAMETER OF
C               'JET-FUNCTION' (DIMENSIONLESS).
C
C     CARD 9 (6F10.5)
C          DELP(1,1 TO NLEVEL) = SMALL CHANGE IN P(1) TO BE USED TO
C               NUMERICALLY CALCULATE DERIVATIVES AND CONVERGENCE
C               CRITERION.
C
C     CARDS 10 THROUGH 31  (6F10.5)
C          REST OF THE 12 DIMENSIONLESS PARAMETERS AND THEIR DELTA'S.
C
C     FOLLOWING THESE 31 PRELIMINARY CARDS COMES THE DATA DECK (THIS
C     DECK IS COMPATIBLE WITH THE DATA DECK FOR PROGRAM JETDAT EXCEPT
C     THAT THE LAST BLANK CARD MUST BE REMOVED).
C
C     CARD 1 (3F10.5)
C          XP = X-COORDINATE OF STATION (FT.)
C          YP = Y-COORDINATE OF STATION (FT.)
C          DEPTH = DEPTH OF WATER (M.)
C
C     CARDS 2 (6F10.5) (DATA AT DIFFERENT LEVELS - TWO LEVELS PER CARD)
C          TEMP(K) = TEMPERATURE AT K-TH LEVEL (DEG.-C)
C          VEL(K) = SPEED (CM./SEC.)
C          DIR(K) = DIRECTION OF CURRENT W.R.T NORTH (DEG.)
C          TEMP(K+1) =
C          VEL(K+1) =
C          DIR(K+1) =
C
C     REPEAT FOR EACH STATION UP TO 'NPTS' STATIONS (<=60).
C
C
C
C     DETAILS OF 'JET-FUNCTION'
C
C     A COORDINATE SYSTEM IS CHOSEN SUCH THAT THE +Y-AXIS IS DIRECTED
C     IN THE OFF-SHORE DIRECTION.  THE +Z-AXIS IS DIRECTED VERTICALLY
C     UPWARD, AND THE +X-AXIS IS SUCH AS TO BE ORTHOGONAL TO THE OTHER
C     TWO AND SO AS TO FORM A RIGHT HANDED COORDINATE SYSTEM IN THE
C     CONVENTIONAL SENSE (X,Y,Z).
C
C     THE PARAMETERS OF 'JET-FUNCTION' ALONG WITH TYPICAL VALUES FOR
C     SOME POINT BEACH UNIT NO. 1 DATA ARE GIVEN BELOW.
C
C          P(1) = A (1.0)
C          P(2) = ALPHA (4.0)
C          P(3) = C (0.5)
C          P(4) = GAMMA (0.33)
C          P(5) = RT (1.0)
C          P(6) = KT (RANGES FROM ABOUT -1.0 TO +1.0)
C          P(7) = B (1.0)
C          P(8) = BETA  (4.8)
C          P(9) = D  (0.5)
C          P(10) = DELTA (0.19)
C          P(11) = RV (1.0)
C          P(12) = KV (RANGES FROM ABOUT -1.0 TO +1.0)
C
C
C     TEMPERATURE PART OF 'JET-FUNCTION'
C
C          CENTERLINE TRAJECTORY----
C          X=XSI*COS(RT*BETA0)-(0.01*KT/B0)*XSI**2*SIN(RT*BETA0)
C          Y=XSI*SIN(RT*BETA0)+(0.01*KT/B0)*XSI**2*COS(RT*BETA0)
```

```
C               WHERE XSI IS INTRODUCED ONLY DUE TO THE PARAMETRIC
C               FORM OF THE EQUATIONS (BENDS LEFT FOR KT>0, BENDS
C               RIGHT FOR KT<0)
C
C          CENTERLINE TEMPERATURE EXCESS RATIO----
C          (TC-TA)/(TO-TA)=A   IF S<ALPHA*BO
C                         =A*SQRT(ALPHA*BO/S)   IF S>ALPHA*BO
C               WHERE S IS THE DISTANCE FROM THE OUTFALL MEASURED ALONG
C               THE CENTERLINE
C
C          TEMPERATURE WIDTH (TO 1/2 THE CENTERLINE VALUE)----
C          WT/BO=C+GAMMA*S/BO
C
C
C      VELOCITY PART OF 'JET FUNCTION'
C
C          THE CENTERLINE TRAJECTORY EQUATIONS HAVE THE SAME FORM AS
C          THE ABOVE WITH KT REPLACED BY KV AND RT REPLACED BY RV.
C
C          CENTERLINE VELOCITY RATIO DECAY----
C          UC/UO=B   IF S<BETA*BO
C               =B*SQRT(BETA*BO/S)   IF S >BETA*BO
C               WHERE UC IS VELOCITY IN EXCESS OF AMBIENT CURRENT
C
C          VELOCITY WIDTH (TO 1/2 THE CENTERLINE VALUE)----
C          WU/BO=D+DELTA*S/BO
C
C
C      WARNING:
C          BE VERY CAREFUL OF ATTACHING ANY SIGNIFICANCE TO THE
C          INDIVIDUAL VALUES OF THE PARAMETERS (P(1) - P(12)), THEY ARE
C          USUALLY NOT UNIQUELY DETERMINED BY THE DATA.  DO NOT USE
C          THESE PARAMETERS TO EXTRAPOLATE TO VALUES OF  S  BEYOND
C          (OR BEFORE) THE DATA.
C
C
      DIMENSION TITLE(20),CON(6),ALIMT(6),ALIMV(6),P(12,6),DEPTH(60),BT(
     16),BV(6),EPSB(6),AREA(6)
      COMMON/HAVE/DELP(12,6),TEMP(60,6),VEL(60,6),DIR(60,6),XP(60),YP(60
     1),AMTEMP(6),AMCUR(6),BETAO,BO,ANGN,TO,UO,NPTS,DR,RD,K
      EXTERNAL FTSIG
      EXTERNAL FVSIG
      DR=0.0174532925
      RD=57.295780
      IMAX=27
C
C     FORMAT STATEMENTS ----
C
90    FORMAT(20A4)
91    FORMAT(2I5,5F10.5)
92    FORMAT(6F10.5)
93    FORMAT(3F10.5)
94    FORMAT('1PROGRAM JETFIT',//,' JET STUDY - INPUT DATA',/,5X,20A4,//
     1)
95    FORMAT(' NUMBER OF STATIONS =', I3, /, ' NUMBER OF LEVELS =', I2,
     1/, ' ANGLE OF NORTH W.R.T. +X-AXIS =', F8.2, ' DEG.', /, ' FULL WI
     2DTH OF OUTFALL =', F7.2, ' FT.', /, ' ANGLE OF OUTFALL W.R.T. +X-A
     3XIS =', F7.2,' DEG.', /, ' OUTFALL TEMPERATURE (TO) =', F7.2, ' DE
     4G.-C', /, ' AVERAGE OUTFALL VELOCITY (UO) =', F7.2, ' CM./SEC.', /
     5/, ' LEVEL', 2X, 'AMB. TEMP.', 2X, 'AMB. CURRENT', 2X, 'CONV. FACT
     6OR', 2X, 'LIMIT(TEMP)', 2X, 'LIMIT(VEL)', /, 10X, '(DEG.-C)', 4X,
     7'(CM./SEC.)', /)
```

```
96     FORMAT(4X, I2, 5X, F7.2, 6X, F8.2, 6X, F8.5, 6X, F7.1, 5X, F7.1)
97     FORMAT(///,' INITIAL PARAMETERS OF JET-FUNCTION (ALL ARE DIMENSION
      1LESS)',//,' LEVEL',8X,'P(1)',8X,'P(2)',8X,'P(3)',8X,'P(4)',8X,'P(5
      2)',8X,'P(6)',/)
98     FORMAT(4X,I2)
99     FORMAT(6X,6(2X,F10.6))
900    FORMAT(//,' LEVEL',8X,'P(7)',8X,'P(8)',8X,'P(9)',7X,'P(10)',7X,'P(
      111)',7X,'P(12)',/)
901    FORMAT('1DATA DECK'//,5X,20A4,//,' STATION',14X,'X',11X,'Y',3X,'DE
      1PTH',2X,'LEVEL',4X,'TEMP.',7X,'SPEED',2X,'DIRECTION',/,18X,'(FT.)'
      2,7X,'(FT.)',4X,'(M.)',8X,'(DEG.-C)',2X,'(CM./SEC.)',5X,'(DEG.)',/)
902    FORMAT(5X, I3, 5X, F10.2, 2X, F10.2, 2X, F6.2)
903    FORMAT(48X, I2, 5X, '----', 8X, '----', 7X, '----')
904    FORMAT(48X,I2,2X,F7.2,5X,F7.2,4X,F7.2)
905    FORMAT('1LEVEL',I2,3X,'(TEMPERATURE FIT)',//,5X,20A4,//)
906    FORMAT(//,' FINAL TEMPERATURE RESULTS FOR',I2,'-TH LEVEL',//,8X,'S
      1IGMA =', F8.3,'  AFTER',I6,' ITERATIONS.',//)
907    FORMAT(10X,'P(',I2,') =',F10.6)
908    FORMAT('1COMPARISON OF DATA AND FIT RESULTS FOR THE',I2,'-TH LEVEL
      1.',//,5X,20A4,//,2X,'STATION',11X,'X',11X,'Y',2X,'TEMP.(DATA)',2X,
      2'TEMP.(CALC.)',3X,'BETAT(CALC.)',2X,'SPEED(DATA)',2X,'SPEED(CALC.)
      3',3X,'BETAV(CALC.)',/,16X,'(FT.)',7X,'(FT.)',5X,'(DEG.-C)',6X,'(DE
      4G.-C)',9X,'(DEG.)',3X,'(CM./SEC.)',4X,'(CM./SEC.)',9X,'(DEG.)',/)
909    FORMAT(6X,I3,2X,F10.2,2X,F10.2,6X,F7.2,7X,F7.2,8X,F7.2,6X,F7.2,7X,
      1F7.2,8X,F7.2)
910    FORMAT(//,' TABLE OF JET-FUNCTION (TEMPERATURE PART)',//,9X,'XSI',
      111X,'S',10X,'XC',10X,'YC',2X,'(TC-TA)/(TO-TA)',2X,'W(1/2)/BO',5X,'
      2BETA',/,7X,'(FT.)',7X,'(FT.)',7X,'(FT.)',7X,'(FT.)',31X,'(DEG.)',/
      3)
911    FORMAT(2X,F10.2,2X,F10.2,2X,F10.2,2X,F10.2, 9X,F8.4,3X,F8.3,2X,F7.
      12)
912    FORMAT(//,' TABLE OF JET-FUNCTION (VELOCITY PART)',//,9X,'XSI',11X
      1,'S',10X,'XC',10X,'YC',4X,'UC/UO',2X,'(UC+UA)/UO',2X,'W(1/2)/BO',5
      2X,'BETA',/,7X,'(FT.)',7X,'(FT.)',7X,'(FT.)',7X,'(FT.)',35X,'(DEG.)
      3',/)
913    FORMAT(2X,F10.2,2X,F10.2,2X,F10.2,2X,F10.2,2X,F7.4,4X,F8.4,3X,F8.3
      1,2X,F7.2)
914    FORMAT(/,' TOO MANY DATA POINTS.',/)
915    FORMAT(/,' TOO MANY LEVELS.',/)
916    FORMAT('1LEVEL',I2,3X,'(VELOCITY FIT)',//,5X,20A4,//)
917    FORMAT(//,' FINAL VELOCITY RESULTS FOR', I2, '-TH LEVEL', //, 8X,
      1'SIGMA =', F8.3, '  AFTER', I6, ' ITERATIONS.', //)
918    FORMAT('1APPROXIMATE EXCESS TEMPERATURE ISOTHERM AREAS AND JET DEP
      1THS.', //, 5X, 20A4, ///, 2X, 'TEMP. EXCESS', 6X, 'AREA(ACRES) - L
      2EVEL',/,6X,'(C-DEG.)', 11X, '1', 11X, '2', 11X, '3', 11X, '4', 11X
      3, '5', 11X, '6', /)
919    FORMAT(7X,F7.2,6(2X,F10.4))
920    FORMAT(////, 11X, 'S', 2X, 'TEMP. EXCESS', 4X, 'DEPTH', 6X, 'ETA(F
      1T.) - LEVEL', /, 7X, '(FT.)', 6X, '(C-DEG.)', 2X, '(LEVEL)', 9X, '
      21', 9X, '2', 9X, '3', 9X, '4', 9X, '5', 9X, '6', /)
921    FORMAT(2X,F10.2,7X,F7.2, 2X, F7.3, 6(2X, F8.2))
922    FORMAT(////, 11X, 'S', 3X, 'VEL. EXCESS', 4X, 'DEPTH', 6X, 'ETA(FT
      1.) - LEVEL', /, 7X, '(FT.)', 4X, '(CM./SEC.)', 2X, '(LEVEL)', 9X,
      2'1', 9X, '2', 9X, '3', 9X, '4', 9X, '5', 9X, '6', /)
923    FORMAT(//, ' GOODNESS OF FIT:', /, 20X, 'TEMPERATURE', F8.2, ' %',
      1/, 20X, 'VELOCITY', F11.2, ' %')
C
C      READ IN DATA
33     READ(5,90,END=30)(TITLE(I),I=1,20)
       READ(5,91) NPTS,NLEVEL,ANGN,BO,BETAO,TO,UO
       IF(NPTS-60)1,1,31
1      IF(NLEVEL-6)7,7,32
```

```
7       READ(5,92) (AMTEMP(K),K=1,6)
        READ(5,92) (AMCUR(K),K=1,6)
        READ(5,92) (CON(K),K=1,6)
        READ(5,92) (ALIMT(K),K=1,6)
        READ(5,92) (ALIMV(K),K=1,6)
        DO 2 J=1,12
        READ(5,92) (P(J,K),K=1,6)
        READ(5,92) (DELP(J,K),K=1,6)
2       CONTINUE
        DO 6 I=1,NPTS
3       READ(5,93) XP(I),YP(I),DEPTH(I)
        IF(XP(I).NE.0.0) GOTO 4
        IF(YP(I).NE.0.0) GOTO 4
        IF(DEPTH(I).NE.0.0) GOTO 4
        GOTO 3
4       ANUM=NLEVEL
        ANUM=ANUM/2.0+0.75
        N=ANUM
        N=2*N
        DO 5 K=1,N,2
5       READ(5,92) TEMP(I,K),VEL(I,K),DIR(I,K),TEMP(I,K+1),VEL(I,K+1),DIR(
       1I,K+1)
6       CONTINUE
C
C       PRINT OUT DATA
C
        WRITE(6,94) (TITLE(I),I=1,20)
        WRITE(6,95) NPTS,NLEVEL,ANGN,B0,BETA0,T0,U0
        DO 8 K=1,NLEVEL
8       WRITE(6,96) K,AMTEMP(K),AMCUR(K),CON(K),ALIMT(K),ALIMV(K)
        WRITE(6,97)
        DO 9 K=1,NLEVEL
        WRITE(6,98) K
        WRITE(6,99) (P(J,K),J=1,6)
        WRITE(6,99) (DELP(J,K),J=1,6)
9       CONTINUE
        WRITE(6,900)
        DO 10 K=1,NLEVEL
        WRITE(6,98) K
        WRITE(6,99) (P(J,K),J=7,12)
        WRITE(6,99) (DELP(J,K),J=7,12)
10      CONTINUE
        WRITE(6,901) (TITLE(I),I=1,20)
        DO 11 I=1,NPTS
        WRITE(6,902) I,XP(I),YP(I),DEPTH(I)
        DO 11 K=1,NLEVEL
        IF(TEMP(I,K))13,14,14
13      IF(VEL(I,K))15,14,14
15      WRITE(6,903) K
        GOTO 11
14      WRITE(6,904) K,TEMP(I,K),VEL(I,K),DIR(I,K)
11      CONTINUE
C
C       START LOOP THROUGH LEVELS (COMPLETE ONE LEVEL AT A TIME).
C
        DO 16 K=1,NLEVEL
C       IF(ALIMT(K).EQ.0.0.AND.ALIMV(K).EQ.0.0) GOTO 16
        M=6
C
C       FIT TO TEMPERATURE DATA.
C
        SIGT=0.0
```

```
      DELMAX=0.0
      DO 17 J=1,M
      BT(J)=P(J,K)
      DELMAX=DELMAX+DELP(J,K)
17    EPSB(J)=DELP(J,K)*CON(K)
      DELMAX=0.16666667*DELMAX
      L=ALIMT(K)
C     IF(L.EQ.0) GOTO 12
      WRITE(6,905) K,(TITLE(I),I=1,20)
      CALL GMIN(FTSIG,M,BT,SIGT,EPSB,L,ITER,DELMAX)
      CALL LABEL(ITER)
      WRITE(6,906) K,SIGT,L
      DO 18 J=1,M
      P(J,K)=BT(J)
18    WRITE(6,907) J,BT(J)
      WRITE(6,910)
      DO 24 I=1,IMAX
      ANUM=I-1
      XSI=ANUM*50.0
      ANUM=0.01*BT(6)/B0
      THETA=DR*BT(5)*BETA0
      STH=SIN(THETA)
      CTH=COS(THETA)
      A1=2.0*XSI*ABS(ANUM)
      IF(A1-0.1)34,34,35
34    S=XSI*(1.0+0.16666667*A1*A1-0.025*A1**4)
      GOTO 36
35    A2=SQRT(1.0+A1*A1)
      S=0.5*XSI*(A2+ALOG(A1+A2)/A1)
36    X=XSI*CTH-ANUM*XSI*XSI*STH
      Y=XSI*STH+ANUM*XSI*XSI*CTH
      T=BT(1)
      IF(S-BT(2)*B0)25,25,26
26    T=T*SQRT(BT(2)*B0/S)
25    A1=STH+2.0*ANUM*XSI*CTH
      A2=CTH-2.0*ANUM*XSI*STH
      BETAT=RD*ATAN2(A1,A2)
      WB0=BT(3)+BT(4)*S/B0
24    WRITE(6,911) XSI,S,X,Y,T,WB0,BETAT
C
C     FIT TO VELOCITY DATA.
C
12    SIGV=0.0
      DELMAX=0.0
      DO 19 J=1,M
      BV(J)=P(J+M,K)
      DELMAX=DELMAX+DELP(J+M,K)
19    EPSB(J)=DELP(J+M,K)*CON(K)
      DELMAX=0.16666667*DELMAX
      L=ALIMV(K)
C     IF(L.EQ.0) GOTO 52
      WRITE(6,916) K,(TITLE(I),I=1,20)
      CALL GMIN(FVSIG,M,BV,SIGV,EPSB,L,ITER,DELMAX)
      CALL LABEL(ITER)
      WRITE(6,917) K,SIGV,L
      DO 20 J=7,12
      P(J,K)=BV(J-M)
20    WRITE(6,907) J,BV(J-M)
      WRITE(6,912)
      DO 27 I=1,IMAX
      ANUM=I-1
      XSI=ANUM*50.0
```

```
      ANUM=0.01*BV(6)/BO
      THETA=DR*BV(5)*BETAO
      STH=SIN(THETA)
      CTH=COS(THETA)
      A1=2.0*XSI*ABS(ANUM)
      IF(A1-0.1)37,37,38
37    S=XSI*(1.0+0.16666667*A1*A1-0.025*A1**4)
      GOTO 39
38    A2=SQRT(1.0+A1*A1)
      S=0.5*XSI*(A2+ALOG(A1+A2)/A1)
39    X=XSI*CTH-ANUM*XSI*XSI*STH
      Y=XSI*STH+ANUM*XSI*XSI*CTH
      VC=BV(1)
      IF(S-BV(2)*BO)28,28,29
29    VC=VC*SQRT(BV(2)*BO/S)
28    A1=STH+2.0*ANUM*XSI*CTH
      A2=CTH-2.0*ANUM*XSI*STH
      BETAV=ATAN2(A1,A2)
      VD=VC+COS(BETAV)*AMCUR(K)/UO
      BETAV=RD*BETAV
      WBO=BV(3)+BV(4)*S/BO
27    WRITE(6,913) XSI,S,X,Y,VC,VD,WBO,BETAV
C
C     PRINT OUT TABLE OF COMPARISON OF CALCULATIONS FROM 'JET-FUNCTION'
C     TO DATA FOR THIS LEVEL.
C
52    WRITE(6,908) K,(TITLE(I),I=1,20)
      ANUM=0.0
      A1=0.0
      A2=0.0
      DO 21 I=1,NPTS
      IF(TEMP(I,K))22,23,23
22    IF(VEL(I,K))21,23,23
23    CALL TEMVEL(XP(I),YP(I),BT,BO,BETAO,RT,BETAT)
      T=RT*TO-RT*AMTEMP(K)+AMTEMP(K)
      BETAT=BETAT*RD
      A1=A1+(TEMP(I,K)-AMTEMP(K))**2
      CALL TEMVEL(XP(I),YP(I),BV,BO,BETAO,RV,BETAV)
      DEVBET=(ANGN-DIR(I,K))*DR-BETAV
      VD=VEL(I,K)*COS(DEVBET)
      VC=RV*UO+AMCUR(K)*COS(BETAV)
      BETAV=RD*BETAV
      A2=A2+VD*VD
      ANUM=ANUM+1.0
      WRITE(6,909) I,XP(I),YP(I),TEMP(I,K),T,BETAT,VD,VC,BETAV
21    CONTINUE
      ANUM=ANUM-6.0
      IF(ANUM.LT.0.5) ANUM=1.0
      A1=100.0*(1.0-SIGT/SQRT(A1/ANUM))
      A2=100.0*(1.0-SIGV/SQRT(A2/ANUM))
      WRITE(6,923) A1,A2
C
C     END OF LOOP THROUGH LEVELS.
C
16    CONTINUE
C
C     CALCULATES ISOTHERM AREAS AND JET DEPTHS.
C          DEPTH IS DEFINED AS THE EQUIVALENT TWO-DIMENSIONAL DEPTH.
C
      WRITE(6,918) (TITLE(I),I=1,20)
      IT=TO-AMTEMP(NLEVEL)
41    TE=IT
```

```
      DO 40 K=1,NLEVEL
40    AREA(K)=TAREA(TE,P)
      WRITE(6,919) TE,(AREA(K),K=1,NLEVEL)
      IT=IT-1
      IF(IT.GE.1) GOTO 41
      WRITE(6,920)
      DO 42 I=1,IMAX
      ANUM=I-1
      S=50.0*ANUM
      T=P(1,1)*(TO-AMTEMP(1))
      IF(S.LE.P(2,1)*BO) GOTO 43
      T=T*SQRT(P(2,1)*BO/S)
43    T=0.5*T
      DO 44 K=1,NLEVEL
44    AREA(K)=ETAT(S,T,P)
      A1=0.0
      IF(AREA(1).LT.(0.1*BO)) GOTO 46
      A1=0.5*AREA(1)
      DO 45 K=2,NLEVEL
45    A1=A1+AREA(K)
      A1=A1/AREA(1)+1.0
46    WRITE(6,921) S,T,A1,(AREA(K),K=1,NLEVEL)
42    CONTINUE
      WRITE(6,922)
      DO 47 I=1,IMAX
      ANUM=I-1
      S=50.0*ANUM
      VC=P(7,1)*UO
      IF(S.LE.P(8,1)*BO) GOTO 48
      VC=VC*SQRT(P(8,1)*BO/S)
48    VD=0.5*VC
      DO 49 K=1,NLEVEL
49    AREA(K)=ETAV(S,VD,P)
      A1=0.0
      IF(AREA(1).LT.(0.1*BO)) GOTO 51
      A1=0.5*AREA(1)
      DO 50 K=2,NLEVEL
50    A1=A1+AREA(K)
      A1=A1/AREA(1)+1.0
51    WRITE(6,921) S,VD,A1,(AREA(K),K=1,NLEVEL)
47    CONTINUE
C
      GOTO 33
C
31    WRITE(6,914)
      GOTO 30
32    WRITE(6,915)
30    CALL EXIT
      STOP
      END
C*****************************************************************C
C                                                                 C
      SUBROUTINE GMIN(FUNC,M,X,F,EPS,LIMIT,ITER,DELMAX)
C                                                                 C
C*****************************************************************C
C
C     ROUTINE FINDS THE MINIMUM BY A SEARCH TECHNIQUE OF THE
C     FUNCTION (CALCULATED IN SUBROUTINE FUNC) WITH RESPECT TO ITS
C     PARAMETERS  X(I), I=1,M.  FIRST THE DIRECTION OF STEEPEST
C     DECENT IS SELECTED BY EVALUATING THE GRADIENT OF THE FUNCTION
C     WITH RESPECT TO THE  M  PARAMETERS.  THEN A STEP IS TAKEN ALONG
C     THAT DIRECTION.  THE SIZE OF THE STEP IS PRESET BUT MULTIPLES OR
```

```
C     FRACTIONS OF THIS STEP SIZE ARE USED IF NECESSARY.
C
      DIMENSION X(10),G(10),EPS(10),XZ(10),DUM(10)
      EXTERNAL FUNC
C
      L=0
      LP=0
      IF(LIMIT.EQ.0) GOTO 35
      IP=1
      IF(LIMIT.LT.0) IP=0
      LIMIT=IABS(LIMIT)
      IF(IP.EQ.0.OR.LIMIT.GE.100) WRITE(6,2)
2     FORMAT(17X,'FUNC',5X,'PARAMETERS',/)
C
1     ITER=1
      L=L+1
      LP=LP+1
      IF(LP.GE.100) LP=0
      CALL FUNC(M,X,F,G,ITER)
      IF(IP.EQ.0.OR.LP.EQ.0) WRITE(6,3) F,(X(J),J=1,M)
3     FORMAT(6X,7F15.8)
      IF(ITER.EQ.0) GOTO 15
      ITER=2
      GNORM=0.0
      DO 4 I=1,M
4     GNORM=GNORM+G(I)*G(I)
      GNORM=SQRT(GNORM)
C     IF(IP.EQ.0.OR.LP.EQ.0) WRITE(6,3) GNORM,(G(J),J=1,M)
      IF(GNORM.LE.0.0) GOTO 15
C
      DO 5 I=1,M
      G(I)=G(I)*DELMAX/GNORM
5     XZ(I)=X(I)-G(I)
      CALL FUNC(M,XZ,FZ,DUM,ITER)
      IF(FZ.LT.F) GOTO 40
C
32    KK=0
      DO 33 I=1,M
      G(I)=0.5*G(I)
      IF(ABS(G(I)).GT.EPS(I)) KK=1
33    XZ(I)=X(I)-G(I)
      CALL FUNC(M,XZ,FZ,DUM,ITER)
      IF(FZ.LT.F) GOTO 13
      IF(KK.EQ.1) GOTO 32
      ITER=3
      GOTO 15
13    DO 11 I=1,M
11    X(I)=XZ(I)
      F=FZ
      GOTO 12
C
40    F=FZ
      DO 41 I=1,M
      X(I)=XZ(I)
41    XZ(I)=X(I)-G(I)
      CALL FUNC(M,XZ,FZ,DUM,ITER)
      IF(FZ.LT.F) GOTO 40
C
12    IF(L.LT.LIMIT) GOTO 1
      IF(ITER.EQ.0) GOTO 15
      ITER=4
```

```
15    LIMIT=L
      RETURN
C
C
35    ITER=2
      CALL FUNC(M,X,F,DUM,ITER)
      GOTO 12
C
      END
C*****************************************************************************C
C                                                                             C
      SUBROUTINE LABEL(ITER)
C                                                                             C
C*****************************************************************************C
C
      I=ITER+1
      GOTO(5,10,15,20,25),I
5     WRITE(6,6)
6     FORMAT(//,'    ARGUMENT OUT OF RANGE.')
      RETURN
10    WRITE(6,11)
11    FORMAT(//,'    SUCCESSIVE ITERATIONS NOT REDUCING FUNCTION.')
      RETURN
15    WRITE(6,16)
16    FORMAT(//,'    GRADIENT TOO SMALL FOR USEFUL ITERATION.')
      RETURN
20    WRITE(6,21)
21    FORMAT(//,'    ERROR CRITERIA SATISFIED.')
      RETURN
25    WRITE(6,26)
26    FORMAT(//,'    MAXIMUM NUMBER OF ITERATIONS ATTAINED.')
      RETURN
      END
C*****************************************************************************C
C                                                                             C
      SUBROUTINE TEMVEL(X,Y,B,BO,BETAO,R,RBETA)
C                                                                             C
C*****************************************************************************C
C
C     ROUTINE RETURNS R (LOCAL EXCESS TEMPERATURE OR VELOCITY RATIO)
C     AT THE POINT (X,Y) AS DETERMINED BY 'JET-FUNCTION' WITH PARAMETERS
C     B(I), OUTFALL FULL WIDTH BO, AND OUTFALL ANGLE BETAO W.R.T. THE
C     X-AXIS.  ROUTINE ALSO RETURNS RBETA (THE ANGLE IN RADIANS THE
C     CENTERLINE ASSOCIATED WITH THE POINT (X,Y) MAKES WITH THE X-AXIS).
C
      DIMENSION B(6)
C
      AK=0.01*B(6)/BO
      ABSAK=ABS(AK)
      THETA=0.0174532925*B(5)*BETAO
      STH=SIN(THETA)
      CTH=COS(THETA)
      XO=X*STH-Y*CTH
      YO=X*CTH+Y*STH
      W=27.0*AK*AK*YO*YO+2.0*(1.0+2.0*AK*XO)**3
      IF(YO.LT.0.0) GOTO 3
C
C     FOLLOWING FOR CASE WHERE YO.GE.0.0
C
      IF(W.LT.0.0) GOTO 2
      A1=0.25*YO*ABSAK
      A2=SQRT(0.00231481481481*W)
```

```
      IF(A1.LT.0.03*A2) GOTO 1
      XSI=(CUBRT(A1+A2)+CUBRT(A1-A2))/ABSAK
      GOTO 4
1     XSI=Y0*CUBRT(2.0/W)
      GOTO 4
2     A1=SQRT(-1.0-2.0*AK*X0)
      S=(3.674234613*Y0*ABSAK)/(A1*A1*A1)
      S=ARCOS(S)*0.333333333
      XSI=(0.8164965809*A1*COS(S))/ABSAK
      GOTO 4
C
C     FOLLOWING IS FOR THE CASE WHERE Y0.LT.0.0
C
3     IF(W.GT.0.0) GOTO 12
      GOTO 2
C
C     NOW HAVE VALUE FOR  XSI.
C
4     A1=2.0*XSI*ABSAK
      IF(A1-0.1)5,5,6
5     S=XSI*(1.0+0.166666667*A1*A1-0.025*A1**4)
      GOTO 7
6     A2=SQRT(1.0+A1*A1)
      S=0.5*XSI*(A2+ALOG(A1+A2)/A1)
C
C     NOW HAVE VALUE FOR  S .
C
7     ETASQ=(X0+AK*XSI*XSI)**2+(Y0-XSI)**2
      A1=STH+2.0*AK*XSI*CTH
      A2=CTH-2.0*AK*XSI*STH
      RBETA=ATAN2(A1,A2)
      W=B(3)*B0+B(4)*S
      IF(W.LE.0.0) GOTO 8
      A1=0.6931471806*ETASQ/(W*W)
      IF(A1.GE.25.0) GOTO 8
      A1=EXP(-A1)
      GOTO 9
8     A1=0.0
9     IF(S-B(2)*B0)10,10,11
10    R=B(1)*A1
      RETURN
11    R=B(1)*A1*SQRT(B(2)*B0/S)
      RETURN
12    R=0.0
      RBETA=THETA
      RETURN
      END
C*********************************************************************C
C                                                                     C
      FUNCTION CUBRT(X)
C                                                                     C
C*********************************************************************C
C
C     ROUTINE CALCULATES THE CUBE-ROOT OF A REAL NUMBER.
C
      Y=X
      SIGN=1.0
      IF(Y)1,3,2
1     SIGN=-1.0
      Y=-Y
2     Y=0.333333333*ALOG(Y)
      CUBRT=SIGN*EXP(Y)
```

```
      RETURN
3     CUBRT=0.0
      RETURN
      END
C*****************************************************************************C
C                                                                               C
      SUBROUTINE FTSIG(M,BT,SIGT,G,ITER)
C                                                                               C
C*****************************************************************************C
C
C     ROUTINE CALCULATES THE STANDARD DEVIATION OF THE TEMPERATURE DATA
C     FROM 'JET-FUNCTION' WITH PARAMETERS BT.  ON CERTAIN CALLS, THE
C     DERIVITIVES OF THIS DEVIATION WITH RESPECT TO EACH PARAMETER IS
C     ALSO CALCULATED.
C
      DIMENSION BT(6),G(6),BB(6)
      COMMON/HAVE/DELP(12,6),TEMP(60,6),VEL(60,6),DIR(60,6),XP(60),YP(60
     1),AMTEMP(6),AMCUR(6),BETA0,B0,ANGN,T0,U0,NPTS,DR,RD,K
C
      CALL TSIG(BT,SIGT)
      IF(ITER.EQ.2) RETURN
      DO 1 J=1,M
      DO 2 I=1,M
2     BB(I)=BT(I)
      BB(J)=BT(J)+DELP(J,K)
      CALL TSIG(BB,SIGP)
      BB(J)=BT(J)-DELP(J,K)
      CALL TSIG(BB,SIGM)
1     G(J)=0.5*(SIGP-SIGM)/DELP(J,K)
      RETURN
      END
C*****************************************************************************C
C                                                                               C
      SUBROUTINE FVSIG(M,BV,SIGV,G,ITER)
C                                                                               C
C*****************************************************************************C
C
C     ROUTINE DOES THE SAME THING AS FTSIG EXCEPT FOR THE VELOCITY
C     PART OF 'JET-FUNCTION' AND THE VELOCITY DATA.
C
      DIMENSION BV(6),G(6),BB(6)
      COMMON/HAVE/DELP(12,6),TEMP(60,6),VEL(60,6),DIR(60,6),XP(60),YP(60
     1),AMTEMP(6),AMCUR(6),BETA0,B0,ANGN,T0,U0,NPTS,DR,RD,K
C
      CALL VSIG(BV,SIGV)
      IF(ITER.EQ.2) RETURN
      DO 1 J=1,M
      DO 2 I=1,M
2     BB(I)=BV(I)
      BB(J)=BV(J)+DELP(J+M,K)
      CALL VSIG(BB,SIGP)
      BB(J)=BV(J)-DELP(J+M,K)
      CALL VSIG(BB,SIGM)
1     G(J)=0.5*(SIGP-SIGM)/DELP(J+M,K)
      RETURN
      END
C*****************************************************************************C
C                                                                               C
      SUBROUTINE TSIG(BT,SIGT)
C                                                                               C
C*****************************************************************************C
```

```
C
C       ROUTINE CALCULATES THE STANDARD DEVIATION OF THE TEMPERATURE
C       DATA FROM 'JET-FUNCTION' OF PARAMETERS BT.
C
        DIMENSION BT(6)
        COMMON/HAVE/DELP(12,6),TEMP(60,6),VEL(60,6),DIR(60,6),XP(60),YP(60
       1),AMTEMP(6),AMCUR(6),BETAO,BO,ANGN,TO,UO,NPTS,DR,RD,K
C
        SIGT=0.0
        ANUM=0.0
        DO 2 I=1,NPTS
        IF(TEMP(I,K))2,1,1
1       CALL TEMVEL(XP(I),YP(I),BT,BO,BETAO,RT,RBETA)
        SIGT=SIGT+(TEMP(I,K)-RT*TO+RT*AMTEMP(K)-AMTEMP(K))**2
        ANUM=ANUM+1.0
2       CONTINUE
        DEGFR=ANUM-6.0
        IF(DEGFR.LT.0.5) DEGFR=1.0
        SIGT=SQRT(SIGT/DEGFR)
        RETURN
        END
C*************************************************************************C
C                                                                         C
        SUBROUTINE VSIG(BV,SIGV)
C                                                                         C
C*************************************************************************C
C
C       ROUTINE DOES THE SAME THING AS TSIG ONLY FOR VELOCITY.
C
        DIMENSION BV(6)
        COMMON/HAVE/DELP(12,6),TEMP(60,6),VEL(60,6),DIR(60,6),XP(60),YP(60
       1),AMTEMP(6),AMCUR(6),BETAO,BO,ANGN,TO,UO,NPTS,DR,RD,K
C
        SIGV=0.0
        ANUM=0.0
        DO 2 I=1,NPTS
        IF(VEL(I,K))2,1,1
1       CALL TEMVEL(XP(I),YP(I),BV,BO,BETAO,RV,RBETA)
        DEVBET=(ANGN-DIR(I,K))*DR-RBETA
        SIGV=SIGV+(VEL(I,K)*COS(DEVBET)-RV*UO-AMCUR(K)*COS(RBETA))**2
        ANUM=ANUM+1.0
2       CONTINUE
        DEGFR=ANUM-6.0
        IF(DEGFR.LT.0.5) DEGFR=1.0
        SIGV=SQRT(SIGV/DEGFR)
        RETURN
        END
C*************************************************************************C
C                                                                         C
        FUNCTION TAREA(TE,P)
C                                                                         C
C*************************************************************************C
C
C       FUNCTION CALCULATES THE APPROXIMATE ISOTHERM AREAS OF 'JET-
C       FUNCTION' NEGLECTING THE CURVATURE OF THE CENTERLINE.
C
        DIMENSION P(12,6)
        COMMON/HAVE/DELP(12,6),TEMP(60,6),VEL(60,6),DIR(60,6),XP(60),YP(60
       1),AMTEMP(6),AMCUR(6),BETAO,BO,ANGN,TO,UO,NPTS,DR,RD,K
C
        TAREA=0.0
        R=P(1,K)*(TO-AMTEMP(K))/TE
```

```
      IF(R.LT.1.0) GOTO 10
      SMAX=P(2,K)*B0*R*R
      NSTP=0.1*SMAX
      IF(NSTP.GT.100) NSTP=100
      AI=NSTP
      DELS=SMAX/AI
      S=0.0
      TAREA=0.5*ETAT(S,TE,P)
      NSTP=NSTP-1
      DO 11 I=1,NSTP
      AI=I
      S=AI*DELS
11    TAREA=TAREA+ETAT(S,TE,P)
      TAREA=DELS*TAREA*4.592E-5
10    RETURN
      END
C*****************************************************************************C
C                                                                               C
      FUNCTION ETAT(S,TE,P)
C                                                                               C
C*****************************************************************************C
C
C     FUNCTION CALCULATES THE LATERAL DISTANCE OUT TO THE TE TEMPERATURE
C     EXCESS ISOTHERM.
C
      DIMENSION P(12,6)
      COMMON/HAVE/DELP(12,6),TEMP(60,6),VEL(60,6),DIR(60,6),XP(60),YP(60
     1),AMTEMP(6),AMCUR(6),BETA0,B0,ANGN,T0,U0,NPTS,DR,RD,K
C
      ETAT=0.0
      TC=P(1,K)*(T0-AMTEMP(K))
      IF(S.LE.P(2,K)*B0) GOTO 12
      TC=TC*SQRT(P(2,K)*B0/S)
12    IF(TE.GT.TC) GOTO 13
      ETAT=1.44269504*ALOG(TC/TE)
      ETAT=SQRT(ETAT)*(P(3,K)*B0+P(4,K)*S)
      IF(ETAT.LT.0.0) ETAT=0.0
13    RETURN
      END
C*****************************************************************************C
C                                                                               C
      FUNCTION ETAV(S,VE,P)
C                                                                               C
C*****************************************************************************C
C
C     FUNCTION CALCULATES THE LATERAL DISTANCE OUT TO THE VE VELOCITY
C     EXCESS POINT.
C
      DIMENSION P(12,6)
      COMMON/HAVE/DELP(12,6),TEMP(60,6),VEL(60,6),DIR(60,6),XP(60),YP(60
     1),AMTEMP(6),AMCUR(6),BETA0,B0,ANGN,T0,U0,NPTS,DR,RD,K
C
      ETAV=0.0
      VC=P(7,K)*U0
      IF(S.LE.P(8,K)*B0) GOTO 10
      VC=VC*SQRT(P(8,K)*B0/S)
10    IF(VE.GT.VC) GOTO 11
      ETAV=1.44269504*ALOG(VC/VE)
      ETAV=SQRT(ETAV)*(P(9,K)*B0+P(10,K)*S)
      IF(ETAV.LT.0.0) ETAV=0.0
11    RETURN
      END
```

APPENDIX D

Fitting Parameters and Results

This Appendix contains the final values of the sets of 12 parameters (six parameters for the fit to the temperature measurements and six for the fit to the velocity data) obtained from the fitting procedure described in Sec. V. The results for the five jet studies analyzed in this manner are included. Values are tabulated (Tables D.1-D.5) for each depth at which sufficient data were available to make the fitting procedure meaningful. Also given are outfall and ambient temperatures and velocities used. In addition, the differences between the measured values at each station and the values calculated from the final fitted functions are tabulated. The quantity ΔT is defined as the calculated temperature excess minus the measured temperature excess at each data location; the quantity Δu is defined as the difference between the calculated jet centerline component of the local jet velocity for each data point and the component of the measured velocity parallel to the fitted velocity centerline. Also included are the root-mean-square deviations σ_T and σ_u defined in Sec. V and $\overline{\Delta T}$ and $\overline{\Delta u}$, which are the average of the absolute values of the tabulated deviations. The quantities $\overline{\Delta T}_{all}$ and $\overline{\Delta u}_{all}$ are the average deviations for all depths.

TABLE D.1. Results of the Fitting Procedure for May 18, 1972, Data

T_o = 17.7°C

U_o = 54.7 cm/scc

U_A = 0.0 cm/sec

	0.5 m	1.0 m	1.5 m	2.0 m	2.5 m	3.0 m
T_A (°C)	9.2	8.5	8.3	7.7	7.6	7.5
θ_o (C°)	8.5	9.2	9.4	10.0	10.6	10.2
A	0.84	0.71	0.78	0.68	0.80	
α	3.8	4.8	3.9	3.0	3.3	
C	0.8	1.3	0.4	2.0	0.2	
γ	0.39	0.35	0.41	0.13	0.19	
R_T	0.77	0.75	0.81	0.72	0.61	
K_T	1.41	1.29	0.85	2.85	3.27	
B	1.47	1.32	1.28	1.24	0.83	
β	4.6	3.7	3.4	3.0	1.4	
D	0.4	0.8	0.5	0.9	0.9	
δ	0.20	0.12	0.12	0.06	0.01	
R_u	1.04	0.96	1.02	1.03	0.85	
K_u	0.55	1.24	0.63	0.42	1.98	

TABLE D.1 (Contd.)

Station #	$\Delta T = T_{calc.} - T_{data}$ (C°)					
	0.5 m	1.0 m	1.5 m	2.0 m	2.5 m	3.0 m
1	0.0	0.5	---	-0.7	---	
2	-0.6	-0.6	-0.4	-0.5	-0.2	
3	---	1.0	---	-0.9	0.2	
4	-0.7	-0.4	-0.2	-0.7	-0.4	
5	-1.8	-1.0	-0.7	-0.8	0.0	
6	0.4	0.2	0.7	0.5	-0.5	
7	---	---	---	---	---	
8	0.5	0.5	1.0	---	---	
9	0.4	0.5	-0.3	-0.8	0.2	
10	0.9	0.0	0.0	1.1	0.1	
11	0.6	0.6	---	1.1	---	
12	-1.4	0.1	0.0	---	---	
13	0.7	0.9	1.7	---	---	
14	-1.5	-2.0	-1.9	-1.4	---	
15	0.2	0.4	0.6	0.3	---	
16	-0.2	0.0	0.4	0.5	---	
17	1.6	0.8	1.0	1.1	0.0	
18	-1.0	-1.2	-2.0	-0.7	---	
σ_T	1.2	1.0	1.3	1.1	0.5	
$\overline{\Delta T}$	0.8	0.6	0.8	0.8	0.2	

$\overline{\Delta T}_{all} = 0.7$ C°

TABLE D.1 (Contd.)

Station #	$\Delta U = U_{calc.} - U_{data}$ (cm/sec)					
	0.5 m	1.0 m	1.5 m	2.0 m	2.5 m	3.0 m
1	5	3	--	0	--	
2	0	0	-2	-3	-5	
3	--	-2	--	0	0	
4	0	2	3	1	0	
5	1	3	-1	-2	-1	
6	-5	-1	3	0	0	
7	--	--	--	--	--	
8	1	1	0	--	--	
9	-2	-4	-7	-2	1	
10	1	-4	4	10	0	
11	6	3	--	1	--	
12	0	0	0	--	--	
13	2	3	4	--	--	
14	-6	-4	-5	-8	--	
15	9	9	9	3	--	
16	-10	-8	-11	-5	--	
17	-3	0	-3	3	-1	
18	-8	1	0	0	--	
σ_u	6	5	7	5	4	
$\overline{\Delta U}$	4	3	4	3	1	

$\overline{\Delta U}_{all} = 3$

TABLE D.2. Results of the Fitting Procedure for May 23, 1972, Data

T_o = 21.6 °C

U_o = 55.5 cm/sec

U_A = 0.0 cm/sec

	0.5 m	1.0 m	1.5 m	2.0 m	2.5 m	3.0 m
T_A (°C)	14.3	12.6	12.1	11.6	11.3	10.8
θ_o (C°)	7.3	9.0	9.5	10.0	10.3	10.8
A	0.84	0.91	0.87	0.85	0.85	0.96
α	5.6	4.4	3.9	3.7	3.8	2.7
C	1.0	0.7	0.7	0.9	0.9	0.5
λ	0.27	0.37	0.32	0.21	0.14	0.20
R_T	1.28	1.26	1.33	1.22	1.28	1.58
K_T	-2.56	-2.58	-3.56	-1.88	-2.64	-7.06
B	1.04	0.98	0.92	0.93	0.80	0.93
β	4.8	4.7	5.1	3.6	2.6	3.7
D	0.8	0.9	0.8	0.8	0.9	0.6
δ	0.17	0.09	0.04	0.03	0.02	0.01
R_u	1.29	1.24	1.25	1.28	1.38	1.49
K_u	-2.11	-1.76	-1.90	-2.03	-2.84	-3.93

TABLE D.2 (Contd.)

Station #	$\Delta T = T_{calc.} - T_{data}$ (C°)					
	0.5 m	1.0 m	1.5 m	2.0 m	2.5 m	3.0 m
1	-0.6	-2.2	-2.6	---	---	---
2	0.8	0.8	1.3	1.9	1.6	---
3	-0.3	0.0	-0.5	-0.8	-0.5	-0.6
4	-0.9	-0.7	-1.1	-1.7	-1.5	0.3
5	-1.4	-1.8	-2.3	-2.9	-2.9	-0.8
6	-2.2	-3.1	-3.0	-1.9	-1.2	0.3
7	1.4	2.8	3.4	3.1	3.0	---
8	0.4	0.2	0.6	2.3	---	---
9	1.5	1.8	1.0	---	---	---
10	-0.3	0.2	0.5	0.6	0.6	---
11	0.0	0.6	1.4	0.0	1.2	---
12	-0.1	0.2	-0.8	0.1	-1.2	---
13	-0.4	-1.3	-1.7	-2.1	-2.6	---
14	-0.1	1.5	0.0	1.1	---	---
15	1.0	-0.1	0.4	-0.2	---	---
16	0.2	0.2	0.1	-0.3	0.7	---
17	0.1	-0.2	0.8	0.0	0.8	---
18	0.0	-0.6	-1.0	-2.1	---	---
19	0.4	0.5	0.7	-0.1	---	---
20	0.6	-0.4	-0.2	-0.6	-0.6	-0.8
21	-0.3	-1.2	-1.4	-0.9	-0.1	-0.3
22	1.4	1.8	1.8	1.4	1.6	1.8
23	-1.2	-0.7	-0.6	-0.6	0.1	-0.6
24	0.0	0.0	-1.4	0.0	0.0	0.0
25	-0.6	-0.3	-0.9	-1.1	-1.6	-0.8
26	0.2	-1.1	-1.5	0.0	-1.1	-1.2
27	-0.3	-0.1	0.4	1.0	1.0	0.3
28	-0.6	-0.5	-0.3	-0.2	-0.8	-0.7
29	0.2	0.1	0.4	0.4	0.3	0.6
σ_T	0.9	1.3	1.6	1.5	1.7	1.0
$\overline{\Delta T}$	0.6	0.9	1.1	1.0	1.1	0.6

$\overline{\Delta T}_{all} = 0.9$ C°

TABLE D.2 (Contd.)

Station #	$\Delta U = U_{calc.} - U_{data}$ (cm/sec)					
	0.5 m	1.0 m	1.5 m	2.0 m	2.5 m	3.0 m
1	-2	0	0	---	---	---
2	33	28	21	24	16	---
3	-4	0	2	-2	5	-1
4	-12	-11	-14	-12	3	2
5	-28	-21	-25	-31	-30	-6
6	-13	-21	-19	-7	-2	7
7	13	13	11	13	18	---
8	39	33	23	21	---	---
9	-2	-2	12	---	---	---
10	-11	-16	2	6	-13	---
11	-11	4	10	-4	-5	---
12	-1	0	1	-1	-4	---
13	1	-2	2	3	1	---
14	-6	-5	-6	-6	---	---
15	-7	0	-12	-1	---	---
16	2	2	-1	2	8	---
17	-1	-8	-4	1	2	---
18	4	6	5	2	---	---
19	1	1	0	2	---	---
20	6	-2	-5	-10	-10	-6
21	2	0	7	4	7	0
22	0	-5	-5	-1	3	0
23	-7	0	0	0	3	3
24	0	0	0	0	0	0
25	-8	-8	-8	0	0	0
26	5	2	-3	0	4	0
27	2	5	5	6	0	0
28	0	0	0	0	0	0
29	6	-2	0	0	0	0
σ_U	14	13	11	11	11	4
$\overline{\Delta U}$	8	7	7	6	6	2

$\overline{\Delta U}_{all}$ = 6 cm/sec

TABLE D.3. Results of the Fitting Procedure for July 13, 1972, Data

T_o = 20.3 °C

U_o = 54.7 cm/sec

U_A = 5.7 cm/sec

	0.5 m	1.0 m	1.5 m	2.0 m	2.5 m	3.0 m
T_A (°C)	13.0	12.2	11.4	11.0	10.6	10.3
θ_o (C°)	7.3	8.1	8.9	9.3	9.7	10.0
A	0.92	0.89	0.70	0.89	0.81	
α	6.2	4.4	4.6	4.3	4.9	
C	0.3	0.5	4.1	0.7	0.8	
R_T	0.97	0.97	0.88	0.94	0.98	
K_T	-0.74	-0.73	0.07	0.05	-0.26	
B	1.26	1.22	1.05	1.26	0.95	
β	7.4	5.3	4.8	7.5	4.3	
D	0.1	0.4	0.3	0.7	0.6	
δ	0.24	0.18	0.16	0.03	-0.01	
R_u	0.94	0.93	0.98	0.96	0.96	
K_u	-0.09	-0.11	-0.18	-0.24	-0.07	

TABLE D.3 (Contd.)

Station #	$\Delta T = T_{calc.} - T_{data}$ (C°)					
	0.5 m	1.0 m	1.5 m	2.0 m	2.5 m	3.0 m
1	0.1	0.3	1.3	0.8	0.0	
2	0.3	0.0	0.6	0.0	1.4	
3	-0.6	-0.6	-0.9	-0.3	-0.6	
4	0.4	0.6	-1.2	-0.1	---	
5	0.0	-0.1	0.9	---	---	
6	-0.4	-0.8	-0.6	-2.1	-1.4	
7	0.8	1.0	0.8	1.0	-0.4	
8	-0.5	-1.1	-0.8	-1.0	-0.9	
9	-0.9	-1.1	-1.3	-0.5	-1.6	
10	0.8	0.4	0.4	-1.0	-0.7	
11	-0.3	-0.6	-0.1	---	---	
12	-0.1	0.2	0.2	1.1	-0.7	
13	0.1	0.4	0.5	0.8	1.1	
14	0.1	0.6	1.1	1.1	1.5	
15	0.4	0.7	-0.2	0.0	-0.7	
16	-0.2	0.3	-0.8	-0.6	-0.4	
17	0.1	1.1	0.2	0.8	0.2	
σ_T	0.6	0.8	1.0	1.2	1.3	
$\overline{\Delta T}$	0.4	0.6	0.7	0.8	0.8	

$\overline{\Delta T}_{all} = 0.6$ C°

TABLE D.3 (Contd.)

Station #	$\Delta U = U_{calc.} - U_{data}$ (cm/sec)					
	0.5 m	1.0 m	1.5 m	2.0 m	2.5 m	3.0 m
1	9	5	-2	5	1	
2	-4	-4	5	6	0	
3	3	2	-7	-7	2	
4	-4	-1	-5	-5	---	
5	-6	-4	4	---	---	
6	2	6	4	2	1	
7	-3	-5	0	-1	5	
8	2	-3	2	9	0	
9	-9	-5	-12	-13	-5	
10	2	-2	-3	0	-1	
11	0	3	7	---	---	
12	7	5	1	2	3	
13	7	10	16	2	2	
14	2	6	10	6	3	
15	-4	-2	-1	3	4	
16	-1	4	3	8	7	
17	10	6	5	4	3	
σ_U	7	6	8	8	4	
$\overline{\Delta U}$	4	4	5	5	3	

$\overline{\Delta U}_{all} = 4$ cm/sec

TABLE D.4. Results of the Fitting Procedure for September 9, 1972, Data

T_o = 24.5°C

U_o = 54.7 cm/sec

U_A = 2.2 cm/sec

	0.5 m	1.0 m	1.5 m	2.0 m	2.5 m	3.0 m
T_A (°C)	16.3	15.2	14.4	14.1	13.9	13.8
θ_o (C°)	8.2	9.3	10.1	10.4	10.6	10.7
A	0.79	0.68	0.66	0.88	0.31	
α	4.5	3.7	2.1	2.0	0.4	
C	0.1	1.1	2.1	2.0	0.8	
λ	0.64	0.58	0.45	0.26	0.61	
R_T	0.98	1.07	1.22	1.34	1.21	
K_T	-0.44	-1.25	-2.18	-3.08	-0.45	
B	1.03	0.85	1.00	0.99		
β	4.4	3.0	4.0	3.9		
D	0.8	0.6	1.2	1.2		
δ	0.22	0.20	-0.02	-0.06		
R_u	0.98	0.98	0.97	1.01		
K_u	0.58	1.24	0.82	0.60		

TABLE D.4 (Contd.)

Station #	$\Delta T = T_{calc.} - T_{data}$ (C°)					
	0.5 m	1.0 m	1.5 m	2.0 m	2.5 m	3.0 m
1	-0.9	0.0	---	---	---	
2	0.6	0.9	1.0	---	---	
3	-0.7	-1.4	-0.2	0.6	---	
4	-1.2	0.0	-1.5	-1.4	---	
5	1.6	0.7	2.2	1.3	---	
6	-0.4	-0.3	-0.6	-0.1	---	
7	0.2	-0.2	-0.8	-0.9	0.0	
8	0.1	-0.2	-0.7	-0.2	0.2	
9	0.1	0.6	-0.6	0.3	-0.5	
10	0.6	0.0	0.2	0.1	-0.6	
11	0.5	0.1	-0.4	0.6	0.2	
12	-0.2	0.3	0.2	-0.6	0.1	
13	-0.2	-0.1	0.2	-0.4	0.2	
14	-0.3	0.3	0.6	0.8	0.5	
15	-0.6	0.0	1.0	1.4	0.4	
16	-0.4	0.1	0.0	0.8	0.3	
17	0.0	-0.9	-1.6	0.3	-0.4	
σ_T	0.8	0.7	1.2	1.0	0.5	
$\overline{\Delta T}$	0.5	0.4	0.7	0.7	0.3	

$\overline{\Delta T}_{all} = 0.5$ C°

TABLE D.4 (Contd.)

Station #	$\Delta U = U_{calc.} - U_{data}$ (cm/sec)					
	0.5 m	1.0 m	1.5 m	2.0 m	2.5 m	3.0 m
1	6	3	---	---		
2	3	2	3	---		
3	-5	-6	-3	-4		
4	-4	2	2	2		
5	1	2	-1	-2		
6	-4	-1	6	7		
7	3	5	0	0		
8	3	3	0	1		
9	6	2	0	0		
10	0	-3	-4	-7		
11	0	-10	-6	0		
12	0	1	3	4		
13	7	4	0	0		
14	0	2	0	0		
15	-3	-3	1	1		
16	-4	-3	1	0		
17	1	0	0	1		
σ_U	5	5	4	4		
$\overline{\Delta U}$	3	3	2	2		

$\overline{\Delta U}_{all} = 3$ cm/sec

TABLE D.5. Results of the Fitting Procedure for October 10, 1972, Data

T_o = 22.2 °C

U_o = 42.3 cm/sec

U_A = 0.0 cm/sec

	0.5 m	1.0 m	1.5 m	2.0 m	2.5 m	3.0 m
T_A (°C)	13.9	13.0	12.7	12.8	12.7	12.7
θ_o (C°)	9.2	9.2	9.5	9.6	9.5	9.5
A	0.85	0.59	0.48			
α	4.6	1.4	0.8			
C	2.0	0.6	0.2			
λ	0.52	0.85	0.46			
R_T	1.02	1.13	1.18			
K_T	0.29	-0.93	0.61			
B	0.52	0.58	0.22			
β	1.9	0.8	0.2			
D	0.2	0.2	0.7			
δ	0.29	0.19	0.00			
R_u	1.27	1.12	1.16			
K_u	-8.29	3.14	1.28			

TABLE D.5 (Contd.)

Station #	$\Delta T = T_{calc.} - T_{data}$ (C°)					
	0.5 m	1.0 m	1.5 m	2.0 m	2.5 m	3.0 m
7	0.2	-0.7	0.5			
8	0.3	0.9	0.8			
9	-0.1	-0.6	-2.1			
10	1.0	2.2	1.3			
11	0.3	0.2	---			
12	-1.0	0.0	---			
13	0.8	2.1	---			
14	-0.3	-2.0	-1.2			
15	-1.2	---	---			
16	-0.7	-1.1	1.0			
17	0.7	-0.2	-0.5			
18	0.0	-0.6	-0.8			
19	-0.1	0.9	-0.2			
20	0.2	-1.0	-0.5			
21	-0.2	-0.9	0.7			
22	-0.2	-0.1	0.7			
23	-0.4	0.8	0.1			
24	1.0	0.7	-0.6			
25	-0.4	-0.6	-0.8			
σ_T	0.7	1.3	1.2			
$\overline{\Delta T}$	0.5	0.9	0.8			
	$\overline{\Delta T}_{all} = 0.7$ C°					

TABLE D.5 (Contd.)

Station #	$\Delta U = U_{calc.} - U_{data}$ (cm/sec)					
	0.5 m	1.0 m	1.5 m	2.0 m	2.5 m	3.0 m
7	0	1	2			
8	-2	3	2			
9	1	0	2			
10	9	2	3			
11	1	5	---			
12	5	4	---			
13	7	6	---			
14	-10	-5	-2			
15	7	---	---			
16	-7	0	-1			
17	-7	0	1			
18	2	2	2			
19	-1	0	-1			
20	-9	-2	-2			
21	2	2	-1			
22	-3	1	0			
23	2	-2	0			
24	1	-1	4			
25	-4	3	0			
σ_U	6	3	2			
$\overline{\Delta U}$	4	2	2			

$\overline{\Delta U}_{all}$ = 3 cm/sec

ACKNOWLEDGMENTS

In a study requiring extensive field work the cooperation and help of a number of people besides the principal authors is often required. In this regard we would like to acknowledge the help of Messrs. Conrad Tome, Paul Siebold, and Richard Zeren. We would particularly like to acknowledge Mr. Barton Hoglund for his general help and assistance in the design and implementation of the field program.

We are grateful for the critical comments and suggestions made by Mr. William Dunn involving the JETFIT fitting procedure and model-data comparisons, and we appreciate the programming assistance of Mr. Stanley Zawadzki in reference to the analytical models evaluated in this study.

We are also grateful to Messrs. Walter Clapper and Robert Neisius for their graphic art contributions, and we would particularly like to acknowledge Ms. Maria Pacholok's typing and retyping several drafts of this report.

REFERENCES

1. J. A. Hoopes, R. W. Zeller, and G. A. Rohlich, *Heat Dissipation and Induced Circulations From Condenser Cooling Water Discharges Into Lake Monona,* Report No. 35, Department of Civil Engineering, The University of Wisconsin (Feb 1968).

2a. T. Hayashi and N. Shuto, "Diffusion of Warm Water Jets Discharged Horizontally at the Water Surface," *Proceedings of the International Association for Hydraulic Research,* Colorado State University, Fort Collins, Colorado, Vol. 4, pp. 47-59, September 1967.

2b. T. Hayashi and N. Shuto, "Diffusion of Warm Cooling Water Discharged from a Power Plant," *Proceedings of the 11th Conference on Coastal Engineering,* Institution of Civil Engineers, Session AVI, pp. 13-16, September 16-20, 1968.

3. A. Wada, "Numerical Analysis of Distribution of Flow and Thermal Diffusion Caused by Outfall of Cooling Water," *Proceedings of the Thirteenth Congress of the International Association for Hydraulic Research,* pp. 335-342, August 31-September 5, 1969.

4. H. H. Carter, *A Preliminary Report on the Characteristics of a Heated Jet Discharged Horizontally into a Transverse Current, Part 1--Constant Depth,* Tech. Report No. 61, Chesapeake Bay Institute, The Johns Hopkins University, Baltimore, Md. (Nov 1969).

5. L. H. Motz and B. A. Benedict, *Heated Surface Jet Discharged Into A Flowing Ambient Stream,* Department of Environmental and Water Resources Engineering, Vanderbilt University, Nashville, Tennessee, Report No. 4 (Aug 1970).

6a, 7. R. C. Y. Koh and L. Fan, *Mathematical Models for the Prediction of Temperature Distributions Resulting from the Discharge of Heated Water Into Large Bodies of Water,* National Environmental Protection Agency Report, Water Pollution Control Research Series 16130 DWO 10/70 (Oct 1970).

6b. R. C. Y. Koh, *Two-Dimensional Surface Warm Jets,* ASCE, J. Hydraul. Div., 819-836 (June 1971).

8a. R. E. Barry and D. P. Hoffman, "Computer Model for a Thermal Plume," Mechanical Division, The Detroit Edison Company, Detroit, Mich., paper presented at *ASCE National Resources Engineering Meeting,* Phoenix, Arizona, January 11-15, 1971.

8b. D. P. Hoffman, "Thermal Plume Model," Mechanical Division, The Detroit Edison Company, Detroit, Mich., paper presented at *Fifteenth Conference on Great Lakes Research,* Madison, Wis., April 5-7, 1972.

9. K. Stolzenbach and D. R. F. Harleman, *An Analytical and Experimental Investigation of Surface Discharges of Heated Water,* Ralph M. Parsons Laboratory for Water Resources and Hydrodynamics, Massachusetts Institute of Technology, Cambridge, Report No. 135 (Feb 1971).

10a. R. W. McLay, M. S. Hundal, F. Martinek, and E. B. Henson, *Mathematical Modeling of Nuclear Plant Thermal Effluents in Lake Champlain,* ASME, Winter Annual Meeting, Paper No. 71-WA/Pwr-4, November 26-December 2, 1971.

10b. M. S. Hundal, F. Martinek, E. B. Henson, and R. W. McLay, "A Computer Model for Predicting Thermal Discharges in Large Lakes," Department of Mechanical Engineering, University of Vermont, Burlington, paper presented at *Fifteenth Conference on Great Lakes Research,* Madison, Wis., April 5-7, 1972.

10c. R. W. McLay, M. S. Hundal, F. Martinek, and E. B. Henson, *A Mathematical Analysis of Thermal Pollution of Lakes and Estuaries,* Department of Mechanical Engineering, University of Vermont, Burlington (May 1972).

11a. H. Stefan, *Surface Discharge of Heated Water, Part I: Three Dimensional Jet-Type Surface Plumes in Theory and in the Laboratory,* Department of Civil and Mineral Engineering, St. Anthony Falls Hydraulic Laboratory, Project Report No. 126, University of Minnesota, Minneapolis (1971).

11b. H. Stefan, "Analytical Jet-Type Model of Heated Water Surface Plumes," Department of Civil and Mineral Engineering, St. Anthony Falls Hydraulic Laboratory, University of Minnesota, Minneapolis, Minnesota, paper presented at *Fifteenth Conference on Great Lakes Research,* Madison, Wis., April 5-7, 1972.

12. E. Prych, *A Warm Water Effluent Analyzed as a Buoyant Surface Jet,* Sveriges Meteorologiska Och Hydrologiska Institut, Serie Hydrologi. Nr. 21, Stockholm, 1972.

13. J. F. Paul and W. J. Lick, "A Numerical Model for a Three-Dimensional Variable-Density Jet," School of Engineering and Department of Geology, Case Western Reserve University, Cleveland, Ohio, paper presented at the *16th Conference on Great Lakes Research,* Huron, Ohio, April 16-18, 1973.

14. F. Engelund and F. Pedersen, *Surface Jet at Small Richardson Numbers,* J. Hydraul. Div., Proc. Am. Soc. Civil Eng. *99*(HY3), Proc. Paper 9588, pp. 405-416 (Mar 1973).

15a. W. Waldrop and R. Farmer, *Three-Dimensional Computation of Buoyant Plumes,* Coastal Studies Institute and Department of Chemical Engineering, Louisiana State University, Baton Rouge (Oct 1973).

15b. R. Farmer and P. Bryant, *A Mathematical Model for the Los Angeles-Long Beach Harbor,* research proposal submitted to the Environmental Protection Agency by the Chemical Engineering Department, Louisiana State University, Baton Rouge (Oct 1972).

16. A. Wada, *Numerical Analysis of Distribution of Flow and Thermal Diffusion Caused by Outfall of Cooling Water,* Coastal Eng. in Japan *11* (1968).

17. D. Pritchard, "Design and Siting Criteria for Once-Through Cooling Systems," presented at *American Institute of Chemical Engineers, 68th Annual Meeting,* Houston, Texas, March 2, 1971.

18. T. R. Sundaram, C. C. Easterbrook, K. R. Piech, and G. Rudinger, *An Investigation of the Physical Effects of Thermal Discharges Into Cayuga Lake (Analytical Study),* CAL No. VT - 2616-O-2, Cornell Aeronautical Laboratory, Inc. (Nov 1969).

19a. J. B. Bryce, W. R. Etter, and E. H. Dye, *Water Environmental Studies and Water Quality Control at Ontario Hydro,* The Hydro-Electric Power Commission of Ontario, Generation Projects Division, Toronto, Canada (June 16, 1971).

19b. R. V. Elliott and D. G. Harkness, "A Phenomenological Model for the Prediction of Thermal Plumes in Large Lakes," The Hydro-Electric Power Commission of Ontario, Toronto, Canada; paper presented at *Fifteenth Conference on Great Lakes Research,* Madison, Wisconsin, April 5-7, 1972.

20. W. Giles, N. Johnson, G. McComb, F. Morris, J. Schell, and J. Young, *A Thermal Effluent Analysis for Electric Power Generating Plants,* Reentry and Environmental Systems Division, General Electric, Technical Information Series No. 71SD257 (Sept 20, 1971).

21. L. A. Loziuk, J. C. Anderson, and T. Belytschko, *Hydrothermal Analysis by the Finite Element Method,* ASCE, J. Hydraul. Div. *98,* No. HY11 (Nov 1972).

22. D. Brady and J. Geyer, *Development of a General Computer Model for Simulating Thermal Discharges in Three Dimensions,* Report No. 7, Department of Geography and Environmental Engineering, The Johns Hopkins University, Baltimore, Md. (Feb 1972).

23. H. Till, *A Computer Model for Three-Dimensional Simulation of Thermal Discharges into Rivers,* doctoral dissertation, Department of Nuclear Engineering, University of Missouri, Rolla (1973).

24. D. W. Pritchard, "Fate of and Effect of Excess Heat Discharged Into Lake Michigan with Specific Application to the Condenser Cooling Water Discharge from the Zion Nuclear Power Station," testimony at *AEC Licensing Hearings for Zion Operating Permit,* Chicago, Ill. (June 1973).

25. H. H. Carter, E. W. Schiemer, and R. Regier, *The Buoyant Surface Jet Discharging Normal to An Ambient Flow of Various Depths,* Technical Report No. 81, Chesapeake Bay Institute, The Johns Hopkins University, Baltimore, Md. (Feb 1973).

26. B. R. Morton, *On a Momentum-Flux Diagram for Turbulent Jets, Plumes, and Wakes,* J. Fluid Mech. *10* (1961).

27. L. Fan, *Turbulent Buoyant Jets into Stratified or Flowing Ambient Fluids,* Tech. Report No. KH-R-15, W. M. Keck Laboratory of Hydraulics and Water Resources, California Institute of Technology, Pasadena (June 1967).

28. G. N. Abramovich, *The Theory of Turbulent Jets,* M.I.T. Press, Massachusetts Institute of Technology, Cambridge (1963).

29. T. Ellison and J. Turner, *Turbulent Entrainment in Stratified Flows,* J. Fluid Mech. *6,* 423 (1959).

30. F. L. Scarpace and T. Green III, *Dynamic Surface Temperature of Thermal Plumes,* Water Resources Research *9*(1) (Feb 1973).